Medicinal Cannabis for Neuropathic Pain

A thesis

submitted in partial fulfilment

of the requirements for the degree

of

Doctor of Philosophy in Health

at

The University of Waikato

by

Marion Constance McKinnon

THE UNIVERSITY OF
WAIKATO
Te Whare Wānanga o Waikato

2022

Abstract

Neuropathic pain is caused by a dysfunction of the nervous system. It differs from normal pain sensations as it is no longer protective and can be present in the absence of a stimulus. It affects eight percent of the population worldwide and has several causes. Diabetes is the most prevalent cause, with about half of those diagnosed developing diabetic neuropathy. Other causes are genetic diseases (e.g. Charcot-Marie-Tooth disease), immune disorders or medications (e.g. chemotherapy drugs) or injury. Neuropathic pain, regardless of its cause, is often poorly managed leading to poor quality of life for those patients. The currently available analgesic options show little efficacy and are often dose-limiting due to adverse effects. Treatments that improve efficacy or offer lower adverse effects need to be investigated; one such potential treatment is medicinal cannabis. To this end, cannabis isolates and a high CBD whole extract were tested to determine efficacy to relieve neuropathic pain symptoms in a pre-clinical mouse model of neuropathy.

A dose-response trial using gene expression biomarkers was completed in wildtype mice. This was to determine what doses of orally administered CBD (25 - 150 mg/kg) in an olive oil vehicle had a biological effect in the dorsal root ganglia of peripheral nerves of mice. CBD (6.25 - 100 mg/kg), a high CBD whole extract (containing CBD 12.5 mg/kg and THC 0.867 mg/kg) and a pure CBD:THC mix (at the same concentrations) were then used to determine efficacy in ameliorating neuropathic pain in a CMT2A mouse model. Finally, a single high-dose streptozotocin-induced diabetic neuropathy mouse model was characterised to determine the parameters of peripheral neuropathy and neuropathic pain symptoms in male wildtype B6:D2 mice.

The dose-response results showed that orally administered CBD produces a U-shaped dose-response curve. This was mimicked in analgesic efficacy in CMT2A mice, with a pure isolate of 12.5 mg/kg CBD showing the greatest efficacy in treating thermal hyperalgesia symptoms. This paralleled a clinically relevant dose of gabapentin (40mg/kg) in efficacy for improving thermal hyperalgesia, both as a single dose and in multiple doses across eight hours. Of the cannabinoids tested, high CBD whole extract showed greater efficacy in improving thermal hyperalgesia symptoms in CMT2A mice, with a wider therapeutic window than either CBD

alone or CBD:THC. This indicates that in addition to THC, other components in cannabis may contribute to efficacy, or be the result of an entourage effect.

Characterisation of the diabetic neuropathy model was completed, with two-thirds of the mice developing high blood glucose (≥ 17 mmol/L) within two weeks of a single high dose of streptozotocin. All diabetic mice showed thermal hyperalgesia symptoms and 40% of those also developed mechanical allodynia; with symptoms evident from as early as week four post-streptozotocin. There was no loss of motor function seen across the trial period of 13 weeks. Sciatic nerve tissue taken from these mice showed a marked loss of acetylated α-tubulin in both proximal and distal sciatic nerves when compared to the wildtype control group.

Acknowledgements

Undertaking a PhD is not a small thing, and without help and support from so many others it would not have been possible. The first set of thanks goes to A. Prof. Brett Langley, my Chief Supervisor. Thank you for setting up and offering this project to me. I have appreciated the opportunity to learn from you over this time. It has been a difficult journey, made even more so with the challenges of COVID, so to know that you have been able to offer help and guidance throughout has been much appreciated. Thank you for being the foundation block for my career path. I would also like to thank Dr Cristina Picci, who was a big part of my honors journey and then at the beginning of my PhD. Thank you teaching me and passing on your knowledge, particularly your expertise of working with and testing the mice.

Thank you to Cannasouth and Callaghan for funding this project. The team at Cannasouth has been a big part of this project and my PhD journey. There has been a lot of change on the team and several people who have been part of this. There are some individuals who I would like to acknowledge separately, David Gill and Philip Squire. You have both been amazing support throughout and continued to keep in contact with a quick online meeting during lock downs, which was a nice boost to long weeks of isolation. Thanks, Phil, for always being prepared to head over to the mice with me on dosing and testing days. I also appreciate the exposure by highlighting my work via your platforms. I have very much enjoyed working with all of you over the last few years.

There were times in this project where I felt like I practically lived at the animal facility. Bobby Smith and Gen Sheriff need to have a big thanks from me too. Bobby was a great friend during this time and has taught me a lot. Thanks to Bobby, I am now an expert at doing a cardiac punch in the mice. Thank you, Gen, for sorting out our MPI transfers so quickly, and ensuring I could still get into the facility during Covid lockdowns, it made things so much easier to be able to carry out my research. Thank you both for the time you spent looking after our mice and assisting me when I needed it.

Dr Will Kelton came on later in the project as a secondary supervisor but had also been a big help at times before that as well. I really appreciated having someone else to go to for help when I needed it. Thank you so much for reading and providing feedback on my writing.

To Sharna, Olivia and Annmaree, you have been constant friends and such a great support network throughout the highs and lows of this journey. Olivia, you have been such a big part of my whole academic journey, right from undergrad to completion. You were a role model to show me that it could be done, I could not have done what I did without your support and guidance. Annmaree, it was nice to go through this journey together, with you being able to understand what I was going through as you were in the same situation of completing your PhD at the same time. Sharna, I always appreciated our catch ups between the animal testing, it made those long tedious days a bit brighter to know I could pop out for a timed break with a cup of tea and a catch up with you.

Thanks also goes to Keely who read some of my thesis chapters and gave feedback. Thank you to all those others as well in the C2 lab group, for friendship, support and the chats over lunch or tea, it is great to have such a supportive group to work with.

Anthony, Emily, Jessica, and Joseph, you have dealt with so much over the last few years, and without your help at home I couldn't have done this. I hope I have been a good role model and shown you that you can achieve your goals.

Mum and Dad, your support has meant that I could carry out this massive undertaking. I have appreciated that much more than I can express. Mum, you have been my biggest cheerleader, reminding me to put my achievements into perspective, remembering that what I am doing is impressive and my work matters.

Caroline, you have been my touchstone through-out this journey, your support and encouragement has meant so much to me throughout this journey. This hasn't been an easy journey, but knowing you are there for me, and that we can just talk it out has made such a big difference.

Finally, my thanks must go to Neil, you have been my constant support throughout this whole process. You have ridden the highs and lows with me, from 3 am support sessions to the excitement of things going well and getting good results. I am sure there have been times when you are sick of hearing about western blots, problems with diabetic mice and other frustrations with my writing! But to know you were there made all the difference. I am pleased you have been by my side for this journey.

Table of Contents

List of figures

List of tables

List of Abbreviations

2-AG	2-Arachidonoylglycerol
5-HT	5-Hydroxytryptamine
AEA	Anandamide
AGEs	Advanced glycation end products
ANOVA	Analysis of variance
ATP	Adenosine triphosphate
CA^{2+}	Calcium
cAMP	Cyclic adenosine monophosphate
CB	Cannabinoid receptor
CB1	Cannabinoid receptor 1
CB2	Cannabinoid receptor 2
CBC	Cannabichromene
CBCA	Cannabichromic acid
CBD	Cannabidiol
CBDA	Cannabidiolic acid
CBDV	Cannabidivarine
CBG	Cannabigerol
CBGA	Cannabigerolic acid
CBN	Cannabinol
CCI	Chronic constriction injury
cDNA	Complementary DNA
CGRP	Calcitonin gene-related peptide
CINP	Chemotherapy induced neuropathic pain
CMT	Charcot-Marie-Tooth disease
CMT2A	Charcot-Marie-Tooth disease, type 2A
CNS	Central nervous system
CoA	Certificate of analysis
COX	Cyclooxygenase

COX 1	Cyclooxygenase 1
COX 2	Cyclooxygenase 2
Ct	Cycle threshold
Cq	Quantification cycle
DMSO	Dimethyl sulfoxide
DNA	Deoxyribonucleic acid
DRG	Dorsal root ganglia
ECL	Enhanced chemiluminescence
EDTA	Ethylenediamine tetra-acetic acid
FAAH	Fatty acid amine hydrolase
FDA	U.S. Food & Drug Administration
FPKB	Fragments per kilobase
GABA	Gamma-aminobutyric acid
GAPDH	Glyceraldehyde 3-phosphate dehydrogenase
GDP	Guanosine diphosphate
GLUT2	Glucose transporter 2
GPCR	G-protein coupled receptor
GPN	Gabapentin
GTP	Guanosine triphosphate
HDAC	Histone deacetylase
HIV	Human immunodeficiency virus
HRP	Horse radish protein
IASP	International Association for the Study of Pain
IP	Intraperitoneal
IV	Intravenous
LD50	Lethal dose (50%)
MAG L	Monoacylglycerol lipase
MAP kinase	Mitogen-associated protein kinase
MFN2	Mitofusion 2
MG^{2+}	Magnesium
MGI	Mouse Genome Informatics International Database

mRNA	Messenger RNA
NCBI	National Centre for Biotechnology Information
NMDA	N-methyl-D-aspartate receptor
PBS	Phosphate buffered saline
PCR	Polymerase chain reaction
PGE_2	Prostaglandin-endoperoxide 2
PKA	Protein kinase A
PNS	Peripheral nervous system
PTGS	Prostaglandin-endoperoxide synthase
qPCR	Real-time PCR
REST	Relative expression software tool
RNA	Ribonucleic acid
RPM	Revolutions per minute
RT	Reverse transcription
RT-qPCR	Reverse transcription qPCR
SAC	Small animal centre
SE	Standard error
SNRI	Serotonin-noradrenalin reuptake inhibitors
SOP	Standard operating procedure
STZ	Streptozotocin
TAE	Tris base acetic acid and EDTA buffer
TBE	Tris borate EDTA buffer
TCA	Tricyclic antidepressants
THC	Δ9-Tetrahydrocannabinol
THCA	Tetrahydrocannabinolic acid
TRP	Transient receptor potential
TRPV1	Transient receptor potential vanilloid type 1
TSH	Thyroid-stimulating hormone
UCSC	University of California Santa Cruz
UV	Ultra violet
WEX	High CBD whole extract

WHO	World Health Organisation
WT	Wildtype

1 Literature Review

1.1 Nociception

Pain is a normal, protective response to a harmful stimulus. It plays a role in preventing damage by avoidance and can help facilitate healing by protecting a damaged area (Latremoliere & Woolf, 2009; Woolf & Mannion, 1999). The process of detecting a harmful stimulus is called nociception and is carried out by specialised nerve endings known as nociceptors that are found throughout the peripheral nervous system (PNS) (Yam et al., 2018).

Different nerve fibre types detect harmful chemical, thermal or mechanical stimuli (Yam et al., 2018). There are two nociceptor nerve types: Aδ fibres and C fibres (Meyer, 2006). Aδ type fibres are myelinated and have medium diameter axons, therefore the signal is fast and localised; these fibres elicit a sharp pain and are activated by thermal and mechanical stimuli (Menorca et al., 2013; Meyer, 2006; Ringkamp et al., 2018). By contrast, C fibres are unmyelinated, have small diameter axons and send slow, long-lasting pain signals that typically represent a more diffuse throbbing pain (Basbaum et al., 2009; Dubin & Patapoutian, 2010; Meyer, 2006). The C fibres are activated by thermal, mechanical and chemical stimuli (Basbaum et al., 2009; Dubin & Patapoutian, 2010; Meyer, 2006). Once these PNS nociceptors have been stimulated and reached an activation threshold, a signal is transduced along the nerve fibre to the dorsal horn of the spinal cord within the central nervous system (CNS) where they can be relayed to higher brain centres to elicit a response (Yam et al., 2018).

Transduction involves converting the noxious stimulus to an electrochemical signal (an action potential), which is then transmitted along the nerve fibre (Bridgestock & Rae, 2013). Nerve fibres have a resting membrane potential that is maintained by the distribution of charged ions of sodium and potassium on either side of the membrane (Yam et al., 2018). Voltage-gated channels can be opened and allow the movement of the ions across the membrane leading to depolarisation of the nerve axon (Yam et al., 2018). The consecutive depolarisation along the nerve fibre propagates the signal, in the form of an action potential, to the axon terminus (Yam et al., 2018). At the axon terminus, the signal can be passed to another neuron via synaptic transmission (Yam et al., 2018). Membrane depolarisation at the presynaptic

neuron terminus (where the signal is coming from) causes calcium channels to open, leading to an influx of calcium and the release of glutamate as their primary neurotransmitter; although other peptides, such as substance P or calcitonin gene-related peptide (CGRP) may facilitate neurotransmission (Latremoliere & Woolf, 2009). Glutamate diffuses across the synaptic cleft and binds to glutamate receptors on the post-synaptic neuron (where the signal is going) (Latremoliere & Woolf, 2009). Under normal conditions, these receptors are turned off by magnesium (Mg^{2+}) ions (Latremoliere & Woolf, 2009). When a sustained depolarization of the membrane occurs, Mg^{2+} ions are forced off receptors allowing the binding of the glutamate (Latremoliere & Woolf, 2009). This acts as a protective function as only a sustained depolarization can lead to a pain signal being sent, otherwise binding of an errant neurotransmitter could send a false pain signal. The binding of glutamate to its receptors triggers the opening of the post-synaptic calcium channels, Ca^{2+} influx, and the depolarization of the post-synaptic neuron (Latremoliere & Woolf, 2009). This allows the movement of the pain signal from the peripheral nerve fibre to the spinal cord neurons, and propagation of the signal to the thalamus in the brain (Bridgestock & Rae, 2013). This type of pain is reversible once the stimulus is removed or in the case of damage, once the tissue has healed (Woolf & Mannion, 1999).

1.2 Pain and Inflammation

Inflammation often comes hand in hand with pain. When tissue damage occurs inflammatory cytokines are released, which mediate the excitation of nociceptors by lowering their activation threshold (Chen et al., 2017; Garland, 2012). These inflammatory mediators upregulate cyclooxygenase (COX) enzymes that synthesise prostaglandins from arachidonic acid (Vane et al., 1998), which can lead to swelling, pain and fever (Vane & Botting, 2003). There are two COX enzymes in humans, COX 1 and COX 2 (Vane et al., 1998). COX 1 is constitutively expressed in almost all cell types and produces prostaglandins for homeostatic functions (Vane et al., 1998). COX 1 is found within the brain with the highest concentrations found in the forebrain (Vane et al., 1998). COX 2, by contrast, is inducible and produces prostaglandins, in particular prostaglandin E_2 (PGE_2), establishing inflammatory effects in response to injury (Vane et al., 1998). COX 2 is induced by inflammatory cytokines such as interleukin-1B, bacterial lipopolysaccharides, and tumour necrosis factor-α (Park et al., 2006;

Vane et al., 1998); whereas anti-inflammatory cytokines and corticosteroids decrease the induction of COX 2 (Vane et al., 1998). Inhibition of COX enzymes lead to relief from pain and inflammation and is how common non-steroidal anti-inflammatory drugs (e.g., aspirin, paracetamol, and ibuprofen) have their action (Vane et al., 1998).

The inflammation pathway has an important defensive function, as inflammatory mediators trigger an influx of immune cells to the site of injury, where they can clear pathogens and cellular debris and stimulate tissue repair (Chen et al., 2017; Garland, 2012). To protect compromised tissue during healing, a cascade of events lead to peripheral sensitisation (Bridgestock & Rae, 2013). The increased presence of inflammatory mediators ultimately leads to a decrease in the activation threshold of the affected neurons (Chen et al., 2017). This causes the affected area to be more sensitive, therefore the area will be more protected as the organism will want to avoid anything touching the area, enhancing the healing process. As the area heals and there are fewer inflammatory mediators and this sensitisation declines (Bridgestock & Rae, 2013).

1.3 Neuropathic Pain

Neuropathic pain differs from normal pain sensations as it is stimulus-independent or arises from innocuous stimuli and is usually persistent (Treede et al., 2008). Neuropathic pain has been defined by the International Association for the Study of Pain (IASP) as "pain that arises as a direct consequence of a lesion or disease of the somatosensory nervous system" (Murnion, 2018). Neuropathic pain affects about 8% of the world population, is more prevalent in people over 50 years of age, and more common in women than men; 8% and 5.7%, respectively (Bouhassira et al., 2008). Neuropathic pain impacts anxiety, depression, sleep and quality of life to a greater extent when compared to chronic nociceptive pain (Schembri, 2019). Individuals suffering from neuropathic pain often have a diminished capacity to work, which can impact both their mental health and finances (Jensen, 2002; Murnion, 2018; Woolf & Mannion, 1999). These individuals will also require more intensive health care, leading to greater pressure on the health system (Jensen, 2002; Murnion, 2018; Woolf & Mannion, 1999).

A defining feature of neuropathic pain is that it is chronic rather than acute. This chronic pain is maintained by changes to the pain pathway, leading to central sensitisation. Central sensitisation is caused by the amplification of neural signalling within the CNS, leading to hypersensitivity (Woolf, 2011). It can also become stimulus independent or caused by innocuous stimuli (Lekan et al., 1996; Mannion et al., 1996; Shortland et al., 1997; Woolf, 2011). The development of central sensitisation leads to hyperalgesia (an increased pain perception from a noxious stimulus) and allodynia (pain from an innocuous stimulus that should not elicit a pain response) (Dubin & Patapoutian, 2010; Woolf, 2011).

1.3.1 Central sensitisation

Central sensitisation is a phenomenon where there is a reduced inhibition of neuronal firing and increased excitability, causing subthreshold signals to send a pain signal to the brain (Latremoliere & Woolf, 2009). As such, this reduced activation threshold and increased excitability can lead to non-noxious stimuli causing a pain response (Latremoliere & Woolf, 2009). The result is that the pain is no longer associated with a noxious stimulus and is no longer a protective function (Latremoliere & Woolf, 2009). These changes occur in the CNS,

and more specifically in the dorsal horn (Latremoliere & Woolf, 2009). Central sensitisation can be induced due to the plasticity of the sensory system and comes about by changes in glutamate receptors and neural gene transcription (Latremoliere & Woolf, 2009). Membrane excitability is increased by the phosphorylation of glutamate channels by protein kinase C, leading to the removal of the Mg^{2+}, which normally stops the binding of glutamate until there has been sustained depolarization (Latremoliere & Woolf, 2009). This allows the increased binding of glutamate and the influx of calcium into the cell, leading to hyperexcitability (Latremoliere & Woolf, 2009). Protein kinase C also decreases excitatory inhibition at the dorsal horn by reducing the levels of GABA, which is an inhibitory neurotransmitter (Latremoliere & Woolf, 2009). This leads to the dorsal horn being more susceptible to activation by Aß-type touch fibres and propagating a pain response (Latremoliere & Woolf, 2009).

Inflammation also contributes to the establishment of central sensitisation, as nerve damage increases levels of pro-inflammatory cytokines (Latremoliere & Woolf, 2009). In this case, an increased amount of COX 2 in the dorsal horn leads to the production of PGE_2, which can also lead to a reduction of inhibitory GABA as well as increased glutamate release (Latremoliere & Woolf, 2009). All of these mechanisms lead to the increased signalling and establishment of neuropathic pain that is independent of noxious stimuli.

1.3.1.1 Allodynia

With central sensitisation there is an increased response to the tactile Aß fibres, leading to allodynia. Allodynia is defined as a pain response caused by an innocuous stimulus that should not cause pain (Dubin & Patapoutian, 2010; Woolf, 2011). This is driven by changes in the dorsal horn leading to lowered inhibition and increased excitability with an exaggerated response to a stimulus (Woolf & Mannion, 1999). It occurs when the larger myelinated Aß nerve fibres, which normally detect tactile/touch signals, sprout into a different level in the dorsal horn lamina (Woolf, 2011). This sprouting is triggered by damage to the smaller diameter and unmyelinated C-type nerve fibres in the PNS (Latremoliere & Woolf, 2009). The dorsal horn is split into layers, with different lamina having different linking neurons, with each nerve type terminating in a particular lamina level (Latremoliere & Woolf, 2009; Woolf & Thompson, 1991). C-type fibres terminate in the upper lamina (lamina levels I and II) where

they connect to inter-neurons (Yam et al., 2018). The tactile Aß nerve fibres normally terminate in the deeper levels, IV and V, of the dorsal horn (Woolf, 2011). Damage to the C-type nerve fibres promote the sprouting of the tactile Aß fibres into lamina levels I and II, thus causing the Aß fibres to now stimulate a pain response to touch and tactile stimuli (Latremoliere & Woolf, 2009).

1.3.1.2 Thermal hyperalgesia

Thermal hyperalgesia is an altered perception of thermal stimuli. A stimulus that normally causes a "warm" signal and should not cause a pain response is now perceived as painful. This is mediated by small diameter sensory nerve C-fibres, which contain transient receptor potential cation channel subfamily V member 1 (TRPV1) channels (also known as the vanilloid or capsaicin receptors) (Jensen & Finnerup, 2014; Ma et al., 2005; Planells-Cases et al., 2005). Evidence suggests that damage to these nerve fibres alters the expression levels of the TRPV1 receptors (Hudson et al., 2001; Jensen & Finnerup, 2014). Damaged fibres show a decrease in the number of receptors, and to compensate for this, there is an increase in the number of receptors in the uninjured fibres (Hudson et al., 2001; Jensen & Finnerup, 2014; Ma et al., 2005). This coupled with the hypersensitivity of the TRPV1 receptors, mediates the development of thermal hyperalgesia (Caterina & Julius, 2001; Planells-Cases et al., 2005).

1.3.2 Distinguishing neuropathic pain from nociceptive pain

The measurement and quantification of pain can be difficult as pain is relative, and patients display differing tolerances to pain. It is therefore important to have quantifiable and repeatable tests to determine the level of neuropathic pain that is exhibited, and thus, changes in pain due to different treatments. Neuropathic pain can also be difficult to distinguish from nociceptive pain. Current methods for quantifying neuropathic pain in patients involve laboratory testing, quantitative sensory testing, bedside exams and questionnaires (Cruccu & Truini, 2009). Nerve conduction testing can be undertaken to determine if there is nerve fibre damage, but this is not useful for accurately quantifying neuropathic pain (Cruccu & Truini, 2009). The first step for determining neuropathic pain is to take a patient's history and establish if there is, or has been, neurological damage or disease. This is then followed by a clinical exam and then diagnostic tests (Finnerup et al.,

2016). A grading scale is used to determine the level of certainty that a patient is presenting with neuropathic pain (Finnerup et al., 2016). Once established, treatments can be trialled to ease the level of the patient's pain and improve their quality of life, though effective options are limited.

1.3.3 Causes of neuropathic pain

Neuropathic pain is caused by a malfunction of the nervous system due to a variety of diseases, injury to nerves, or some types of medications. The symptoms of neuropathic pain from these sources are varied and include both gain of function and loss of function symptoms (Baron, 2016). Gain of function symptoms includes dysesthesia (abnormal sensations like burning or itching), paresthesia (pins and needles), and mechanical and thermal hyperalgesia and allodynia (Baron, 2016). Loss of function symptoms includes mechanical and thermal hypoesthesia (reduced perception/numbness), hypoalgesia (reduced reaction to painful stimuli) and complete or partial sensory deficits (Baron, 2016; Woolf & Mannion, 1999). These symptoms can be debilitating and often lead to further injury.

Diseases that can lead to neuropathic pain include diabetes, genetic disorders like Charcot-Marie-Tooth disease, multiple sclerosis, HIV, and shingles. Nerve injury can result from surgery, sciatica, or accidents; including the loss of a limb or amputation, though this can often be a result of diseases; for example, diabetes is the leading cause of both neuropathic pain and amputation (Argoff et al., 2006; Leone et al., 2012). Medications that can cause neuropathic pain include a range of chemotherapy drugs, which can lead to dose limitations when treating cancer (Quasthoff & Hartung, 2002). In some cases, alcohol abuse can also lead to neuropathy and neuropathic pain (Chopra & Tiwari, 2012). Of these causes, diabetes and Charcot-Marie-Tooth disease are further discussed below.

1.3.3.1 Diabetic-induced neuropathic pain

Diabetes is a group of metabolic disorders that are caused by impaired insulin secretion and/or action leading to hyperglycemia (American-Diabetes-Association, 2013). Chronic hyperglycemia leads to damage or failure of many organs, particularly the eyes, kidneys, heart, and nerve tissue (American-Diabetes-Association, 2013). Diabetes is the most prevalent cause of neuropathic pain (Yagihashi et al., 2011), affecting up to 400 million people

worldwide (Wild et al., 2004; World-Health-Organization, 2018). Neuropathies are the most common complication among diabetic patients, with approximately 50% of diabetic patients suffering from neuropathy (Yagihashi et al., 2011). In diabetic patients, a progressive, length-dependent, distal loss of sensory neurons occurs over time (Zilliox & Russell, 2011) and as the disease progresses it can affect autonomic nerves and damage motor neurons (Feldman et al., 2019). Older patients (over 50 years of age) have a higher incidence of diabetic neuropathy (Feldman et al., 2019), with the duration of diabetes directly related to an increased risk of neuropathy (Feldman et al., 2019). Most patients with diabetic-induced neuropathy notice mild discomfort, but up to 25% of these have significant neuropathic pain (Zilliox & Russell, 2011). In extreme cases, patients with sensory loss can suffer unnoticed injuries to the feet, which can contribute to the development of ulcers and lead to amputation (Russell & Zilliox, 2014). Indeed, diabetes is the leading cause of foot amputation (Leone et al., 2012). The only effective current treatment to prevent nerve damage from diabetes is tight control over the patient's blood glucose levels (Yagihashi et al., 2011), though this is often hard to maintain for many patients.

1.3.3.2 Charcot–Marie–Tooth disease, type 2A

Genetically inherited diseases that cause neuropathic pain are often harder to treat as the disease tends to affect the structure or function of the nerves. One such example is Charcot-Marie-Tooth (CMT) disease. CMT is a collection of relatively rare inherited PNS neurological disorders affecting 1:2500 people and are caused by autosomal dominant, autosomal recessive, or X-linked mutations to genes that affect the structure or function of the peripheral nerve (Martinou et al., 2010). Depending on the gene(s) affected, symptoms vary in severity and presentation and may impact sensory neurons, motor neurons, or both (Padua et al., 2006). Motor symptoms include lower limb weakness, muscle loss, foot drop, hammer toe, and frequent tripping (McCorquodale et al., 2016). Sensory neuron dysfunction leads to neuropathic pain, which can be quite severe, requiring life-long analgesia (Carter et al., 1998). CMT currently has no cure and disease management is largely restricted to analgesics, physical therapy and orthopaedic devices (McCorquodale et al., 2016). These include gait therapy, occupational therapy, assistive orthopaedic devices, and surgery for foot deformities (McCorquodale et al., 2016). Since there is no cure and treatment is difficult, neuropathic pain can dominate the lifestyle of these patients.

CMT can be divided into five main categories: CMT1, CMT3, CMT4, and CMTX1, which all affect the myelin sheath that surrounds peripheral nerves; and CMT2, which affects the axon. A nerve conduction test can be carried out to determine the CMT type, with demyelinating types having a slowed conduction velocity of less than 38 m/s, while CMT2 has more normal nerve conduction velocities (more than 38 m/s) (Shy et al., 2002). CMT1 tends to have an early onset, usually within the first 10 years of life, and due to the earlier onset, the symptoms can become more severe. By contrast, CMT2 tends to have a later onset, often in the patients' 20's but it can be as late as 70 years of age (Harding & Thomas, 1980). Although it is sometimes useful to know the precise type of CMT that a patient has, genetic testing is not always performed as treatment is the same regardless of disease type (McCorquodale et al., 2016). Situations when it can be helpful to know the genetic involvement include when the inheritance pattern needs to be understood to make well-informed reproductive decisions, and for clinical trials that target a particular CMT type. When genetic testing is carried out it should be paired with genetic counselling (McCorquodale et al., 2016).

Within the axonal CMT2 type, the disease is divided into 16 subtypes, depending on the specific gene affected. CMT2A is the most common form of CMT2, making up approximately 90% of CMT2 cases (Saito et al., 1997), and is characterised by progressive axonal degeneration, with dieback occurring from the distal end of the nerve and the longest nerves being affected first (Scherer, 2011; Skre, 1974). CMT2A has the earliest onset of the CMT2 subtypes, and because of this, it is the most severe form of CMT2 (Feely et al., 2011). CMT2A is caused by an autosomal dominant mutation in the mitofusion 2 (*mfn2*) gene (Saito et al., 1997; Scherer, 2011). More than 30 different mutations have been identified in this gene (Detmer & Chan, 2007), with the most common being a missense mutation in exon 4 that results in an arginine to glutamine (R94Q) substitution (De Vriendt et al., 2006).

1.3.4 Current treatment options for neuropathic pain

Neuropathic pain is often poorly managed causing reduced quality of life (Jensen, 2002; Murnion, 2018; Woolf & Mannion, 1999). Treatments that currently exist for neuropathic pain are often ineffective or dose-limiting due to adverse side effects (Kingery, 1997; Woolf & Mannion, 1999). Neuropathic pain is best managed by treating the primary disease causing the pain. For example, painful diabetic neuropathy can be somewhat managed by keeping

blood glucose levels tightly controlled, which reduces the risk of developing or worsening diabetic-induced neuropathic pain (Murnion, 2018). Other causes of neuropathic pain, for example, genetic diseases, cannot be treated in this way. Most patients will turn towards analgesic medication to help ease the pain. Many of these are ineffective for the treatment of chronic neuropathic pain, have the potential for addiction and abuse, and have adverse side effects (Murnion, 2018). Analgesics are used in a trial-and-error approach as each patient and pain symptomology will differ in the reaction to the drug (Murnion, 2018; Woolf & Mannion, 1999).

First-line drugs for the treatment of chronic neuropathic pain are antidepressants and anticonvulsants. Antidepressants have been shown to have a moderate effect on neuropathic pain that is independent of their antidepressant activity (Obata, 2017; Saarto & Wiffen, 2007; Woolf & Mannion, 1999). The two main types of antidepressants used to treat neuropathic pain are tricyclic antidepressants (TCAs), and serotonin-noradrenalin reuptake inhibitors (SNRIs) (Fornasari, 2017). These work by blocking voltage-gated sodium channels and NMDA receptors in the spinal cord, which can decrease central sensitisation (Fornasari, 2017). The side effects of these drugs vary depending on the particular antidepressant taken but include headaches, dizziness, gastrointestinal upsets, insomnia, sexual dysfunction and weight gain (Ferguson, 2001). TCAs also can have an anticholinergic effect (Fornasari, 2017), whereby decreased acetylcholine action can lead to physical and mental impairment (Lieberman, 2004).

In contrast to antidepressants, anticonvulsants act on voltage-gated calcium channels in the CNS (in particular, NMDA receptors) (Fornasari, 2017). Gabapentin, one such anticonvulsant, is the current 'go-to' treatment for neuropathic pain (Wiffen et al., 2017). It is an anti-epileptic drug that has been used with some success as a first-line treatment drug to treat neuropathic pain associated with postherpetic neuralgia and diabetic neuropathy (Kukkar et al., 2013; Maneuf et al., 2006). Gabapentin is an analogue for GABA (an inhibitory neurotransmitter in the CNS (Bowery & Smart, 2006)) and is lipophilic so can move across the blood-brain barrier (Bennett & Simpson, 2004). As such, it was originally thought that gabapentin's mechanism of action was through the GABA receptors (Bennett & Simpson, 2004), but further study showed that this was not the case and that the main receptor target for gabapentin is the voltage-dependent $\alpha 2\delta$ subunit on the calcium channel (Kukkar et al., 2013). These receptors

are highly concentrated in the dorsal horn of the spinal cord (Kukkar et al., 2013; Maneuf et al., 2006; Rose & Kam, 2002) and their activation by gabapentin inhibits the release of excitatory neurotransmitters, which decreases signalling, and interrupts propagation of the neuropathic pain signal (Bennett & Simpson, 2004).

Gabapentin has few drug interactions but does have side effects, the most common being dizziness and sleepiness, nausea and vomiting (Jensen, 2002). Less common, affecting less than 10% of patients, are the more adverse side effects of ataxia and swelling in the extremities of the limbs (Kukkar et al., 2013; Rose & Kam, 2002). Additionally, the New Zealand Med-Safe data sheet indicates use with caution in those over 18 years of age to treat neuropathic pain, as the risk of suicidal ideation was increased twofold when compared to a placebo group (Pfizer, 2020). The efficacy of gabapentin in neuropathic pain patients is reported to be somewhere between 30% to 38% of patients reporting at least a 50% reduction in pain (Bennett & Simpson, 2004; Wiffen et al., 2017). It has good bioavailability at lower doses, with increasing doses of gabapentin having reduced bioavailability; this is hypothesised to be due to saturation of transport mechanisms at the higher doses (Bennett & Simpson, 2004).

Second-line drugs for treating neuropathic pain include topical treatments. These are often used for pain that has a local generation site. Commonly used topical treatments are capsaicin (8%) or lidocaine (Murnion, 2018). Lidocaine can block voltage-gated sodium channels in the nerves, inhibiting the action potential from being propagated (Fornasari, 2017). This drug is only able to penetrate the skin a small distance and will only act locally where it has been applied (Fornasari, 2017) and often make little to no long-term difference in relieving a patient's suffering.

Finally, stronger analgesics like tramadol and other opioid drugs (e.g. morphine, oxycodone and hydromorphone) make up the last-line of drugs for neuropathic pain (Murnion, 2018). Opioid drugs work predominantly in the CNS by binding to G protein-coupled opioid receptors (Fornasari, 2017) and act to stop the release of neurotransmitters (Fornasari, 2014). This in turn leads to a lowered number of nociceptive signals reaching the brain causing a lowered perception of pain (Fornasari, 2014). Opioids have better efficacy than the first- and second-line drugs for minimizing neuropathic pain, but they have many drawbacks that limit their use. The tolerability of opioids is often low, with about 50% of patients suffering from an

adverse effect (Labianca et al., 2012). They are also highly addictive and extended use results in a decrease in efficacy due to tolerance, leading to a need for increased dosage, which in turn increases the side effects (Labianca et al., 2012). The most common side effects of opioid drugs are nausea, vomiting, constipation, pruritis, and cognitive impairment (Fornasari, 2014). Due to these issues, opioids must be used with care when treating neuropathic pain. Though often these drugs can be of some help, they are not the 'silver bullet' to treat chronic neuropathic pain.

1.4 Cannabis for Neuropathic Pain

Due to the number of patients who suffer from neuropathic pain, it is important to investigate other ways in which pain can be mitigated or minimised in a safe and tolerable way. Effective treatments need to target neuropathic pain without a host of unwanted and unintended side effects to provide a patient with a better quality of life. One potential treatment option is cannabis. There are many historical accounts of the use of cannabis to treat pain (Fine & Rosenfeld, 2014) and more recently, a number of pre-clinical and clinical trials have indicated that cannabinoids may be useful for treating neuropathic pain symptoms (Vučković et al., 2018). Cannabinoids can activate the endocannabinoid system, which plays a major role in the pain pathway (Woodhams et al., 2015). Unlike other analgesic drugs, there are very few adverse effects associated with the use of cannabis, and of those, most are well tolerated (Ware et al., 2015).

1.4.1 Cannabis

Cannabis is a plant from the family Cannabaceae, which is also sometimes referred to as marihuana or marijuana. It is an annual dioecious plant that grows well in most climates and can be found worldwide (Laursen, 2015; Russo, 2007). Cannabis has a long history with written records of its use dating back to 5000 years ago (Zuardi, 2006). It is one of the earliest known plants cultivated by humans in ancient China due to its versatility (Zuardi, 2006). The plant has many uses: the seeds are used for food and fuel; the stalks for fibre and rope; and the unfertilized flowers for medicinal or recreational purposes (Bridgeman & Abazia, 2017; Russo, 2007; Zuardi, 2006). There are many strains and there is great debate about their taxonomy and lineages as it has been cultivated by humans for so long (Laursen, 2015); however, it is generally agreed upon that there are three major species of cannabis, *C. Sativa, C. Indica* and *C. Ruderalis,* with a great number of subspecies within these (Laursen, 2015). *C. Sativa* is much taller and has a lower Δ^9-tetrahydrocannabinol (THC) content (Hartsel et al., 2016). It is the strain that is commonly used for fibre due to its longer stem (Hartsel et al., 2016). *C. Indica* is shorter with denser branches and a high THC content (Hartsel et al., 2016). *C. Ruderalis* is the smallest of the three strains, has a very low THC and is not often used for medicinal or recreational uses, but is commonly cross-bred with the other strains (Hartsel et al., 2016).

The cannabis plant flowers at the end of summer as the light hours become shorter. The active compounds are found in trichomes of the unfertilized flowers on the female cannabis plant (Dayanandan & Kaufman, 1976); with over 500 different compounds that have been isolated to date (Katalin & Attila, 2017). These compounds include cannabinoids, flavonoids, terpenes, hydrocarbons, phenols, nitrogen-containing compounds, carbohydrates and fatty acids (McPartland & Russo, 2001). The cannabinoids are the most well-known isolates, with the most studied being THC and cannabidiol (CBD). Though, many more have recently been extracted and characterised, with some of these having a much greater biological activity than the major cannabinoids (McPartland & Russo, 2001).

Recreational use of the plant has probably been going on for as long as it has been cultivated by humans (Ameri, 1999; Lee, 2012). Recreational use increased greatly in the United Kingdom and other Western countries during the 1960s and 1970s, leading to increased research on the topic (Pertwee, 2006). Much of this research focused on how the psychoactive effects are mediated and their effectiveness in treating pain symptoms (Pertwee, 2006). Cannabis products can be inhaled via smoking, ingested, or absorbed through the skin or mucosal membranes (Jett et al., 2018). The main reason it is used recreationally is for the feeling of euphoria and relaxation. Other psychoactive effects of cannabis include increased sensory perception, tachycardia, antinociception, loss of concentration, and memory impairment (Ameri, 1999). This psychoactivity is mainly attributable to the THC, found in the flowers and leaves of the plant (Jett et al., 2018), which interacts with the CNS once it is in the bloodstream (Ameri, 1999). Because of its psychoactive effects, it is illegal to grow and use cannabis or cannabis products in many countries, and there is a lot of controversy surrounding the plant. Despite this, in 2016 the World Health Organization (WHO) indicated that cannabis was the most widely used illicit drug, with 2.5% of the world population consuming it (WHO, 2016). In recent times there has been a shift in its acceptability, with a growing number of countries having legalized cannabis for recreational and/or medicinal use.

1.4.2 History of cannabis for treating pain symptoms

Historical evidence of cannabis preparations being used to treat pain in China, Egypt, Greece, Europe and India dates back as much as 5000 years ago (Fine & Rosenfeld, 2014). Cannabis

has been commonly used as a medicine, most frequently as a treatment for pain (Brand & Zhao, 2017). Many ancient Egyptian, Chinese and Indian texts mention the use of cannabis for treating a variety of malaises (Russo, 2007). Traditional Chinese texts also describe the use and preparation of the plant material (Brand & Zhao, 2017). There are records of cannabis preparations used to treat pain associated with gout, headache, and menstrual pain, and to treat the pain associated with broken bones (Brand & Zhao, 2017). Other uses, recorded in the *Bencao* from around 200 A.D., include itching, convulsions, anaemia and the treatment of mania (Brand & Zhao, 2017). Interestingly, within this text, there is mention of cannabis being the unsurpassed treatment for 'a pain that restricts movement', which Brand and Zhao (2017) suggest could be interpreted as neuropathic pain. Cannabis is again mentioned much later on as a treatment to soothe neuropathic pain in 9th century A.D Egypt (Russo, 2007). Today the most commonly cited reason for using medical cannabis is pain, usually chronic pain (Vučković et al., 2018); with many patients self-reporting that cannabis can help to alleviate their pain symptoms (Ogborne et al., 2000).

With thousands of years of evidence from a variety of cultures in which cannabis has been used as a treatment for pain, there is a good indication that cannabis contains beneficial compounds that could lead to analgesia.

1.4.3 Exogenous cannabinoids

Exogenous cannabinoids are those coming from outside the body, which can be from cannabis plants or synthesised in a laboratory (Lu & Mackie, 2016). Cannabinoids found in cannabis plants are also known as phytocannabinoids. Cannabinol (CBN), a metabolite of THC, was the first phytocannabinoid to be isolated from cannabis in the late 19th century, with the structure elucidated in the early 1930s (Pertwee, 2006). The next two phytocannabinoids identified were cannabidiol (CBD) and THC, in 1940 and 1942, respectively (Pertwee, 2006).

CBD is found in high concentrations in cannabis extracts, making up about 40% of total compounds and is non-psychoactive (Mechoulam et al., 2007). The first effects noted for CBD were a reduction in seizure activity in patients with treatment-resistant epilepsy (Friedman & Sirven, 2017). CBD has since been shown to have analgesic, anti-inflammatory, anti-convulsant and anxiolytic effects (Vučković et al., 2018).

THC is produced in the plant as tetrahydrocannabinol acid (THCA) and is decarboxylated to THC when heated (Perrotin-Brunel et al., 2011). THC usage leads to altered brain function and the psychotropic effects of feeling 'high' which include euphoria, anxiety, paranoia, cognitive impairment, and depression of motor activity (Vučković et al., 2018). These effects occur because the THC can bind to cannabinoid receptors in the brain (Demuth & Molleman, 2006). THC has been shown to have analgesic, anti-inflammatory, anti-oxidant, anti-pruritic, and antispasmodic effects as well as being a muscle relaxant and bronchodilator (Vučković et al., 2018). In the body, THC is metabolized in the liver by cytochrome P450 to Δ^{11}-THC, which is much more psychoactive (Turkanis et al., 1991). This is known as first-pass metabolism. Thus, the effects of cannabis taken orally differ from those when it enters the bloodstream directly via inhalation as it bypasses the first-pass metabolism.

In addition to CBD and THC, there are also many other phytocannabinoids present in cannabis. While many are uncharacterised, or poorly characterised, it is recognised that they play a role in the effects that cannabis has, particularly in analgesia. CBD and THC when used together do not provide the same level of efficacy as whole cannabis extract leading to the hypothesis that minor phytocannabinoids either play an entourage role or that some minor phytocannabinoids have much greater potency than CBD and THC (Russo, 2019).

1.4.4 Biological effects of cannabinoids

Cannabis, particularly when used recreationally, has some well-known side effects, notably the effect of intoxication or feeling "high". When cannabis is used medically it is desirable that the psychoactive effects are avoided, while maintaining the clinically relevant analgesic or anti-inflammatory effects. Some of the effects noted in mice due to the presence of THC include hypothermia, postural hypotension, tachycardia, catalepsy, and a reduction in spontaneous activity (Smirnov & Kiyatkin, 2008; Whitlow et al., 2002). Some of these are due to the activation of the CB1 receptors, for example catalepsy and analgesia, while others, for example hypothermia, are due to impairment of vasodilation in the thermoregulation system (Paton, 1973). These effects need to be considered when there is a change in the behaviour of the test animals. Testing can be carried out for spontaneous activity, catalepsy, hypothermia and analgesia in mice (Fride et al., 2006). Changes to body temperature can be recorded via a thermometer (Fride et al., 2006), and often when using mice to test

cannabinoids, keeping them in a warmer environment can help overcome the drop in body temperature and accompanying behavioural changes (Fride et al., 2006).

A better option is to prevent this group of effects by avoiding THC, and thus determining other compounds in the cannabis that will lead to analgesia. In addition, as evident in the literature, whole cannabis extract has better efficacy than THC and/or CBD alone (Russo, 2011). When the psychoactive effects of cannabis are decreased or removed (for example, decreasing or removing THC content), the most common adverse effects that have been reported are mild learning, memory and motor deficits, dizziness and nausea; all of which are minimal and usually well tolerated in humans (Deshpande et al., 2015; Rog et al., 2007). In the context of current drug treatments for neuropathic pain, which come with a raft of adverse effects (as discussed in section 1.3.4), cannabis could provide a better way to manage chronic and debilitating pain (Lee et al., 2018).

1.4.5 Endocannabinoid system

Many studies investigating cannabis isolates and their effect on the body have been carried out over the years. As well as the psychoactive effects, cannabis also affects the cardiovascular system, respiratory system (particularly if inhaled), immune system, and endocrine system (Ashton, 2001). It was originally assumed that exogenous cannabinoids elicit these systemic actions by binding to cell membranes due to their lipid nature (Lawrence & Gill, 1975). However, it was later discovered that cells have specific receptors that cannabinoids interact with; these were aptly called cannabinoid receptors and are the targets of endogenous cannabinoids (Pertwee, 2006; Zou & Kumar, 2018).

The endocannabinoid system consists of cannabinoid receptors, endocannabinoids, and the enzymes responsible for the synthesis and degradation of the endocannabinoids (Burston & Woodhams, 2014; Mackie, 2006; Woodhams et al., 2015). It is a neuromodulation system that regulates stress recovery by helping endocrine, nervous and behavioural systems maintain homeostasis (Mucke et al., 2018). It maintains energy balance via the regulation of food intake, utilization and storage (Mucke et al., 2018), and is involved in brain activities like learning, memory, anxiety, and drug addiction (Vučković et al., 2018). Most importantly, immune, and inflammatory responses to a noxious stimulus and pain can be modulated by the endocannabinoid system (Mucke et al., 2018; Woodhams et al., 2015).

1.4.5.1 Cannabinoid receptors

Two types of cannabinoid receptors are found throughout the body: type 1 (CB1) and type 2 (CB2). Both are G-protein-coupled receptors (GPCRs) (Howlett et al., 2002) and can act as on/off switches for the cell; the receptors bind cannabinoids outside the cell and facilitate a signalling cascade causing a change inside the cell (Tikhonova & Costanzi, 2009). Cannabinoid receptor type 1 is highly expressed in the central nervous system on pre-synaptic nerve terminals (Pertwee, 2008; Woodhams et al., 2015). These were first discovered in 1988 in the brains of rats during studies to determine where cannabinoids bind to have their action (Devane et al., 1988). This led to the discovery of CB1 receptors in the CNS of humans and other mammals in 1990 (Matsuda et al., 1990). Cannabinoid receptor type 2 was discovered a few years after the CB1 receptors, in 1993 (Munro et al., 1993). They are mainly found on

immune cells and play a role in the suppression of the immune system (Basu et al., 2011; Woodhams et al., 2015). When CB2 receptors are activated, there is a reduction in the production of pro-inflammatory cytokines causing a decrease in inflammatory responses (Kaminski, 1996; Shang & Tang, 2017). This in turn leads to reduced neuronal activation and antinociception in inflammatory pain states (Shang & Tang, 2017). Because both types of cannabinoid receptors are ubiquitously expressed in the CNS, PNS, and on immune cells, following their discovery, it was assumed that they must have endogenous ligands that bind and activate them (Lu & Mackie, 2016; Munro et al., 1993).

1.4.5.2 Endogenous cannabinoids

Endogenous cannabinoids are synthesised in the body (Stout & Cimino, 2014) and were discovered in the early 1990s, after the discovery of the cannabinoid receptors (Burston & Woodhams, 2014; Mackie, 2006; Woodhams et al., 2015). The two most abundant and well-studied endogenous cannabinoids are anandamide (AEA) and 2-arachidonoylglycerol (2-AG). These are lipid-based molecules that are synthesised on demand from the precursor molecule arachidonic acid (Barrie & Manolios, 2017; Lu & Mackie, 2016). They are released during high neuronal activity, as indicated by increased intracellular calcium levels (Zou & Kumar, 2018), to modulate pain signalling (Lu & Mackie, 2016). Both endocannabinoids, AEA and 2-AG, are rapidly degraded in the body and the effects are short-lived and highly specific (Woodhams et al., 2015). Of the two endocannabinoids, 2-AG is found at much higher levels in the brain (Woodhams et al., 2015) and has the greatest affinity for CB1 receptors (Mackie, 2006), but can also bind to CB2 receptors (Woodhams et al., 2015). AEA interacts with both CB1 and CB2 receptors as well as TRPV1 receptors (Rosenbaum & Simon, 2006).

1.4.6 Modulation of pain and inflammatory systems by the endocannabinoid system

The pain and inflammation responses are, in part, modulated by the endocannabinoid system. In periods of high neuronal signalling, endocannabinoids are synthesised in the post-synaptic membrane (Hosking & Zajicek, 2008). The endocannabinoids then diffuse across the synaptic cleft in a retrograde direction towards the pre-synaptic nerve and can bind to CB1 receptors (Hosking & Zajicek, 2008). They are unusual as they work in a retrograde fashion,

from the post-synaptic cells to the pre-synaptic cells (Alger, 2013). The binding of endocannabinoids to CB1 receptors on the pre-synaptic nerve causes inhibition of neurotransmitter release stopping the pain signal from being sent any further (Hosking & Zajicek, 2008). Increasing the amount or the activity of endocannabinoids to help with analgesia would seem like a promising target in patients suffering from chronic or inflammatory pain; however, as they are only synthesised on demand and are rapidly degraded in the body, their effects are short-lived and a systemic effect is not seen (Woodhams et al., 2015; Zou & Kumar, 2018).

Inflammation is also regulated by the endocannabinoid system. Endocannabinoids bind to the CB2 receptors on the immune cells leading to reduced levels of proinflammatory cytokines, reducing neuronal activity and antinociception in inflammatory pain states (Shang & Tang, 2017). The levels of the cytokines are tightly regulated by the endocannabinoid system throughout the whole inflammatory response (Donvito et al., 2018).

Investigating other exogenous cannabinoids that can interact with these receptors and have a more systemic response could prove valuable. Exogenous cannabinoids are not as quickly metabolised as endogenous cannabinoids, and the effects are longer-lasting when compared to endogenous cannabinoids (Hosking & Zajicek, 2008). THC and CBD can bind to the cannabinoid receptors mimicking the effects of endogenous cannabinoids, AEA and 2-AG (Howlett et al., 2002; Lotsch et al., 2018; Mackie, 2006). They also tend to have a more systemic action compared to the highly specific and on-demand synthesis of endogenous cannabinoids, as they are freely circulating and can bind to any unoccupied cannabinoid receptors (Pertwee, 2008). THC has a high affinity for both CB1 and CB2 receptors, while CBD has a very low affinity for them (Pertwee, 2008), though there is evidence that CBD can act as an antagonist for both CB1 and CB2 receptors, in the presence of THC (Vučković et al., 2018). Through this mechanism, CBD is thought to modulate the psychoactive effects of THC when taken together (McPartland & Russo, 2001). CBD action is proposed to be mediated mainly through TRPV1 receptors (Muller et al., 2019).

1.4.7 Clinical and pre-clinical studies and their limitations

As previously stated, the most common reason given for the medicinal use of cannabis is to treat chronic pain, and there are a variety of pre-clinical and clinical trials that validate this

(Vučković et al., 2018). Current knowledge of cannabis for medical use indicates that it is safe to use and has minimal undesirable side effects (Ware et al., 2015). When looking at neuropathic pain in particular, clinical evidence in humans suggests that there is a perceived pain reduction when cannabinoids are taken (Banerjee & McCormack, 2019; Rabgay et al., 2019; Rog et al., 2007; Ware et al., 2015; Wilsey et al., 2013), with most patients noting an improvement in pain scores (Rog et al., 2007). A common finding in many of these studies is that the use of THC for chronic pain leads to a reduction in unpleasantness rather than true analgesia (Lotsch et al., 2018).

While it is possible that each neuropathic pain aetiology may need to be investigated separately with the cannabinoid composition, dosage and administration route all tailored to each disease, a lack of defined and systematic procedure in cannabinoid clinical studies have complicated its mainstream clinical use (Rabgay et al., 2019). For example, in one clinical trial, patients would self-titrate the number of sprays they felt they needed and there was no reporting on the purity or concentrations of the cannabinoids used (Rog et al., 2007). This is an issue particularly when a whole extract is used as there is a great deal of variation in the levels of cannabinoids within different varieties and strains of the plants. The downside to many clinical studies is that they rely on patient self-reporting, and are often uncontrolled open-label trials (Rog et al., 2007). This introduces bias as patients were aware of what they are taking and are not compared to a control placebo group. Self-reporting of pain can also be dubious, change day to day, and be influenced by mood or emotional well-being. In many of the studies, there was evidence that the whole cannabis had a greater effect than the single cannabis isolates (Russo, 2011).

Several pre-clinical trials have used cannabis isolates to ameliorate neuropathic pain symptoms. As is seen with the clinical trials, the pre-clinical trials show considerable variation in the route of administration, type of cannabinoid given and effective dose (**Table 1-1**, **Table 1-2**, **Table 1-3**, **Table 1-4** & **Table 1-5**). Further complicating these pre-clinical trials, many of the studies use an intraperitoneal route for administration. Considering the route of administration is very important, as most patients will not be injecting the cannabis products, and the drug will undergo first-pass metabolism when taken orally. This leads to variations in the action and bioavailability of the drug. This is where robust scientific research with known

and reproducible cannabis constituents, regulated doses, and administration routes needs to be conducted.

***Table 1-1**. Rodent models of neuropathic pain show the efficacy of intraperitoneally injected CBD to ameliorate some of the pain symptoms.*

CBD via intraperitoneal injection				
Effective dose	**Frequency**	**Vehicle**	**Disease**	**Reference**
20mg/kg	Every second day for 7 days	Ethyl alcohol, Cremophore and saline (1:1:18)	Chemo-induced neuropathic pain	(King et al., 2017)
5mg/kg	1 x day for 10 days	Ethyl alcohol, Cremophore and saline (1:1:18)	Diabetic-induced neuropathic pain	(Lehmann et al., 2016)
5mg/kg	1 x day for 10 days	Ethyl alcohol, Cremophore and saline (1:1:18)	Arthritic induced pain	(Malfait et al., 2000)
2mg/kg	1 dose	Ethyl alcohol, Cremophore and saline (1:1:18)	Cisplatin-induced neuropathic pain	(Harris et al., 2016)
0.5 – 2mg/kg	1 x day for 6 days	Ethyl alcohol, Cremophore and saline (1:1:18)	Cisplatin-induced neuropathic pain	(Harris et al., 2016)

***Table 1-2**. Rodent models of neuropathic pain show the efficacy of intraperitoneally injected THC to ameliorate some of the pain symptoms.*

THC via intraperitoneal injection				
Effective dose	**Frequency**	**Vehicle**	**Disease**	**Reference**
10mg/kg	Every second day for 7 days	Ethyl alcohol, Cremophore and saline (1:1:18)	Chemo-induced neuropathic pain	(King et al., 2017)
2mg/kg	1 dose	Ethyl alcohol, Cremophore and saline (1:1:18)	Cisplatin-induced neuropathic pain	(Harris et al., 2016)
0.5 – 2mg/kg	1 x day or 6 days	Ethyl alcohol, Cremophore and saline (1:1:18)	Cisplatin-induced neuropathic pain	(Harris et al., 2016)
2.5mg/kg	1 x day for 4 days	DMSO 8%, Tween 20 1%, saline	Ethanol-induced locomotor sensitisation	(Filev et al., 2017)

***Table 1-3**. Rodent models of neuropathic pain show the efficacy of intraperitoneally injected CBD: THC mix to ameliorate some of the pain symptoms.*

CBD: THC via intraperitoneal injection				
Effective dose	**Frequency**	**Vehicle**	**Disease**	**Reference**
0.16 +0.16mg/kg	Every second day for 7 days	Ethyl alcohol, Cremophore and saline (1:1:18)	Chemo-induced neuropathic pain	(King et al., 2017)
2.5 + 2.5mg/kg	1 x day for 4 days	DMSO 8%, Tween 20 1%, saline	Ethanol-induced locomotor sensitisation	(Filev et al., 2017)

***Table 1-4**. Rodent models of neuropathic pain show the efficacy of orally administered CBD to ameliorate some of the pain symptoms.*

CBD via oral gavage				
Effective dose	**Frequency**	**Vehicle**	**Disease**	**Reference**
30mg/kg	1 x day for 8 days	Ethyl alcohol, Cremophore and saline (1:1:18)	STZ diabetic neuropathic pain	(Comelli et al., 2009)
25mg/kg	1 x day for 10 days	Olive oil	Arthritis	(Malfait et al., 2000)

***Table 1-5**. Rodent models of neuropathic pain show the efficacy of orally administered THC to ameliorate some of the pain symptoms.*

THC via oral gavage				
Effective dose	**Frequency**	**Vehicle**	**Disease**	**Reference**
150mg/kg	1x day for 6 days	Corn oil	STZ diabetic neuropathic pain	(Li et al., 2001)
17.8 mg/kg	1 dose	15% DMSO, 5% tween80 and saline	CCI model	(Mitchell et al., 2021)

1.5 Objectives of this Research

This study is set out to determine the efficacy of specific cannabis extracts to provide analgesia in pre-clinical models of neuropathic pain.

There were three main aims of this work:

1) A dose-response trial to identify relevant biomarkers that could be used to determine an efficacious orally administered dose of a pure CBD isolate.
2) To determine the efficacy of CBD and other specific cannabis extracts to lead to analgesia in a pre-clinical neuropathic pain model of CMT2A mice by measuring changes to thermal hyperalgesia and mechanical allodynia responses with treatment.
3) To characterise a B6:D2 male mouse model of a single high dose of STZ-induced diabetic neuropathy and neuropathic pain that could be used to further test the efficacy of CBD and other specific cannabis extracts.

2 Dose-Response

2.1 Introduction

Cannabis has long been used by humans for recreational purposes and is most commonly taken by smoke inhalation or orally (Grotenhermen, 2003; Russell et al., 2018). When the cannabis is inhaled the active compounds enter the bloodstream without first being metabolised, and take effect quickly (Grotenhermen, 2003; Russell et al., 2018). Conversely, taking cannabis products orally results in the cannabinoids being metabolized and has a longer-lasting effect when compared to inhalation (Grotenhermen, 2003). Oral administration of cannabinoids is a clinically relevant way to ensure a controlled and repeatable dose. Given that oral administration is also the preferred route for prescription or over-the-counter drugs in the human population, an orally administered cannabinoids dose-response trial was performed in mice to determine a safe and potentially effective therapeutic dose.

Published pre-clinical and clinical studies using whole extract or cannabis isolates display a wide range in the “effective dose”. This is due to variation in the type of cannabinoid given, the administration route, and different strains of the cannabis plant. To determine the most effective and clinically relevant dose of a particular cannabinoid, highly refined and characterised cannabis isolates and a high CBD whole extract were obtained from Cannasouth Bioscience Limited. These isolates were prepared under sterile conditions, with a high purity and known concentrations.

Evidence from published pre-clinical trials using mice treated by oral gavage, with CBD and tetrahydrocannabinol (THC) by oral gavage was collated to guide what might be safe and effective starting doses of the cannabinoids (**Table 2-1**). It was noted that oral doses of more than 50mg/kg CBD in sesame oil repeated for 10 days showed hepatotoxicity and a single dose of 2460mg/kg CBD also became toxic (Ewing et al., 2019). THC LD50 for mice was found to be 42.5mg/kg by IV and 482mg/kg when given orally (Beaulieu, 2005). This analysis guided a safe range of starting doses to treat neuropathic pain symptoms.

***Table 2-1**. Effective dosages of cannabinoids for treating various diseases in mice*

CBD				
Effective dose	**Frequency**	**Vehicle**	**Disease**	**Reference**
30mg/kg	1 x day for 8 days	Ethyl alcohol, Cremophore and saline (1:1:18)	STZ diabetic neuropathic pain	(Comelli et al., 2009)
25mg/kg	1 x day for 10 days	Olive oil	Arthritis	(Malfait et al., 2000)
120mg/kg	1 dose	Ethyl alcohol, Cremophore and saline (1:1:18)	Obsessive-compulsive disorder	(Deiana et al., 2012)
THC				
150mg/kg	1x day for 6 days	Corn oil	STZ diabetic neuropathic pain	(Li et al., 2001)

2.1.1 Pharmacokinetics and pharmacodynamics of cannabinoids in mice

The efficacy of a drug can vary due to many different factors; bioavailability, plasma drug concentration, time taken to reach maximum concentration (t_{max}), elimination rate and duration of action. There are also genetic factors that determine how well a certain individual metabolises a drug. Together, these factors determine the efficacy and toxicity of a drug. The reported pharmacokinetics of cannabis products vary greatly due to both the route of administration and the vehicle it is administered in. Additionally, while there is limited information available on the major cannabinoids: CBD and THC; many of the other cannabinoids do not have well-established pharmacokinetics or pharmacodynamics. This can be problematic when trying to set parameters for assessing cannabinoids dosing, particularly around timing of testing or tissue harvesting. **Table 2-2** shows the t_{max} values of various cannabinoids circulating in the blood when given to rodents by oral gavage. Some of these as indicated were given in a lipid-based vehicle.

Table 2-2. *t_{max} of circulating cannabinoids in the blood of rodents that were administered by oral gavage. Some of these were administered in a lipid vehicle as indicated.*

Product	Dose	Location	t_{max}	Reference
CBD	10mg/kg (rats)	Serum	2 hours	(Hložek et al., 2017)
CBD	120mg/kg (mice)	Plasma	1 hour	(Deiana et al., 2012)
CBD	20mg/kg (mice)	Plasma	2 hours	(Xu et al., 2019)
CBD (in lipids)	12mg/kg (rats)	Plasma	3 hours	(Zgair et al., 2017)
CBDV	60mg/kg (mice)	Plasma	30 mins	(Deiana et al., 2012)
THC	400mg/kg (mice)	Plasma	1 hour	(Liao et al., 2014)
THC (in lipids)	12mg/kg (rats)	Plasma	3 hours	(Zgair et al., 2017)
THC	10mg/kg (rats)	Serum	2 hours	(Hložek et al., 2017)
THCV	30mg/kg (mice)	Plasma	30 mins	(Deiana et al., 2012)
CBG	120mg/kg (mice)	Plasma	2 hours	(Deiana et al., 2012)

As previously mentioned, the use of cannabinoids in a clinical setting will most likely entail the use of oral administration. One of the biggest problems with the oral administration of cannabinoids so far is the limited bioavailability (Deiana et al., 2012; Mechoulam & Hanuš, 2002; Millar et al., 2018). This is due to the first-pass metabolism where most of the cannabis metabolites are excreted by the kidneys before they can have an effect (Huestis, 2007). This issue can be somewhat overcome by the administration of the cannabinoids with lipids (Zgair et al., 2017; Zgair et al., 2016). The use of a lipid or oil-based vehicle for oral administration of cannabinoids has been shown to have a longer onset of action leading to a delayed t_{max} in the body (McClements, 2020; Zgair et al., 2017). This same trend was also seen when the cannabinoids were administered by intraperitoneal injection (I.P injection), along with an prolonged time until elimination of the cannabinoids, when compared to a non-lipid carrier (Anderson et al., 2019). Based on these findings, the cannabinoids were suspended in an olive oil vehicle as it is highly palatable to mice and to make use of the longer therapeutic window. Any other cannabis isolates used were then based on the effective therapeutic dose of the CBD.

2.1.2 Tissue collection and biomarker expression

2.1.2.1 Dorsal root ganglions

Dorsal root ganglia (DRGs) are composed of a cluster of sensory nerve cell bodies located adjacent to the spinal cord in each intervertebral foramina of the spinal column (Nascimento et al., 2018). The axons of these neurons contain a mix of nerve fiber types, including low-threshold mechanosensory fibers, higher-threshold Aβ nociceptors, and Aδ fibers (Ahimsadasan et al., 2022). DRGs have been well researched for their role in the development and maintenance of neuropathic pain (Latremoliere & Woolf, 2009; Woolf, 2011). Because the DRGs house the cell bodies, where the majority of the proteins and cell components are produced (Waymire, 2018), any changes to gene transcription will be seen there (Martin et al., 2019). Gene expression within a cell can be altered due to environment, internal changes in chemistry, or administration of drugs (Singh et al., 2018). Therefore, transcriptional changes in the cell bodies due to the administration of cannabinoids can be quantified by extracting mRNA from the DRGs and measuring changes in the gene expression levels using qPCR.

Following dose escalation in mice, gene expression of cyclooxygenase enzymes (COX 1 and COX 2) were used as biomarkers to determine what doses induce a biological effect and develop a CBD dose-response profile. COX 1 and COX 2 were chosen as biomarkers as they play important roles in pain and inflammation pathways (Vane et al., 1998). In response to pain and inflammation, COX 1 and COX 2 genes are upregulated leading to increased levels of COX 1 and COX 2 mRNA (Adelizzi, 1999). Furthermore, COX 2 expression has been widely used as a first indicator of anti-inflammatory actions of a drug (Vane et al., 1998). As such, primers were designed and used in qPCR analysis to measure any changes to COX 1 and COX 2 mRNA levels in mice administered the specific cannabinoids.

Full transcriptome analysis on mRNA from the dose response trial was also completed to give a more unbiased approach in determining if there were improved biomarkers that could indicate efficacy of CBD to improve analgesia in the mouse model.

2.2 Materials and Methods

2.2.1 Animal work, tissue harvesting and preparation

2.2.1.1 Ethics and animal welfare

Ethics was approved by the University of Waikato Ethics committee, ***approval number 1093*** (Coversheet is found in the Dose Response Appendix A.1.). All relevant standard operating procedures (SOPs) were followed and appropriate training was received before carrying out any animal work. The relevant SOPs are listed in **Table 2-3**.

Table 2-3*. List of relevant standard operating procedures for rodents*

SOP #	**Name**
5	Housing and Care of Lab/Domestic and Wild Rodents
9	Euthanasia of Rodents by CO2 Asphyxiation
10	Administration of a Substance by Intraperitoneal Injection in Rats and Mice
15	Euthanasia of Rodents by CO2 Anaesthesia and Decapitation
22	Administration of a Substance by Oral Gavage in Mice
X	Rodent Genotyping by Ear Punch

Animals were housed in the Ruakura Small Animal Centre (SAC) in standard Thoren mouse cages (Model #19, Mouse cage III), with no more than 5 mice per cage. The mice were housed in temperature-controlled rooms (23-24 °C) with controlled lighting (12 hours light and 12 hours dark). Mice had access to standard rodent feed and water at all times. Cages were environmentally enriched with nesting material (shredded paper), an in-cage shelter, and a hanging ring on the cage to allow climbing.

2.2.1.2 Oral administration of Cannabinoids

Previous data from the literature (Comelli et al., 2009; Deiana et al., 2012; Ewing et al., 2019; Malfait et al., 2000), collated in **Table 2-1** and **Table 2-2**, show a range of effective doses and pharmacokinetics of CBD. Based on this data, a dosing range of 0 mg/kg (control group of olive oil vehicle only), 25 mg/kg, 50 mg/kg, 100 mg/kg and 150 mg/kg of CBD in olive oil was used in experiments. For the dose response work, CBD was administered once daily for 4 days followed by tissue harvest 1 to 2 hours after the final dose (dosing and harvesting schedule is found in the Dose Response Appendix A.2) and then analysis. Five cohorts of mice were used for these experiments: (i) vehicle control, *n* = 6; (ii) dose 1, 25 mg/kg CBD, *n* = 6; (iii) dose 2, 50 mg/kg CBD, *n* = 6; (iv) dose 3, 100 mg/kg CBD, *n* = 6; and (v) dose 4, 150 mg/kg CBD, *n* = 6. Mice (strain B6:D2, wildtype) were randomly assigned to each group, weighed, and this information was recorded along with their identification (ear punches and/or tail markings for short trials). This allowed administration of the appropriate volume of cannabinoid to ensure the appropriate dose, in mg/kg. All cannabis isolates were provided by Cannasouth Bioscience Limited and were suspended in olive oil (sigma 75343-1L, lot # BCBZ4118). Certificate of analysis for the extracts are listed in the Dose Response Appendix, A.2)

For dosing, mice were restrained using the scruff method as this is safe and effective for both the mouse and the handler (Machholz et al., 2012). Once restrained, the cannabinoid was administered by gently placing the tip of a 200 µL micropipette containing the correct amount of the cannabinoid in the mouse's mouth and slowly expelling the contents. The taste preference in mice for olive oil meant that none of the dose was lost and avoided the need for oral administration by gavage. Following administration, the mouse was released and observed for a short period before placing them back into the home cage.

2.2.1.3 Tissue harvesting

To determine the gene expression changes induced by cannabinoids administration to mice, DRGs and spinal cords were harvested on day four of administration of the CBD. This occurred between one and two hours after the final dose of the cannabinoid when the CBD levels reached a maximum blood plasma level (**Table 2-2**). Actual timing of euthanasia of each mouse is set out in the Dose Response Appendix, A.3. The mice were euthanised by CO_2

asphyxiation followed by decapitation as a secondary euthanasia method, as per SOPs and ethics approval (Dose Response Appendix A.1). Following euthanasia, removal of DRGs and spinal cords occurred.

2.2.1.3.1 Harvesting of dorsal root ganglia and spinal cords

The methods of DRGs and spinal cord harvesting were based on those published by Richner et al. (2017); Sleigh et al. (2016); Sleigh et al. (2020). This method allows quick and clean removal of both the spinal cord and the identification of DRGs with minimal tissue damage, unlike the laminectomy method where the spinal column is cut section by section and some damage can be caused to the spinal cord (Sleigh et al., 2016). The euthanised mouse was pinned on a dissection board in a prone position and the fur was wet down with 70% ethanol to reduce contamination. The skin of the neck was pinched up with forceps and cut along the spine in a distal direction towards the tail. The skin was then pulled back to allow visualisation of the spinal column, which was then removed by cutting along the ribs past the pelvic bone on both sides and freeing it from the body. The spinal column was then completely removed by cutting it across below the pelvic bone. The spinal column was trimmed slightly at both caudal and rostral ends to avoid the most S-shaped parts and to ensure the spinal cord was visible at each end. A 5 mL syringe with an adapted unfiltered 200 μL pipette tip on the end was filled with cold phosphate buffered saline (PBS). (The adaptation of the pipette tip involved cutting it with sharp scissors across the top to allow it to fit onto the lure of the 5 mL syringe). The spinal column was held straight in one hand and the syringe was used to remove the spinal cord by hydraulic extrusion. This involved placing the end of the pipette tip into the most distal end of the spinal cord. Steady pressure was applied to the syringe plunger and the PBS was flushed into the spinal column, pushing the spinal cord out in one piece. The spinal cord was then placed into a labelled microcentrifuge tube and frozen at -80 °C. The excess tissue and muscle were then removed from the spinal column, ensuring that the caudal ribs were kept intact to allow identification of the DRGs.

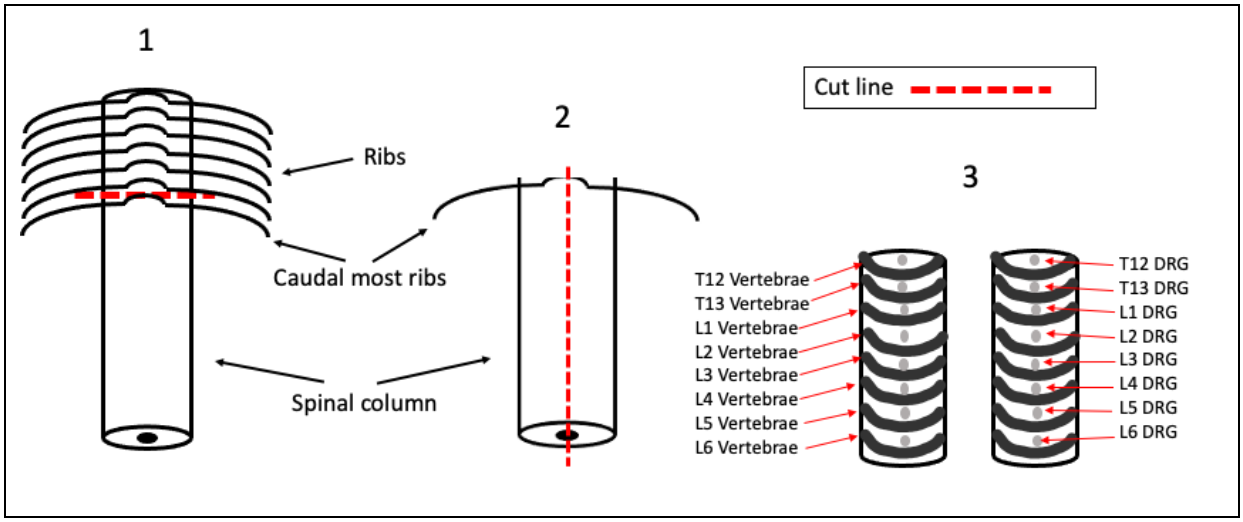

Figure 2-1*.Diagram of how the spinal column was cut to identify and extract dorsal root ganglia (DRGs).* ***1****) Identify the caudal most ribs and using a scalpel blade cut across the spinal column just above these****. 2)*** *Hold the spinal column with forceps and cut the spine open in two pieces.* ***3)*** *Identify the specific DRGs, the most proximal to the ribs will be the T12 DRG. Thoracic vertebrae and DRGs labelled T, lumbar vertebrae and DRGs labelled L.*

The spinal column was cut proximal to the most caudal ribs (**Figure 2-1**– Picture 1) and this section was held firmly with forceps. A scalpel blade was used to cut open the spinal column along the midline (**Figure 2-1**– Picture 2). Both halves were pinned to the board ensuring that the caudal ribs were noted for correct identification of the DGRs (**Figure 2-1**– Picture 3). Using a dissection microscope, the required DRGs were identified; thoracic number 13 (T13) DRGs are below the caudal ribs, and the lumbar number one (L1) to lumbar five or six (L5/6) DRGs follow (Sleigh et al., 2016). The caudal ribs were kept in place to allow for quick and easy identification and removal of the specific DRGs (L3, L4, and L5 DRGs). Under the microscope, the meninges were peeled back from the spinal column allowing easy access to the DRGs which were gently pulled out using forceps and placed directly into labelled microcentrifuge tubes containing cold 300 µL TRIzol™ LS Reagent (ThermoFisher #10296010) and 100 µL RNase free water (Fisher Bioreagents BP561-1 Lot # 194324). The samples were kept on ice during the dissection period to avoid degradation of the mRNA. Following dissection, the DRGs in TRIzol™ were homogenized using a tissue homogenizer (Pro Scientific, # PRO-PK 02200P) with a 5 mm probe (Pro Scientific # 02-05075) and stored at -20 °C until required.

2.2.1.4 mRNA extraction

Samples were removed from -20 °C storage, thawed to room temperature, vortexed briefly and incubated at room temperature for five minutes. After incubation, 80 µL of chloroform was added and the samples were thoroughly mixed and incubated for a further three minutes

at room temperature. The samples were then centrifuged (Eppendorf Centrifuge 5414R) for 15 min at 12,000 x *g* at 4 °C to separate the aqueous, interphase, and phenol phases. The aqueous phase (top phase) containing the RNA was carefully removed and pipetted into a new microcentrifuge tube.

The RNA was then precipitated by adding 200 µL of isopropanol and incubating for 10 min at room temperature. The RNA precipitate was then collected at the bottom of the tube by centrifugation for 10 min at 12,000 x *g* at 4 °C. The supernatant was discarded without disturbing the RNA pellet and the RNA was washed with 400 µL of 75% ethanol by briefly vortexing followed by centrifugation at 7500 x *g* for five minutes at 4 °C. The supernatant was discarded, and the RNA was left to dry for 5 - 10 min. The RNA pellet was resuspended in 25 µL of RNAse-free water (Fisher Bioreagents BP561-1 Lot # 194324) and then incubated in a heating block for 10 min at 55 °C while gently shaking. The concentration and quality of the RNA samples was measured using a Nanodrop (Nanodrop 2000, Invitrogen). This data is found in the Dose Response Appendix, A.4. The RNA was then used to synthesise complementary DNA (cDNA) or stored at -80 °C until needed.

2.2.1.5 cDNA synthesis

The total RNA extracted from the DRGs and spinal cords were used to reverse transcribe (RT) cDNA for real-time polymerase chain reactions (qPCRs). RNA concentration and quality information was used to determine the quantity of each sample to be used in RT reactions (Dose Response Appendix, A.4).

For cDNA synthesis iScript Reverse Transcription Supermix for RT-qPCR (BioRad #1708841) was used according to the manufacturer's instructions. This involved adding 120 ng of RNA to each PCR tube along with 4 µL of iScript RT Supermix and the appropriate amount of RNAse-free water (Fisher Bioreagents BP561-1 Lot # 194324) to make a 20 µL reaction. All reactions were assembled on ice. The samples were placed in the thermal cycler (Biorad T-100) with the protocol in **Table 2-4**.

Table 2-4. *Protocol used for synthesising cDNA from RNA extracted from spinal cords and sciatic nerves.*

STEP	TIME AND TEMPERATURE
PRIMING	5 mins at 25°C
REVERSE TRANSCRIPTION	20 mins at 46°C
REVERSE TRANSCRIPTION INACTIVATION	1 min at 95°C

The resulting cDNA was stored at -20°C until needed.

2.2.2 COX 1 and COX 2 as biomarkers

2.2.2.1 Primer design

This methodology was used to determine changes in COX 1 and COX 2 gene expression in DRGs due to administration of CBD. Primers for the mouse COX 1 and 2 and GAPDH genes were designed using National Centre for Biotechnology Information Gene (NCBI gene) (Sayers et al., 2022), using Gene ID: 19224 for *cox-1,* Gene ID: 19225 for *cox-2* and Gene ID:24383 for *gapdh*. Complementarity and hairpins were checked using Net Primer (Premier Biosoft) (*NetPrimer*, 2022). The resulting primer sequences were input into UCSC in silico PCR (https://genome.ucsc.edu/cgi-bin/hgPcr) to give product sizes. GAPDH primer sequences (to be used as an internal reference gene) and COX 1 and COX 2 primers were obtained from Sigma Aldrich. The COX 1 and COX 2 primers, along with primers for GAPDH are listed in

Table **2-5**.

***Table 2-5**. Table of primers used.*

GENE TARGET	FORWARD PRIMER (5' TO 3')	REVERSE PRIMER (5' TO 3')	SIZE (BP)
COX 1	GGGAATTTGTGAATGCCACC	GGGATAAGGTTGGACCGCA	241
GAPDH1	CGACTTCAACAGCAACTCCCACTCTTCC	TGGGTGGTCCAGGGTTTCTTACTCCTT	175
COX 2	GACGGTGCTTCTAAGTGATGGA	TTGGCATGGTAAGATGTCAGC	353

2.2.2.1.1 Standard PCR

The protocols and designed primers were tested using cDNA synthesised from spinal cord tissue. This was to ensure the primers were specific and the PCR product was of the expected size.

PCR was performed in PCR tubes with: 1.2µL of 10 x PCR buffer with $(NH4)_2SO_4$, (Invitrogen #EP0402); 0.96 µL of 2.5 µM dNTPs (Invitrogen, #R1122); 0.96 µL of 25 µM $MgCl_2$ (Invitrogen, #EP0402); forward and reverse primers at 20 µM; TAQ DNA recombinant polymerase (Invitrogen #EP0402, 5 U/µL); and cDNA and distilled water to make the volume up to 12 µL. The actual PCR cycling protocol depended on the primers used and is set out in **Table 2-6**. A gradient cycle was used to determine the optimum annealing temperature for the primer sets.

PCR products were visualised by agarose gel electrophoresis, using a 1.5% agarose gel (UltraPure™ Agarose Invitrogen #16500100) in TAE buffer (50 X buffer: 242 g Tris, 57.1 mL glacial acetic acid, 100 mL 0.5 M EDTA, pH 8) for 35 min at 100 V.

***Table 2-6**. PCR protocol for each primer sets, COX 1, COX 2, and GAPDH with gradient annealing temperature*

STEP	COX 1	COX 2	GAPDH1
1	95 °C for 5 min	95 °C for 5 min	95 °C for 5 min
2 – DENATURATION	94 °C for 30 s	94 °C for 30 s	94 °C for 30 s
3 – ANNEALING	64-70 °C for 30 s	62-70 °C for 30 s	66-72 °C for 30 s
4 – EXTENSION	72 °C for 30 s	72 °C for 30 s	72 °C for 30 s
CYCLES	34	34	34
5 – FINAL	72 °C for 6 min	72 °C for 6 min	72 °C for 6 min

2.2.2.1.2 Primer Efficiency

Once the primers had been optimised, primer efficiency was calculated using a series dilution and plotting a standard curve in Excel to get a line equation and R^2 value. This was carried out in the MIC qPCR cycler (BioMolecular systems) using the optimized annealing temperature of 65 °C found from the standard PCR (**Table 2-6**) under conditions found in **Table 2-7**.

Table 2-7. *qPCR cycling conditions used to determine efficiency of COX 1, COX 2 and GAPDH primer sets*

	ENZYME ACTIVATION	**95 °C FOR 5 MIN**
40 CYCLES OF:	Denaturation	95 °C for 5 s
	Annealing/Extension	65 °C for 30 s on Green
MELT ON GREEN	Melt from 60 °C to 95 °C at 0.3 °C/s	

2.2.2.2 Real-time PCR

SolisFAST® SolisGreen® qPCR Mix (SolisBiodyne, #28-46-00001) was used following the manufacturer's recommendations. Each 12 µL reaction contained: 2.4 µL of 5x SolisFAST® SolisGreen® qPCR Mix; 0.6 µL of forward primer at 10 µM (for COX 1, M2 COX 2, or GAPDH); 0.6 µL of reverse primer at 10 µM (for COX 1, COX 2, or GAPDH); 6.4 µL of RNAse free water (Fisher Bioreagents BP561-1); and 2 µL of previously synthesised cDNA from the mouse DRGs. This was mixed and briefly centrifuged. Samples were placed into the MIC qPCR cycler (BioMolecular systems) and the cycling conditions used are set out in **Table 2-8**. Realtime PCRs for each sample were performed in duplicate. As with the previous section, 2.2.1.5 cDNA Synthesis, 120 ng of RNA was used to create cDNA. In this case, the RNA from DRGs of wildtype mice dosed with CBD were used.

***Table 2-8**. Cycling protocol for qPCR*

	ENZYME ACTIVATION	**95 °C FOR 2 MIN**
40 CYCLES OF:	Denaturation	95 °C for 5 s
	Annealing/Extension	65 °C for 20 s on Green
MELT ON GREEN	Melt from 60 °C to 95 °C at 0.3 °C/s	

2.2.2.3 Data analysis of qPCR

The delta-delta Ct ($\Delta\Delta$Ct) method is used to calculate the change to relative fold gene expression when doing real-time PCR (Livak & Schmittgen, 2001). It uses the cycle threshold (Ct) where the signal exceeds the base level of fluorescence (Livak & Schmittgen, 2001). This method was used to analyse the qPCR results with GAPDH expression used as an internal reference for normalisation. This is done following the methods set out by Livak and Schmittgen (2001). This involved finding the average Ct value for each sample by averaging the replicates of each sample. ΔCt was calculated by comparing the gene of interest Ct to the reference gene Ct.

$$\Delta Ct = Ct(gene\ of\ interest) - Ct(reference\ gene)$$

The control average for each group (control, 25 mg/kg CBD, 50 mg/kg CBD, 100 mg/kg CBD and 150 mg/kg CBD) was calculated and $\Delta\Delta$Ct was calculated.

$$\Delta\Delta Ct = \Delta Ct(sample) - \Delta Ct(Control\ average)$$

The fold gene expression was then able to be calculated.

$$Fold\ gene\ expression = 2^{-(\Delta\Delta Ct)}$$

This fold expression was graphed to visualise the changes in gene expression when compared to the control samples.

2.2.3 Transcriptomics

Transcriptomics analysis of mRNA from the CBD dose-response trial was sent to GENEWIZ (GENEWIZ Genomics Centre, Suzhou, China) to be analysed using Illumina Next Generation sequencing to determine genes that may be up or down-regulated due to the administration of CBD.

The quality and quantity of the RNA previously extracted, as per section 2.2.1.4, was measured on the Nanodrop. The samples that met the standards of: RNA concentration of > 2 μg, ≥ 50 ng/μL, and a 260/280 ratio of 1.8 – 2.2, were selected and stabilised in GENEWIZ RNA stabilization tubes (GTR5025-GW) to be shipped to GENEWIZ (GENEWIZ Genomics Centre, Suzhou, China). The tubes allow shipping at room temperature without the need for keeping the RNA frozen. At least 20 μL of RNA in RNase-free water (Fisher Bioreagents BP561-1) was added to the bottom of the GENEWIZ RNA stabilization tube which has a stabilization matrix coating on the bottom of the tube. The RNA was left to incubate for five min at room temperature before pipetting up and down 10 times to solubilize and mix the RNA into the matrix. The tubes containing the RNA were placed into a speed vac (Savant SC110) with the lids off to dry out. The temperature was set to ambient temperature and the tubes were spun and dried for approximately 2 h, or until they were completely dry as per a visual inspection. The tubes were capped and then sent to GENEWIZ for sequencing.

A total of 15 tubes were sent for analysis: three from the control group, and three from each dose group (25 mg/kg, 50 mg/kg, 100 mg/kg, and 150 mg/kg of CBD, respectively). The process undertaken by GENEWIZ (GENEWIZ Genomics Centre, Suzhou, China), included RNA extraction from stabilisation tubes, quality assessment of the RNA, sequencing library preparation, library validation and then Illumina sequencing. The quality of the resulting data was then analysed. This included a quality score along the reads, ATGC content distribution, and the content of clean raw reads. Alignment to a reference genome (Mus musculus Ensembl GRCm38.100) was also provided. The returned data included lists of genes that were up-or down-regulated due to the administration of the CBD, with separate lists for each dose. This data was used to choose genes that were potentially up or down regulated by different CBD doses to use for qPCR testing moving forward. A flow chart of the process and data generated for GENEWIZ is found in the Dose Response Appendix A.6.

2.2.4 Real-time PCR with mice using genes from GENEWIZ

A set of six candidate genes that were upregulated across the 25 mg/kg, 50 mg/kg and 100 mg/kg dose groups from the transcriptomics were selected for validation using a different cohort of CBD-treated mice, and confirm their usefulness as biomarkers for CBD dose. The

genes and functions were searched for using the QuickGo Gene ontology program (Binns et al., 2009) and Mouse Genome Informatics International Database (MGI) (Bult et al., 2019).

Primers were designed using NCBI primer blast (https://www.ncbi.nlm.nih.gov/tools/primer-blast/) (NCBI, 2022) and the primers were checked for hairpins and self-dimerization using Net Primer (http://www.premierbiosoft.com/NetPrimer/AnalyzePrimer.jsp) (*NetPrimer*, 2022). Of the six candidate genes, four of these had primers that were deemed suitable after these checks and were then ordered from Sigma-Aldrich.

The list of genes used are:

RPS2-p6 – Ribosomal protein pseudogene. MGI I.D. 3644876 (Bult et al., 2019).

Clec3b – C type lectin, involved in the skeletal system development and bone mineralisation MGI I.D. 104540 (Bult et al., 2019).

RPS3a3 – Ribosomal protein pseudogene MGI I.D. 3643406 (Bult et al., 2019).

Dio2 - Type 2 iodothyronine, converts T4 into T3 MGI 1338833 (Bult et al., 2019). Primers for this target were designed, but no product was amplified so this set of primers was not used past optimisation stages.

The optimisation was carried out using mRNA extracted from spinal cords as per previous methods in section 2.2.2. GAPDH was used as a reference gene. Either one or two primer sets were designed per gene. These are listed in **Table 2-9**.

***Table 2-9**. List of primers designed for qPCR with mouse DRG cDNAs using upregulated candidate genes identified from GENEWIZ transcriptomics analysis for potential biomarkers of the efficacy of CBD.*

Gene	Primer Name	Gene I.D. (NCBI)		Sequence (5' to 3')	Product size (bp)
Rps2-p6	Rps2-p6A	1000043752	Forward	TCAGCTTTACCTCCACGAGC	
			Reverse	ACCCTAAGGAGTGGTACAGGG	294
	Rps2-p6B	1000043752	Forward	TCCCCAATAGCGACCAAAGC	
			Reverse	CCGCTTTCAAATTCAAGCCAGA	448
Rps3a3	Rps3a3-1	668144	Forward	AACCGCCAGTCCAAGAATCA	
			Reverse	AACCCATCAGTCCCTGGAAGC	183
	Rps3a3-2	668144	Forward	TGCTAAGGTTGAGCGAGCTG	
			Reverse	ATCAGTCCCTGGAAGCTATCTG	207
Clec3b	Clec3b-1	21922	Forward	GGACAGAGGAAGGAACACCAA	
			Reverse	ACAGCTATCCTGCACTTACCAG	248
	Clec3b-2	21922	Forward	GAGAAACCAGGAACAGGCAAC	
			Reverse	CTCCAAACAGCTATCCTGCACT	309
Dio2	Dio2	13371	Forward	CTTTCGGTGAGGCAATGGGA	
			Reverse	ACAGCAGCAGTGTGTTAGTG	772
GAPDH	GAPDH1	14433	Forward	CGACTTCAACAGCAACTCCCACTCTTCC	
			Reverse	TGGGTGGTCCAGGGTTTCTTACTCCTT	175

Optimisation of annealing temperature was carried out using a gradient PCR with the conditions as set out in **Table 2-10**. The resulting products were run out on a 1.5% agarose gel to visualise the results and determine the most effective annealing temperature for the primer sets.

***Table 2-10**. PCR conditions for determining the optimal annealing temperature of the primers for qPCR to determine changes to gene expression*

STEP	CONDITIONS	
1	95 °C for 3 min	
2	95 °C for 30 sec	
3	A gradient of 60 °C – 66 °C for 30 s	
4	72 °C for 30 s	Repeat steps 2 – 4 for 35 cycles
5	72 °C for 5 min	

Once the primers had been optimised a second dose response trial was set up with mice, using three mice per dose. These were; vehicle control of olive oil only, 25 mg/kg of CBD, 50 mg/kg of CBD and 100 mg/kg of CBD, giving a total of 12 mice. These were dosed orally using the same methods as 2.2.1.2. Dosing schedule and timing of tissue harvesting is set out in Dose Response Appendix, A.5. Mice were dosed daily for four days and on day four were euthanised between 1-2 hours post-administration and tissues were collected as per methods section 2.2.1.3. Extraction of mRNA, cDNA synthesis, and real-time PCR were carried out as per sections 2.2.1.4, 2.2.1.5, and 2.2.2. Realtime PCRs were performed in duplicate and relative quantification was used to determine changes to the genes of interest, with GAPDH as the reference gene. This was done using the MIC qPCR cycler (BioMolecular systems) built in software.

2.2.5 Statistical analysis

Analysis of the COX 1 and COX 2 gene expression changes in wildtype mice due to the administration of CBD was performed using an Excel spreadsheet with the $\Delta\Delta$Ct method as set out by Livak & Schmittgen (2001) (Livak & Schmittgen, 2001).

The gene expression data for qPCR was analysied using the MIC qPCR cycler (BioMolecular systems) built-in software. This software determines quantification cycle (Cq) values using the LinRegPCR method (Ramakers et al., 2003), the expression ratios are calculated using the Pfaffl method (Pfaffl, 2001), and the data was analysied using the Relative Expression Software Tool (REST).

All other statistical analysis was carried out using SPSS statistics version 28.0.1.0 (142).

All p values were deemed statistically significant at $p \leq 0.05$. Standard error (SE) was used for error bars. One way ANOVA (analysis of variance) with Turkey HSD post-hoc testing was carried out on the data to compare means of the groups and determine if they are statistically significantly different.

2.3 Results

2.3.1 Cox 1 and 2 genes as biomarkers

Changes in expression levels of COX 1 and COX 2 have been widely used as first indicators of the anti-inflammatory actions of a drug, as they play an integral role in pain and inflammation pathways (Vane et al., 1998). For this reason, COX 1 and COX 2 gene expression levels were measured to determine their use as biomarkers for CBD dosing, with primer sets described in section 2.2.2, **Table 2-5**. The RNA quality and quantity used for this can be found in the Dose Response Appendix, A.4. The efficiency of the primers were 0.953 for COX 1 and 1.0853 for COX 2 (**Figure 2-2**). Additionally, the efficiency for GAPDH was 1.066 (**Figure 2-2**). All of these primer sets were deemed to have acceptable efficiency of values between 0.9 – 1.10 (Bustin et al., 2009).

A. COX 1

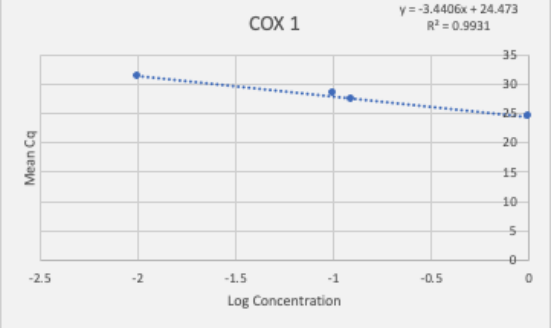

Slope -3.4406

Efficiency 0.953

B. COX 2

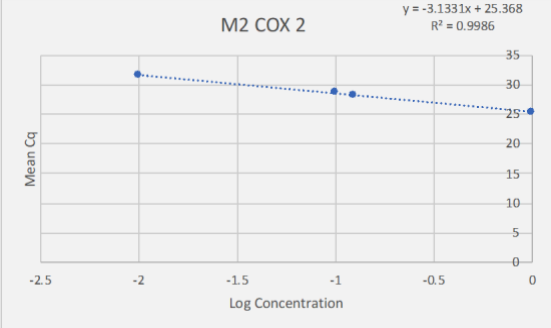

Slope -3.1331

Efficiency 1.0853

C. GAPDH1

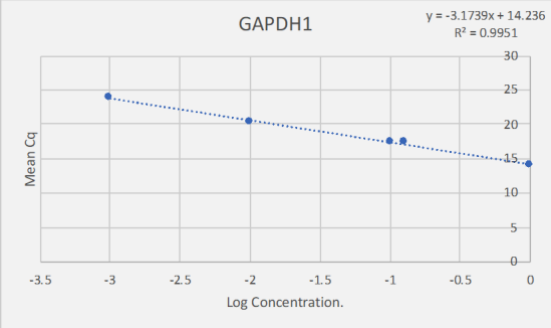

Slope -3.1739

Efficiency 1.066

Figure 2-2. *A standard curve with primers to determine the efficiency of primers for qPCR. Formula; y = mx+c, with m = slope. Efficiency = -1 + $10^{(-1/m}$. · A) COX 1 primer pair set standard curve. B) COX 2 primer pair set standard curve. C) GAPDH reference gene primer pair set standard curve.*

The COX 1 and COX 2 primers were used to measure changes to the gene expression of COX 1 and COX 2 in the DRGs of wildtype mice given a range of CBD doses. Changes to the gene expression were calculated as mean ratios and were all compared to the vehicle control group of 0 mg/kg of CBD (olive oil vehicle only). For COX 1, as the dose of CBD increased there was not a statistically significant change to the *cox-1* expression levels (**Figure 2-3**). Moreover, a high variation in *cox-1* expression was seen within the groups (note large error bars; **Figure 2-3**).

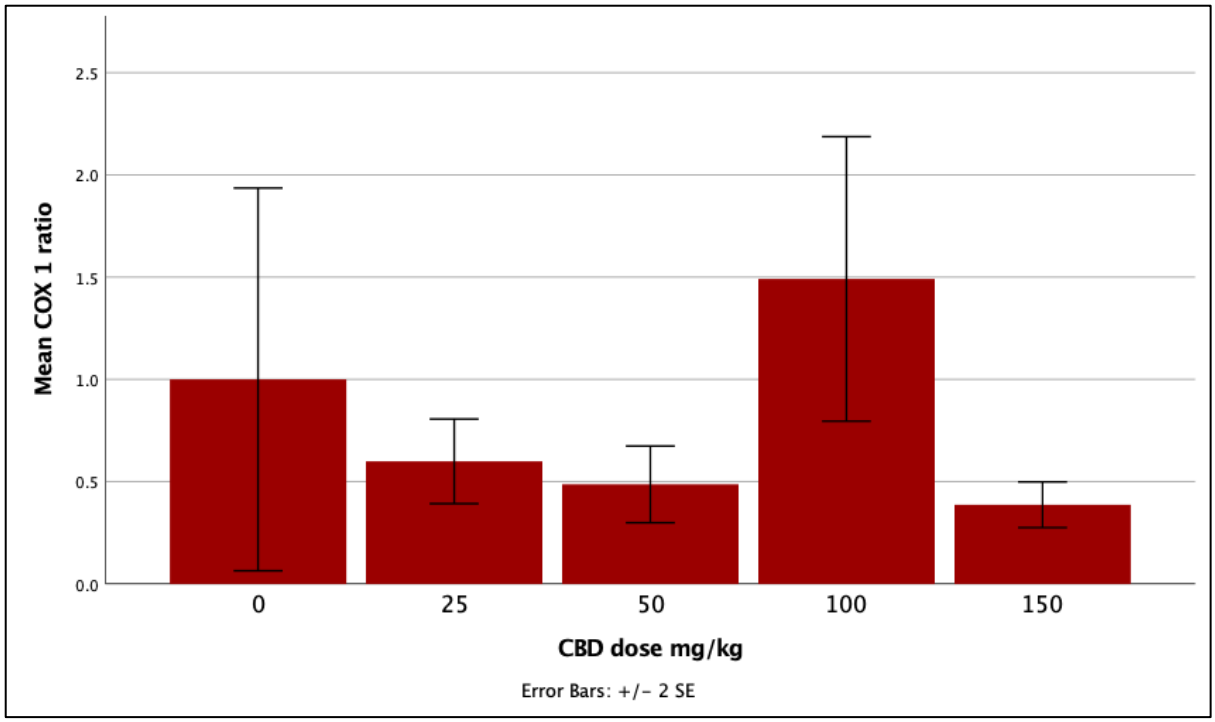

***Figure 2-3**. Changes to relative gene expression of COX 1 in wildtype mice administered CBD orally in olive oil once daily for four days (biological replicates n = 6, duplicates n=2). One-way ANOVA with Turkey HSD post-hoc testing. SE = standard error. P values when compared to the control group; 25 mg/kg - 0.829, 50 mg/kg - 0.665, 100 mg/kg = 0.699, and 150 mg/kg = 0.506.*

Similarly, for COX 2, different doses of CBD did not result in any statistically significant change in *cox-2* expression (**Figure 2-4**). As with COX 1, there was high variation shown within some of the groups.

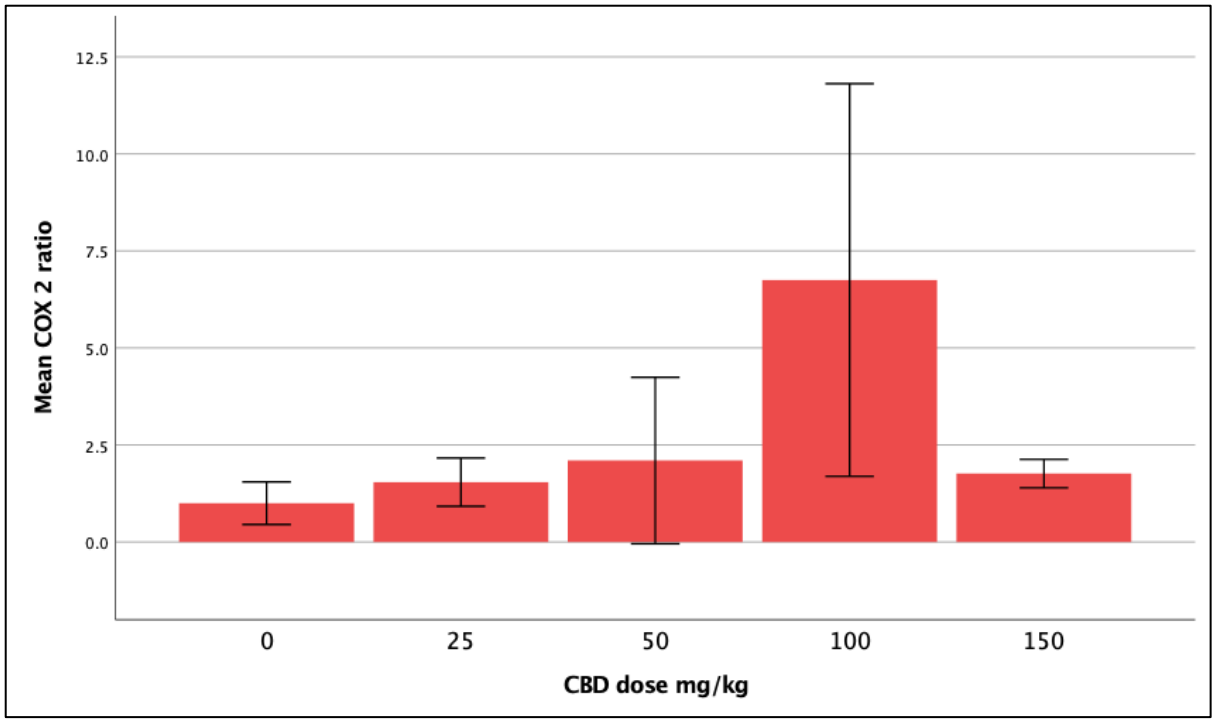

Figure 2-4. *Changes to relative gene expression of COX 2 in wildtype mice administered CBD orally in olive oil once daily for four days. (Biological replicates n = 6, duplicates n = 2). One-way ANOVA with Turkey HSD post-hoc testing. P values when compared to the control group; 25 mg/kg – 0.999, 50 mg/kg – 0.991, 100 mg/kg = 0.158, and 150 mg/kg = 0.998.*

2.3.2 Transcriptomics

Since COX 1 and COX 2 gene expression was highly variable within treatment groups and no significant changes were detected at different doses, they were deemed unsuitable as biomarkers for this study. As a result, an unbiased search for other potential biomarker genes was undertaken. To this end, total RNA from DRGs of mice treated with a range of CBD doses was sent to GENEWIZ for whole genome transcriptomics. The resulting data was of high quality, with a base call accuracy of greater than 99.9% (1 in 1000 probability of an incorrect base call) and mapped well to the reference genome (Mus musculus Ensembl GRCm38.10). From this, gene expression changes were calculated. A total of 200 genes were upregulated and a total of 56 genes were downregulated across all the doses of CBD (**Figure 2-5**). Volcano plots of each dose compared to the control were also supplied by GENEWIZ (Dose Response Appendix, A.7)

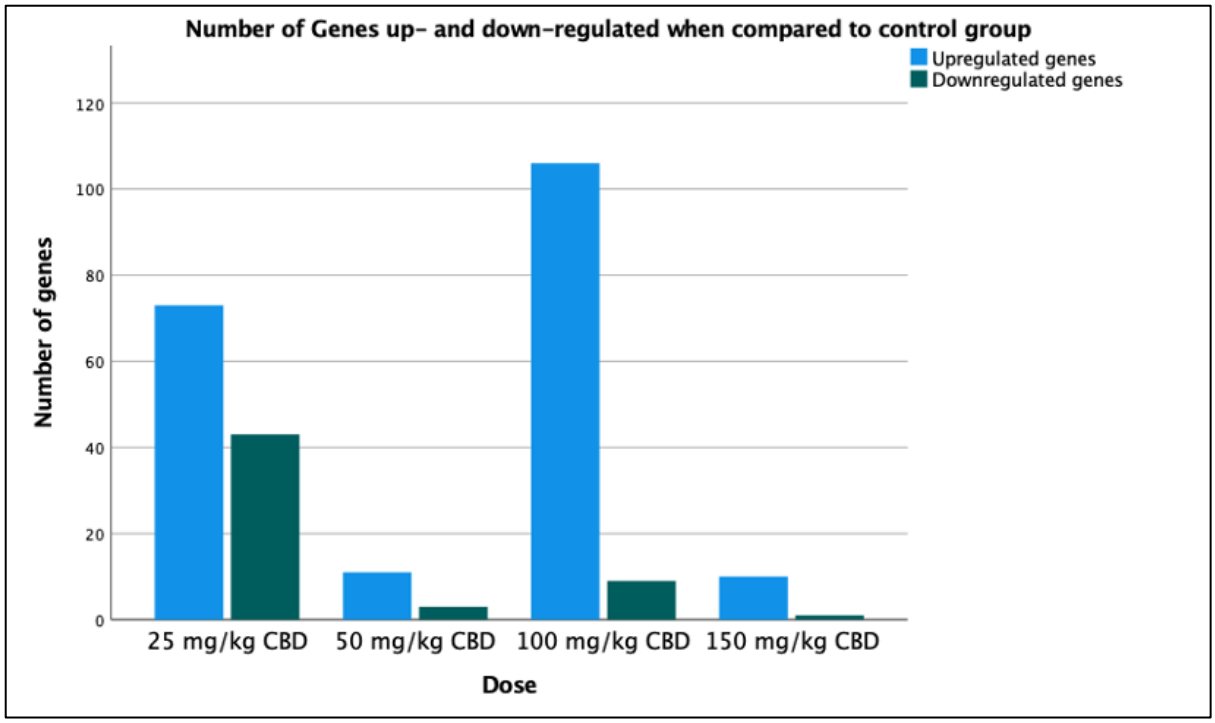

Figure 2-5*. Differential gene expression - number of genes significantly up-or down-regulated when compared to control group with administration of CBD to WT mice. The graph was plotted using data from GENEWIZ.*

The greatest change in overall gene expression (based on number of genes changed) was seen with 25 mg/kg and 100 mg/kg of CBD (116 and 115, respectively), while the least change in gene expression was seen with 50 mg/kg and 150 mg/kg of CBD (14 and 11, respectively; **Figure 2-5**). The number of genes that were similar between these groups was small, with only one gene, *hist1h2al,* upregulated across all treatment groups. This gene is involved in DNA packaging, allowing the DNA to be condensed in the cell (Peterson & Laniel, 2004). Three other genes were significantly differentially expressed across three of the experiment groups. Two of these were *rsp3a2* and *rsp2-ps6*, which encode ribosomal proteins (Bult et al., 2019), and the third was *dio2*, which encodes a deiodinase involved in the production of the T3 hormone and the regulation of thyroid-stimulating hormone (TSH) (Bult et al., 2019). The number of genes common between the CBD doses is shown as a Venn diagram (**Figure 2-6**). This information was used to select the genes, *rps2-p6, rps3a3, clec3b* and *dio2* that were used as biomarkers in the next trial and are listed in the methods section 2.2.4. *rps2-p6* was upregulated in the 25, 50 and 100 mg/kg CBD doses at 2.46, 3.13 and 5.49 fragments per kilobase (FPKB), and the other genes, *rps3a3, clec3b* and *dio2* were upregulated in the 25

mg/kg dose at 76.41, 146.09, and 1.12 FPKB, respectively, and at 96.25, 31.45, and 1.16 FPKB, respectively in the 100 mg/kg CBD dose.

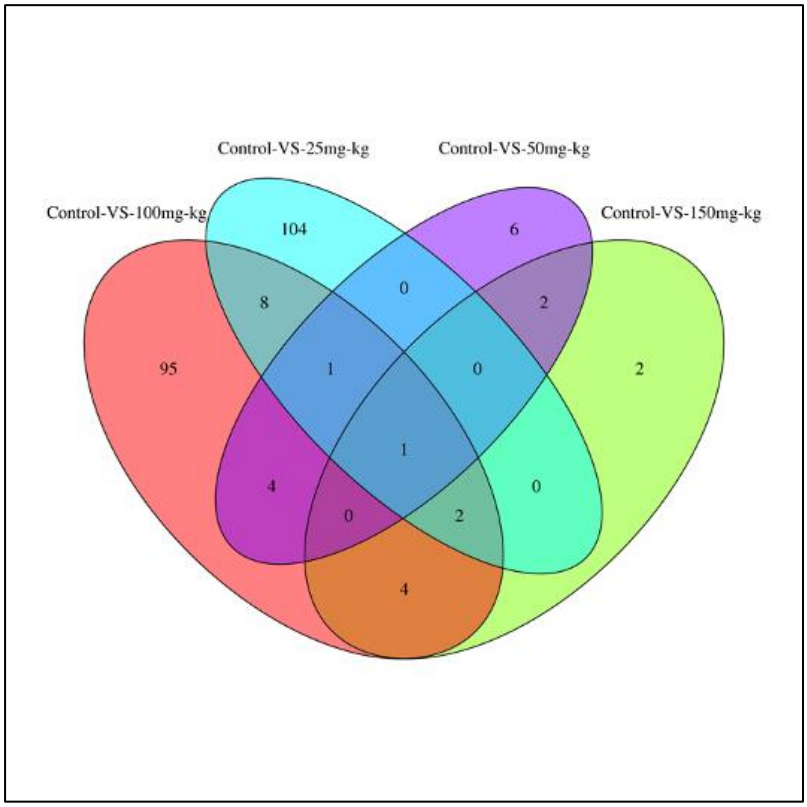

Figure 2-6. *Venn diagram of differentially expressed genes with the administration of CBD to wildtype mice. Picture and data from GENEWIZ*

2.3.3 Real-time qPCR results for Rps2-p6, Rps3a3, Clec3b, and Dio2 gene expression in mice

Primers for Rps2-p6, Rps3a3, Clec3b, and Dio2 qPCRs were designed as described in Section 2.2.4. Optimisation of annealing temperature was carried out for each primer set, with 65 °C used for all primers. Efficiencies were not manually calculated as the MIC software has that function built in to its automatic analyses.

Once the primers were designed, optimisation of annealing temperature was carried out and the results of this are shown on an agarose gel image (**Figure 2-7**).

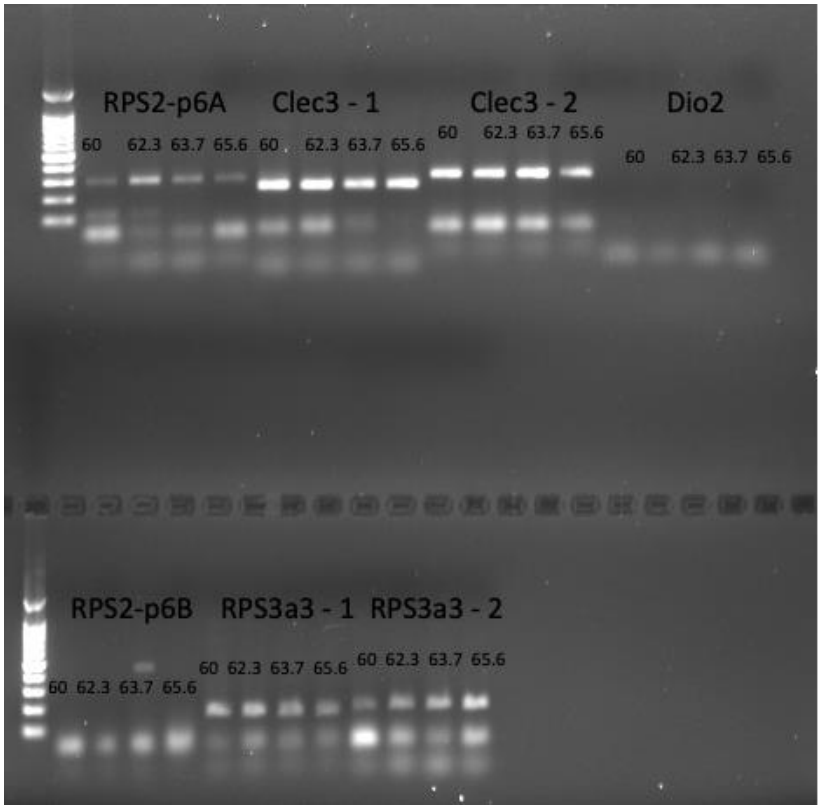

Figure 2-7*. Gel electrophoresis results of a temperature gradient with the primers designed for qPCR. Annealing temperature ranged from 60 °C to 65.6 °C as indicated by the numbers on each band in the agarose gel.*

Primer sets were used to determine Rps2-p6, Rps3a3, and Clec3b gene expression changes in DRG neurons of mice treated with 0 mg/kg, 25 mg/kg, 50 mg/kg, or 100 mg/kg of CBD. As Dio2 primers did not amplify a product it was not used moving froward. Gene expression ratios from qPCR are shown in **Figure 2-8** for each of the genes and doses. There is a clear U-shaped response seen across all the genes tested, with a higher gene expression ratio (1.129 - 3.216, and 0.822 – 5.768) seen at 25 mg/kg and 100 mg/kg and a lower ratio (0.039 - 0.488) at 50 mg/kg of CBD (Table **2-11**).

Table 2-11. *Gene expression ratios of primer sets used for qPCR.*

Primer set	Expression ratio 25 mg/kg CBD	Expression ratio 50 mg/kg CBD	Expression ratio 100 mg/kg CBD
Rps2-p6A	2.279	0.448	1.443
Rps2-p6B	2.513	0.039	1.638
Rps3a3-1	2.565	0.209	0.892
Rps3a3-2	1.129	0.146	0.822
Clec3-1	3.216	0.175	1.352
Clec3-2	2.256	0.406	5.768

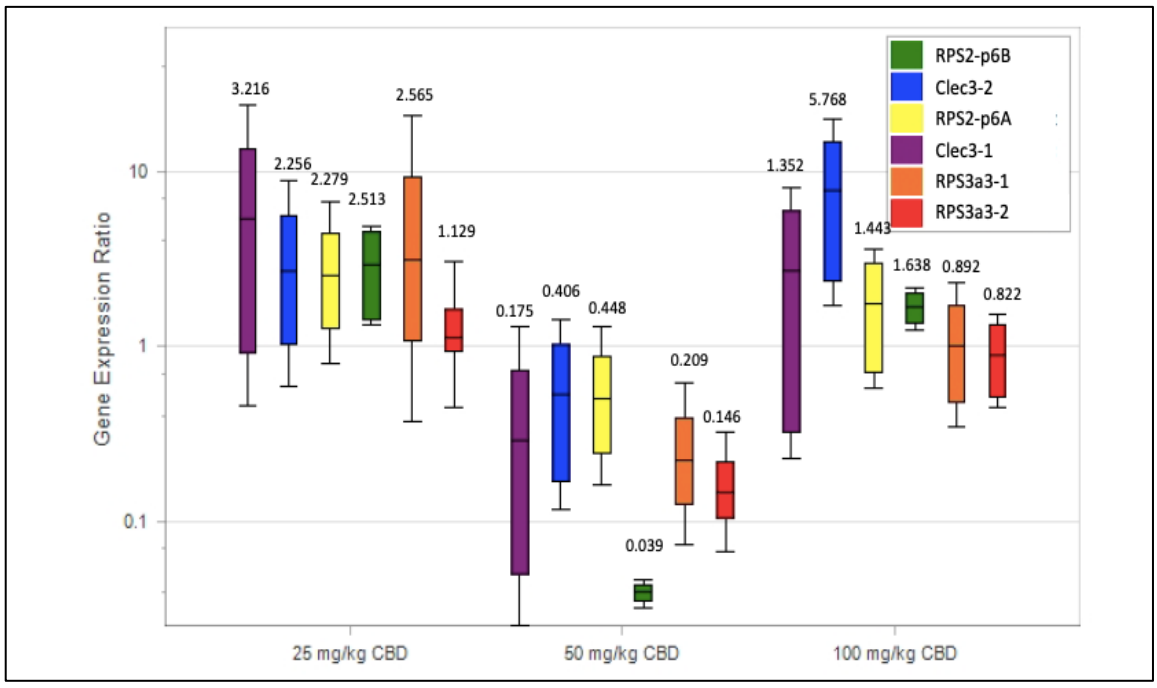

Figure 2-8. *Graph of gene expression ratios from DRG tissues from mice administered CBD in olive oil. Gene expression ratios for each gene at each dose are indicated above each bar. Error bars represent a 95% confidence interval.*

2.4 Discussion

The aim of this chapter was to determine if a biomarker could be identified and used to indicate what CBD doses induce biological effects in mouse DRGs and then to develop a CBD dose-response profile. This proved not to be as straightforward as was expected, with the first selected biomarkers, COX 1 and COX 2, not showing any significant difference between doses. Whole genome transcriptomics was then completed to determine if there were any other candidate genes that would change in a dose-dependent manner with the administration of CBD to the mice. There were no adverse effects noted in any of the mice administered with the CBD over the four days, indicating that the concentrations of CBD (25 mg/kg to 150 mg/kg) as part of the dose-response trial were safe across this time period. There is some evidence that a larger dose of CBD can lead to hepatoxicity (Ewing et al., 2019), so this combined with the fact that there was no statistically significant change seen with the administration of 150 mg/kg of CBD, led to this dose being discontinued moving forward.

2.4.1 COX 1 and COX 2 as biomarkers

Cannabidiol is reported in the literature to have anti-inflammatory effects (Atalay et al., 2020; Burstein, 2015; Cabrera et al., 2021; Henshaw et al., 2021); however, the pathways responsible for mediating these anti-inflammatory effects are less clear (Izzo et al., 2009; Vučković et al., 2018). There is some evidence that using CBD in rodent models of inflammation can lead to a decrease in COX downstream enzymes, in particular, prostaglandin E_2 (PGE_2). Because the PGE_2 is readily associated with inflammatory responses it is often used as an indicator of COX activity (Giuliano & Warner, 2002). In rats, for example, Freund's adjuvant-induced paw oedema and chronic sciatic nerve constriction injury are used as models of inflammatory and neuropathic pain, respectively. In these models, CBD at 20 mg/kg resulted a statistically significant decrease in blood plasma levels of PGE_2 compared to untreated controls (Costa et al., 2007). Although this study did not directly measure COX expression, PGE_2 production is rate limited by COX 2 (Giuliano & Warner, 2002), therefore, it can be used as an indirect measure of COX 2 activity. By contrast, there is also conflicting evidence that CBD decreases COX expression. In a cell culture model of human colon adenocarcinoma, treatment with CBD (100 mg/mL) lead to an increase in COX 2 expression (Ruhaak et al., 2011); however, this study did show a downregulation of COX 1 and COX 2

enzymes with other cannabis isolates, including tetrahydrocannabinolic acid (THCA; the precursor to THC), Cannabidiolic acid (CBDA), cannabigerol (CBG) and cannabigerolic acid (CBGA) (Ruhaak et al., 2011).

Our results showed that there was no statistically significant change in gene expression levels of *cox-1* and *cox-2* in DRGs of wildtype mice after the oral administration of CBD between 25 mg/kg and 150 mg/kg (**Figure 2-3** and **Figure 2-4**). Since CBD is thought to downregulate *cox-1* and *cox-2*, it is possible that if inflammation was primed in the mice prior to CBD treatment, thus elevating *cox-1* and *cox-2* expression, a statistically significant reduction in expression level may have been observed. However, these results led to the conclusion that COX 1 and COX 2 would not be suitable to use as biomarkers of CBD's biological effects in mouse DRGs. This was further supported by the high variability in *cox-1* and *cox-2* expression seen in both CBD-treatment and vehicle-treatment groups. Thus, transcriptomics was carried out to unbiasedly identify genes whose expression change with the administration of oral CBD in mice and identify potential biomarkers.

2.4.2 Transcriptomics

There were a large number of genes with changed expression levels in DRGs following administration of CBD to the mice. This is consistent with reports in the literature that multiple pathways are targeted by the use of medicinal cannabis (Izzo et al., 2009; Vučković et al., 2018). Historically, the cannabinoid type 1 (CB1) and type 2 (CB2) receptors were thought to be the pathway used to produce analgesia (Rahn et al., 2007), but CBD has since been shown to interact in many more biological pathways, including those involved in pain and inflammation (Morales et al., 2017; Pertwee, 2005; Vučković et al., 2018). CBD, when used with tetrahydrocannabinol (THC) has an antagonistic role at the cannabinoid receptors (McPartland & Russo, 2001; Pertwee, 2008; Vučković et al., 2018). CBD has also been shown to interact with G-protein coupled receptors, 5-hydroxytryptamine (5HT) receptors (also known as serotonin receptors), and transient receptor potential (TRP) channels (Izzo et al., 2009; Vučković et al., 2018). With CBD having so many different targets in pain and other pathways, it can be difficult to identify a particular one to use as an indication of therapeutic efficacy.

The genes selected to be used as biomarkers in this case are involved in a range of processes. The genes were selected based on the greatest increase in transcription and those that were common across at least two of the doses (25 mg/kg, 50 mg/kg and 100 mg/kg CBD); the overlap of the number of genes between the CBD doses is shown in **Figure 2-6**. The list of genes were selected were *rps2-p6, rps3a3*, and *clec3b* (**Table 2-9**). *rps2-p6 and rps3a3* are both pseudogenes for ribosomal subunits and were upregulated across all the CBD doses. Clec3b is involved in bone growth and formation (Bult et al., 2019). CBD has been indicated in improved bone healing in other studies (O'Connor et al., 2020; Raphael-Mizrahi & Gabet, 2020). Bone healing is mediated in part through the endocannabinoid system and it is thought that CBD interacting on the CB1 and CB2 receptors is able to increase the bone formation. This interaction was shown in pre-clinical studies (O'Connor et al., 2020), with CBD leading to enhanced fracture healing in a rodent model (Raphael-Mizrahi & Gabet, 2020). CBD administered daily at 5 mg/kg to rats with a femoral fracture were shown to have a marked improvement in healing process and bone strength after healing when compared to a control group (Kogan et al., 2015). All of these studies indicate that the increase in transcription of the Clec3b gene across the CBD doses should be expected.

Interestingly, there was no indication of up or down-regulation of *cox-1* or *cox-2* in the transcriptomics data provided by GENEWIZ. This is consistent with the initial qPCR experiments for *cox-1* and *cox-2* expression, which indicated no significant change to the expression levels of these genes; though, as previously mentioned, it is possible that inflammation (and therefore elevated *cox-1* or *cox-2* expression) needs to be present for CBD to have a measurable effect, further emphasising that the CBD is not having any analgesic action through these pathways.

There was a vast amount of data that was generated by the transcriptomics work (Dose Response Appendix, A.6), but for this study, only the data concerning differentially expressed genes were considered. Included in this data are alternative splicing analyses, novel transcription predictions and gene ontology enrichment. Future work using this data set could indicate other genes or relevant pathways to better identify biomarkers to determine the efficacy of CBD and other cannabinoids in these *in vivo* studies.

2.4.3 U-shaped dose-response

In both the transcriptomic data (**Figure 2-5**) and an independent (different animals and treatments) dose-response qPCR experiment (**Figure 2-8**) a U-shaped gene expression response to increasing doses of CBD is observed. This is indicated by a greater gene expression changes at 25 mg/kg and 100 mg/kg, and a lower gene expression changes at 50 mg/kg orally administered CBD. This being observed in both sets of data suggests that these expression changes are a biological response to the CBD. This is also consistent with evidence in the literature where a U-shaped curve is associated with CBD, in both pre-clinical and clinical studies (Guimarães et al., 1990; Linares et al., 2018; Nazario et al., 2015; Nedelescu et al., 2022; Zuardi et al., 2017). Many of these studies explore changes to anxiety levels in animals and humans. In an elevated plus-maze, male Windsor rats were given CBD by intraperitoneal injection at 2.5 mg/kg, 5 mg/kg, 10 mg/kg and 20 mg/kg and ratios of entry into open arms were calculated (Guimarães et al., 1990). CBD doses of 2.5 mg/kg to 10 mg/kg resulted in statistically significantly different arm entry ratios compared to vehicle treated rats, with a peak at 5 mg/kg whereas 20 mg/kg was not significantly different to the vehicle animals (Guimarães et al., 1990). This effect on anxiety is duplicated in human subjects undergoing public speaking in two studies. One used a real situation (Zuardi et al., 2017) and the other a simulated condition (Linares et al., 2018). What they both showed was the lowest (100 mg and 150 mg respectively) and highest dose (900 mg and 600 mg respectively) of CBD had little to no difference when compared to control; and the middle dose (300 mg and 300 mg respectively) showed anxiolytic affects.

There is a lot of variation with what is classified as a high, medium, and low dose of CBD, particularly with animal studies. It varies with each study and disease aetiology. Despite the many observations of CBD having this U-shaped effect with ‘high’ and ‘low’ doses showing a greater measured efficacy when compared to the ‘medium’ dose, there is no clear consensus in the literature on why the CBD acts in this way. Cannabis used in a medicinal setting seems to be a complicated drug, and even CBD as a single isolate has many known pathways (Izzo et al., 2009). This means that it is not a simple task to determine why CBD has this U-shaped dose response curve, and is well outside the scope of this work.

Because the greatest CBD effects in this dose-response work was seen at 25 and 100 mg/kg, both of these doses were selected for use in assessing whether CBD is efficacious in treating

neuropathic pain associated with Charcot Marie Tooth peripheral neuropathy. In addition to these doses, the 50 mg/kg dose was selected to determine if analgesic efficacy might mirror the gene expression dose-response results.

2.5 Conclusion

What can be concluded from this dose-response work is three-fold: Firstly, that orally administered CBD does not change the expression levels of *cox-1* and *cox-2*. This was shown both with the qPCR and transcriptomics data. COX 1 and COX 2 proved to be poor biomarkers for this study. Secondly, we have identified three genes, *rps2-p6, rps3a3*, and *clec3b* that are reliably upregulated in mouse DRGs by oral administration of CBD. These genes may have utility as biomarkers for CBD and potentially other cannabinoids. The expression patterns of these genes display a U-shaped curve in response to CBD dose. These genes were identified through an unbiased transcriptomics approach and were confirmed by qPCR in independent experiments. A U-shaped response curve is not unusual for CBD as evident in the literature and supports the notion that these gene expression changes reflect a biological activity of the CBD. Thirdly, the U-shaped gene expression response curve suggests that 25 mg/kg and 100 mg/kg might be effective doses, while 50 mg/kg and 150 mg/kg would be less effective; however, it was not possible to identify what might be a single "effective" dose to move forward into mouse behaviour trials. Based on the results from this chapter, it was determined that the doses 25 mg/kg, 50 mg/kg, and 100 mg/kg CBD should be used in behavioural testing studies

3 Efficacy of Cannabinoids to Treat Neuropathic Pain in a Mouse Model of Charcot-Marie-Tooth Disease, type 2A

3.1 Introduction

Charcot-Marie-Tooth disease is the most common inherited PNS neurological disorder, affecting 1 in 2500 people (Martinou et al., 2010). It is a collection of peripheral neuropathies, caused by mutations to genes that affect the structure or function of the peripheral nerve. CMT can be further subdivided depending on the gene affected. One such subdivision is CMT2A, which is characterised by progressive length-dependent axonal die back from the distal end of nerves (Scherer, 2011; Skre, 1974). CMT2A is caused by mutations to the *mfn2* gene, of which more than 30 different mutations have been identified (Detmer & Chan, 2007). The most common *mfn2* mutation in humans is a missense mutation in exon 4, resulting in an arginine to glutamine ($MFN2^{R94Q}$) substitution (De Vriendt et al., 2006). CMT2A has the earliest onset of the CMT2 types, and because of this, it is the most severe form of CMT2 (Feely et al., 2011).

The symptoms of CMT vary in severity and presentation affecting both motor and sensory neurons (Padua et al., 2006). Symptoms include lower limb weakness, muscle loss, foot drop, hammer toe, frequent tripping, and neuropathic pain (McCorquodale et al., 2016). Interestingly, some CMT types can also affect optic nerves, even though they are part of the CNS (Züchner et al., 2004). CMT currently has no cure and is managed in part by physical therapy, surgery and orthopaedic devices. This treatment can include gait therapy, occupational therapy, assistive orthopaedic devices, and surgery for tendon transfers and foot deformities (McCorquodale et al., 2016). Neuropathic pain associated with CMT diseases can be quite severe, requiring life-long analgesia(Carter et al., 1998). Work carried out by Carter et al. (1998) found that 22% of patients needed opioid based analgesics to manage their pain symptoms. As previously stated in the literature review section 1.3.4, there are a long list of problems with opioid use. Another common treatment for neuropathic pain is gabapentin (Kukkar et al., 2013; Maneuf et al., 2006). Gabapentin (also known as Neurontin) has several common side effects, the most common are dizziness and sleepiness. Less commonly, affecting approximately 10% of patients, are ataxia and swelling in the extremities

of the limbs (Kukkar et al., 2013; Rose & Kam, 2002). There is also the possibility of respiratory depression when taking gabapentin combined with opioids (Pfizer, 2020) and there is some indication that gabapentin use can lead to increased suicidal ideation and self-harm (Andersohn et al., 2010; Patorno et al., 2010; Pfizer, 2020). Despite these side effects, gabapentin has some efficacy with treating neuropathic pain symptoms, with somewhere between 30% to 38% of neuropathic pain patients reporting at least a 50% reduction in pain (Bennett & Simpson, 2004; Wiffen et al., 2017).

With both opioids and gabapentin having unwanted side effects, and not able to reliably treat the pain associated with neuropathic diseases it is important to find effective alternative analgesics for those suffering with any neuropathic pain including, CMT2A patients. Pre-clinical investigations in this chapter use CMT2A mice and wildtype littermates as a neuropathic pain model to test the efficacy of different cannabinoids in providing analgesia.

3.1.1 Mouse model of CMT2A

Like that seen in CMT2A patients, CMT2A mice show a progressive degeneration of peripheral nerves, with dieback occurring from the distal end of long nerves (Scherer, 2011; Skre, 1974). This mouse model was created by the Martinou lab using the most common human CMT2A mutation $MFN2^{R94Q}$ (Martinou et al., 2010). Named *MitoCharc1* or B6; D2-Tg (Eno2-MFN*R94Q) L51Ugfm, CMT2A mice have one copy of the mutant human *mfn2* (mh*Mfn2*) gene (with an R94Q substitution) under the control of a neuron specific enolase promoter. These CMT2A mice are a good model for human CMT2A disease as shown by both motor and sensory function testing (Picci et al., 2020). The CMT2A mice show thermal hyperalgesia and mechanical allodynia from as early as can be measured (by four weeks of age) and a progressive decline in motor performance with significant deficits seen between 20 and 22 weeks of age (Picci et al., 2020). These are animals that have been used in previous work in this laboratory and are well characterised (Picci et al., 2020).

3.1.2 Genotyping

Mice were genotyped to determine their CMT2A status before sorting them into treatment and control groups. The mice are maintained as mh*Mfn2* hemizygotes (as homozygotes are not viable) and bred to wildtype (non-carrier) mice from the same colony. It is therefore

important to determine if mice are wildtype or CMT2A, both for the purpose of testing and breeding. Due to the symptoms of CMT2A in mice being mild but chronic, the CMT2A mice are not visually different to their wildtype littermates, with their CMT2A status not able to be determined by casual observation. Rather, determining CMT2A status was achieved by genotyping, which involved the extraction of DNA from ear punch tissue, PCR to amplify the mh*Mfn2* gene, and agarose gel electrophoresis to visualize the resulting banding pattern on an agarose gel. Two sets of primers were used; oIMR10453 and oIMR10454 which amplify a 200bp fragment of the mouse *mfn2* gene, and oIMR8744 and oIMR8745 which amplify a 300bp fragment of the hm*mfn2* gene (**Table 3-3**). Thus, wildtype mice have a single 200bp band and the transgenic mice have both a 200bp and 300bp band. The primers for hm*mfn2* target a specific part of the transgene, that is not present in the mouse wildtype gene.

3.1.3 Behaviour

von Frey, Hargreaves, and Rotarod testing have been used with good results to detect neuropathic pain (mechanical allodynia and thermal hyperalgesia) and changes to motor function, co-ordination, and grip strength in CMT2A mice (Colleoni & Sacerdote, 2010). For this work von Frey and Hargreaves tests were used to determine if any changes to mechanical allodynia and thermal hyperalgesia occurred in CMT2A mice when cannabinoids were administrated.

3.1.3.1 von Frey

Allodynia is a pain reaction to a stimulus, such as touch, that should not cause pain, and is a symptom of neuropathic pain (Chaplan et al., 1994). Mechanical allodynia in mice can be measured using von Frey filaments. These are nylon monofilaments of varying stiffness mounted onto a handle that are designed to bend at a precise and known force allowing a reliable and repeatable force to be applied (Levin et al., 1978). The use of von Frey filaments for testing allodynia is advantageous as it is reliable, repeatable, shows graded responses, and does not place the non-restrained mouse under stress (Chaplan et al., 1994). The filament is applied to the plantar surface of the paw of the mouse, and the mouse is free to remove its paw if the sensation is uncomfortable (Levin et al., 1978). The paw withdrawal threshold – which filament induces a withdrawal response, in grams of force – can then be calculated

(Levin et al., 1978). Treatments that lead to relief of mechanical allodynia will cause a change in the paw withdrawal threshold, making this an important tool to determine if there has been a relief of neuropathic pain symptoms due to the cannabinoid treatment.

3.1.3.2 Hargreaves

Hyperalgesia is an overreaction to a pain signal, in which a stimulus elicits an exaggerated pain response and is often seen in neuropathic pain. It can be tested for by presenting a hot or cold stimulus and noting the response of the animal. One method that is commonly used is Hargreaves testing. This method uses non-restrained mice in a cage with a glass bottom and a radiant heat source, which is applied to a plantar surface of the paw (Hargreaves et al., 1988). The time for the animal to remove its paw is termed paw withdrawal latency and is calculated in seconds, giving a quantitative measurement (Hargreaves et al., 1988). Typically, animals suffering with hyperalgesia will have a different withdrawal latency when compared to non-hyperalgesic animals (Cheah et al., 2017). Hargreaves testing employs the use of a movable infrared generator that is placed under the glass panel bottom. The rodent is placed upon the glass in an observation chamber (Figure 3-4). This method has also been shown to be reliable and repeatable without inducing stress to the animal (Hargreaves et al., 1988). It can detect small changes in sensitivity, making this an important additional tool to identify changes in neuropathic pain symptoms that cannabinoid treatment might elicit.

3.1.4 Gabapentin

Gabapentin is commonly used as a treatment for neuropathic pain in patients. Because of its clinical usage, it is used in this study to compare CBD efficacy in the pre-clinical neuropathic pain model used. Many pre-clinical trials using gabapentin in models have been carried out to date, with effective doses of gabapentin in different mouse models of neuropathic pain shown in **Table 3-1**. Oral doses vary between 10 mg/kg to 50 mg/kg, with more variation observed in the intraperitoneal injections, ranging from 3 mg/kg to 100 mg/kg. An oral dose of 10 mg/kg in mice has a bioavailability of 99.8%, decreasing to approximately 80% bioavailability at 50 mg/kg (Radulovic et al., 1995). The maximum blood plasma concentration of gabapentin in mice peaks at two hours after an oral dose (Kusunose et al., 2010; Radulovic et al., 1995). It is water-soluble and is easily dissolved into water-based vehicles (Rose & Kam,

2002). Most studies have dissolved it directly into distilled water or saline to administer to the mice (Table **3-1**).

***Table 3-1**. Effective doses of gabapentin in mouse models of neuropathic pain.*

Dose	Route of administration	Vehicle	Treatment	Reference
10 – 40 mg/kg	Oral	Distilled water	Diabetic induced NP	(Reda et al., 2016)
10 - 30 mg/kg	Oral	Saline	Chemotherapy induced NP	(Matsumoto et al., 2006)
3 mg/kg	I.P.	Saline	Fibromyalgia	(Nishiyori & Ueda, 2008)
100 mg/kg	I.P	Saline	Chronic constriction injury	(Atwal et al., 2019)
50, 100 & 150 mg/kg	I.P	Saline	Partial sciatic nerve ligation	(Kusunose et al., 2010)
10 mg/kg & 100 mg/kg	I.P.	Distilled water	Pharmacokinetic trial	(Scuteri et al., 2020)
50 mg/kg	Oral	Distilled water	Chronic constriction injury	(Vincenzetti et al., 2019)

Research on the efficacy of gabapentin to alleviate diabetic induced neuropathic pain carried out by Reda et al. (2016) showed efficacy to rescue hyperalgesia with hot plate testing to vehicle levels at 10 mg/kg gabapentin, but in von Frey testing for allodynia this was not achieved until 40 mg/kg gabapentin. Matsumoto et al. (2006) showed close to rescue of function at 30 mg/kg gabapentin with von Frey and complete rescue with Hargreaves testing at the same dose. This data paired with the bioavailability that is inversely related to the dose, a lower, but effective, oral dose is preferred. Based on this data 40 mg/kg of gabapentin was chosen and given orally, and was prepared in distilled water and made up to the correct concentration with olive oil.

3.1.5 Multiple doses over time

Clinically, patients need sustained pain relief across the day. It is important to determine if additional doses will lead to an improved or sustained response over time. To test this, the most effective dose of CBD was administered multiple times to CMT2A mice in an 8 hour study. This was compared to olive oil vehicle control and 40 mg/kg gabapentin to determine if there would be sustained pain relief across the 8 hours.

3.1.5.1 Rationale for using CBD in the multiple dose study

Several factors were considered in deciding to use CBD (as opposed to high CBD whole extract or CBD:THC) in the multiple dose study. Any cannabis product containing more than 2% THC is classified as a controlled drug in New Zealand ("Misuse of Drugs Act," 1975). This classification makes cannabis products with >2% THC, such as the high CBD whole extract more challenging to work with and store. For a single dose in the mice this controlled drug was able to be administered with a certified person from Cannasouth present and the drug returned promptly. With multiple doses across a longer eight hour period it is not as practically feasible. The mice were habituated to one person being in the room at the time of testing and having extra people could unsettle the mice and lead to changes in their responses and introduce variance in the results. Conversely, CBD product is not a controlled drug in New Zealand ("Misuse of Drugs Act," 1975), therefore, is much more accessible to work with in these situations. In New Zealand, CBD is already able to be purchased by patients when prescribed by a NZ general practitioner (GP), therefore, it is more clinically relevant to test this at this point in time.

Working with a single pure cannabinoid isolate leads to more consistency, as the purity and strength can be guaranteed. A whole extract, containing minute fractions of the lesser cannabinoids and other compounds that are harder to detect and test for will not be as consistent. As noted in the discussion section (3.4.3.1 & 3.4.3.2) there are many other cannabinoids, terpenes and flavonoids that could lead to changes in the analgesic response. These compounds can differ in concentration depending on plant types or different growing condition, leading to changes in drug composition and therapeutic inconsistencies in patients.

3.2 Materials and Methods

3.2.1 Genotyping CMT2A mice

Ear punching was used to identify and genotype mice. The mice were gently restrained in a scruff hold and then an ear punch tool was used to place a small 2mm hole in the ear corresponding to their identification number. The ear tissue from the punch was collected into a labeled microcentrifuge tube and used for genotyping. This was achieved by adding 180 µL of 10% Chelex solution (Sigma, # C7901-25G) to the tube. The tissue sample in the Chelex solution was heated at 99°C for at least 30 min in a Thermomixer heating block (Eppendorf). The samples were then incubated at 4 °C for at least 24 hours up to one week. Following this, the samples were again incubated at 99 °C for 30 min then removed from the heating block and centrifuged at 16,000 x *g* (5415R, Eppendorf) at room temperature for 3 min. The resulting supernatant was used directly in a PCR reaction to genotype the mice. Remaining supernatant was stored at 4 °C. The PCR components and final concentrations are listed in Table **3-2**. The primers used are listed in **Table 3-3**. PCR was performed in PCR tubes with; 1.2µL of 10 x PCR buffer with $(NH4)_2SO4$ (Invitrogen #EP0402), 0.96 µL of 2.5 µM dNTPs (Invitrogen, #R1122), 0.96 µL of 25 µM $MgCl_2$ (Invitrogen, #EP0402), forward and reverse primers at 20 µM TAQ DNA recombinant polymerase (Invitrogen #EP0402, 5 U/µL), and 4 µL of DNA and distilled water to make up a total volume of 12 µL.

***Table 3-2**. Components in each 12μL PCR tube reaction for genotyping the mice. DNA is extracted from the ear punch tissue..*

PCR COMPONENT	VOLUME ADDED
DDH2O	1.97 μL
10 X PCR BUFFER $(NH_4)_2SO_4$	1.2 μL (1x)
2.5μM DNTPS	0.96 μL (0.2 μM)
25μM $MGCL_2$	1.44 μL (2 μM)
20μM OIMR10453	0.6 μL (0.5 μM)
20μM OIMR10454	0.6 μL (0.5 μM)
20μM OIMR8744	0.6 μL (0.5 μM)
20μM OIMR8745	0.6 μL (0.5 μM)
TAQ DNA POLYMERASE	0.03 μL (0.15 U)
DNA	4 μL
TOTAL VOLUME	**12 μL**

***Table 3-3**. Primers used for genotyping of the mice*

Transgene	Sequence (5' – 3')	Size
oIMR8744	ATG CAT CCC CAC TTA AGC AC	
oIMR8745	CCA GAG GGC AGA ACT TTG TC	300bp
Wildtype		
oIMR10453	CAA ATG TTG CTT GTC TGG TG	
oIMR10454	GTC AGT CGA GTG CAC AGT TT	200bp

PCR conditions were as follows:

1) 94 °C for 3 min for initial denaturing of the DNA, and to activate the Taq DNA polymerase (Invitrogen, Lot # 1850672)
2) 35 cycles of:
    a. 94 °C for 30 s (Denaturing)
    b. 62 °C for 30 s (Annealing)
    c. 72 °C for 30 s (Elongation)
3) Final elongation at 72 °C for 2 min
4) Hold at 4 °C indefinitely

The resulting PCR product was analysed by agarose gel electrophoresis. A 1.5% agarose gel in TAE was used to visualize the PCR products. The agarose gel was made by mixing UltraPure™

Agarose powder (Invitrogen, #16500-100) into 50 mL of 1 x TAE buffer (1 X buffer: 242 g Tris, 57.1 mL glacial acetic acid, 100 mL 0.5 M EDTA, pH 8, distilled water to make up to 1 X) and microwaving until molten. 2 μL of ethidium bromide at 10 mg/mL (Sigma Aldrich, # E1510) was added, and then the resulting solution was cast in a 12-well gel mold. Once set, the gel was submerged in 1 x TAE running buffer, and 10 μL of PCR product plus 2 μL of 6 X DNA loading dye (Thermo Fisher #R0611) was loaded into each well. A 100 bp molecular weight marker (Solis BioDyne #07-11-00050) was used to determine product size. The electrophoresis was performed for 30 min at 100V. Gels were imaged by ethidium bromide fluorescence using a UV gel documentation system (ibright FL1000 imager).

3.2.2 Power analysis for group sizes

Mice can be used to model human neuropathy and neuropathic pain, which cannot be modeled in non-sentient models. The number of mice needed for each aim needs to be balanced carefully to ensure the smallest number of mice that can give significant data are used. To determine this power calculations were carried out for each of the behaviour tests. The group size for experiments involving CMT2A mice was based on power analysis using SPSS statistical analysis software and the information from a previous study using the variables of sensory and locomotor differences between the CMT2A and wildtype mice (Picci et al., 2020) The p value was set at 0.05, and the power was 0.80.

Power analysis for the group size (*n*) needed to see a significant difference between control and treatment groups for von Frey was eight mice (**Table 3-4**).

***Table 3-4**. Power analysis for von Frey testing with CMT2A mice.*

Power Analysis Table

	N[b]	Actual Power[c]	Test Assumptions			
			Power	Std. Dev.[d]	Effect Size	Sig.
Test for Mean Difference[a]	8	.856	.8	.040	1.250	.05

a. Two-sided test.

b. Number of group pairs.

c. Based on noncentral t-distribution.

d. Standard deviation of the mean difference.

Power analysis for the group size (*n*) needed to see a significant difference between control and treatment groups for Hargreaves testing was four mice (**Table 3-5**). The numbers needed were smaller than with the von Frey testing but as the same group of mice was used for both tests the larger number generated for statically significant differences in the von Frey was used, *n* = 8. At least eight mice per group were therefore used for the dose response and the behavioural studies.

***Table 3-5**. Power analysis for Hargreaves testing in CMT2A mice*

Power Analysis Table

	N[b]	Actual Power[c]	Test Assumptions			
			Power	Std. Dev.[d]	Effect Size	Sig.
Test for Mean Difference[a]	4	.963	.8	1.340	2.955	.05

a. Two-sided test.

b. Number of group pairs.

c. Based on noncentral t-distribution.

d. Standard deviation of the mean difference.

3.2.3 Cannabidiol dosing and oral administration

The cannabinoid preparations used in this chapter are: a CBD isolate dosed at 6.25 mg/kg, 12.5 mg/kg, 25 mg/kg, 50 mg/kg and 100 mg/kg, a high CBD whole extract dosed at 12.5 mg/kg CBD also containing THC at 0.867 mg/kg and other compounds at a lower concentration, and a CBD:THC isolate dosed at 12.5 mg/kg CBD and 0.867 mg/kg THC. Certificate of analysis for these are found in the (Appendices, A.2, B.1 and B.2) Once mice had been genotyped and group numbers determined, mice were separated based on genotype and sex and randomly assigned to four genotype/treatment groups: wildtype control (*n* = 8); wildtype treatment (*n* = 8); CMT2A control (*n* = 8); and CMT2A treatment (*n* = 8). The age of the mice at the beginning of testing ranged from 12 to 14 weeks across all of the cohorts, and each group had an even mix of males and females. Mice were weighed to determine oral dose, and this was administered as described in methods section 2.2.1.2.

Prior to treatment, baseline von Frey and Hargreaves testing of the mice was performed. Following treatment, mice were tested at set timepoints post administration; 30 min, 1 hour, 1.5 hours, 2 hours, 3 hours, and 4 hours. The mice were returned to their home cages after

the 2- and 3-hour timepoints to rest and returned to testing chambers to settle for 15 min before the next time point testing.

A range of CBD doses were used to determine whether CBD had any efficacy in alleviating neuropathic pain in the CMT2A mice; 6.25 mg/kg, 12.5 mg/kg, 25 mg/kg, 50 mg/kg, and 100 mg/kg of CBD. The first doses to be tested were; 25 mg/kg, 50 mg/kg and 100 mg/kg, based on the Dose Response data (Section 2.3.3). Following this, lower doses of 12.5 mg/kg and 6.25 mg/kg were also completed to determine the lowest therapeutic dose. In later experiments, the most effective CBD dose was chosen to base both the high CBD whole extract and the CBD:THC dosing on.

There was a washout period of at least seven days between any treatments to ensure cannabinoids were removed from the mouse's system. Cannabinoids are lipophilic and can accumulate in the fatty tissues, but within five days, 90% of the THC will have been excreted in a human (Huestis, 2005). Giving the mice at least seven days between doses allowed for clearance of any cannabinoids or their metabolites from their systems.

3.2.4 Behavioural testing

von Frey testing and Hargreaves were carried out on CMT2A mice and age matched wildtype littermates prior to and after administration of cannabinoids.

3.2.4.1 von Frey materials and methods

To determine changes to mechanical allodynia in the mice with the administration of cannabinoids, von Frey testing was carried out. This involves placing clear walled testing chambers on a wire mesh floor frame as shown in Figure 3-1. The wire floor grid platform was set up on a table of appropriate height so that mice were at eye level when seated and placed away from walls giving ample room to move around the platform. The arenas and wire mesh platform were cleaned and sanitised with 70% ethanol between each

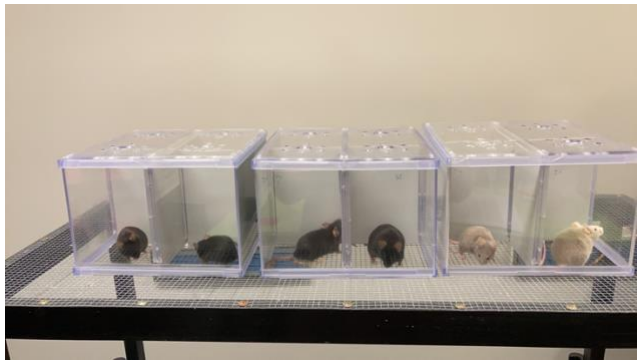

Figure 3-1*. Photograph of mice in the von Frey set up including a wire mesh floor and clear open floored observation arenas.*

use and paper towels were placed under the wire mesh on the table. Testing took place in the light phase of the circadian cycle of the animal housing facility at approximately the same time each day.

Prior to testing, a mouse-apparatus acclimatisation was carried out, which consisted of placing the animals in the observation arena for 30 - 50 minutes every second day for two weeks to allow mice to become familiar with the apparatus and to settle more quickly (Cheah et al., 2017). For testing, the animals were placed in the observation arena and the identification of the mouse and any other relevant data (e.g., time of dose or what compound was dosed) was written on the outside of the observation arena. The mice were given at least 20 minutes to acclimatise to the apparatus before testing began, and if the mice were still active after this period additional time was given. Once the mice had been determined to have settled the testing and presentation of the von Frey filaments (0.04 g – 4 g, Ugo Basile) began. The filament was pressed to the middle of the plantar surface of the hind paw (**Figure 3-2**) with sufficient pressure causing the filament to bend. The filament was held in place for 3 seconds and a withdrawal response noted. Testing involved using an up- down method, beginning with the presentation of the 0.4g filament. A positive withdrawal response of flicking, lifting, or licking of the paw was noted on the data sheet with an X. A non-response was recorded as an O (**Figure 3-3**). Each filament was presented three consecutive times and three positive withdrawals constituted a positive response. When a positive response was seen the next lower filament in the series was presented. If there was a negative response the next highest filament was presented. This continued until a consistent reading was gained from the mice, with at least five positive readings. Each positive response was recorded in a table (**Figure 3-3**) with mouse identification and treatment group also noted.

***Figure 3-2**. Indication of the correct positioning of the von Frey filament to the mid-plantar surface of a mouse hind paw.*

Force (g)																																											
0.04																																										
0.07																																										
0.16																																										
0.4	x	x	o										x	o	o																			o	o	o						
0.6				x	o	o				x	x	x				x	x	o				x	o	o				o	o	o				x	x	x				o	x	x		
1							x	x	x										x	x	x				x	x	x				x	x	x									x	x	x
1.4																																											
2																																										
3																																										
4																																										

Figure 3-3. *Example data entered into a von Frey data sheet with seven positive results.*

The mean of these data points was determined, giving a single mean paw withdrawal threshold for each mouse. This data was then grouped according to treatment group and again the mean of this data was found to give a paw withdrawal threshold in grams of force for each group and changes between groups due to treatment were then analysied.

3.2.4.2 Hargreaves materials and methods

The clear walled testing chambers were placed on top of a glass platform for Hargreaves testing and the mice placed into the chambers (**Figure 3-4**). The identification of the mouse and any other relevant data was written on the outside of the observation arena. The mice were given at least 30 minutes to acclimatise to the apparatus before testing began and if the mice were still active after this period additional time was given (Cheah et al., 2017). Any liquid on the glass top was removed before testing was carried out to ensure the heat did not dissipate and lead to inaccurate results. (Cheah et al., 2017).

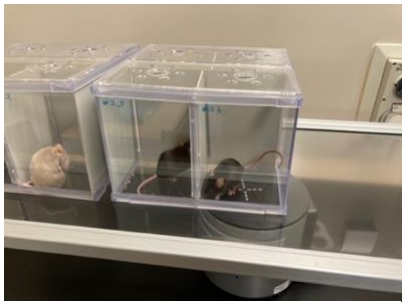

Figure 3-4*. Hargreaves set up showing mice in testing chambers on a clear glass floor, with a movable infrared generator (Ugo Basile, Italy).*

The control unit (UGO Basile, Italy #37370-001) was turned on and set up with at an infrared intensity of 30 (IR 30) and with a cut-off at 20 seconds to ensure that no damage to the paw occurred. The infrared emitter/detector (UGO Basile, Italy #37370-002) was lined up and centered directly beneath the plantar surface of the rear paw of the mouse (positioned in the same way as for von Frey (**Figure 3-2**)). The start button was pressed to start the infrared emission and the timer automatically started. The timer automatically stopped when the mouse removed the paw. The withdrawal response was monitored to ensure it was not an involuntary movement and was a positive response due to the discomfort of the heat. A

positive response was accompanied with response of flicking, lifting, or licking of the paw. The time taken to withdrawal, in seconds, of a positive withdrawal was recorded. At least three and no more than five positive trials occurred for each mouse. There was an interval of at least 3 min between each test on the same paw of each mouse to avoid sensitisation between trials. The withdrawal latency in seconds for each mouse was recorded and each set of trials were averaged to give a single mean paw withdrawal latency. The animals were then grouped according to treatment and the averages for these were determined. After testing was completed, mice were returned to their home cages. The glass top and the cages were cleaned and then sanitised with 70% ethanol before the next group of mice.

3.2.5 Gabapentin materials and methods

Based on literature review of gabapentin dosing and use in mice (**Table 3-1**), gabapentin (Sigma-Aldrich, #PHR1049) was prepared as a 20 mg/ml solution with distilled water and olive oil (Sigma; 75343-1L, Lot #BCBZ4118) to administer orally to the mice at 40 mg/kg.

To make up 1 mL of gabapentin, 20 mg of gabapentin powder was weighed and dissolved into 200 μL of distilled water. Once the gabapentin was dissolved, 800 μL of olive oil was added and the solution was mixed well. Oral administration of gabapentin in mice followed the same methods as the cannabinoid administration, as set out in section 2.2.1.2 (Dose Response). The timepoints for von Frey and Hargreaves testing were the same as that set out for the cannabis extracts and control (Section 3.2.3).

3.2.6 Multiple dose materials and methods

Mice were administered cannabinoid extracts at 2-hour intervals across an 8-hour time period to examine if therapeutic effect could be maintained using multiple administrations. Drug administration and Hargreaves behaviour methods followed those described in sections 2.2.1.2 and those in section 3.2.4.2, respectively.

The drugs that were administered were 12.5 mg/kg CBD in olive oil, olive oil vehicle control, or 40 mg/kg gabapentin in distilled water and olive oil.

CMT2A mice were dosed at 0 h, 2 h, 4 h and 6 h time points. Testing occurred prior to the first dose (baseline) and then hourly from 1 h through to 8 h post administration of the first dose. At the 2 h dosing time point mice were tested then removed from testing chambers and

administered drug. They were placed into their home cage for a rest period for 30 min after dosing. After this time the mice were then returned to the testing chamber to settle to allowing testing again on the hour. This occurred again at both four and six hour timepoints. The longest period the mice spent in the testing chambers without a break was two hours.

3.2.7 Statistical analysis

All statistical analysis was carried out using SPSS statistics version 28.0.1.0 (142). Graphs were created using SPSS, using standard error to create error bars. One way ANOVA (analysis of variance) was used to compare differences between testing groups and post hoc analysis using TURKEY HSD was carried out as the group sizes were matched throughout the behaviour experiments. All p values were deemed statistically significant at $p \leq 0.05$. Those p values that were close to being significant were noted and the actual value was written on the graphs. Error bars were set for +/- 2 standard error (SE) as this gave a good visual representation to determine if the results are statistically significantly different. This is the same as a 95% confidence interval. Spline interpolation was used between some data points on line graphs.

3.3 Results

3.3.1 Genotyping results

The mice are maintained *as* mh*Mfn2* hemizygotes (as homozygotes are not viable) and bred to wildtype (non-carrier) mice from the same colony. To determine whether mice were wildtype or CMT2A for breeding and testing purposes, CMT2A mice were ear punched and genotyped after weaning. An example of the results is as shown in **Figure 3-5**. CMT2A mice show two distinct bands at 200 and 300 bp, while wildtype mice show a single band at 200 bp. These results, along with the mouse identification ear punch data, were recorded both on the mouse home cage card and in a notebook for future reference.

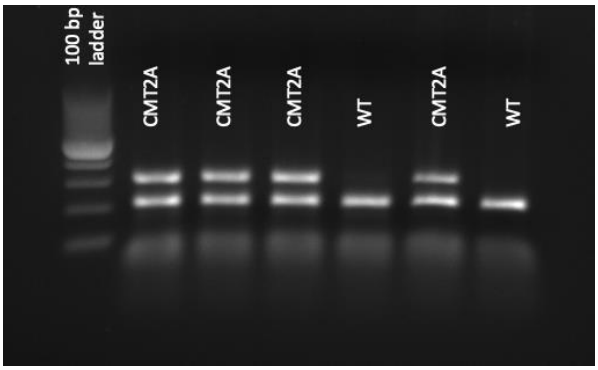

***Figure 3-5**. Example of an agarose gel image used to genotype the CMT2A status of the mice.*

3.3.2 Efficacy of a single oral dose of CBD to ameliorate neuropathic pain symptoms in CMT2A mice

To determine whether CBD could ameliorate neuropathic pain symptoms in CMT2A mice, mice were treated with a single oral dose of CBD (described in section 2.2.1.2) and analysed six times over a four hour window using von Frey and Hargreaves tests (described in sections 3.1.3.1 and 3.1.3.2). In the results, to enable ease of visualising the data in the graphs, the wildtype controls of each dose of CBD were removed, as they were not significantly different to the wildtype olive oil control group. This also indicates that there is no change from baseline in wildtype mice given any of the doses of CBD that we administered. These graphs are available in the Efficacy in CMT2A Appendix, B.3 and B.4.

3.3.2.1 Mechanical allodynia

An increase in paw withdrawal threshold (g) in CMT2A mice administered CBD would indicate that the CBD had some efficacy to lead to an improvement in mechanical allodynia. When the testing was carried out there was no statistically significant difference in paw withdrawal

threshold (mechanical allodynia) between any of the treatment groups orally administered CBD in olive oil and the CMT2A control group (**Figure 3-6**). This indicates that the CBD alone is not having an effect on mechanical allodynia symptoms in the CMT2A mice at any of the doses given in this study.

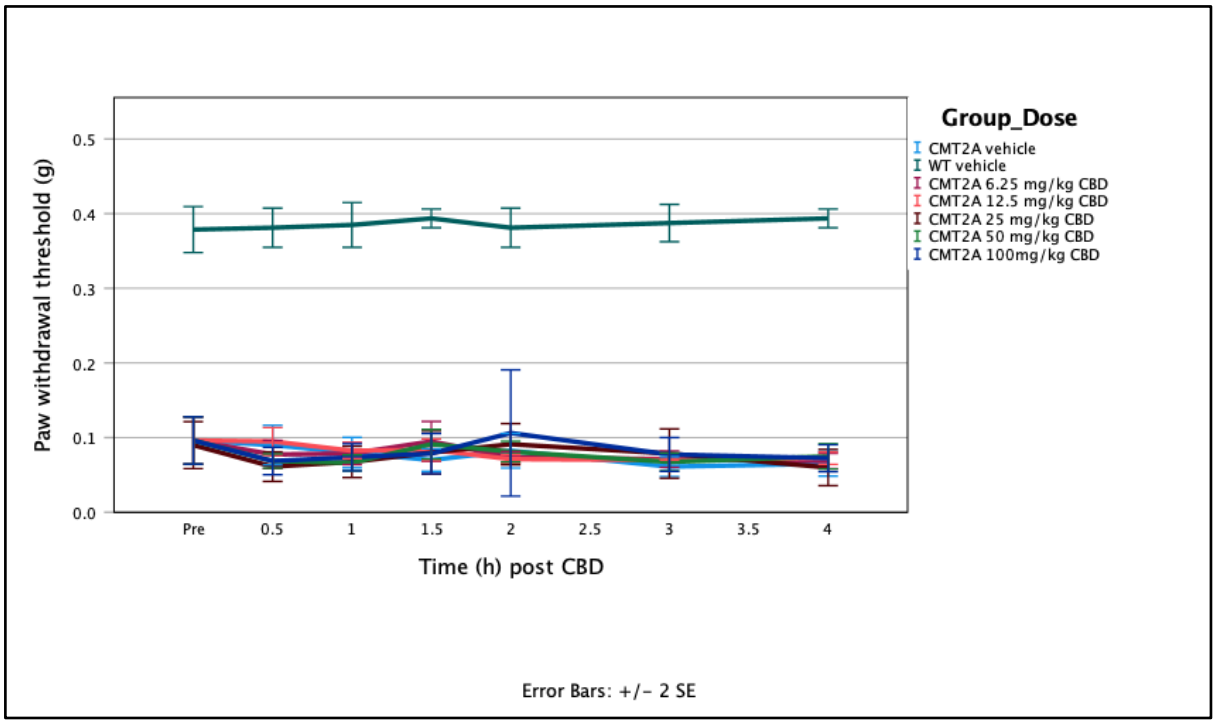

Figure 3-6. *Changes to paw withdrawal threshold (g) to a mechanical stimuli in CMT2A and wildtype (WT) mice given orally administered CBD in olive oil. n = 8 in each group with an equal mix of male and female mice.*

3.3.2.2 Thermal hyperalgesia

Thermal hyperalgesia is another symptom of neuropathic pain, and as such, an improvement in paw withdrawal latency (s) would indicate that the CBD had some efficacy in improving these symptoms. All doses of CBD administered in this study lead to some relief of thermal hyperalgesia symptoms in CMT2A mice when compared to the control group (**Figure 3-7**). All CBD doses given showed a gradual increase in paw withdrawal latency to a peak at 2 h post CBD administration and a gradual decrease back to baseline by 4 h post CBD administration. It is interesting to note that the timing of efficacy and peak analgesia seen here in **Figure 3-7**,

mirror blood plasma levels of CBD which has been reported in the literature (Deiana et al., 2012; Viudez-Martínez et al., 2019; Xu et al., 2019).

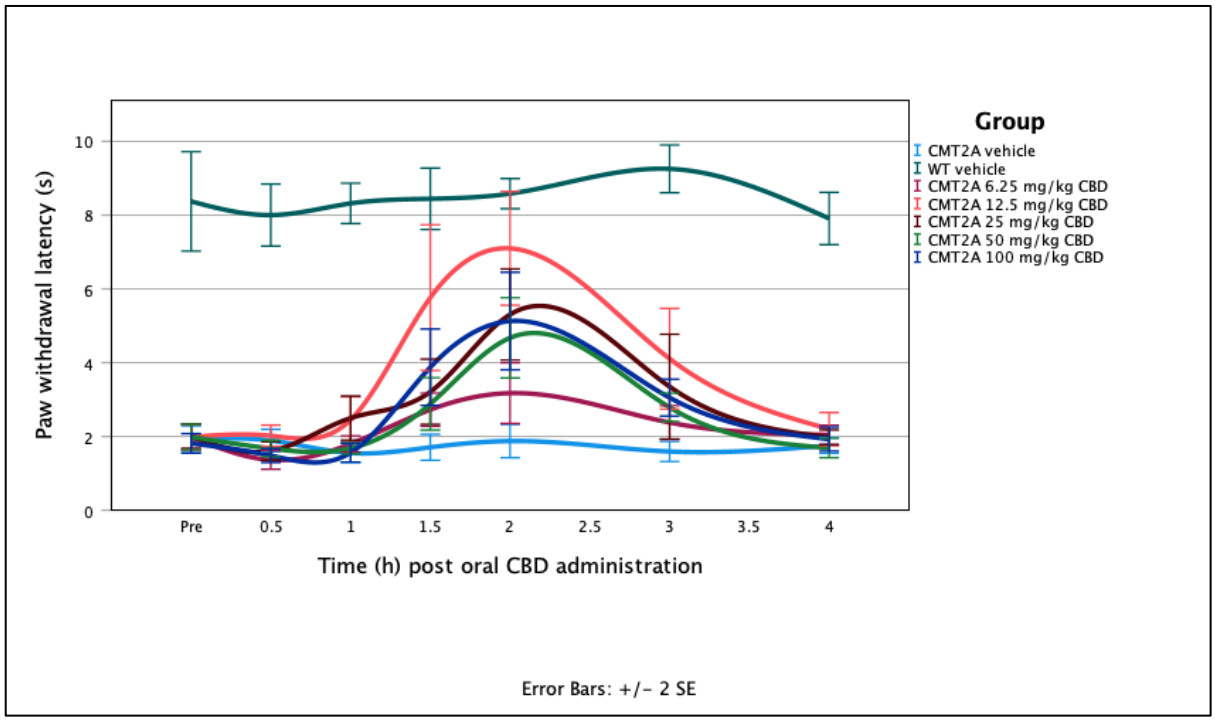

***Figure 3-7**. Hargreaves results showing changes in paw withdrawal latency (s) in CMT2A and wildtype (WT) mice given CBD orally in olive oil. n = 8 in each group with an equal mix of male and female mice.*

By 2 h post CBD administration all of the doses of CBD, except the 6.25 mg/kg dose, caused a statistically significant change in paw withdrawal latency compared to the CMT2A control group (**Figure 3-8**). In addition to the 2 h time point, the 12.5 mg/kg dose also resulted in statistically significant change in paw withdrawal latency at the 1.5 and 3 h time points then returned to baseline by 4 h post administration.

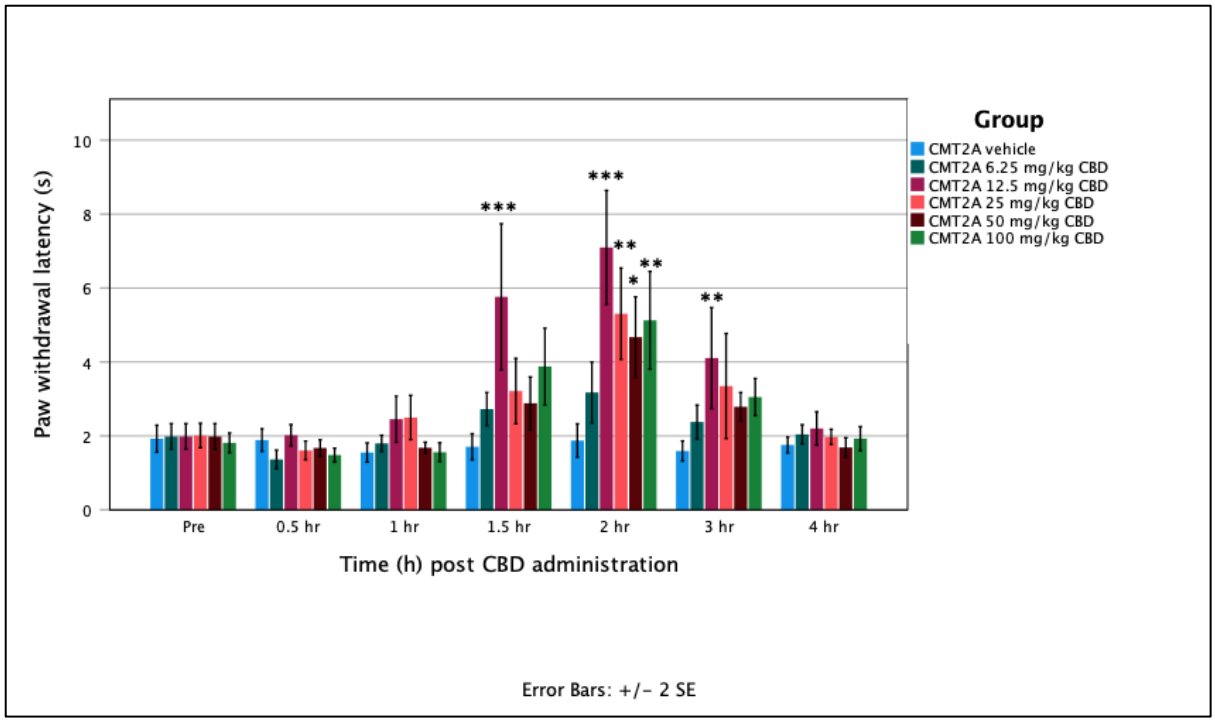

***Figure 3-8**. Changes to paw withdrawal latency (s) in CMT2A mice given orally administered CBD. n = 8. ANOVA with Turkey HSD post hoc testing. Comparison is against the CMT2A control group. p ≤. 0.058 *, p ≤ 0.01 **, p ≤ 0.001 ***. At 2 h post administration 50 mg/kg CBD - p = 0.058. Error bars ±2 SE.*

The greatest change to paw withdrawal latency across all CBD doses is seen at 2 h post administration. The data from this time point was taken and graphed to more easily visualise the differences between each of the CBD doses (**Figure 3-9**). This shows that CBD given orally at 12.5 mg/kg is the most efficacious dose to treat thermal hyperalgesia symptoms of CMT2A mice of all the doses given. The least efficacious dose is 6.25 mg/kg, followed by 50 mg/kg of CBD. There is similar efficacy shown at both 25 mg/kg and 100 mg/kg of CBD.

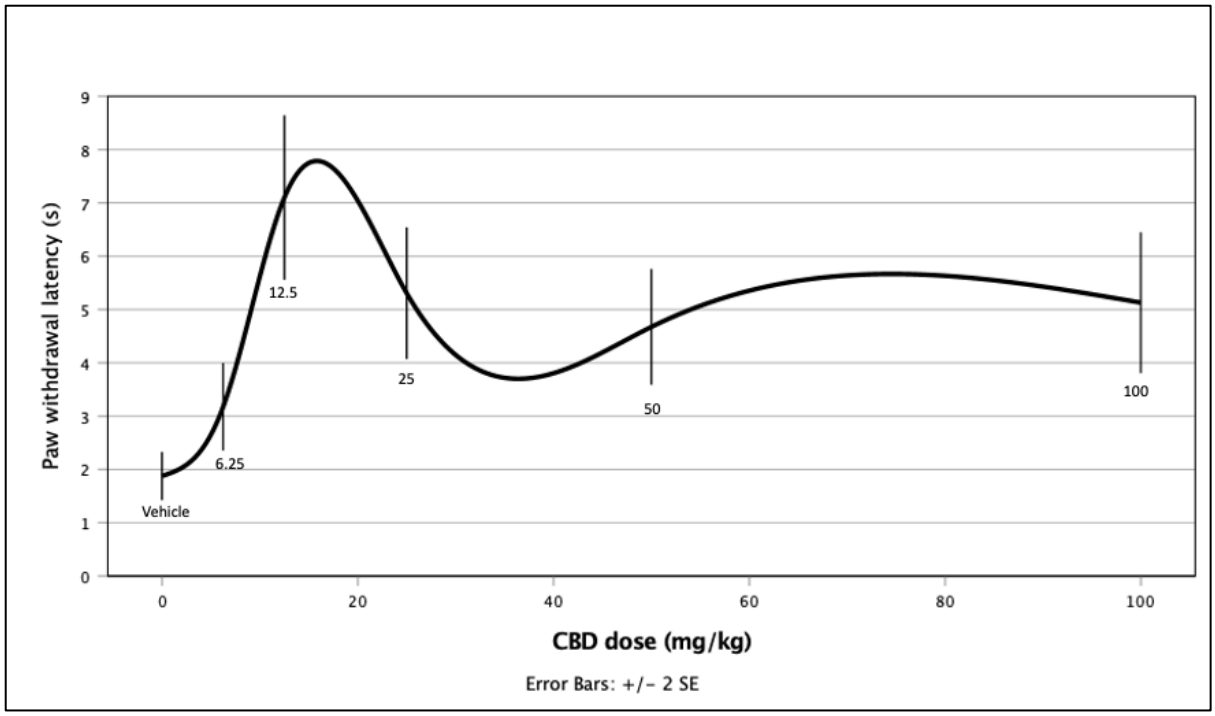

Figure 3-9*.Changes to peak paw withdrawal latency (s) in CMT2A mice given oral CBD. Measured at 2 h post administration (n = 8). Error bars represent +/- 2 standard errors. Spline interpolation was used between the points to give a more realistic behavioural dose response curve.*

3.3.3 Comparison of CBD to gabapentin

As shown in the previous results, a single oral dose of CBD has shown some efficacy in ameliorating thermal hyperalgesia symptoms in the CMT2A mice. It is therefore important to compare the efficacy of CBD to a relevant control drug. In this case gabapentin was chosen to compare to the efficacy of CBD in the mouse model as it is commonly used to help treat neuropathic pain symptoms in patients. Gabapentin was administered orally at a clinically relevant dose of 40 mg/kg. Mice were treated with a single dose of gabapentin and analysed six times over a four hour window using von Frey and Hargreaves tests.

3.3.3.1 Mechanical allodynia

The therapeutic profile of a single oral dose of 40 mg/kg of gabapentin to improve mechanical allodynia in CMT2A mice across four hours post administration is shown in **Figure 3-10**. There is a clear improvement in mechanical allodynia in the mice given the gabapentin with statistically significant differences in paw withdrawal thresholds between the treatment group and the control group at 1.5 and 2 h time points. Comparison to the 12.5 mg/kg CBD is

not carried out for this as there was no statistically significant difference between this and the control group for this testing (**Figure 3-6**).

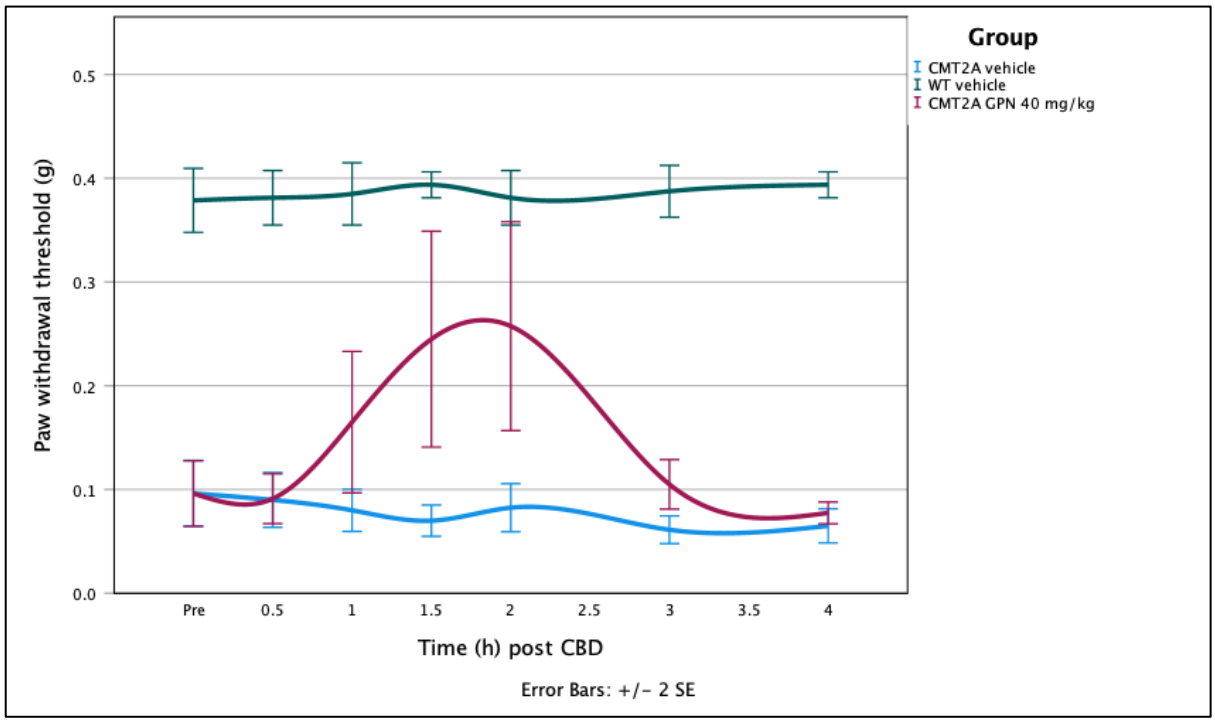

Figure 3-10. *Changes to paw withdrawal threshold (g) in CMT2A mice given orally administered gabapentin at 40 mg/kg. n = 8 in each group with an equal mix of male and female mice. GPN = gabapentin, WT = wildtype.*

3.3.3.2 Thermal hyperalgesia

As was seen previously in results section 3.3.2.2, the most efficacious dose of CBD to lead to relief of thermal hyperalgesia symptoms was 12.5 mg/kg. This dose was compared to a clinically relevant dose of 40 mg/kg gabapentin. CBD given orally at 12.5 mg/kg seems to have a very similar efficacy profile in improving thermal hyperalgesia symptoms in the CMT2A mice as the gabapentin (**Figure 3-11**). The therapeutic profile over time for gabapentin in neuropathic pain models reported in the literature is very similar to what was seen in this study; a sharp upward trend at about 2 h post administration and a gradual decline back to baseline by 4 to 6 h post administration (Atwal et al., 2019; Gustafsson et al., 2003; Kusunose et al., 2010).

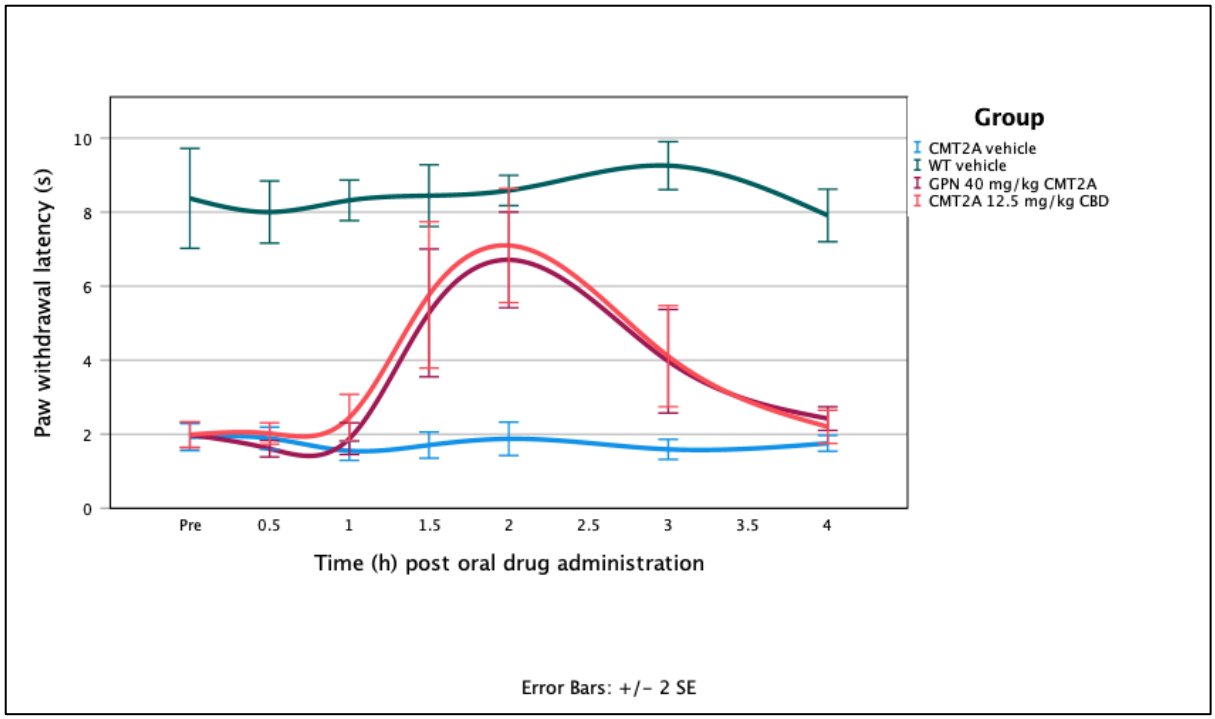

***Figure 3-11**. Changes to paw withdrawal latency (s) in CMT2A mice given gabapentin at 40 mg/kg or CBD at 12.5 mg/kg. n = 8 in each group with an equal mix of male and female mice. GPN = gabapentin, WT = wildtype.*

In contrast to the mechanical allodynia symptoms, thermal hyperalgesia symptoms in the CMT2A mice were improved with both the gabapentin and CBD. Both the 40 mg/kg gabapentin and the 12.5 mg/kg of CBD are statistically significantly different from the CMT2A control group at the 1.5 and 2 h time points as indicated in **Figure 3-12**. It is very close to being statistically significant for the 12.5 mg/kg of CBD at the 3 h time point as indicated by the p value of 0.057.

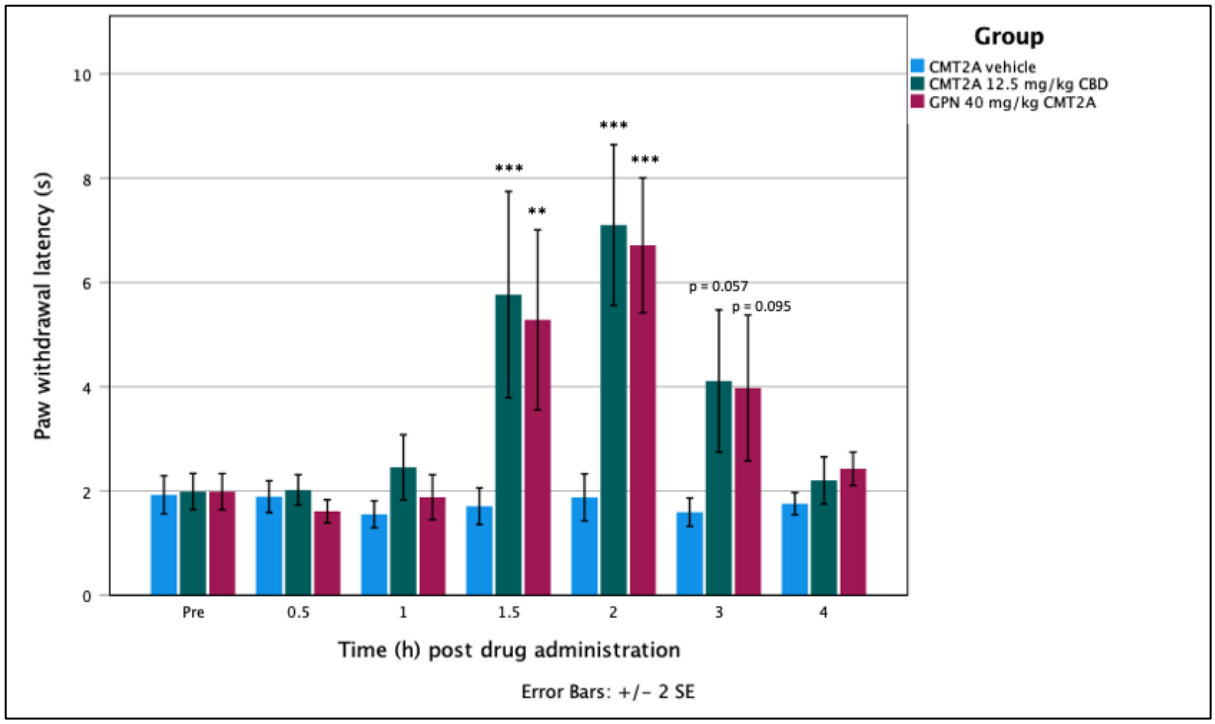

Figure 3-12**. Bar graph comparing the efficacy of gabapentin (GPN) and CBD to ameliorate thermal hyperalgesia in CMT2A mice. ANOVA with Turkey HSD post hoc testing. Comparison is against the CMT2A control group. p ≤ 0.05 *, p ≤ 0.01**, p ≤ 0.001 *

There is no significant difference between the dose of 12.5 mg/kg of CBD and gabapentin at any of the time points tested.

3.3.4 High CBD whole extract and CBD:THC

CBD has shown efficacy to ameliorate the thermal hyperalgesia symptoms in this mouse model, but the CBD is only a part of the whole plant. There are many minor cannabinoids present in cannabis, and the role of a number of those in leading to analgesia is still unknown. To test whether THC or other minor cannabinoid fractions may play an additional role in providing analgesia in neuropathic pain, CBD was compared to a high CBD whole extract and CBD:THC. As the 12.5 mg/kg oral dose of CBD in olive oil vehicle showed the most improvement in pain behaviour symptoms in CMT2A mice, whole plant extract was used at a dose that contained 12.5 mg/kg CBD. The CBD whole extract was extracted from a high CBD strain and the certificate of analysis is available in the Efficacy in CMT2A Appendix, B.1. This extract contained 55% CBD and 3.82% THC, leaving other compounds that are present in the extract making up 41.18% of the total profile. At this CBD concentration, the THC content in the dose given to mice was 0.867 mg/kg.

The other treatment examined was CBD:THC. This was also dosed to provide a CBD concentration of 12.5 mg/kg. At this concentration the THC content in the dose given to mice was at 0.867 mg/kg, containing no other compounds. The certificate of analysis for this is in the Efficacy in CMT2A Appendix, B.2. As in the study that used CBD alone, CBD whole extract and CBD:THC were tested with both von Frey and Hargreaves across four hours.

3.3.4.1 Mechanical allodynia

With the previous testing on CBD alone, there was no improvement in mechanical allodynia seen (Section 3.3.2.1). To determine if this could to be improved, the high CBD whole extract also containing THC and other minor cannabinoids, and the CBD:THC were tested in the mice. Both the high CBD whole extract and the CBD:THC showed efficacy in treating mechanical allodynia symptoms (**Figure 3-13**), which was not seen with the CBD alone (**Figure 3-6**).

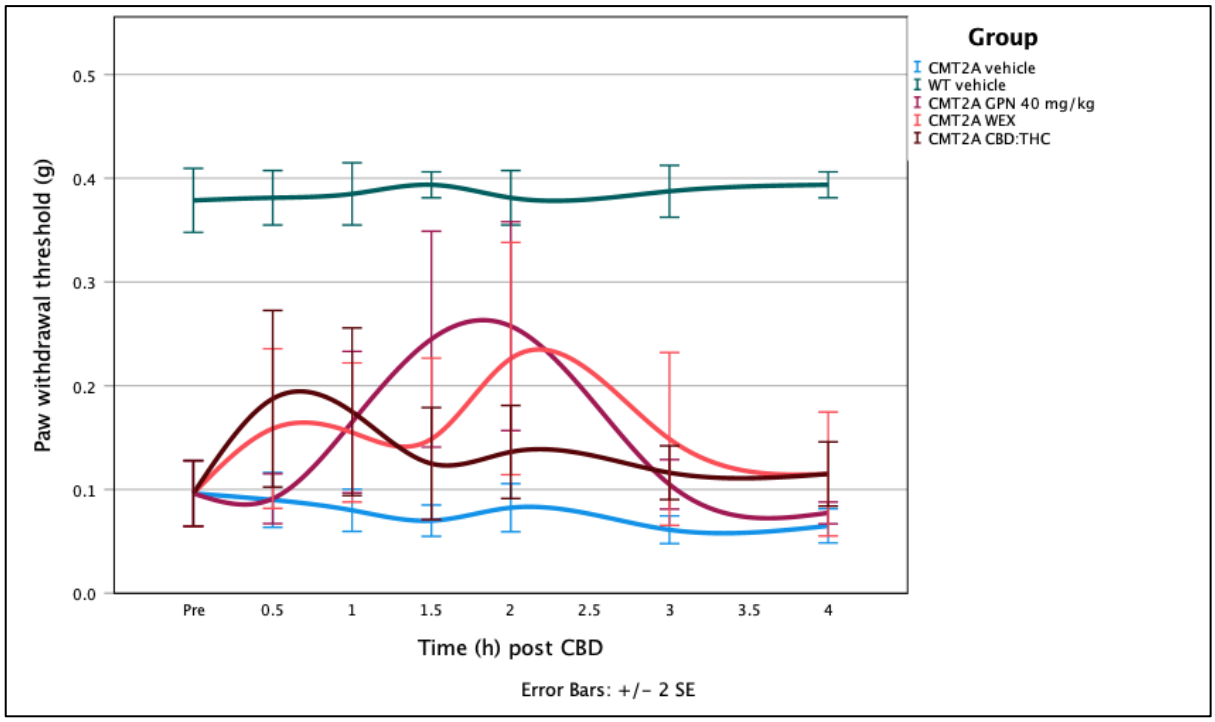

Figure 3-13. *Changes to mechanical allodynia in CMT2A mice given High CBD whole extract (WEX) and a CBD:THC mix. n = 8 with a mix of males and females. 40 mg/kg Gabapentin(GPN) was left on the graph as a comparison. WT = wildtype.*

The high CBD whole extract (labelled WEX on the graphs) showed a peak change in paw withdrawal threshold at 2 h post administration (**Figure 3-14**), which was statistically

significantly different when compared to the CMT2A control group. This statistically significant difference was also seen at the 3 h time point.

The CBD:THC showed a trend of slightly increased paw withdrawal thresholds, with statistically significant differences seen at 0.5 h and 1 h post administration (**Figure 3-14**).

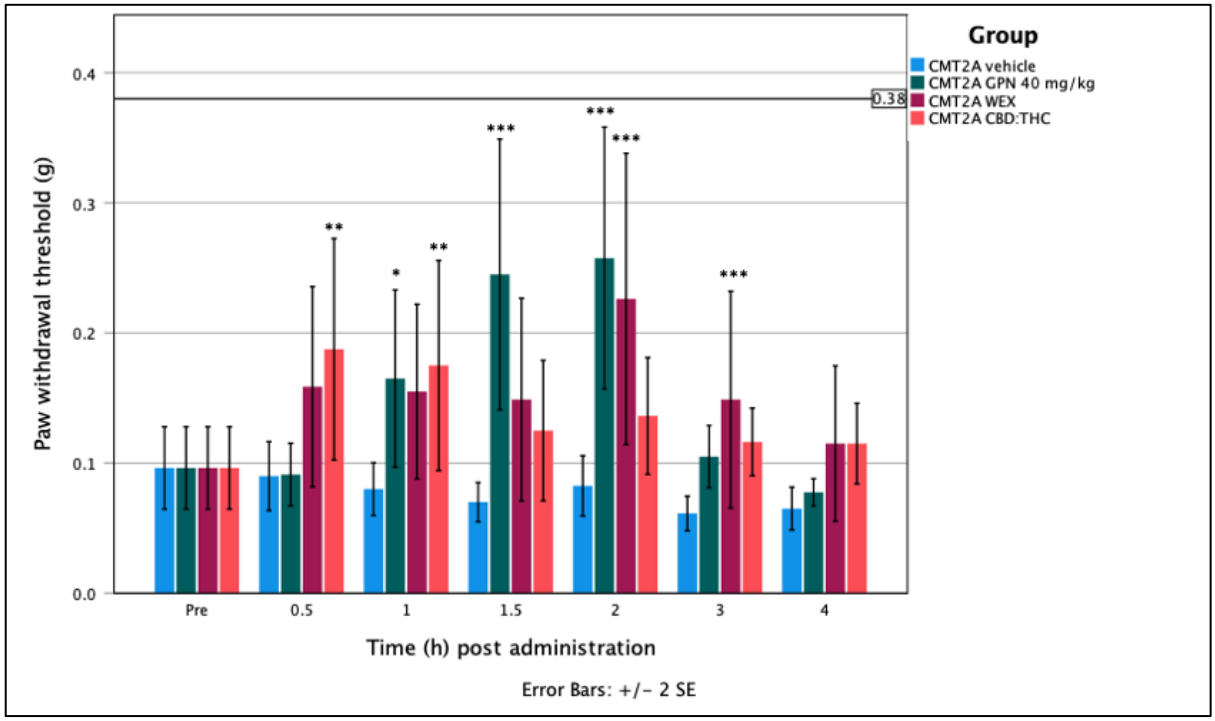

***Figure 3-14**. Changes to paw withdrawal threshold (g) in CMT2A mice (n = 8) given high CBD whole extract (WEX) and a CBD:THC mix. Gabapentin (GPN) at 40 mg/kg was left on to allow for a comparison. n = 8. Groups are compared to the CMT2A control group. ANOVA with Turkey post hoc testing. Comparison is against the CMT2A control group. p ≤ 0.05 *, p ≤ 0.01**, p ≤ 0.001 ***. The wildtype average paw withdrawal threshold of 0.38 g was left on as a reference line.*

Neither of the drug compounds administered as a single dose were as efficacious as the gabapentin in leading to changes to mechanical allodynia in the CMT2A mice. None of the drug compounds given were able to show a rescue to wildtype levels. There is also no statistically significant difference between the two drug compounds (high CBD whole extract and CBD:THC) at their ability to ameliorate mechanical allodynia in CMT2A mice (**Figure 3-15**).

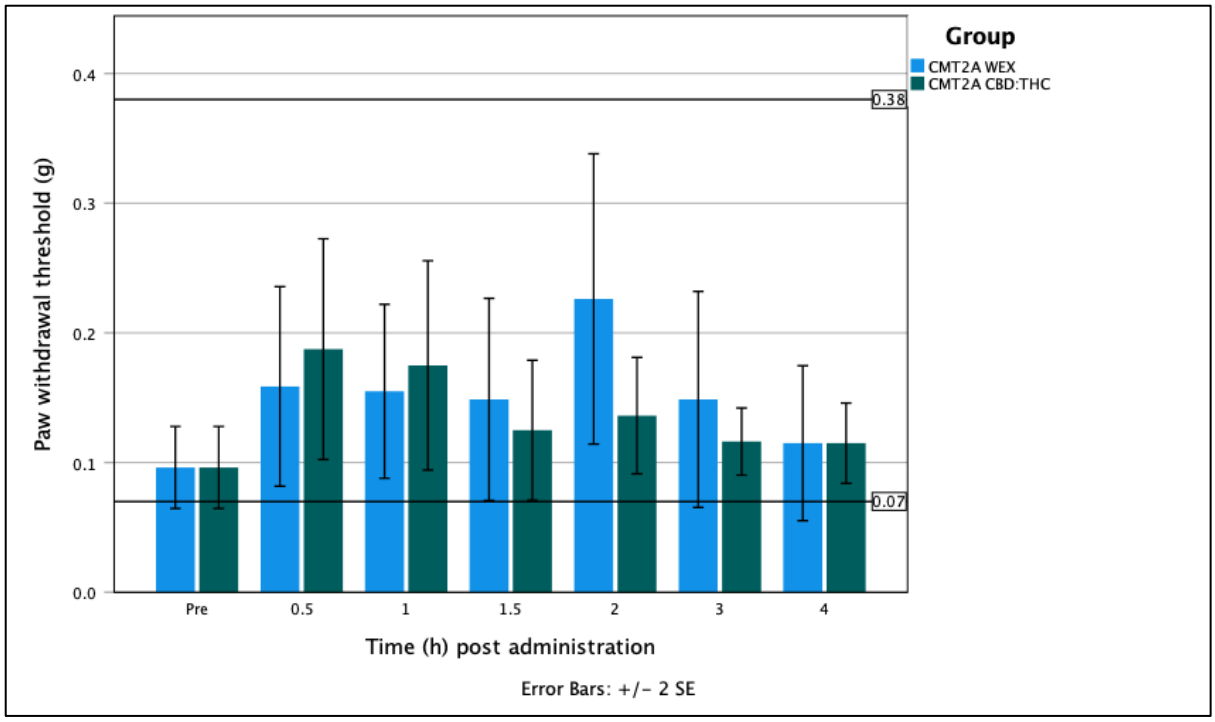

***Figure 3-15**. Comparison of high CBD whole extract (WEX) and CBD:THC to ameliorate mechanical allodynia symptoms in CMT2A mice. n = 8. A reference line of average wildtype control testing has been added at 0.38 g, and the average CMT2A control reference line of 0.07 g. Two sided t-test for comparison of means was used.*

3.3.4.2 Thermal hyperalgesia

In contrast to the von Frey results there is a clear efficacy noted in the improvement of thermal hyperalgesia symptoms in the CMT2A mice with both the high CBD whole extract and the CBD:THC (**Figure 3-16**). The CBD:THC has a very similar shaped curve to the 12.5 mg/kg CBD dose and the 40 mg/kg of gabapentin, with a slightly higher peak at the 2 h time point.

The high CBD whole extract dose followed a slightly different curve than the CBD alone or CBD:THC in that it shows a slightly earlier onset and a longer duration of action (**Figure 3-16**). Paw withdrawal thresholds were statistically significantly different from the CMT2A control group by the 1 h time point, which was not the case for either CBD:THC or gabapentin (**Figure 3-17**). Both the high CBD whole extract and the CBD:THC clearly showed statistically significant differences at 3 h post administration.

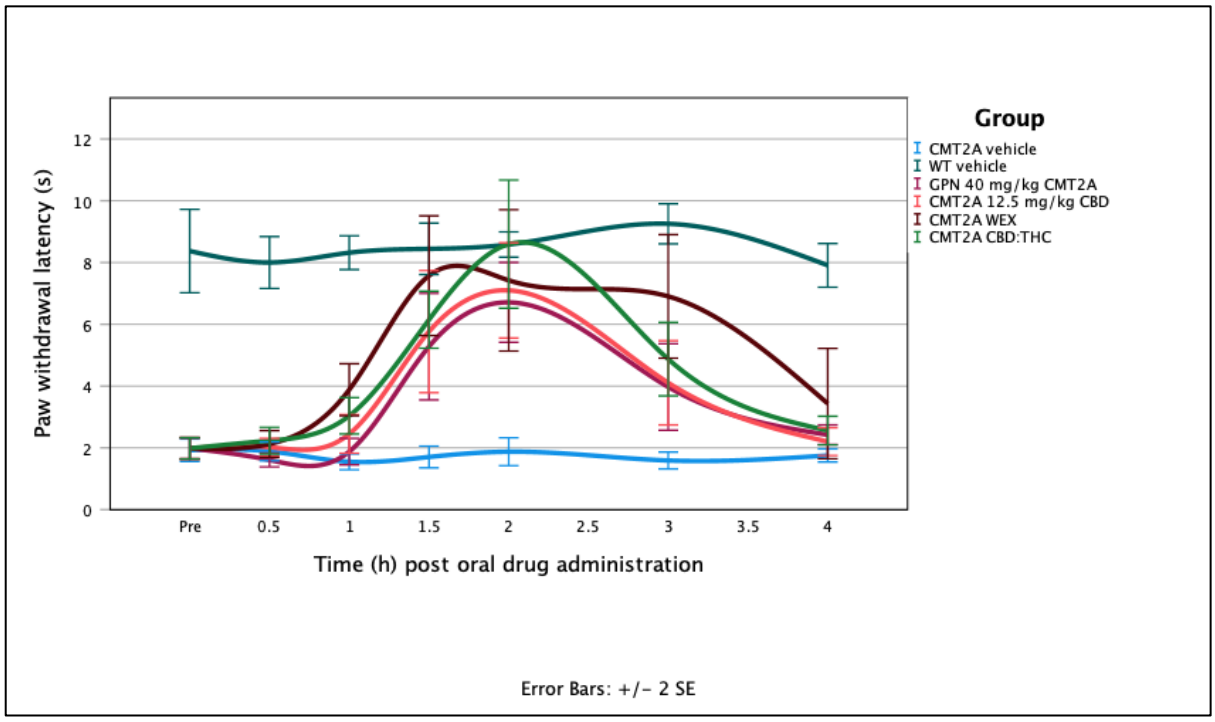

Figure 3-16. *Therapeutic curve of changes to paw withdrawal latency (s) of CMT2A mice given 40 mg/kg gabapentin (GPN), CBD:THC and high CBD whole extract (WEX). n = 8 in each group with an equal mix of male and female mice. WT = wildtype.*

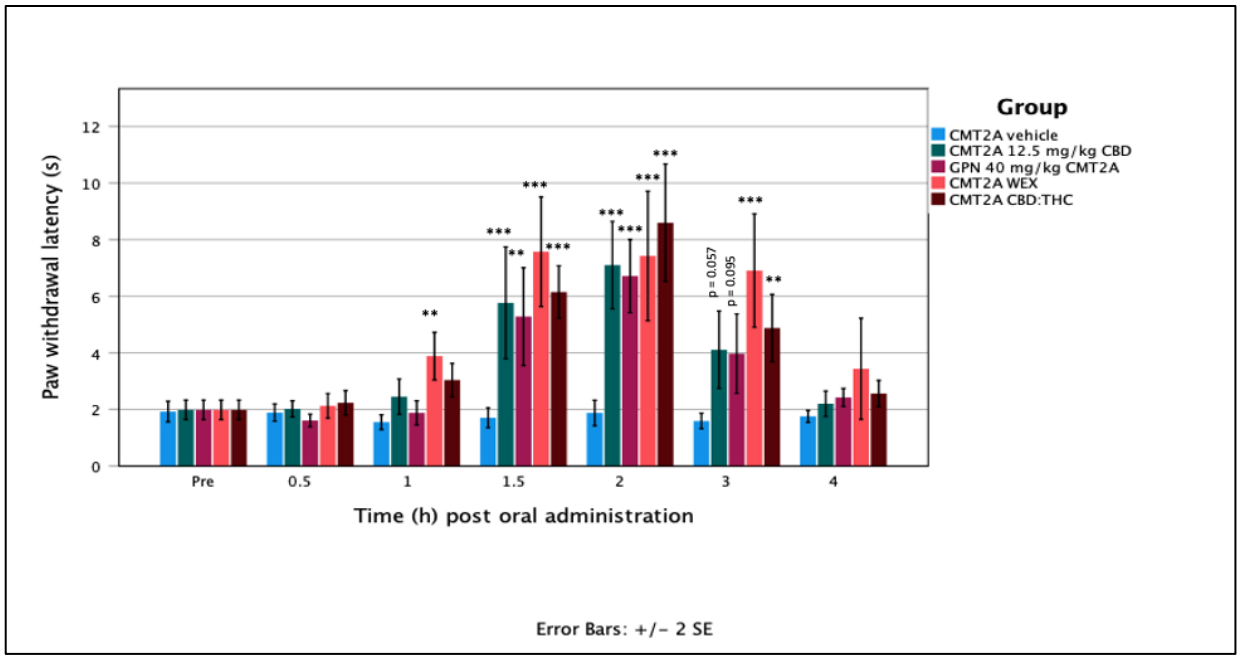

Figure 3-17*. Bar chart showing changes to paw withdrawal latency in CMT2A mice given cannabis drugs and tested across four hours. ANOVA with Turkey post hoc testing. Comparison is against the CMT2A control group. p ≤ 0.05 *, p ≤ 0.01**, p ≤ 0.001 ***. GPN = gabapentin, WEX = high CBD whole extract, WT = wildtype.*

3.3.5 Multiple doses over time

In the earlier section (3.3.2), 12.5 mg/kg CBD was shown to be the most effective dose to ameliorate the thermal hyperalgesia symptoms in the CMT2A mouse model. Although this is important, in a clinical setting patients will want a sustained analgesic effect. Therefore, multiple doses of 12.5 mg/kg CBD were given across a set time period of eight hours to determine the therapeutic profile. As in the previous section 3.3.3, the CBD was compared to gabapentin. CMT2A mice were dosed with control olive oil, 12.5 mg/kg CBD or 40 mg/kg gabapentin every two hours at time points indicated in **Figure 3-18**. Wildtype mice were not tested across the eight hours as they test consistently across all other trials, but a reference line of an average paw withdrawal latency (8.41 s) for this group of mice was added to the graph.

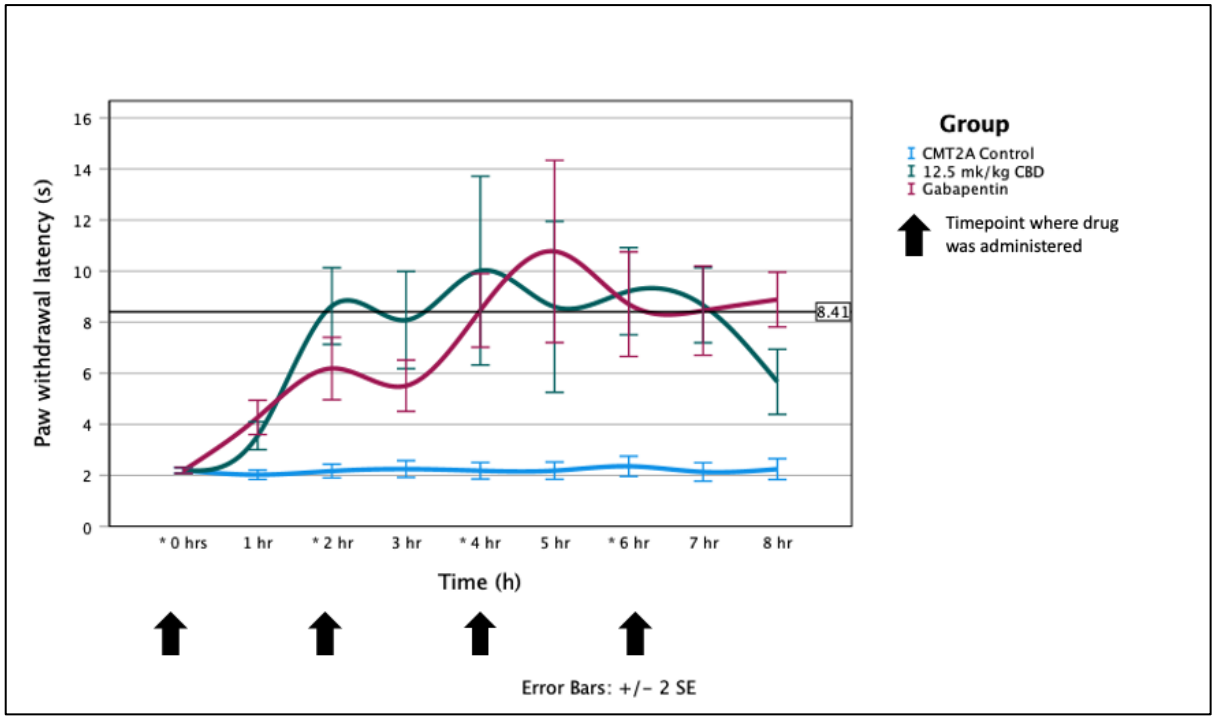

Figure 3-18. *Sustained dose of 12.5 mg/kg CBD and a comparison of 40 mg/kg gabapentin verses CMT2A control. n = 8. A reference line of wildtype littermates average paw withdrawal latency was added at 8.41 s.*

Paw withdrawal latencies for both the 12.5 mg/kg CBD and gabapentin treated CMT2A mice were statistically significantly different to those of control CMT2A mice at all time points tested from 1 h through to 8 h (**Figure 3-18**). CBD treatment had a more robust onset than

gabapentin, with paw withdrawal latencies increasing to wildtype levels by the 2 h time point. CBD showed slight decreases between treatments (time points of 3 and 5 h), but none of these were statistically significantly different to the 2, 4 and 6 h time points. Following the 6 h dose of CBD, there was a decrease in paw withdrawal latency between the 7 and 8 h time points; however, at the 8 h time point (2 h after the last CBD dose) paw withdrawal thresholds were still significantly higher than the CMT2A control group.

Compared to gabapentin, CBD treatment every two hours showed a statistically significant difference in paw withdrawal latency the 2 and 3 h time points (**Figure 3-19**). Across the 4 to 7 h time points there was no statistically significant difference in paw withdrawal latency between the CBD and the gabapentin treatment. By 8 h, a time point in which paw withdrawal latency decreased in the CBD treated group, the gabapentin treated group had a statistically significantly higher paw withdrawal latency.

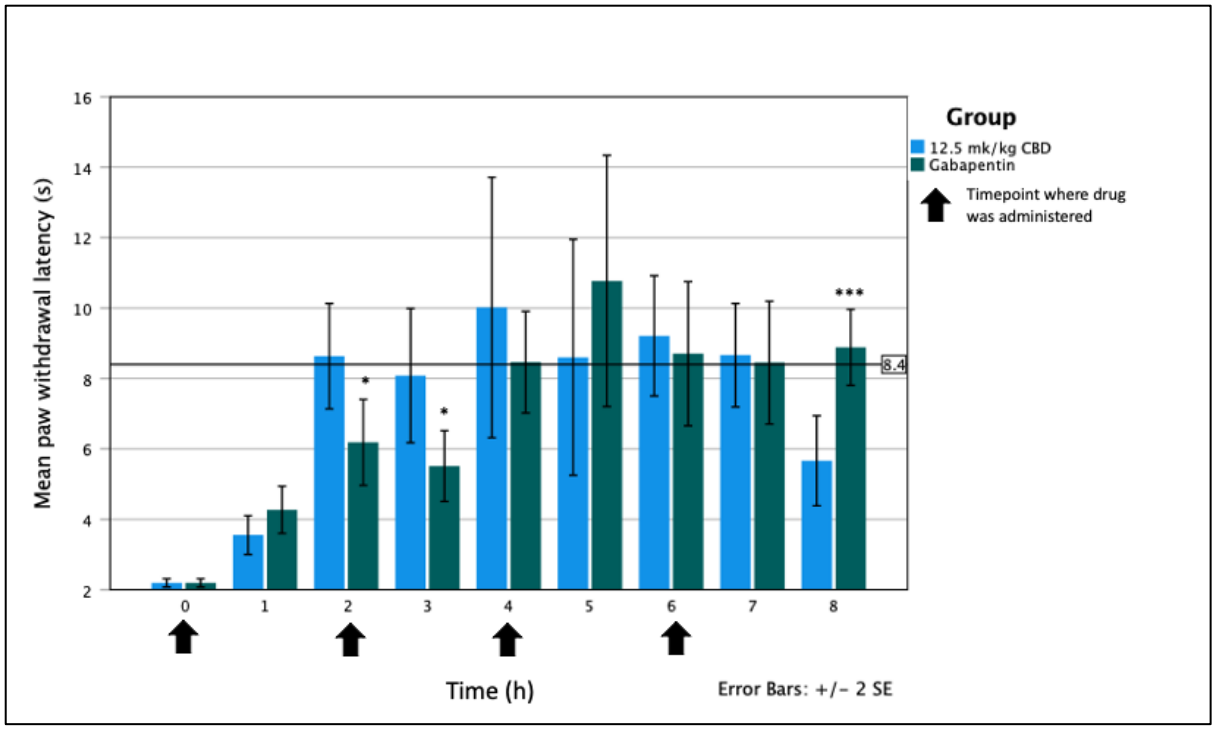

Figure 3-19*. Comparison of gabapentin and 12.5 mg/kg of CBD to alleviate thermal hyperalgesia in CMT2A mice. n = 8. Reference line of average wildtype paw withdrawal latency of 8.4 s. Two tailed t-test. p ≤ 0.05 *, p ≤ 0.01**, p ≤ 0.001 ***.*

3.3.6 Comparison of all doses at two hours post administration – thermal hyperalgesia

As has been shown here, a single oral dose of the various cannabinoids administered in this study have peak efficacy at 2 h post administration for improvement of thermal hyperalgesia. To directly compare the efficacy of each of these treatments a box and whisker plot with this data was generated and is shown in **Figure 3-20**. The paw withdrawal latency (s) from the peak efficacy at two hours post administration was used. As mechanical allodynia did not show a clear peak of efficacy at the same time (**Figure 3-13**) this data was not plotted. Gabapentin at 40 mg/kg, CMT2A vehicle and wildtype (WT) vehicle were also shown as a comparison.

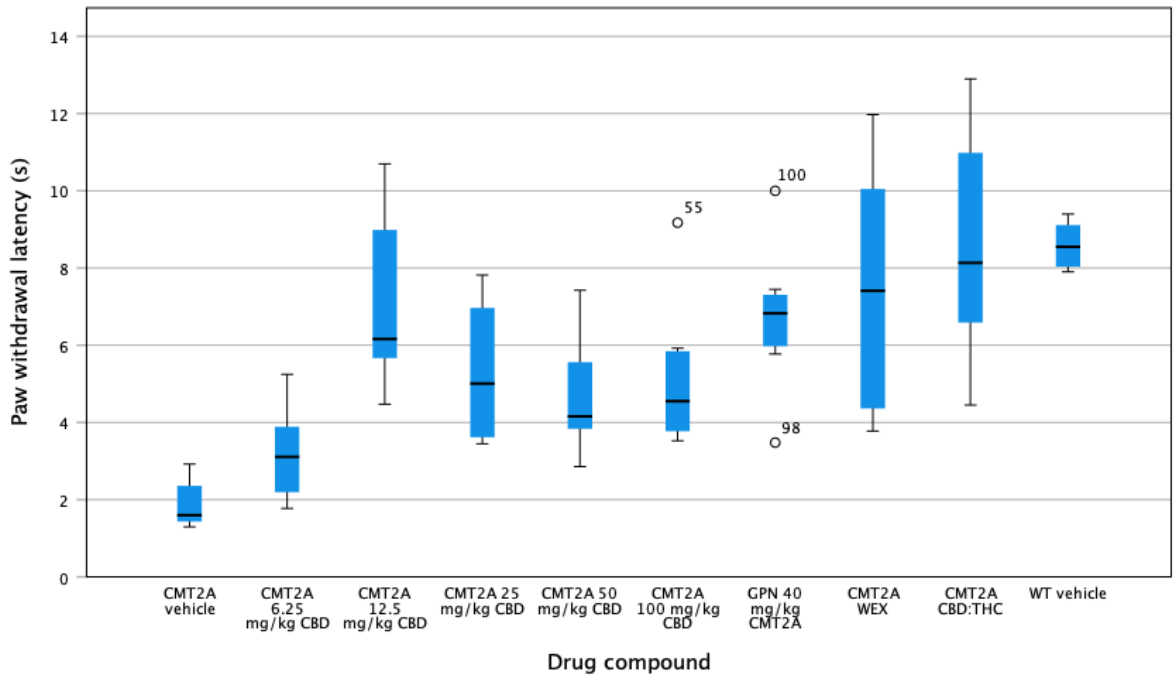

***Figure 3-20**. Box and whisker plot showing changes to thermal hyperalgesia in CMT2A and wildtype mice at two hours post drug administration. n = 8, with an even mix of male and female mice. GPN = gabapentin, WEX = high CBD whole extract, WT = wildtype.*

There is a large inter-quartile range seen in the high CBD whole extract (WEX) and the CBD:THC indicating that there was more variation seen in these data sets. Most of the cannabis based drugs showed a large range when compared to the control groups of CMT2A vehicle, wildtype vehicle and 40 mg/kg gabapentin.

3.4 Discussion

The aim of the study described in this chapter was to determine if orally administered cannabinoids could lead to an amelioration of neuropathic pain symptoms in a CMT2A genetic mouse model of peripheral neuropathy. The neuropathic pain symptoms of hyperalgesia and allodynia were considered and tested, using pure CBD from 6.25 mg/kg to 100 mg/kg. CBD dosed at 12.5 mg/kg was shown to be the most effective in ameliorating thermal hyperalgesia symptoms. This dose was also shown to be comparable in efficacy to gabapentin; both as a single oral dose treatment or as multiple doses across an eight hour period. Mechanical allodynia symptoms were harder to treat with a single oral dose of CBD, but some efficacy was seen when the mice were administered high CBD whole extract and a CBD:THC mix. Overall the high CBD whole extract showed the greatest improvement in pain scoring in the CMT2A mice.

3.4.1 Efficacy of a single oral dose of CBD to ameliorate neuropathic pain in CMT2A mice

Most doses of orally administered CBD given in this study showed efficacy in improving thermal hyperalgesia symptoms in this mouse model of CMT2A. Conversely, there was no change observed to mechanical allodynia in the same mouse model given a single oral dose of CBD. The improvement in thermal hyperalgesia was not linear with dose, as a lower dose of 12.5 mg/kg CBD showed the greatest change in thermal hyperalgesia symptoms (**Figure 3-8**). CBD has been shown to be effective at ameliorating neuropathic pain symptoms in other diseases as seen in **Table 2-1**. There is currently no published research looking at the use of CBD to ameliorate thermal hyperalgesia or mechanical allodynia in CMT2A mice (as of November 2022). This pre-clinical work is valuable as it can lead to clinical research to help patients suffering with neuropathic pain associated with CMT2A.

3.4.1.1 Differences in response to CBD – thermal hyperalgesia and mechanical allodynia

There was a clear difference in the ability of single orally administered dose of CBD to ameliorate neuropathic pain symptoms of thermal hyperalgesia and mechanical allodynia in this CMT2A model. This difference could be due to a number of factors; differences in nerve

fibre type associated with allodynia and hyperalgesia, differing mechanisms that develop and establish hyperalgesia and allodynia, or CBD may need to build up in the system with doses given more frequently across a few days to lead to a change in mechanical allodynia.

Thermal hyperalgesia and mechanical allodynia mechanisms are mediated in different ways, with different fibre type responsible for the development and maintenance of the symptoms. Mechanical allodynia is mediated by large myelinated Aß fibres which normally terminate in the deeper levels, IV and V of the laminae in the dorsal horn of the spinal cord (Jensen & Finnerup, 2014; Sandkühler, 2009; Todd, 2010). When nerve damage has occurred and has led to the development of central sensitisation, the Aß fibres sprout into the upper laminae levels I and II, causing tactile sensations to be sent as a pain signal (Jensen & Finnerup, 2014; Sandkühler, 2009; Todd, 2010). In contrast, thermal hyperalgesia is mediated by C type fibres, which are smaller diameter, unmyelinated, and terminate in the upper laminae levels, I and II, of the dorsal horn (Jensen & Finnerup, 2014; Lefaucheur, 2019; Shir & Seltzer, 1990; Todd, 2010). When damage occurs to these nerve types there is a transcriptional change to the TRPV1 receptors leading to increased number of receptors on the uninjured fibres (Hudson et al., 2001; Jensen & Finnerup, 2014; Ma et al., 2005). This increase in numbers and an increase of sensitivity of the channels leads to the onset of thermal hyperalgesia (Hudson et al., 2001; Jensen & Finnerup, 2014; Ma et al., 2005). The notion that these nerve types have different pathways and mechanisms leading to neuropathic pain could point to the difference in responses with the testing carried out.

It is well established that there is a progressive, length-dependent degenerative nerve loss seen in CMT2A patients, with the longest nerves affected first (Scherer, 2011; Skre, 1974). The sciatic nerve is the longest in the body, and is made up of both motor and sensory nerves, with a mix of both myelinated and unmyelinated fibres (Schmalbruch, 1986). The damage occurring to the nerve tissue of the mice as the disease progresses, will lead to transcriptional changes in the C-type fibres and the development of thermal hyperalgesia as seen by a decreased threshold to a radiant heat source. The Increase in number and hypersensitisation of the TRPV1 receptors, lead to a thermal heat causing a painful response much more quickly in the CMT2A mice when compared to their wildtype littermates. Administration of CBD in this model led to an improved paw withdrawal latency (**Figure 3-7**). Many studies have shown that CBD interacts with the TRPV1 receptors as an agonist (Anand et al., 2020; Costa et al.,

2004; de Almeida & Devi, 2020; Iannotti et al., 2014). The TRPV1 channels are able to be activated and then quickly desensitised by CBD (Iannotti et al., 2014), leading to the analgesic effects seen with the thermal hyperalgesia testing (Costa et al., 2004).

Mechanical allodynia is driven by central sensitisation in the CNS (Sandkühler, 2009). Why a single oral dose of CBD was not able to lead to any improvement of mechanical allodynia in CMT2A mice is unclear. It may be that this is harder to treat, due to the involvement of the CNS. One study, using a chronic constriction method of inducing mechanical allodynia, did show that CBD given as a single dose with a subcutaneous injection (30 mg/kg) was able to improve mechanical allodynia at two hours post administration (Casey et al., 2017). It is possible that the different mode of administration may have led to improved outcomes, as with oral administration it is well known that the bioavailability of the CBD is much lower compared to other modes of administration that do not involve first pass metabolism (Huestis, 2005; Millar et al., 2018). This is unlikely to be the case in this research, as the higher doses of oral CBD (25, 50 & 100 mg/kg) did not show greater efficacy. Most rodent studies that have shown an improvement in mechanical allodynia have used CBD across multiple days (De Gregorio et al., 2019; Jesus et al., 2019; Silva-Cardoso et al., 2021; Ward et al., 2014), whereas, this work used a single oral dose. Other work showed again that multiple daily doses of CBD are able to prevent development of mechanical allodynia in a mouse model of chemotherapy induced neuropathic pain (Ward et al., 2014; Ward et al., 2011). Another rodent study looking at behavioural effects of CBD and a CBD analogue (KLS-13019) showed that pre-treatment with oral and IP administered CBD before onset of chemotherapy-induced neuropathic pain was effective at preventing mechanical allodynia, but was not able to reverse mechanical allodynia once it had been established (Foss et al., 2021). The CMT2A mice used in this work had well established mechanical allodynia, and therefore similar to this paper, did not show any improvement in the von Frey testing with CBD alone. CMT2A mice have also been shown to have a difference in rescue of mechanical allodynia and thermal hyperalgesia in a nerve repair model using HDAC6 inhibitors (Picci et al., 2020), indicating that damage caused to the nerves leading to mechanical allodynia may be harder to treat.

Future work in the CMT2A mice should look at daily dosing of CBD across multiple days, as that could have led to improvement in mechanical allodynia symptoms in the mice, as has

been seen in other studies (De Gregorio et al., 2019; Jesus et al., 2019; Silva-Cardoso et al., 2021; Ward et al., 2014).

3.4.1.2 U-shaped dose response

A U-shaped dose response to the CBD with the thermal hyperalgesia testing is clearly seen (**Figure 3-9**). The lowest dose of 6.25 mg/kg has the least change, 12.5 mg/kg is the most effective dose and the "higher" doses show lowered efficacy (**Figure 3-9**). This U shaped response is also seen in the gene expression results, with the greatest change at 25 mg/kg and 100 mg/kg with the least at 50 mg/kg and 150 mg/kg (**Figure 2-8**, Dose response chapter). This clear similarity between the gene expression changes and behaviour results are a good indicator that there are likely physiological changes behind the behavioural changes.

As set out in section 2.4.3, the literature shows that there is a U-shaped response to CBD. Some rodent studies show a U-shaped response to the CBD in pain behaviour testing (Genaro et al., 2017) or in testing for anxiolytic effects (Campos & Guimarães, 2008; Guimarães et al., 1990). Rats that were subjected to incision pain and given a single IP dose of CBD at 0.3 to 30 mg/kg, showed the greatest improvement in mechanical allodynia with 3 mg/kg of CBD (Genaro et al., 2017). The lowest (0.3 and 1 mg/kg) and the highest (30 mg/kg) were not statistically different from the control group (Genaro et al., 2017). In elevated plus maze testing for antianxiety effects of CBD, doses between 2.5 to 20 mg/kg were injected intraperitoneally and the entry ratio was calculated (Guimarães et al., 1990). The most effective dose was 5 mg/kg, with both 2.5 and 10 mg/kg showing a statistically significant difference when compared to vehicle treated rats, and the 20 mg/kg not showing any difference to the vehicle treated rats (Guimarães et al., 1990).

Why this response is seen is not clear. It could be that each pain aetiology has its own particular response to differing doses. What is consistent is that there is a U shaped response to the CBD. This has been seen both in the behaviour and the gene expression data in this work. There is very little consistency in what dose of CBD is effective for ameliorating pain symptoms in the pre-clinical studies previously mentioned; however given the variation in doses given, the composition of the CBD isolate, the vehicle used to deliver the CBD, pain type assessed, and testing methods, it is not surprising that there is no consensus on what dose is effective for treating a particular type of neuropathic pain. Further work examining gene

expression work at the lower doses used in this work would be advantageous, to see if the gene expression correlates with the behaviour and follows the U shaped dose response curve.

3.4.2 Comparison of CBD and gabapentin

In this study, 12.5 mg/kg CBD has been shown to be as effective as gabapentin to ameliorate thermal hyperalgesia symptoms in CMT2A mice. While this is not seen with mechanical allodynia (though it is possible that multiple doses could have an effect on mechanical allodynia, as discussed in section 3.4.1.1), there are many advantages of the use of CBD to treat neuropathic pain symptoms when compared to gabapentin. Gabapentin has a long list of side effects (as set out in sections 1.3.4 and 3.1.4) and many patients would benefit from the reduced side effects of CBD, with the same analgesic result as gabapentin. There is increasing evidence of the misuse of gabapentin, and although it is much less abused than opioids it is still of some concern (Bonnet et al., 2018; Peckham et al., 2018; Quintero, 2017). There is no evidence that CBD can cause a tolerance (Hoggart et al., 2015), as can happen with other opioid drugs (Buntin-Mushock et al., 2005; Morgan & Christie, 2011). Conversely, THC in cannabis can lead to tolerance (MacCallum & Russo, 2018; Nordstrom & Hart, 2006; Ramaekers et al., 2020; Ramaekers et al., 2011), but clinical and pre-clinical studies have shown that with the addition of CBD to THC there are lowered side effects and psychoactive effects (Karniol & Carlini, 1973; Karniol et al., 1974; Russo & Guy, 2006; Welburn et al., 1976). The importance of this is that there are low side effects seen with CBD alone, while providing the same analgesic response as gabapentin. This leads to more choices for patients suffering with neuropathic pain who find gabapentin ineffective or are unable to tolerate the adverse side effects.

3.4.3 High CBD whole extract and CBD:THC

The results show that there is a greater improvement in the pain symptoms of thermal hyperalgesia in the CMT2A mice, with the high CBD whole extract (WEX) than any of the other compounds trialled (**Figure 3-17**). One reason for this improvement could be due to the addition of the THC. There are many studies showing the efficacy of THC to treat neuropathic pain (Casey et al., 2017; King et al., 2017; Ware et al., 2010). However, this study shows that while there is clearly an improvement with the high CBD whole extract, THC does not appear

to account for all of this difference. When the CBD:THC mix was used, which contains the same concentrations of CBD (12.5 mg/kg) and THC (0.867 mg/kg) as the high CBD whole extract, the efficacy is not as great (**Figure 3-17**). This indicates that there is something else present in the high CBD whole extract that is adding to the pain relief.

It is also interesting to note change in mechanical allodynia in the CMT2A mice with the high CBD whole extract (WEX) or with the addition of THC to the CBD (**Figure 3-14**); something not seen with CBD alone (**Figure 3-6**). Clearly the THC is leading to an improvement with mechanical allodynia, but as discussed for thermal hyperalgesia, differences in mechanical allodynia responses between high CBD whole extract and CBD:THC treatments suggest that the addition of THC does not account for this alone.

The high CBD whole extract dose contained CBD as 55% of the total profile and THC at 3.82%, leaving other compounds that are present in the extract making up 41.18% of the total profile (Efficacy in CMT2A Appendix B.1). The other compounds that make up the remaining portion of the whole extract contains other cannabinoids, terpenes or even flavonoids, which could be contributing to the enhanced analgesic effect. Thus, the improved analgesia seen with the high CBD whole extract could be due to another compound in the extract having an effect at a much smaller concentration or the presence of the entourage effect.

3.4.3.1 Other compounds that could have clinical relevance for treating pain

Over 500 compounds have so far been identified within the whole cannabis plant extract (Katalin & Attila, 2017). While the most prominent and well-documented compounds THC and CBD make up a large proportion of the whole extract, there are many more compounds that could have pharmacological effects. These include cannabinoids, terpenoids, flavonoids, and other compounds, all of which have been identified in the cannabis plant (McPartland & Russo, 2001). Many of the cannabinoids are precursors or derivatives of the major cannabinoids (**Figure 3-21**). There is evidence that some minor cannabinoids have a greater binding affinity for the cannabinoid receptors than THC and CBD and could have a greater effect (Russo, 2011). Many of these compounds show promise to modulate pain and inflammation responses but are not as well characterised within the literature, with little information available on their mechanisms and actions. Some of the cannabinoids that show potential to lead to relief of neuropathic pain are: cannabigerolic acid (CBGA), cannabidiolic

acid (CBDA), tetrahydrocannabinolic acid (THCA), cannabinol (CBN), cannabigerol (CBG) and cannabichromene (CBC) (Evans, 1991; Moreno-Sanz, 2016; Rock et al., 2018; Ruhaak et al., 2011; Russo & Marcu, 2017; Takeda et al., 2008). Their pain relief potential is due to their interaction with pain pathways, either through interaction with cannabinoid receptors (Pertwee, 2005; Verhoeckx et al., 2006) or through inhibition of COX 1 or COX 2 (Ruhaak et al., 2011; Takeda et al., 2008).

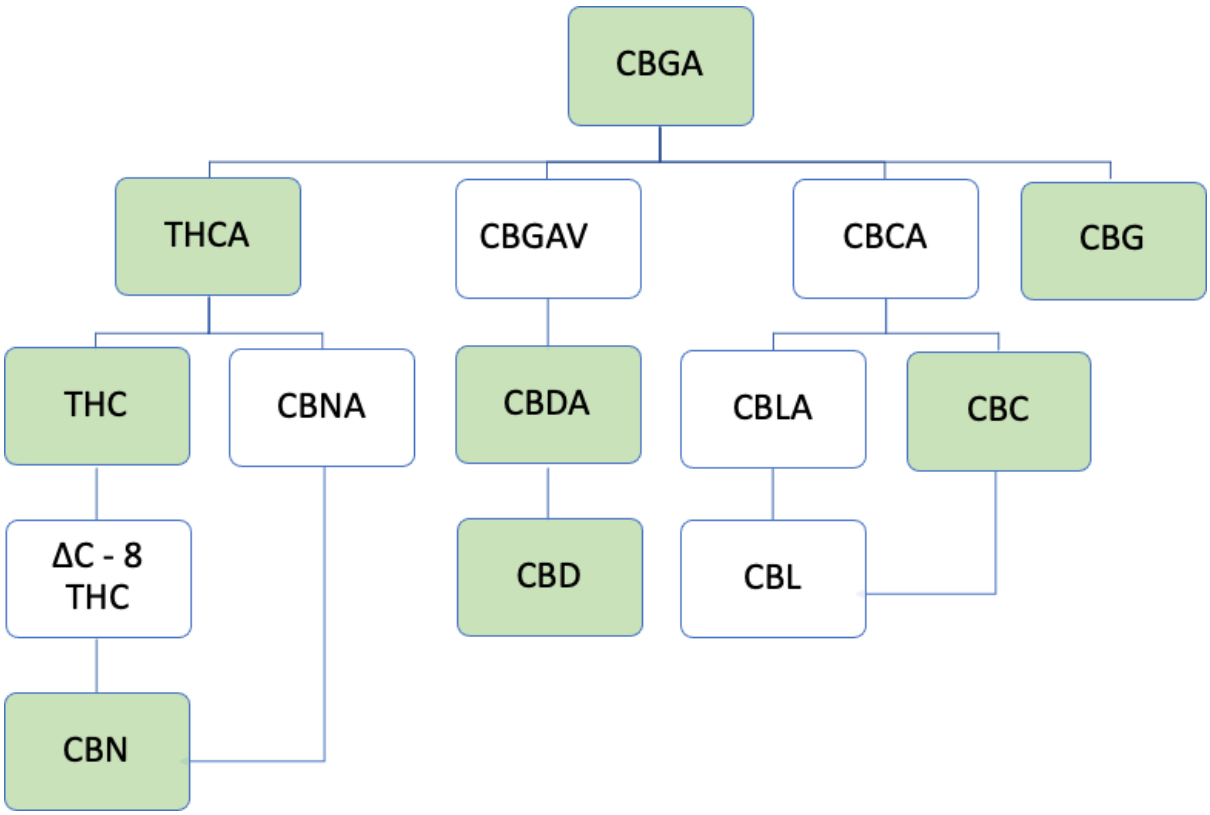

***Figure 3-21**. Flowchart showing the synthesis pathway relationships of precursors and metabolites of some phytocannabinoids within the cannabis plant. Cannabigerolic acid (CBGA) is the precursor molecule to all three major pathways of the phytocannabinoid synthesis. Those highlighted in green show some indication of having anti-inflammatory or analgesic properties.*

Cannabigerolic acid is the precursor to the three prominent cannabinoids: THCA, CBDA, and CBCA (**Figure 3-21**) (Taura et al., 2007). CBGA has only a few mentions in literature, with a limited number of studies on its effects. One paper researching CBGA showed inhibition of both COX 1 and COX 2 *in vitro* (Ruhaak et al., 2011). This lead to the school of thought that CBGA could have analgesic and anti-inflammatory effects, but this is yet to be established.

Cannabidiolic acid is found predominantly in fresh plant material of fibre type plants (Taura et al., 2007) and is the precursor of CBD (Formato et al., 2020). As with some of the other cannabinoids, it is not as well studied and there is little literature on this compound (Formato et al., 2020). There is some indication that CBDA could have anti-inflammatory and analgesic effects due to it showing efficacy at both 10 µg/kg (intraperitoneally injected), and 1- and 100 µg/kg (orally administered) in a paw edema model (Rock et al., 2018). This could be because CBDA has been shown to selectively inhibit COX 2 (Takeda et al., 2008). With CBDA showing some analgesic and anti-inflammatory effects at such low concentrations it could be worthwhile investigating and testing this compound further to see if it has any efficacy to treat neuropathic pain symptoms in CMT2A.

Tetrahydrocannabinolic acid is synthesised from CBGA and is the precursor to THC (Figure **3-21**) (Moreno-Sanz, 2016). Over time most of the THCA in the plant slowly decarboxylates to THC; with this process accelerating when the cannabis is exposed to high heat (Moreno-Sanz, 2016). Contrary to THC, THCA does not possess any psychoactive effects (Moreno-Sanz, 2016), nor is there any evidence that it is converted to THC, *in vivo* (Jung et al., 2009; Moreno-Sanz, 2016; Rock et al., 2013). There is some indication that THCA could have anti-inflammatory, immunomodulatory and neuroprotective properties (Moreno-Sanz, 2016; Ruhaak et al., 2011). The anti-inflammatory effects seem to be modulated by weak inhibition of COX 1 and COX 2 enzymes (Ruhaak et al., 2011). There is conflicting evidence on whether THCA can bind to cannabinoid receptors in the CNS; the current hypothesis is that THCA is only able to bind to CB 1 receptors within the PNS (Moreno-Sanz, 2016). This means that THCA could have a pharmacological effect without the unwanted psychoactive effects associated with activation of the cannabinoid receptors in the CNS.

Cannabinol was the first phytocannabinoid isolated from cannabis in the late 1890s with the structure elucidated in the early 1930s (Russo & Marcu, 2017). CBN is the metabolite of THC in aged cannabis products; often cannabis products that are poorly stored have the THC break down into CBN (Russo & Marcu, 2017). The CBN has much-reduced (approximately 1/10th) psychoactivity when compared to THC (Huestis, 2005). It is thought to inhibit COX enzymes (Russo & Marcu, 2017), though it is more well known for its antibacterial properties (Appendino et al., 2008). It also has a lower binding affinity than THC to both CB 1 and CB 2 receptors (Russo & Marcu, 2017). CB 1 receptors are involved in the psychoactive effects of

cannabinoids (Mackie, 2006) and the lowered binding affinity of the CBN to the CB 1 receptors could explain the decreased psychoactive effects.

Cannabigerol is a precursor to many cannabinoids, including THC and CBD. There is some evidence that CBG is an analgesic and has an action on the sodium channels in the CNS (Evans, 1991). Literature suggests that it is not as potent as THC as an analgesic, however, and that any action of CBG is occurring in peripheral nervous system receptors, rather than the central nervous system (Evans, 1991).

Cannabichromene discovered in 1996, is another compound that is also quite abundant in cannabis, with relatively high concentrations (DeLong et al., 2010; Udoh et al., 2019). It is a non-psychoactive cannabinoid (Marcu, 2016) and has been shown to have some anti-inflammatory effects (DeLong et al., 2010; Udoh et al., 2019; Wirth et al., 1980). There is some thought that CBC works to reduce inflammation through both CB 2 receptors and other alternative pathways other than cannabinoid receptors (Izzo et al., 2012). Oral administration of quite large doses of CBC (240 mg/kg and 480 mg/kg) were given to rats and were found to result in statistically significant changes to carrageenan-induced paw oedema (Wirth et al., 1980). Lower doses given by intraperitoneal injection (120 mg/kg) were also significant (Wirth et al., 1980). There have also been some analgesic effects seen with CBC. Using a tail flick test there was some mild analgesia seen with doses of 25 to 75 mg/kg (no dose related difference was seen between these doses) (Davis & Hatoum, 1983).

Aside from the cannabinoids, the cannabis plant also contains other compounds, including terpenes and flavonoids. There are around 200 terpenes found in cannabis (Russo, 2011). These compounds are the oily fragrant hydrocarbons that are responsible for the plants recognisable smell (Russo, 2011). β-myrcene is the most abundant terpene found in cannabis and it has shown anti-inflammatory properties in a paw rat model of hyperalgesia (Lorenzetti et al., 1991) and has been shown to inhibit prostaglandin E_2 (Baron, 2018). β-caryophyllene, another terpene found in abundance in cannabis plants, has been shown to have analgesic effects that are mediated through the CB2 receptors, and also inhibits prostaglandin E_2. (Klauke et al., 2014; Lorenzetti et al., 1991). Many other terpenes found in cannabis have also been shown to have anti-inflammatory or analgesic properties including α-pinene, humulene, linalool and limonene (Baron, 2018).

In contrast to the terpenes, flavonoid compounds act as antioxidants and are often what give plants and foods their vibrant colours (Baron, 2018). A particular flavonoid that could be of interest in cannabis is cannflavin A. This has previously been shown to inhibit prostaglandin E_2 in human rheumatoid cells at a level that is 30 times more potent than Aspirin (Barrett et al., 1986).

Any or all of these cannabis compounds could be leading to the improved analgesia seen in the high CBD whole extract when compared to 12.5 mg/kg CBD alone and CBD:THC. One way to determine what isolate might be leading to the improved analgesia is to isolate and test each one individually and in combination with the major cannabinoids. This would be outside of the scope of this research.

3.4.3.2 Entourage effect as seen in cannabis

There is also a school of thought that there could be an "entourage effect" within the cannabis extracts where the sum of the parts is more effective than the individual parts alone (Ben-Shabat et al., 1998). This term seems to have been used rather loosely in the literature with no real solid definition. Most papers discuss the action of CBD and THC together rather than the actions of the other compounds present in the cannabis (Cogan, 2020), and this is usually in the context of a reduction of adverse effects of the psychoactive component THC (Cogan, 2020). Although there is ambiguity with the definition and actual mode of action when discussing "entourage effect", the results of this work clearly show there is an increased improvement in thermal analgesia with the high CBD whole extract when compared to CBD alone and CBD:THC. There is still speculation if this is a real "entourage effect" or if it is due to the presence of another compound. Cannabinoids interact with a large number of known biological pathways, many of these are associated with both analgesia and inflammation (Izzo et al., 2009). There are also neuroprotective pathways that are activated by some of these cannabinoids (Izzo et al., 2009). Even with all that is known about these biological pathways, there is still a vast amount of understanding to be gained from studying these molecules and their modes of action in an organism. The "entourage effect" could be as simple as the components in cannabis leading to more activation of different pathways; as noted in the previous section (3.4.3.1) there are numerous compounds within the cannabis plant that have shown to have some analgesic or anti-inflammatory effects. Some work has been done to

look at analgesic effects of combining some of these compounds. A study done by Wirth et al. (1980) looked at a combination of CBC and THC, both of which show anti-inflammatory effects. Combining the two isolates seems to enhance the effect when compared to a single isolate alone (Wirth et al., 1980). In another study done by Davis et al. (1983), THC was shown to be more effective at providing an analgesic effect than the CBC, but the combination of the THC and CBC together was more effective again (Davis & Hatoum, 1983). This was a study using acute pain, rather than chronic or neuropathic pain, and as previously stated there are differences in the pain signalling with central sensitisation. Nevertheless, this study supports the idea that a combination of cannabinoids leads to better outcomes than a single isolate.

3.4.4 Multiple doses over time

There were no adverse effects noted in the mice given multiple doses over an eight hour period for either CBD or gabapentin. CBD administered multiple times across a longer time period was shown to be comparable to gabapentin to alleviate thermal hyperalgesia in the CMT2A mice. When compared to gabapentin, CBD showed an earlier onset, but had a slightly earlier drop-off, in pain scoring. Future work could include continuing this testing past the eight hour time point to determine when each group of mice given the drugs (12.5 mg/kg CBD or 40 mg/kg gabapentin) return to baseline testing.

Both the 12.5 mg/kg CBD and 40 mg/kg gabapentin treatments resulted in a “normalised” pain threshold (comparable to wildtype average testing) when given as multiple doses, which was not seen in the single oral dose of either drug. Gabapentin typically is given at a lower starting dose then titrated up based on the patient’s response. This dose for treating neuropathic pain starts at 900 mg a day given across three doses, then can be titrated to a maximum of 3600 mg/day (Backonja & Glanzman, 2003; Pfizer, 2020). It can take up to four weeks before patients get analgesic results, as it needs to build up in the body. This mechanism could be reflected in this study, with improved responses seen in the thermal hyperalgesia testing after multiple doses of 40 mg/kg gabapentin when compared to a single dose of the same concentration. The same improvement to wildtype baseline testing was seen with multiple doses of 12.5 mg/kg CBD. This increased effect seen with additional doses of CBD is clearly not due to a cumulative effect of dose, (e.g. two separate doses of 12.5 mg combining to give a total of 25 mg). If this was the case the higher doses of CBD (25, 50 and

100 mg/kg) would have had a greater analgesic effect, which was not seen in this study. The therapeutic profile of a single dose of 12.5 mg/kg of CBD showed a gradual increase from baseline to a peak at two hours post administration and then a decrease from there back to baseline. This matched blood plasma levels that have been reported in the literature when CBD was given orally in an oil vehicle to rodents (Deiana et al., 2012; Hložek et al., 2017; Xu et al., 2019; Zgair et al., 2017). The addition of a second dose at the two hour timepoint maintained the therapeutic peak for a longer period. This second and subsequent doses led to the maintenance of the analgesic response, and this was continued for the whole eight hour testing period. Future work could be completed to determine if this response could also be maintained for a longer period.

Work to determine if the blood plasma levels are also maintained in the same way with multiple doses would be advantageous. There is a clear correlation with the single dose, and this could prove to be the same with multiple doses. There is no evidence in the literature that CBD is able to lead to tolerance (Hoggart et al., 2015), indicating that there is no reason that consecutive doses with CBD could not be continued. Therefore, patients could continue taking oral CBD for as long as necessary to achieve analgesic results without a drop off in therapeutic profile.

3.5 Conclusions

Cannabis isolates have shown clear efficacy to improve neuropathic pain symptoms in CMT2A mice. Lower doses of CBD were more efficacious in treating thermal hyperalgesia than higher doses, showing a clear U-shaped dose response. A pure isolate of CBD alone at 12.5 mg/kg showed the greatest efficacy in treating thermal hyperalgesia symptoms, but no change in mechanical allodynia symptoms in the same mice. This difference could be due to the underlying mechanisms in how thermal hyperalgesia and mechanical allodynia are established and maintained after nerve injury, and how CBD is able to interact with different receptors. CBD administered orally at 12.5 mg/kg was comparable to a clinically relevant dose of 40 mg/kg gabapentin, both as a single oral dose and with multiple doses given across an eight-hour period in improving thermal hyperalgesia symptoms in CMT2A mice. This offers patients who suffer from neuropathic pain another effective option to improve their pain symptoms with lowered side effects when compared to gabapentin at a clinically relevant dose.

A single orally administered dose of high CBD whole extract showed the greatest efficacy in improving neuropathic pain symptoms with a wider therapeutic window than 12.5 mg/kg CBD alone or a pure CBD:THC mix given at the same concentration (12.5 mg/kg CBD and 0.867 mg/kg THC). The addition of THC in the high CBD whole extract showed a slight improvement compared to CBD alone but did not account for the whole improvement in pain scoring. This indicates that in addition to THC, other components in the cannabis may be contributing to efficacy. There is a growing number of cannabinoids, terpenes and even flavonoids found in the cannabis plant that are showing some efficacy in treating pain or inflammation symptoms or markers in both cell and animal models. These isolates could be “adding up” and creating an entourage effect leading to the improved pain scoring in the mice, or a single isolate could be responsible for the improved effect seen. Investigation into these lesser studies cannabis derived compounds could lead to insight into their possible analgesic contributions.

4 Streptozotocin-Induced Diabetic Mouse Model

4.1 Introduction

Diabetic neuropathy is the most prevalent cause of peripheral neuropathy and neuropathic pain in humans (Argoff et al., 2006; Leone et al., 2012). As such, a mouse model of diabetic-induced neuropathy is an important and clinically relevant system in which to study this. Type one diabetes can be induced in mice with the administration of streptozotocin (STZ) (Brito-Casillas et al., 2016; Furman, 2015; Jaggi et al., 2011; Tesch & Allen, 2007; Wu & Huan, 2008); and as such, is a commonly used method to mimic the pathology and the resulting complications of type 1 diabetes (Deeds et al., 2011). STZ, when administered to mice, is taken into the pancreas by the glucose transporter, GLUT2, causing the selective death of pancreatic β-islet cells in the islets of Langerhans (Haschek et al., 2013; Yamamoto et al., 1981). As these are the only insulin producing cells found in the body, the death of these cells causes a deficiency of insulin production resulting in uncontrolled blood glucose homeostasis in the mice (Brito-Casillas et al., 2016; Furman, 2015; Jaggi et al., 2011; Tesch & Allen, 2007; Wu & Huan, 2008). As the hyperglycemia continues unchecked, damage to peripheral nerves occurs leading to nerve tissue loss (Brown & Asbury, 1984). The mechanisms behind this loss in diabetic neuropathy is not yet fully understood. This loss causes neuropathic pain symptoms in the forms of tactile allodynia and thermal hyperalgesia (O'Brien et al., 2014).

STZ is commonly administered to mice in one of two ways: either as multiple low doses or a single large dose (Jolivalt et al., 2016). Mice given lower repeated doses have a reduced mortality rate than those given a single large dose but do not reliably develop neuropathy (Jolivalt et al., 2016). Conversely, mice given a single large dose of STZ will reliably display chronic neuropathic pain (Brito-Casillas et al., 2016; Furman, 2015; Jaggi et al., 2011; Tesch & Allen, 2007; Wu & Huan, 2008). This method of inducing hyperglycemia mimics the mechanisms of type 1 diabetes, and while type 2 diabetes is more prominent in society, both type 1 and type 2 diabetes can lead to diabetic neuropathy (Malik, 1997). Indeed, it has been shown that there are no discernible neurophysical differences in the nerves of patients suffering from type 1 and type 2 diabetes (Malik, 1997). This suggests that damage to the nerve tissues occurs due to hyperglycemia and downstream mechanisms rather than the type of diabetes, *per se*.

There is considerable variation in the literature regarding the rate and onset time of neuropathic pain symptoms in diabetic mice. In a review by O'Brien et al. (2014) 18 studies are summarized in a table with onset of diabetic neuropathy symptoms in mice varying from 4 to 16 weeks, depending on mouse strain, mouse age, and the diabetic induction model used.

This Chapter documents the establishment and characterization of a mouse model of diabetic neuropathy. It reports the number of mice that developed diabetic hyperglycemia, how many went on to develop peripheral neuropathy, and the time taken for the onset of different neuropathic pain symptoms (thermal hyperalgesia and mechanical allodynia). It also examines whether motor dysfunction is evident in this mouse model. At the molecular level, axon microtubules in sciatic nerves are examined to determine whether alterations in α-tubulin levels or acetylation is concomitant with diabetic peripheral neuropathy, as seen in other peripheral neuropathies, namely CMT disease type 2A, 2F, 2D (Adalbert et al., 2020; Picci et al., 2020) and chemotherapy-induced neuropathy (Van Helleputte et al., 2018).

4.1.1 Diabetic-induced neuropathic pain and motor dysfunction

In mouse models of diabetic neuropathy, the onset of neuropathic pain typical starts with mild pain sensations leading to moderate and then finally severe pain due to the degeneration of the nerve fibres (O'Brien et al., 2014). As the disease progresses, other symptoms begin to develop, including: sensory loss, numbness and reduced thermal sensitivity (O'Brien et al., 2014). Further progression is marked by reduced motor performance as the mice begin to suffer damage to the large myelinated motor nerves (O'Brien et al., 2014).

The onset and severity of diabetic-induced neuropathic pain can be detected with changes in response to thermal and mechanical stimuli in neuropathic mice (Hargreaves and von Frey testing, respectively). Conversely, the onset and severity of diabetic-induced motor dysfunction can be detected with changes to coordination, balance, and grip strength using a rotarod test (Colleoni & Sacerdote, 2010). The Rotarod consists of a rotating horizontal rod. The mouse being tested is placed on the rod and has to grip, balancing and coordinate walking forwards to stay on the rod (Deacon, 2013). As the rotational velocity of the rod accelerates, the mouse is challenged to remain on the rod, with the time it takes the mouse to fall (the

latency to fall) being measured. As such, this test measures motor function rather than endurance in the mouse (Deacon, 2013).

4.1.2 Axonal transport in the peripheral nervous system

In most cell types of the body, the size of the cytoplasm is small relative to the nucleus, and transport of mitochondria and other cellular components occurs over a short distance (Lodish H, 2000). By contrast, in neuronal cells the axon termini can be a long distance from the nucleus and cell body. In the human sciatic nerves, for example, the axon termini can be up to one meter from the cell body (Burks et al., 2014). The transport of cellular components and mitochondria along the axon to where they are needed is achieved by organised microtubule networks to which molecular motors bind and traffic the various cargos (Kirkpatrick, 1999). Microtubules with neurofilaments also form the cytoskeleton of the axon, providing structural integrity and regulating the diameter of the axon (Al-Chalabi & Miller, 2003; Kirkpatrick, 1999). Microtubules are made up of α- and β-tubulin heterodimers, which polymerise to form a long hollow tube structure (Kirkpatrick, 1999). Microtubules are polar structures with two distinct ends: a fast-growing plus end and a slow-growing minus end. This polarity is not only important in determining the growth of microtubules, but also the direction of molecular motor movement along microtubules, with most kinesin's moving toward the plus end (antegrade) and dynein's moving toward the minus end (retrograde) of microtubules (Kirkpatrick, 1999). The microtubule can undergo post-translational modifications, which can increase the affinity of the molecular motors, leading to improved binding and more efficient transport (Reed et al., 2006). Acetylation of the lysine residue at amino acid position 40 (K40) of α-tubulin, on the inner luminal surface leads to a more stable microtubule that is protected during mechanical stress (Glozak et al., 2005; Janke & Montagnac, 2017).

Peripheral neuropathies, such as CMT2A and diabetic neuropathy, are characterized by a retrograde axonal degeneration, a phenomenon called "dying-back" neuropathy, which typically affects longest nerves first, possibly due to insufficient supply of cellular components and mitochondria from the cell body. Thus initial symptoms are seen in the extremities, with the feet affected first (Scherer, 2011; Skre, 1974). The sciatic nerve, which is the longest in the body, is therefore studied as an early indicator of neuropathic damage (Burks et al., 2014).

This nerve can be easily accessed and removed to study *ex vivo* because of its placement and size. In CMT2A, CMT2D, CMT2F and chemotherapy-induced neuropathy mice there is an early and progressive loss of α-tubulin acetylation in the sciatic nerve (Adalbert et al., 2020; Picci et al., 2020; Van Helleputte et al., 2018). It is hypothesised that the decrease in acetylated α-tubulin seen in these neuropathies decreases the stability of microtubules as well as the binding affinity of molecular motors (Reed et al., 2006). Whether or not acetylation levels of α-tubulin are altered in diabetic neuropathy is unknown.

4.2 Materials and Methods

Six-month-old wildtype male mice (strain B6:D2) were used in this study. Male mice were used in this study as female mice display less response to STZ due to oestrogen protection of the β–islet cells in the pancreas (Deeds et al., 2011; Le May et al., 2006). The mice had an average age of 20 ± 2 weeks and an average weight of 27 ± 3 g at the beginning of the study. Experiments were performed in three independent studies containing 12, 12, and 18 mice, but data from all three cohorts were analysed together. To induce diabetes, mice were administered a single large dose of STZ (180 mg/kg). Prior to STZ administration, baseline blood glucose was measured and baseline behavioural testing was performed. The baseline behavioural data included von Frey and Hargreaves testing, and in a subset of mice, rotarod testing. Following STZ administration, blood glucose monitoring and behavioural testing was performed weekly for 13 weeks, after which time, mice were euthanised and sciatic nerves were harvested from the mice. Proteins from sciatic nerves were used in immunoblot analysis. All mouse numbers and procedures were approved by the University of Waikato Animal Ethics Committee, Approval Number:1093 (Dose Response Appendix, A.1).

4.2.1 Behavioural testing

Hargreaves and von Frey testing was performed as per the methods set out in the methods section 3.1.3.1 and 3.1.3.2. For the first group of diabetic mice (*n* = 8) rotarod testing was also performed to determine if there was any loss of or change to motor function. Behavioural training was performed every two days for two weeks times prior to the administration of STZ to habituate the mice to the tests, overcome learning effects, and develop stable recordings. This was followed by behavioural testing to record baseline values, and behavioural testing for 13 weeks post-STZ administration.

4.2.1.1 Rotarod materials and methods

A Ugo Basile Model 47600 rotarod was used to assess motor performance in mice, this tests a combination of coordination, balance, and grip strength. To habituate the mice to the apparatus and test, the rotarod was set at a constant speed of five revolutions per minute

(RPM). Mice were placed on the rotarod and were given three trials of approximately 10 min each with a five-minute rest period between trials.

For baseline testing, the rotarod was set with the following experimental settings: initial speed of 4 RPM, a maximum speed of 40 RPM, and a uniform acceleration from 4 RPM to 40 RPM over 300 seconds. The mice were then placed on the rotarod (up to five mice per trial) and the rotarod activated. Individual timers for each of the mice automatically started with the rotarod and were stopped automatically when mice fell from the rotating rod and setting off the trip plate. The rotarod would then display the latency to fall in seconds for each mouse. If the trip plate was not activated by the mouse falling, it was turned off manually. Mice that could no longer keep up with the accelerating rod but held on and rotated with the rod for more than two full rotations were classified as fallen and the timer was stopped. Once all the mice had fallen or reached the cut-off time of 300 seconds the experiment was stopped, and all mice were allowed to rest for five minutes before starting another trial. Each mouse was tested three times. After each test session the rod and trip plates were cleaned thoroughly and sanitised with 70% ethanol. The latency to fall in seconds for each mouse was averaged across the three trials. The mice were tested weekly for seven weeks then at week 13 post-STZ (STZ-Induced Diabetes Appendix, C.3).

4.2.2 Blood glucose testing

Two separate blood glucose tests were performed in mice prior to STZ administration in order to determine a baseline blood glucose level. Following STZ administration, weekly blood glucose tests allowed the determination of diabetic onset in the mice. Testing was carried out at approximately the same time each day on unfasted mice.

Blood glucose levels were measured in mice using a CareSens Dual Blood glucose monitoring system (CareSens). Measurements were obtained in a mouse by removing it from its cage and gently wrapping its tail around a small cylinder to expose underside of its tail. A CareLance lancing device was then used to lightly pierce the skin of the tail, near the tip, drawing a drop of blood (~1 μL). The CareSens monitoring system, loaded with a CareSens Pro Blood glucose test strip was placed next to the blood drop, allowing ~0.5 μL of the blood to move into the test strip. The glucose concentration (in mmol/L) displayed on the meter was then recorded. This method proved to be fast, repeatable, and relatively non-invasive with minimal bleeding.

The mice barely noticed the procedure and there was no need for restraint or sedation. Baseline glucose concentrations in the mice averaged 11 mmol/L (196 mg/dL).

4.2.3 Administration of streptozotocin

Once all baseline behavioural and blood glucose data had been collected, mice were weighed and randomly grouped into treatment or control groups. The treatment group received a single large dose of STZ administered at 180 mg/kg in a sodium citrate buffer using 1 mL disposable lure slip tip syringes (Terumo #DVR-5175) with disposable 25 G 25 mm needles (BD Precision Glide #301807) to induce type 1 diabetes. Control mice received sodium citrate buffer only.

To prepare 10 mL of the citrate buffer, 148.5 mg of trisodium citrate - 50 mM, (Sigma Aldrich # 71402-100G) was dissolved into 8 mL of distilled water. In a separate beaker, a citric acid buffer was prepared using 630 mg of citric acid – 1 M, (Sigma Aldrich #C1909 - 500G) mixed with 3 mL of distilled water. The citric acid buffer was slowly added to the trisodium citrate, whilst stirring, until it reached a pH of 4.5. The volume was adjusted to 10 mL with distilled water and filter-sterilised. STZ powder (Sigma Aldrich #S0130) was added to the citrate buffer immediately before administration to give a final concentration of 30 mg/ml. Dosing charts can be found in the STZ-Induced Diabetes Appendix.

The mice were monitored after injection, and then returned to their home cages. Mice had normal access to food but water was replaced with a 10% sucrose water solution for three days. This was to prevent hypoglycaemic shock, which can occur due to the rapid breakdown of β-islet cells and subsequent unregulated release of insulin (Wu & Huan, 2008). After three days the 10% sucrose was replaced with water as per normal. Daily welfare checks were performed and recorded on individual animal welfare forms (STZ-Induced Diabetes Appendix, C.2). Mice that displayed any adverse signs, hypoglycaemic shock, or lost more than 20% of their body weight were euthanised.

Blood glucose levels were recorded at seven days post-STZ and weekly thereafter. Mice were deemed diabetic when blood glucose concentrations were more than 17 mmol/L (300mg/dL).

4.2.4 Collection of tissues

Streptozotocin-induced diabetic mice and citrate buffer-treated, non-diabetic control mice were euthanised at the end of the behavioural study for the collection of sciatic nerve tissue. Mice were euthanised using CO2 asphyxiation followed by decapitation as a secondary euthanasia method. The mice were then pinned on a dissection board in a prone position. The fur was sprayed lightly with 70% ethanol to wet it down and avoid contamination. Forceps were used to lift the skin in the mid-thigh area and cut away the skin from the foot to the front shoulders on both sides of the animal. The sciatic nerve was then identified through the thigh muscle and the muscle was carefully removed to partially expose the sciatic nerve. The nerve was then carefully followed in both directions to the spinal column and the foot. Excess tissue and bone were removed as necessary to expose the full nerve. The nerve was carefully removed and bisected into distal and proximal sections. These sections were placed into labelled microcentrifuge tubes containing 400 μL of RIPA buffer (Thermo Scientific Product # 89900) with protease inhibitor (Thermo Scientific Product #A32955) and frozen at -80°C immediately after dissection.

4.2.5 Immunoblotting

Protein immunoblot analysis was used to determine the amount of total α-tubulin and acetylated α-tubulin in the sciatic nerve portions. GAPDH was used as a loading control.

4.2.5.1 Protein extraction

Sciatic nerve tissue in RIPA buffer was homogenized using a tissue homogenizer (Pro Scientific, # PRO-PK 02200P) with a 5 mm probe (Pro Scientific # 02-05075). The homogenized tissue was incubated on ice for 30 min, vortexing briefly every 10 minutes. The resulting lysate was centrifuged at 10,000 x *g* (Centrifuge 5415R, Eppendorf) for 20 min at 4 °C and the supernatant, containing the proteins, was transferred to a new labelled microcentrifuge tube. This was stored at -80 °C until required.

4.2.5.2 Protein quantification

Protein concentrations in the samples were quantified using a Peirce™ BCA protein assay kit (Product # 23227) as per manufacturer's instructions. This involved the preparation of nine BSA protein standards at concentrations of 0 - 2000 μg/mL. The amount of working reagent needed was calculated based on the number of samples and was made by mixing 50 parts BCA Reagent A with 1 part BCA Reagent B to the correct volume. Using a 96-well microplate, 25 μL of each standard or each protein lysate was added to individual wells, along with 200 μL of working reagent. The 96-well microplate was mixed on a plate shaker for 30 s. The plate was then covered and incubated at 37°C for 30 min. The plate was cooled to room temperature and absorbance measured on a Thermo Scientific MultiSkan plate reader at 562 nm. A standard curve was prepared using the blank-corrected BSA concentration standards, which allowed the quantification of each of the protein samples. The concentration was used to determine 5 μg protein loadings of each sample for the immunoblot analysis (STZ-Induced Diabetes Appendix,C.4).

4.2.5.3 Immunoblot analysis

For SDS Polyacrylamide gel electrophoresis (SDS-PAGE), 5 μg of protein was added to RIPA buffer to give a final volume of 25 μL. Each sample then received 8.3 μL loading buffer (Bolt LDS buffer 4 X Lot#1876348) containing 5% beta-mercaptoethanol and mixed gently. The samples were incubated at 99°C for 3 min in a Thermomixer heating block (Eppendorf) and centrifuged at 16,000 x *g* for 3 min at room temperature. The samples were loaded into a (4% - 12%) gradient Bis-Tris plus Gel (Invitrogen, ThermoFisher #NW04125BOX), along with 3 μL of protein standard (GangNam-STAIN™ prestained protein ladder, #24052) and run at 100 V for approximately 70 min in 1 x Bolt running buffer (Invitrogen, ThermoFisher, #B0002).

Once proteins had migrated through the gel and become separated by molecular mass, as determined by the protein standard, proteins were transferred to a PDVF membrane (Roche, #NR0772). The gel was placed on a PDVF membrane that had been activated in methanol for 30 s and sandwiched together with the filter paper and sponges. The cassette containing the transfer sandwich was placed into the transfer chamber, covered with 1 x cold transfer buffer (20 X bolt transfer buffer, (Invitrogen, ThermoFisher, #BT0006), 10% methanol, and distilled

water to make it up to 1 X) and electrophoresed at 100 V for approximately 1 h 15 min at 4°C with the transfer buffer being circulated using a magnetic flea at 500 RPM.

Once the proteins were transferred to the membrane it was removed from the cassette and placed in a 1 X blocking buffer (Blocker ™ FL Fluorescent Blocking Buffer 10 X, ThermoFisher #37565) for 15 min at room temperature on a rocker. The blocking buffer was removed and replaced with primary antibodies in blocking buffer.

Primary antibodies for immunoblot:

Mouse monoclonal anti-α-tubulin, **1:2000** (Sigma Aldrich, #AA13)

Rabbit monoclonal anti-acetylated-α-tubulin, **1:2000** (Cell signal, #D20G3)

Rabbit monoclonal anti-GAPDH, **1:3000** (Sigma Aldrich, #G9545)

Following an overnight incubation at 4°C on a rocker, the primary antibodies were removed, and the membrane was washed three times in 1 X TBS-T (Pierce™, Thermo Scientific, #28360) for 5 min, on a rocker at room temperature. After the final wash, TBS-T was removed and replaced with secondary antibodies in blocking buffer.

Secondary antibodies for immunoblot:

Goat anti-mouse IgG (H+L) HRP, **1:2000**. (Invitrogen, # 16066, Lot # 47-166-032017)

Goat anti-rabbit IgG (H+L) HRP, **1:2000**. (Invitrogen, # 65-6120, Lot # RL242746A)

Secondary antibodies were incubated with the membrane on a rocker for one hour at room temperature. Secondary antibodies were removed, and the membrane was again washed three times in TBS-T for 5 min on a rocker at room temperature.

Following the final wash, the membrane was incubated with Western Bright ECL spray (Advansta, # K-12049-D50) for 2 min at room temperature, which is used to detect HRP-

conjugated secondary antibodies. The membrane was imaged by detecting a chemiluminescent signal on the iBright FL1000 imager and analysed using Image J software.

Each membrane was first probed with anti-acetylated α-tubulin and anti-GAPDH, imaged, then stripped using Restore™ Stripping Buffer (ThermoScientific USA, Product # 21059) and re-probed with anti-total α-tubulin and anti-GAPDH to avoid discrepancies with loading, running, and transfer differences.

4.2.5.4 Immunoblot quantification.

Western blot bands were quantified by comparing the relative intensity of pixels for each of the acetylated α-tubulin, total α-tubulin and GAPDH chemiluminescence signals using ImageJ software (Schneider et al., 2012). Both the acetylated α-tubulin and total α-tubulin were first normalised to the corresponding GAPDH signal, then the proportion of acetylated α-tubulin was calculated by using the ratio between normalised acetylated α-tubulin and normalised total α-tubulin. Each of these were presented as a percentage of the control group, with the non-diabetic control group set at 100%.

4.2.6 Statistical analysis

All statistical analyses and graphs were created using SPSS statistics version 28.0.1.0 (142). One-way ANOVA (analysis of variance) was used to compare differences between 3 or more conditions with post hoc analysis using TURKEY HSD. All p values were deemed statistically significant at $p \leq 0.05$. Those p values that were close to being significant were noted and the actual value was written on the graphs. Error bars were set for +/- 2 standard error (SE) as this gives a good visual representation to determine if the results are statistically significantly different. This is the same as a 95% confidence interval. In data sets where there were two groups, independent sample t-tests (two-tailed) were carried out. Levene's test of significance was used to determine if equal variances were assumed (significance ≤ 0.05 equal variance not assumed, significance > 0.05 equal variance assumed). Rotarod data for pre-STZ and 13 weeks post was compared using a paired t-test (two-tailed) as the same animals were tested at each time point. Data is presented as mean ± standard deviation (SD).

4.3 Results

4.3.1 Induction of diabetes in B6:D2 male mice by streptozotocin

Following STZ administration, the number of mice that become diabetic, the number that develop neuropathy and neuropathic pain, and the time taken for this to occur varies depending on the genetics of the mice, the sex and age of the mice, and the STZ dosing concentration and regimen. Therefore, a B6:D2 male mouse model of a single high dose of STZ-induced diabetic neuropathy was characterised. Mice were examined for 13 weeks post-STZ injection with testing for rotarod performance, thermal hyperalgesia and mechanical allodynia. Sciatic nerve tissues were harvested at the conclusion (13 weeks post-STZ injection).

A total of 42 B6:D2 male mice with an average age of 20± 2 weeks and an average weight of 27 ± 3 g were used in this study. Eight of these were citrate control mice and the remaining 34 were injected intraperitoneally with 180 mg/kg of STZ. Other studies using this model have found that at least 60% of the mice given a single large dose of STZ are expected to become diabetic (Furman, 2015). Of the 34 mice, 22 became diabetic with blood glucose readings of ≥ 17 mmol/L, while 12 of these did not become diabetic. Two mice administered STZ died within 24 hours of administration. One mouse died within two weeks of STZ administration. A further six mice needed to be euthanised due to excessive weight loss (>20% of initial body weight) between 4 – 8 weeks post-administration. Of the 22 mice that became diabetic, a total of 13 mice were assessed throughout the 13 weeks. This group of mice finished the trial at an average weight of 27± 2 g, keeping a steady weight throughout the trial, in contrast to the citrate control mice that gained weight and were 32 ± 6 g at week 13 (**Figure 4-1**). The diabetic mice displayed polyuria, but otherwise were considered healthy by daily animal welfare observations for overt pain symptoms, signs of distress, and dehydration (STZ-Induced Diabetes Appendix, C.2).

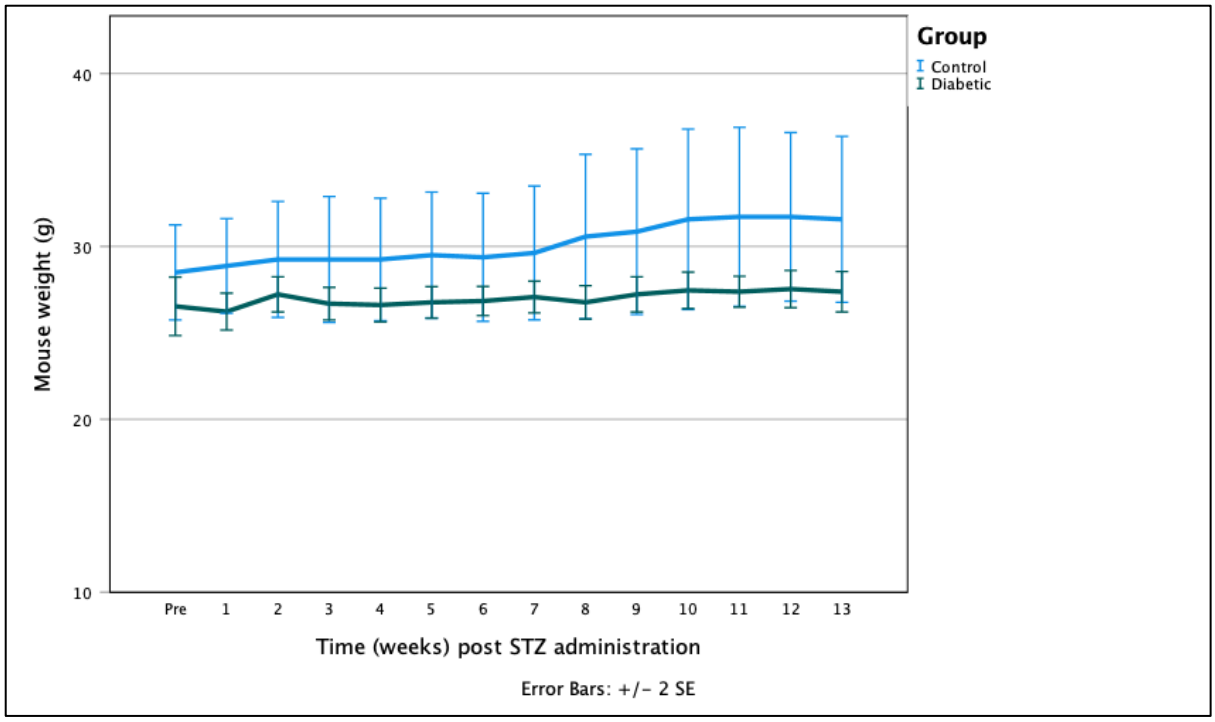

***Figure 4-1**. Average mouse weight per group across the 13 week assessment. Control n = 8, Diabetic n = 13.*

4.3.2 Hyperglycemia

To monitor the onset of hyperglycaemia after administration of STZ, blood glucose concentrations were measured weekly. Two weeks post-STZ injection 22 mice from 34 (65%) displayed blood glucose readings of more than 17 mmol/L, indicating hyperglycaemia (diabetic onset) (**Figure 4-2**). Interestingly, one mouse who had been displaying reliable high blood glucose spontaneously returned to non-diabetic glucose level at eight weeks post-STZ administration. For the 13 mice assessed throughout the 13 weeks, blood glucose measurements remained >17 mmol/L. Many of the diabetic mice had blood glucose readings of ≥ 33.3 mmol/L.

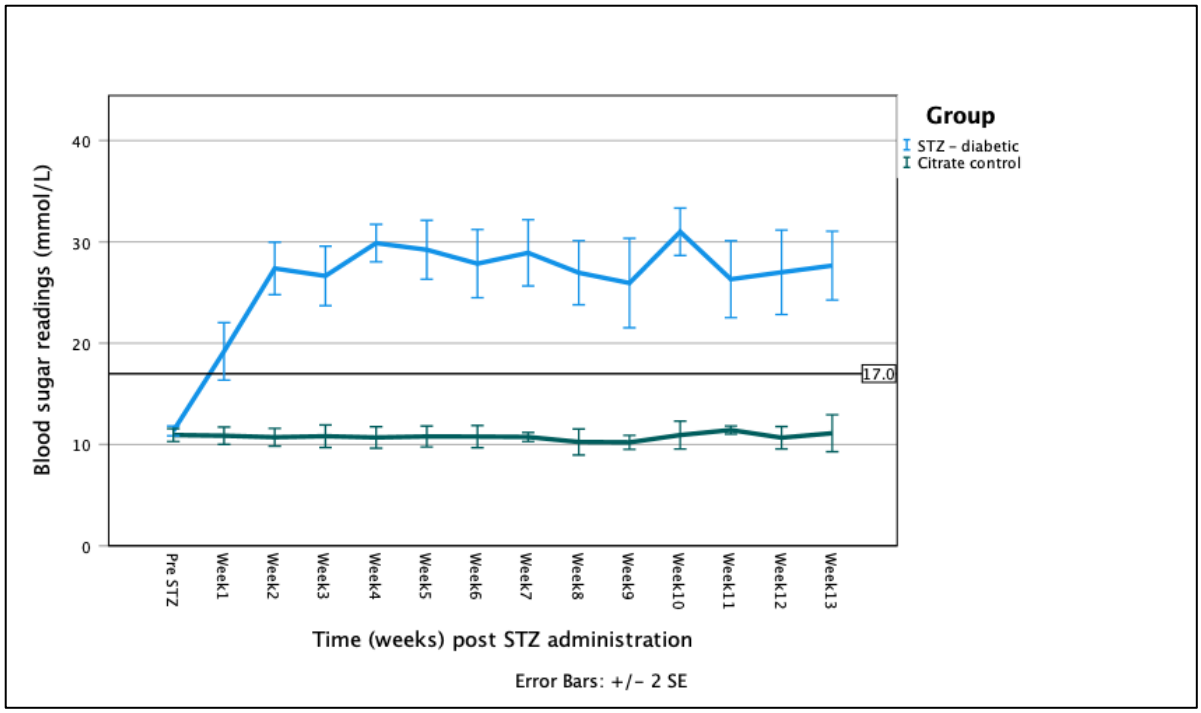

***Figure 4-2**.Line graph of blood glucose readings (mmol/L) of wildtype male mice administered 180mg/kg of STZ by IP injection. Mice who have 3 consistent readings of more than 17 mmol/L (reference line) are considered diabetic. (Total n = 21, Diabetic n = 13, citrate control n = 8). From 1-week post-STZ all time points are statistically significantly different from the citrate control group with p ≤ 0.001.*

4.3.3 Development of diabetic induced neuropathic pain

Male B6:D2 mice were tested weekly to determine any onset of motor dysfunction, thermal hyperalgesia and mechanical allodynia; this involved the use of Rotarod, Hargreaves and von Frey testing, respectively.

4.3.3.1 Rotarod

Although motor dysfunction is a late-onset symptom in diabetes in mice(O'Brien et al., 2014), testing was carried out in the STZ-induced diabetic and non-diabetic mice to determine if there was any change in motor performance that might be attributable to diabetic neuropathy-induced motor neuron dysfunction. Rotarod testing was performed in a subset of the diabetic mice (*n* = 8). Individual readings for each diabetic mouse at baseline (pre-) and 13 weeks post-STZ administration are shown in **Figure 4-3**. Two individual diabetic mice showed a large change in latency to fall across the 13 weeks; one has shown a large decrease

in motor performance across the 13 weeks with a loss of ~200 s, and another has shown an increase in motor performance with an increase of ~150 s.

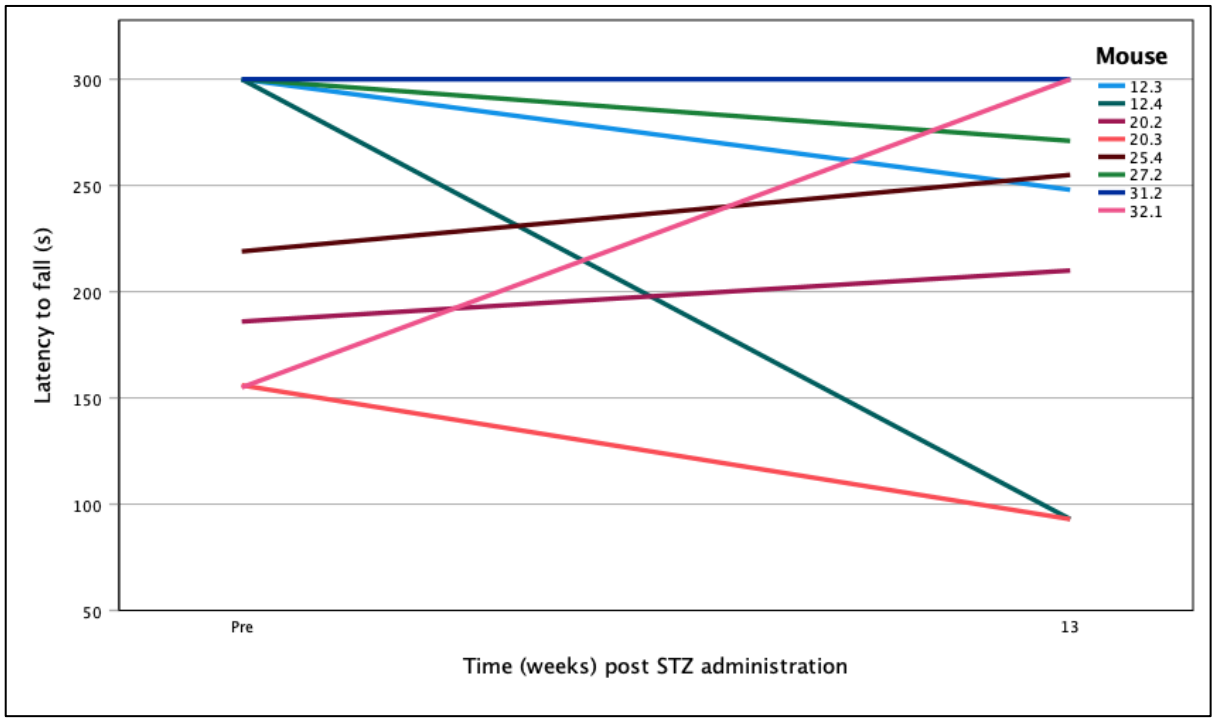

***Figure 4-3**. Rotarod data for individual diabetic mice, n = 8. Baseline and 13 weeks data is shown.*

Despite two mice showing larger changes in latency to fall, there was no statistically significant change in the groups average latency to fall (s) in the diabetic mice across 13 weeks (**Figure 4-4**).

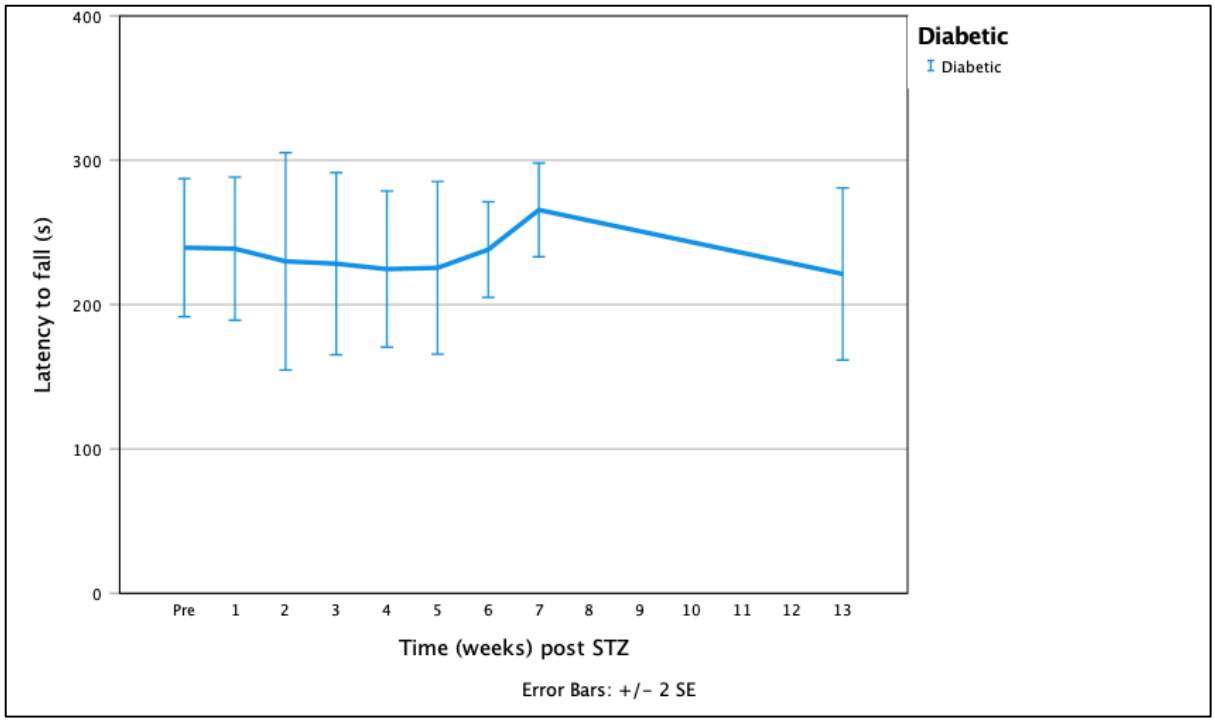

***Figure 4-4**. Bar graph of latency to fall (s) in male diabetic mice across 13 weeks post 180 mg/kg streptozotocin. n = 8*

When pre-STZ latency to fall and 13-week post-STZ latency to fall in this cohort are compared, no statistically significant differences are evident (**Figure 4-5** &**Table 4-1**). Thus, the diabetic mice were deemed to have no loss of motor function by rotarod testing, across the 13 weeks of assessment.

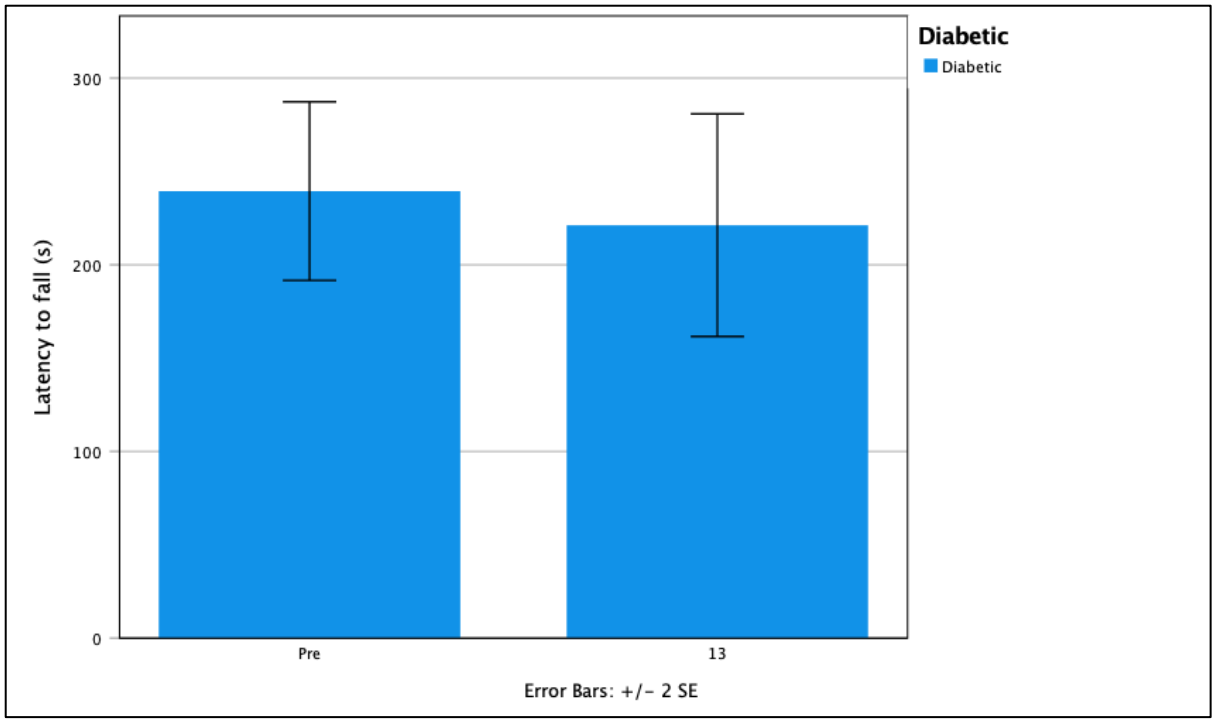

Figure 4-5. *Bar graph comparing latency to fall (s) in male wildtype mice, baseline and 13 weeks post-diabetes. p = 0.741*

Table 4-1*. Paired sample t-test for baseline and 13 weeks post diabetes*

Paired Samples Statistics

		Mean	N	Std. Deviation	Std. Error Mean
Pair 1	Pre	239.50	8	67.650	23.918
	13	221.25	8	84.309	29.808

Paired Samples Correlations

		N	Correlation	Significance One-Sided p	Significance Two-Sided p
Pair 1	Pre & 13	8	.140	.370	.741

4.3.3.2 Thermal hyperalgesia

Thermal hyperalgesia or hypoalgesia is typically the first neuropathic pain symptom observed in diabetic mice (O'Brien et al., 2014). Changes to thermal responses were noted in all mice that became diabetic in this trial. This was indicated by a decrease in paw withdrawal latencies (thermal hyperalgesia) with Hargreaves testing in diabetic mice (**Figure 4-6**). Paw withdrawal latencies for diabetic mice were statistically significantly lower at all time points from week 4 to week 13 post-STZ compared to the citrate buffer-treated, non-diabetic control group (**Figure 4-6**).

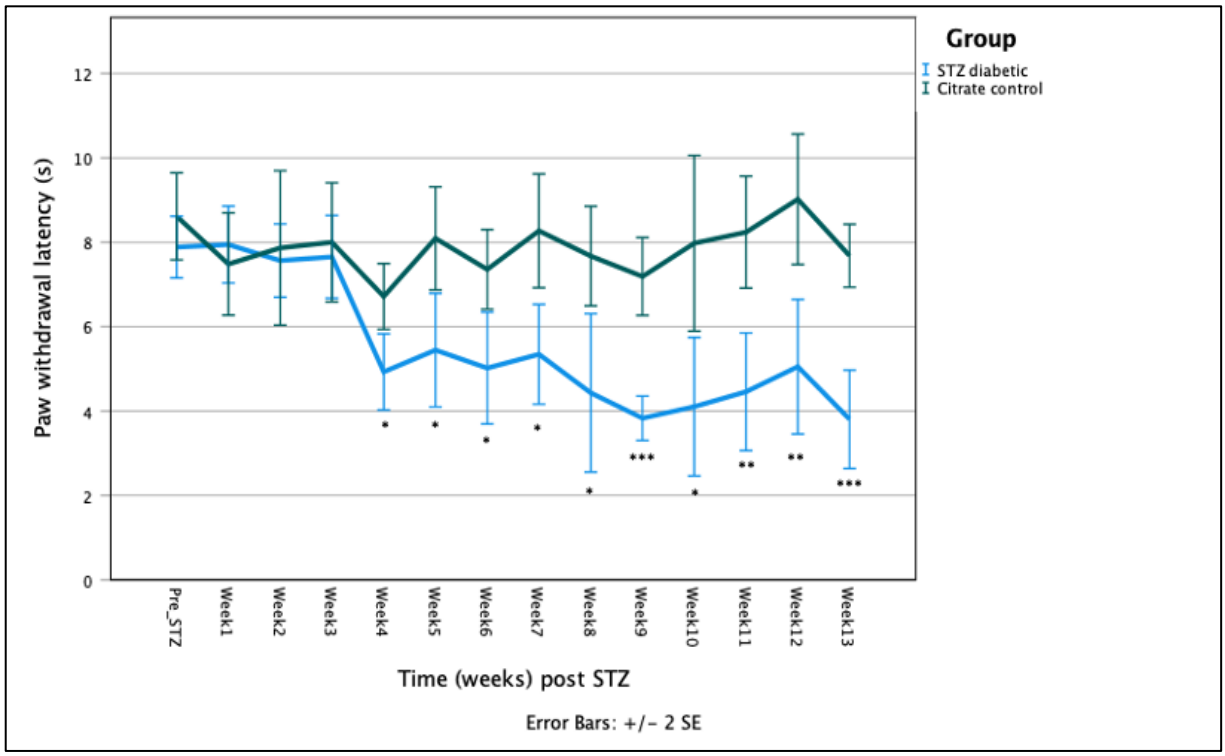

Figure 4-6*. Line graph showing the onset of thermal hyperalgesia in diabetic mice. STZ diabetic n = 13, citrate control n = 8. Two-sided T – test carried out to determine p values. P ≤ 0.05 *, p ≤ 0.01 **, p ≤ 0.001 ****.*

4.3.3.3 Mechanical allodynia

Contrary to the thermal hyperalgesia results, mice that became diabetic displayed mechanical allodynia at a later time point. In the diabetic mice, there is a downward trend in paw withdrawal thresholds by von Frey testing compared to the citrate buffer-treated, non-diabetic controls from week three to week 10 post-STZ. Paw withdrawal thresholds for the diabetic mice group were statistically significantly lower at all time points from week 11 to week 13 post-STZ (**Figure 4-7**).

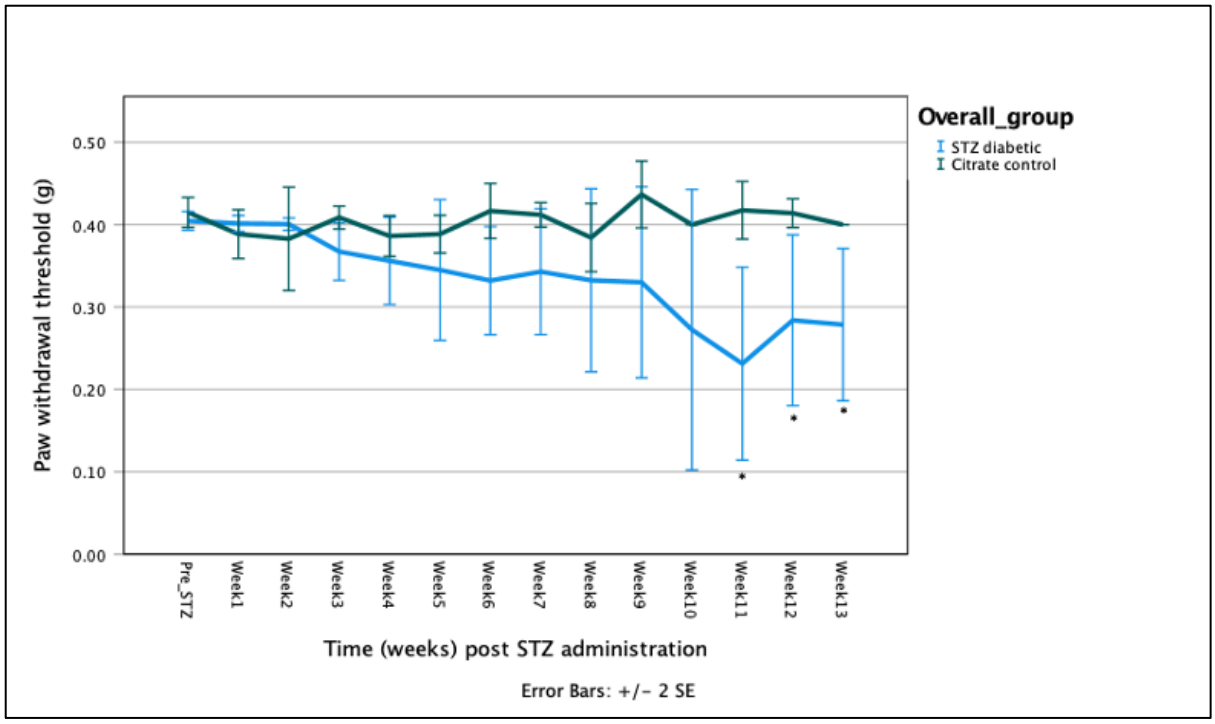

***Figure 4-7**. Time of onset of mechanical allodynia in diabetic male mice after induction of diabetes by a single large dose of 180 mg/kg STZ. STZ diabetic n = 13, citrate control n = 8. Independent sample t-test, two-tailed. p 0.01 ≤ 0.05 *.*

Individual examination of the 13 diabetic mice revealed that five mice displayed clear changes to the paw withdrawal threshold across the 13 weeks of testing mechanical allodynia, while 8 mice showed no consistent changes to paw withdrawal thresholds (**Figure 4-8**). Each mouse deemed to show mechanical allodynia symptoms showed a varying time of onset symptoms from between 4 – 11 weeks.

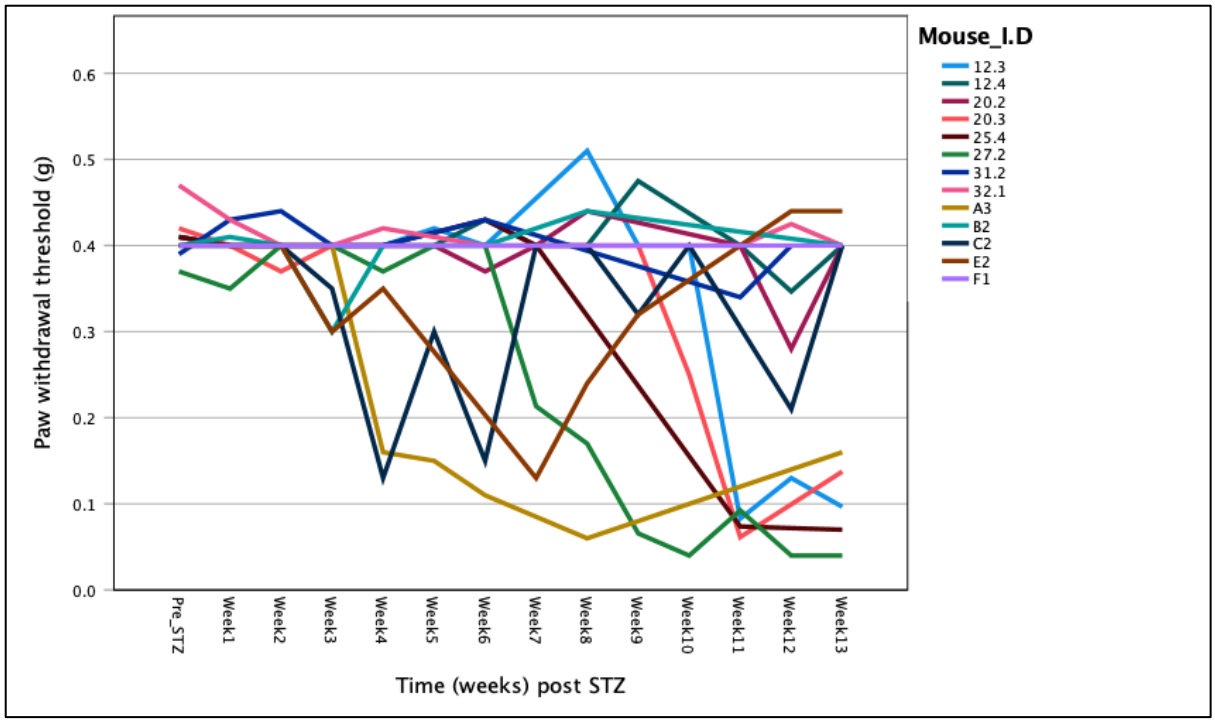

***Figure 4-8**. Changes to paw withdrawal threshold in individual diabetic mice*

The diabetic group was thus separated into those that showed mechanical allodynia and those that did not (**Figure 4-9**) and analysed. The diabetic "allodynia group" were statistically significantly different from both the diabetic "non-allodynia group" and the citrate buffer-treated, non-diabetic control group for weeks 11, 12 and 13.

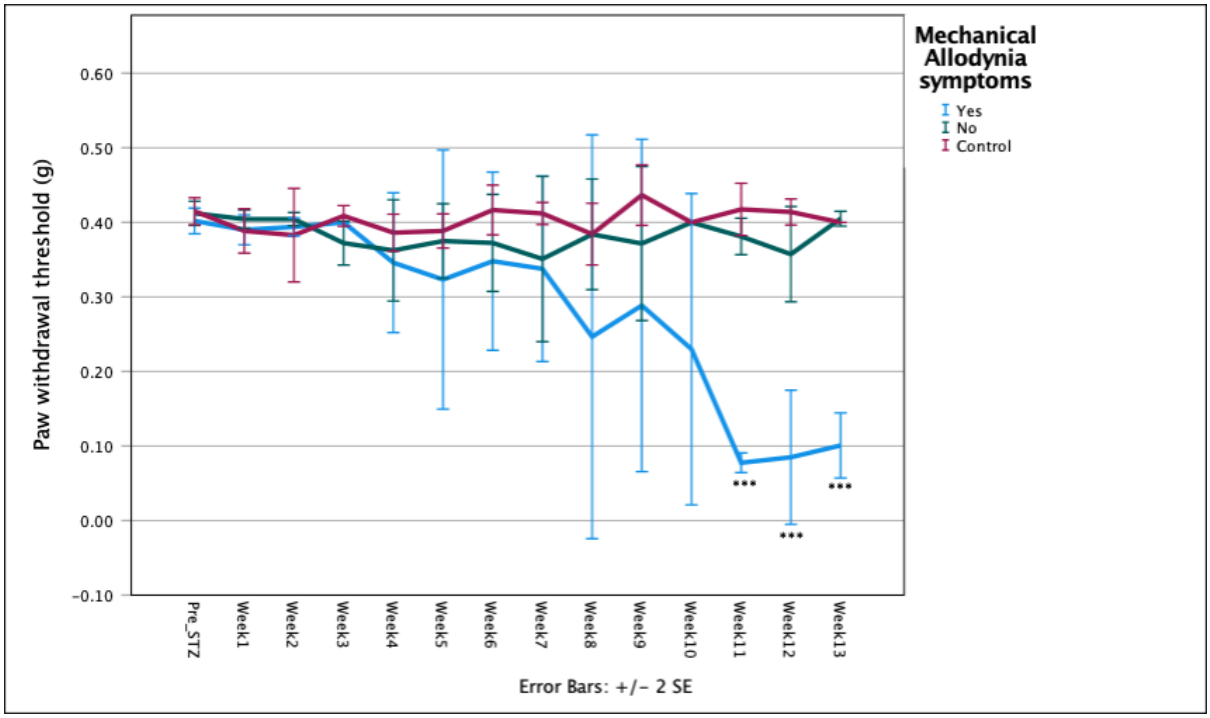

Figure 4-9*. Line graph showing the onset of mechanical allodynia in male diabetic mice. Diabetic mice that showed mechanical allodynia (Yes) n = 5, diabetic mice that did not show mechanical allodynia (No) n = 8, Citrate control group n = 8. Allodynia vs citrate control weeks 11, 12 & 13, p ≤ 0.001 ***.*

4.3.4 Immunoblot analysis for acetylated α-tubulin

In the peripheral neuropathies, CMT2A, CMT2D, CMT2F and chemotherapy-induced neuropathic pain, neuropathy is accompanied by a progressive loss of α-tubulin acetylation (Adalbert et al., 2020; Castelli et al., 2018; Krukowski et al., 2015; Krukowski et al., 2017; Picci et al., 2020; Shen et al., 2021; Van Helleputte et al., 2018; Zhang et al., 2022); however, whether this is a characteristic of diabetic neuropathy is unknown. To determine if α-tubulin acetylation changes are present in diabetic neuropathy, sciatic nerve tissue was taken from diabetic and citrate control non-diabetic mice at the end of the 13 weeks. The nerve was bisected into proximal and distal portions, and levels of total α-tubulin and acetylated α-tubulin was determined by immunoblot analysis.

The analysis used sciatic nerves from eight diabetic mice (13 weeks post-STZ) and sciatic nerves from five citrate buffer-treated, non-diabetic control mice. Of the sciatic nerves taken from diabetic mice, four of the mice displayed mechanical allodynia, and all displayed thermal

hyperalgesia. Immunoblot membranes were first assessed for acetylated α-tubulin and GAPDH, then stripped and assessed for total α-tubulin and GAPDH.

4.3.4.1 Proximal sciatic nerve

Proximal sciatic nerve immunoblots were imaged and the results are shown in **Figure 4-10** and **Figure 4-11**. GAPDH was used as an internal loading control.

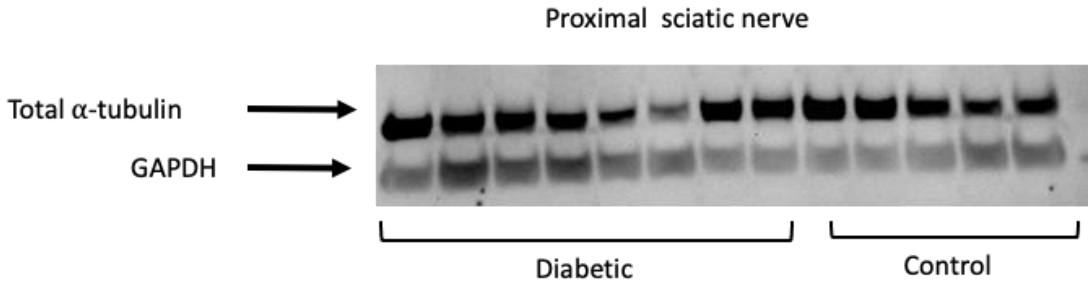

Figure 4-10*.Total α-tubulin in proximal sciatic nerve portions in diabetic and wildtype control mice.*

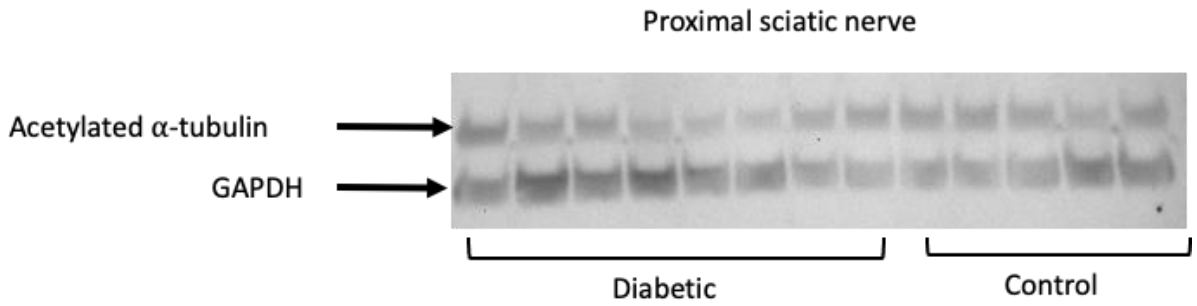

Figure 4-11*. Acetylated α- tubulin in proximal sciatic nerve portions in diabetic and wildtype control mice.*

Image J was used to quantify the respective optical density of acetylated α-tubulin, total α-tubulin, and GAPDH signals and used for analysis. The acetylated α-tubulin and the total α-tubulin were first normalised to GAPDH, then the ratio of acetylated α-tubulin to total α-tubulin was calculated.

The normalised level of total α-tubulin in the proximal sciatic nerves showed no statistically significant difference between the diabetic and the citrate buffer-treated, non-diabetic

control mice (**Figure 4-12**). This suggests that there is no loss of total α-tubulin in the proximal sciatic nerves of diabetic mice.

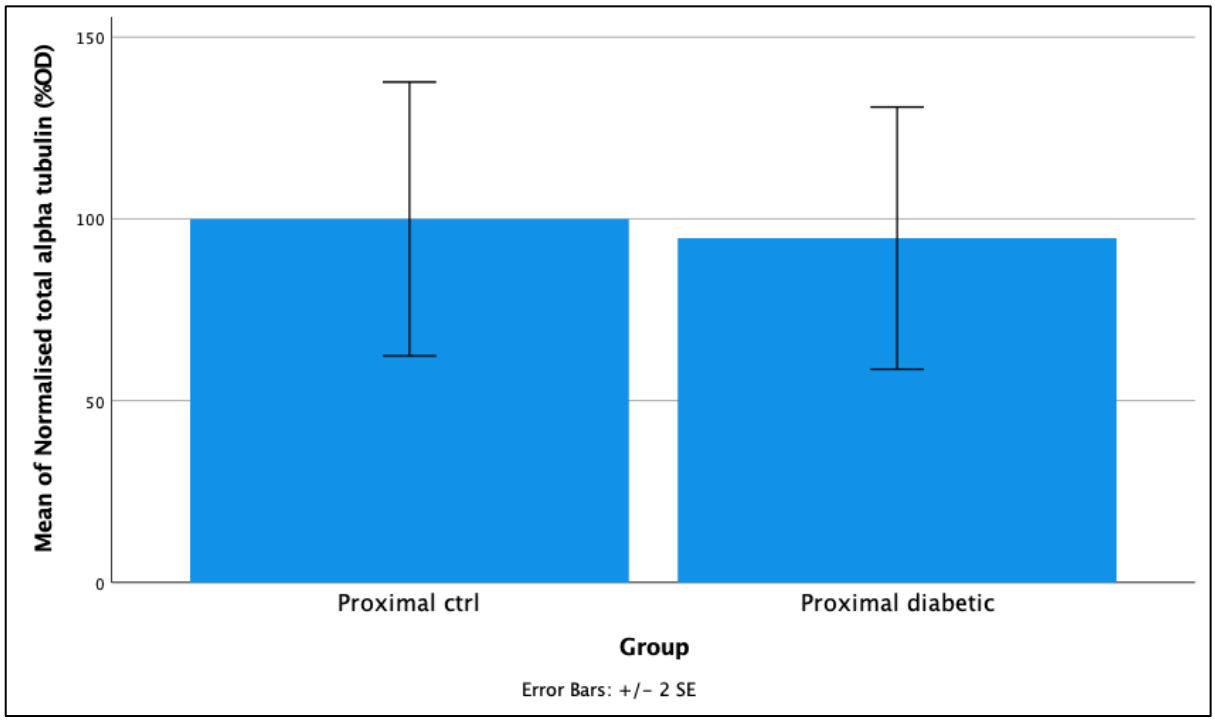

***Figure 4-12**. Mean of normalised total α-tubulin in proximal sciatic nerves. Data is presented as a percentage of control mice and normalised to GAPDH. Distal control n = 5, Distal diabetic n = 8. p = 0.85. Proximal diabetic = 94± 51% of the proximal control group.*

In contrast to total α-tubulin, the proximal nerve of diabetic mice had less acetylated α-tubulin (56 ± 34%) than that of citrate buffer-treated, non-diabetic control mice(**Figure 4-13**). Although this level did not reach statistically significance, with a p value of 0.066, it does suggest a trend of less acetylated α-tubulin in the proximal sciatic nerves of diabetic mice.

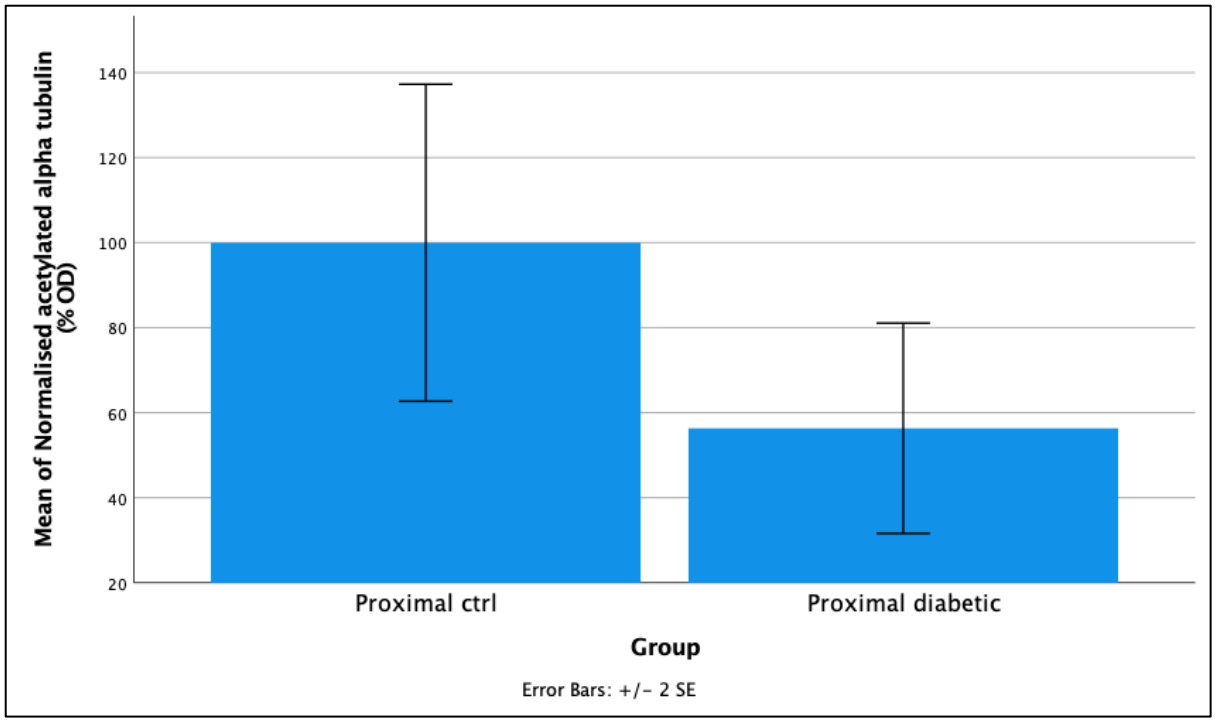

***Figure 4-13**. Mean of normalised acetylated α-tubulin in proximal sciatic nerves. Data is presented as a percentage of control mice and normalised to GAPDH. Distal control n = 5, Distal diabetic n = 8. p = 0.066. Proximal diabetic = 56± 35% of the proximal control group*

When normalised acetylated α-tubulin is expressed as a ratio to total α-tubulin, a statistically significant loss (42%) of acetylated α-tubulin seen in the proximal sciatic nerve when compared to the citrate buffer-treated, non-diabetic control mice (**Figure 4-14**).). This result, when considered with the results in **Figure 4-12**, suggests that there is a loss of the α-tubulin acetylation rather than a loss of total α-tubulin, *per se*, in the proximal sciatic nerves of diabetic mice.

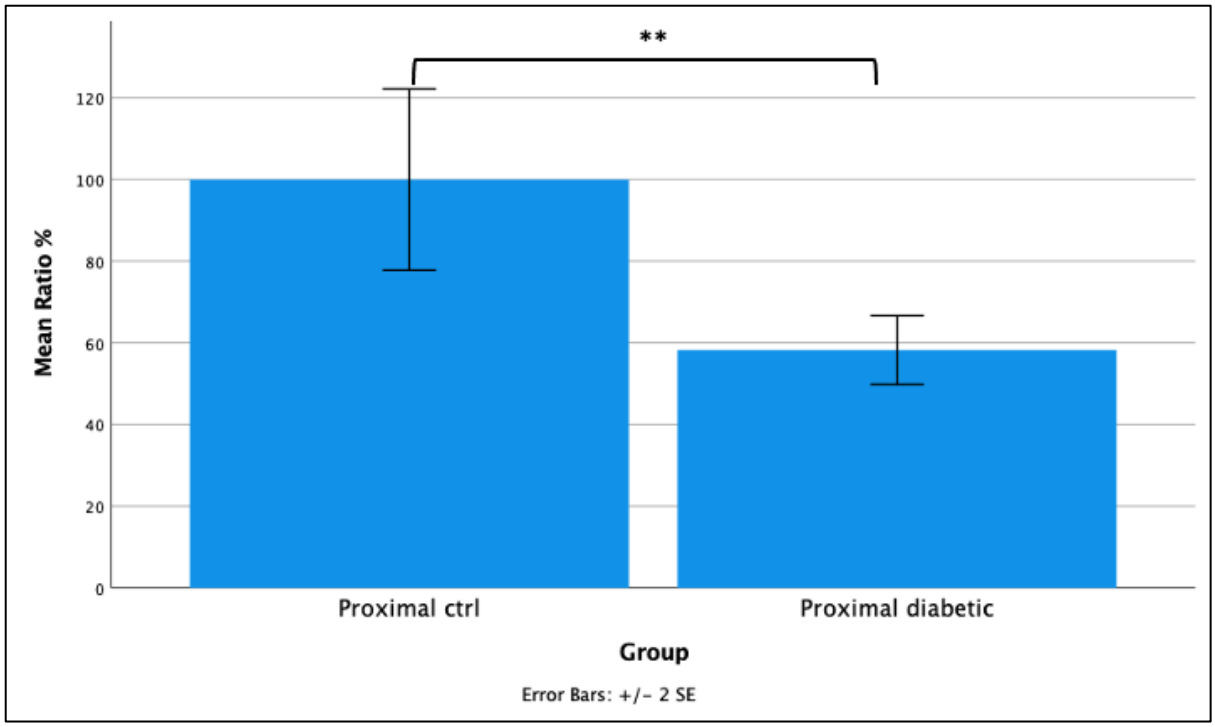

Figure 4-14*. Bar graph showing changes to the ratio of acetylated* α*-tubulin levels in proximal sciatic nerves in diabetic male mice. Error bars +/- 2 SE. Citrate controls n = 5, diabetic mice n = 8. Two-sided t – test carried out to determine p values. p ≤ 0.05 *, p ≤ 0.01 **, p ≤ 0.001 ***. p = 0.002. Proximal diabetic = 58*$\pm$*12% of the Proximal control group*

4.3.4.2 Distal sciatic nerve

Distal sciatic nerve immunoblots were imaged and the results are shown in **Figure 4-15** and **Figure 4-16**. GAPDH was used as an internal loading control. One distal sciatic nerve sample was excluded from the analysis due to uneven loading as indicated by the very low GAPDH band.

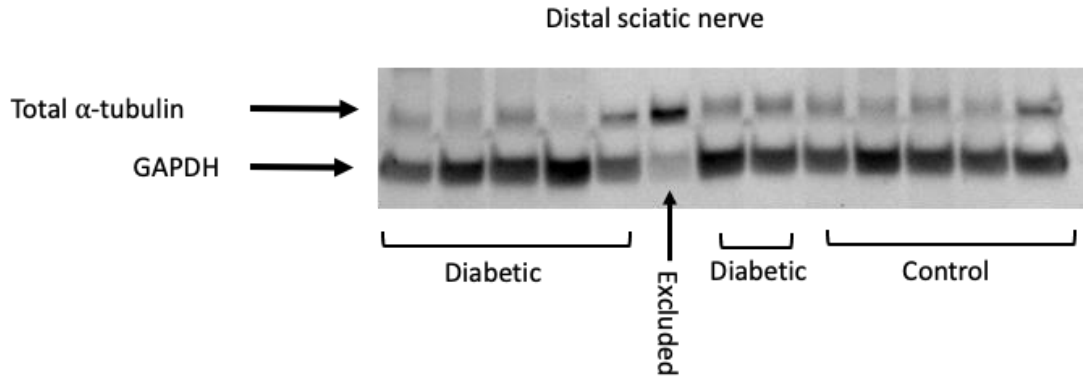

***Figure 4-15**. Total α- tubulin in distal sciatic nerve portions in diabetic and wildtype control mice.*

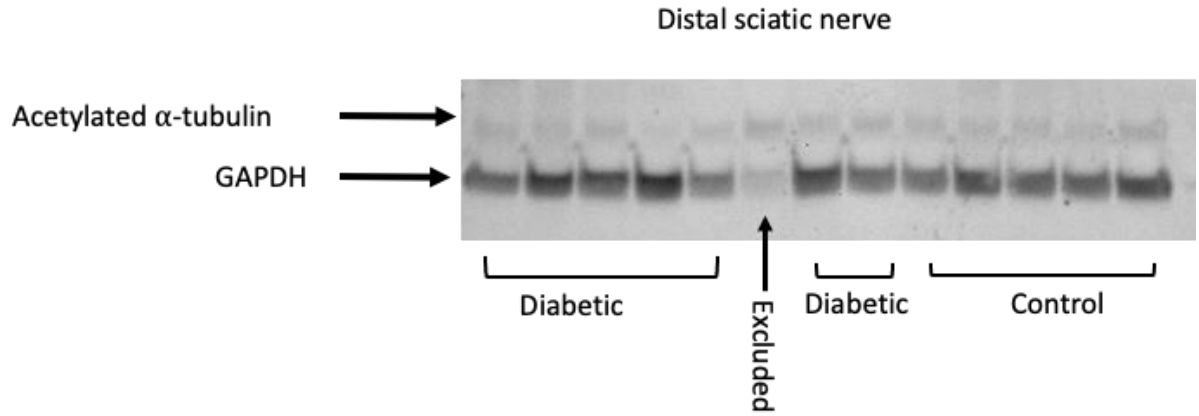

***Figure 4-16**. Acetylated α - tubulin in distal sciatic nerve portions in diabetic and wildtype control mice.*

As with the proximal sciatic nerve section, Image J was used to quantify the respective optical density of distal sciatic nerve acetylated α-tubulin, total α-tubulin, and GAPDH signals and used for analysis. The acetylated α-tubulin and the total α-tubulin were first normalised to GAPDH, then the ratio of acetylated α-tubulin to total α-tubulin was calculated.

No statistically significant difference was seen in the levels of total α-tubulin between the diabetic mice and the citrate buffer-treated, non-diabetic control (**Figure 4-17**). The level of total α-tubulin in the diabetic mice is 142 $\pm$ 73% of that of the control mice.

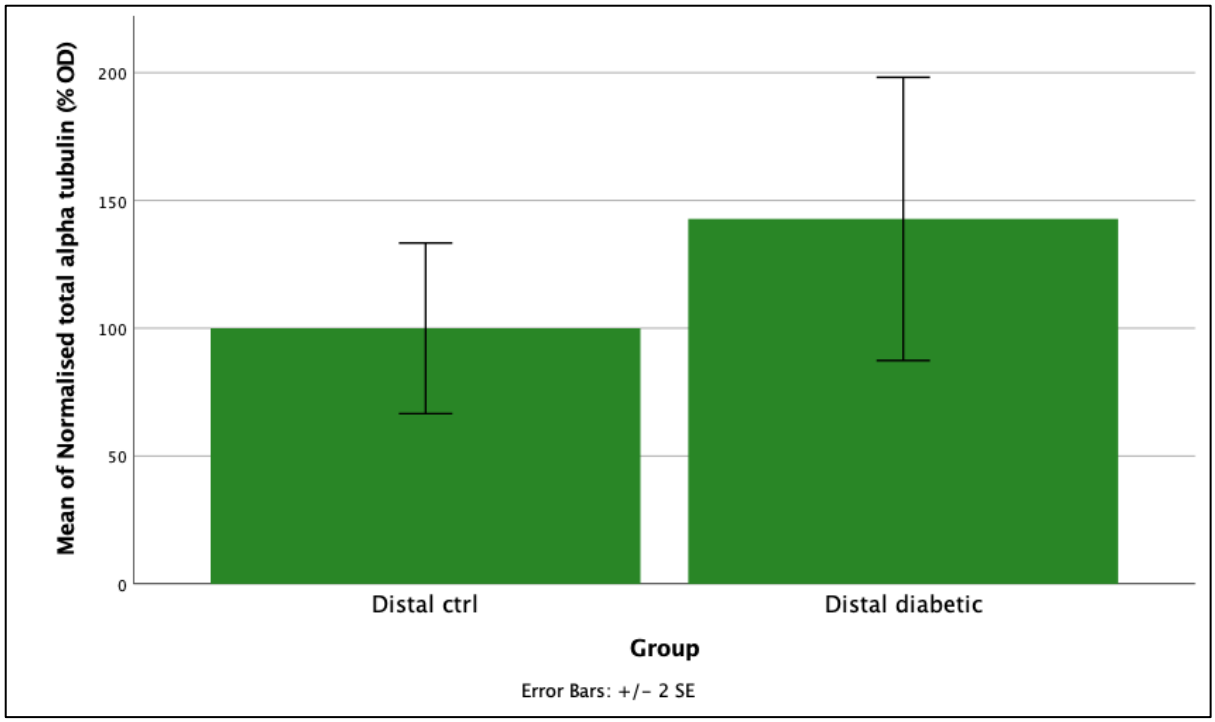

***Figure 4-17**. Mean of normalised total α-tubulin in distal sciatic nerves. Data is presented as a percentage of control mice and normalised to GAPDH. Distal control n = 5, Distal diabetic n = 7. p = 0.262*

In contrast to total α-tubulin, there is statistically significantly ($p < 0.001$) less acetylated α-tubulin in the distal sciatic nerves of the diabetic mice when compared to the citrate buffer-treated, non-diabetic control mice (**Figure 4-18**). The level of acetylated α-tubulin was 64 ± 30% less than the control group.

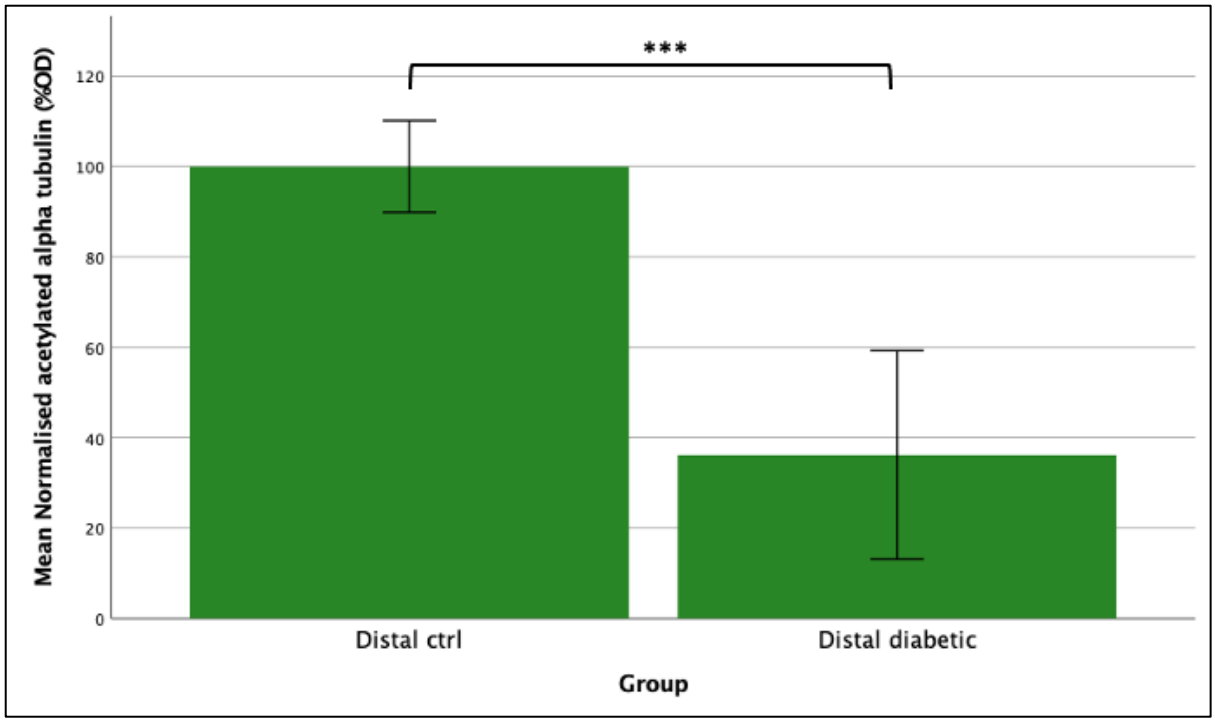

***Figure 4-18**. Mean of normalised acetylated α-tubulin in distal sciatic nerves. Data is presented as a percentage of control mice and normalised to GAPDH. Distal control n = 5, Distal diabetic n = 7. Two-sided t – test carried out to determine p values. p ≤ 0.05 *, p ≤ 0.01 **, p ≤ 0.001 ***.*

When normalised acetylated α-tubulin is expressed as a ratio to total α-tubulin, a statistically significant loss (78 ± 13%) of acetylated α-tubulin seen in the proximal sciatic nerve when compared to the citrate buffer-treated, non-diabetic control mice (**Figure 4-19**). This is a much larger loss of acetylated α-tubulin than that seen in the proximal sciatic nerve (Figure **4-14**). As was also seen with the proximal sciatic nerve this would suggests that there is a loss of the α-tubulin acetylation rather than a loss of total α-tubulin, *per se*, in the proximal sciatic nerves of diabetic mice.

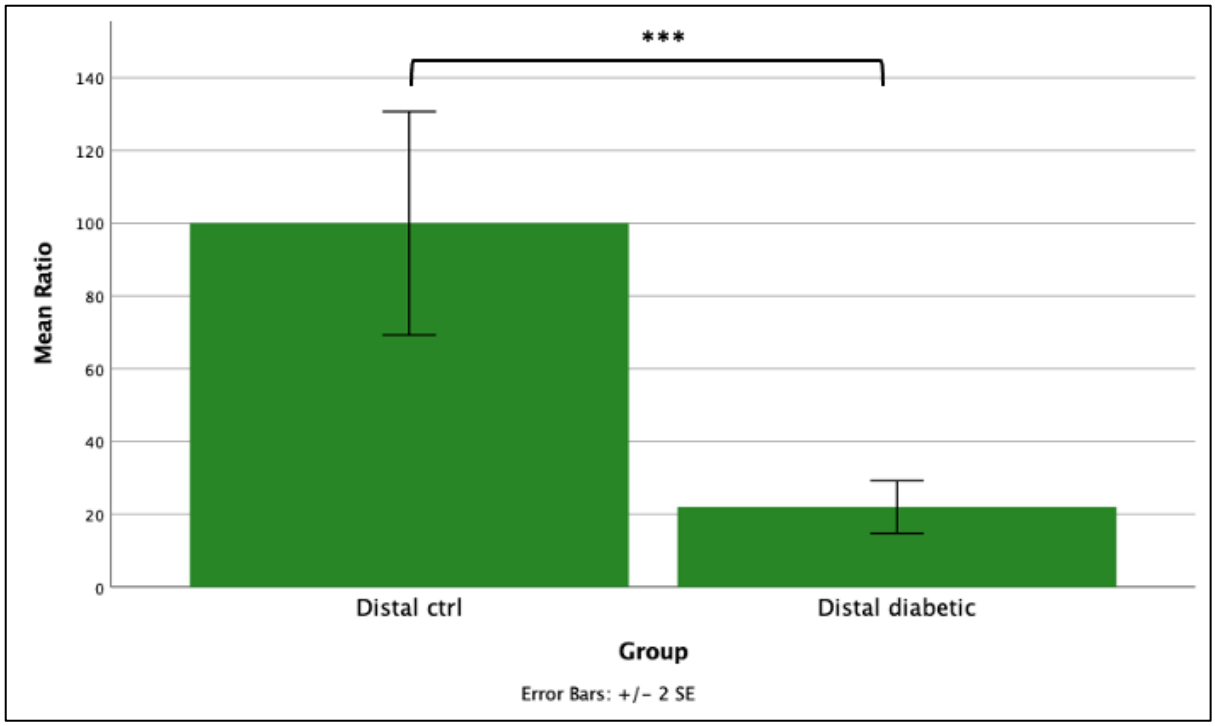

***Figure 4-19**. Bar graph showing changes to acetylated α-tubulin in distal sciatic nerves of diabetic mice. Error bars +/- 2 SE. Wildtype controls n = 5, diabetic mice n = 7. Two-sided t – test carried out to determine p values. p ≤ 0.05 *, p ≤ 0.01 **, p ≤ 0.001 ***.*

Five out of the 13 mice from the diabetic cohort displayed mechanical allodynia symptoms, as indicated by a decreased paw withdrawal threshold (**Figure 4-8**).To determine whether the presence of this symptom correlated with changes in the levels of acetylated α-tubulin and total tubulin in distal sciatic nerves, these mice were compared to diabetic mice that did not show these symptoms. No statistically significant difference was evident in the levels of total α-tubulin and acetylated α-tubulin in the mice that showed mechanical allodynia (*n* = 4) compared to diabetic mice that did not show mechanical allodynia symptoms (*n* = 3). (**Table 4-2** & **Table 4-3**).

Table 4-2. *Results of a two sided t-test to determine any differences between the levels of total α-tubulin in distal sciatic nerves of diabetic mice that displayed mechanical allodynia and those that did not show allodynia*

Group Statistics

	Group	N	Mean	Std. Deviation	Std. Error Mean
Totalalphatub	Mechanical allodynia	4	161.9158	87.90866	43.95433
	Not	3	117.3502	53.08352	30.64778

Independent Samples Test

		Levene's Test for Equality of Variances		t-test for Equality of Means							
						Significance				95% Confidence Interval of the Difference	
		F	Sig.	t	df	One-Sided p	Two-Sided p	Mean Difference	Std. Error Difference	Lower	Upper
Total alpha tub	Equal variances assumed	.466	.525	.77	5	.238	.477	44.56566	57.98515	-104.5	193.62122
	Equal variances not assumed			.83	4.892	.222	.444	44.56566	53.58423	-94.10	183.22995

Table 4-3*. Results of a two sided t-test to determine any differences between the levels of acetylated α-tubulin in distal sciatic nerves in diabetic mice that displayed mechanical allodynia and those that did not show allodynia.*

Group Statistics

	Group	N	Mean	Std. Deviation	Std. Error Mean
Acetylatedalphatub	Mechanical allodynia	4	43.0819	40.22770	20.11385
	Not	3	26.9487	12.15986	7.02050

Independent Samples Test

		Levene's Test for Equality of Variances		t-test for Equality of Means							
						Significance				95% Confidence Interval of the ...	
		F	Sig.	t	df	One-Sided p	Two-Sided p	Mean Difference	Std. Error Difference	Lower	Upper
Acetylated alphatub	Equal variances assumed	2.75	.16	.658	5	.270	.540	16.1332	24.51316	-46.8798	79.1463
	Equal variances not assumed			.757	3.69	.247	.494	16.1332	21.30386	-45.0044	77.2709

4.4 Discussion

4.4.1 Animal welfare

Overall, the administration of a single high STZ dose followed by induction of diabetes was tolerated in the wildtype B6:D2 male mice. Aside from the nine (out of 34) mice that were removed from the study, the mice remained relatively healthy. The number of deaths due to hypoglycaemia, or euthanasia due to weight loss was lower than what has been reported in the literature; with deaths of up to 20% of the mice expected in the first 48 hours and another 20% of the mice expected to be removed due to excessive weight loss across 8 – 10 weeks (Furman, 2015). The loss of insulin signalling and hyperglycaemia in mice has also been reported to result in symptoms that include dehydration, ketoacidosis, reduced growth, weight loss, lethargy, polyuria, and neuropathic pain, and changes to motor activity (Jaggi et al., 2011). Aside from polyuria and static growth rates (**Figure 4-1**) these symptoms were not readily discernable in daily observations of the mice throughout the course of the experiment.

As the mice developed diabetes, there was an observed, but not tested, increase in anxiety-like behaviour. Before baseline testing, mice in this trial were well acclimatized to the testing chamber. They were then exposed to the chambers twice weekly throughout the trial period. Normally, mice in this testing regiment settle quickly as the trial progresses; this was clearly evident in the citrate buffer-treated, non-diabetic control mice. However, as the diabetic mice progressed past 30 days post-STZ, a small number of the diabetic mice began to take a much longer time to settle and showed signs of distress when placed into the chambers, this number varied from week to week. There were some days when individual mice of this cohort gave unreliable results or were unable to be tested. The changes in behaviour were attributed to increased anxiety, which can be a common occurrence in mice and humans with untreated high blood glucose, and is well documented in the literature (Aksu et al., 2012; Gupta et al., 2014).

This anxiety-like behaviour in mice can complicate testing and interpretation of nociceptive tests (Walker et al., 1999). Studies with STZ induced diabetic rats, have found that if the rats are treated with insulin, to normalise blood glucose levels prior to testing, ease of testing improves; however, it has also been shown that neuropathic pain symptoms can be altered under this regime (Fox et al., 1999). It is not clear why this happens, but it is hypotheised that

by normalizing the blood glucose the peripheral nerve damage does not occur as it does in the untreated diabetic rats (Fox et al., 1999). This meant that treating the mice with insulin prior to testing neuropathic pain symptoms was not possible.

Anxiety-like behaviour was mitigated to some degree by placing fewer mice in the testing chambers at a time. Only mice from the same home cage went into adjacent testing chambers, with an empty testing chamber between those who were not cage mates. Mice that showed signs of distress in the testing chambers were removed and placed back into their home cage.

It is recommended that diabetic mice are not left for more than an hour in testing chambers without access to water as they can become dehydrated and not respond appropriately to testing, leading to inconsistent results (Jolivalt et al., 2016). Complicating this, the diabetic mice suffer from polyuria, and in the Hargreaves apparatus, the mice sit on a clear glass floor. The presence of liquid on the glass floor can interfere with the test causing heat to dissipate and give inaccurate results. Therefore, the testing chambers had to be cleaned more frequently, which disturbed the mice and compounded the unsettled behaviour. The increased anxiety-like behaviour, polyuria, and time limitations to prevent dehydration, made testing in this mouse model difficult. Other studies have not noted this difficulty, despite the increased anxiety being well known and documented (Aksu et al., 2012; Gupta et al., 2014).

4.4.2 Development of diabetic-induced neuropathic pain

Both thermal hyperalgesia and mechanical allodynia were observed in the diabetic mice, consistent with what has been reported in several studies (O'Brien et al., 2014). All diabetic mice in this study showed a decreasing trend in paw withdrawal times with Hargreaves testing, with paw withdrawal time becoming statistically significantly different from that of citrate buffer-treated, non-diabetic control mice from four weeks post-STZ administration (**Figure 4-6**). Usually in this type of model, thermal hyperalgesia is the first type of neuropathic pain that presents with the diabetic neuropathy. It begins with a decreased paw withdrawal latency and then, as the nerve damage progresses, there is a loss of sensation and paw withdrawal latency increases above control groups (hypoalgesia) (O'Brien et al., 2014; Obrosova, 2009). There is no set timeframe for thermal hyper- to hypoalgesia development noted in these studies as it varies with the mouse strain and diabetic induction method; in

fact some mouse models display thermal hypoalgesia as a first symptom (O'Brien et al., 2014). Our results showed thermal hyperalgesia symptoms showing up relatively early, from four weeks post-STZ administration; however, there was no indication of thermal hypoalgesia in these mice over the 13-week testing period. The early onset of thermal hyperalgesia indicates that the smaller unmyelinated nerve fibres are becoming dysfunctional or damaged before the larger myelinated Aß fibres that are responsible for mechanical allodynia. This is also consistent with evidence from both type 1 and type 2 diabetic patients in which a loss of these smaller unmyelinated C-type nerve fibres precedes larger myelinated Aß fibre degeneration (Pittenger et al., 2004; Shun et al., 2004; Sumner et al., 2003).

Nearly 40% of the diabetic mice (blood glucose measuring ≥ 17 mmol/L) in this study began to show signs of mechanical allodynia. The time of onset of mechanical allodynia in individual mice varied from week four to week 11 post-STZ. This mimics what is seen in human patients, with 30 to 50% of diabetic patients presenting with mechanical allodynia (Feldman et al., 2019).

No loss of motor function was seen by rotarod testing in these mice during the course of the study (**Figure 4-4** & **Figure 4-5**). These results are similar to what has been noted in other studies looking at changes in rotarod performance in STZ-induced diabetic mice across 6 weeks post-hyperglycaemia (Souayah et al., 2009). However, from our results, we cannot rule out that motor dysfunction presents after 13 weeks, as the disease progresses, as the loss of motor fibres is a much later symptom (O'Brien et al., 2014).

The full mechanism(s) behind how peripheral nerves are damaged in both painful and painless diabetic neuropathy are largely unknown; however, it is hypothesised that the persistent hyperglycaemia and dyslipidaemia that are associated with diabetes cause nerve damage (Rosenberger et al., 2020). In this scheme, high blood and cellular concentrations of glucose and lipids result in increased oxidative stress, inflammation and mitochondrial dysfunction; all of which cause metabolic damage, and structural and functional changes to the peripheral nerves (Rosenberger et al., 2020). This dysregulation can also cause microvascular damage, which in turn can lead to hypoxia causing nerve ischemia (Rosenberger et al., 2020).

When the nerve cells are subjected to increased blood glucose levels, as is the case with diabetes, there has been shown to be a nearly three-fold increase in the presence of advanced glycation end products (AGEs). This is evident from both *in vitro* and *in vivo* studies; for

example in the sciatic nerves of diabetic rats and dogs when compared to non-diabetic control animals (Vlassara et al., 1981). Glycation is random, and non-enzymatic, and can readily occur on lysine residues within proteins (Akio & Ritsuko, 2021) leading to increased AGEs, which have been shown to play a role in the pathogenesis of diabetic neuropathy (Sugimoto et al., 2008). An accumulation of AGEs on neuronal cytoskeleton proteins like tubulin, neurofilament and actin leads to increased oxidative stress triggering fibre loss and slowed axonal transport (Sugimoto et al., 2008). It is therefore interesting to speculate that lysine 40 within α-tubulin might be a target for glycation (Akio & Ritsuko, 2021), and may account for the loss in α-tubulin acetylation observed in both proximal and distal sciatic nerve segments (Glozak et al., 2005; Janke & Montagnac, 2017).

4.4.3 Loss of acetylated α-tubulin

As set out previously in section 4.1.2, the stability of microtubules is essential for efficient transport in nerve cells, and the acetylation of α-tubulin is an important part of this (Reed et al., 2006). Various length-dependent peripheral neuropathies, like CMT and chemotherapy-induced neuropathy, display a loss of acetylation of α-tubulin (Adalbert et al., 2020; Picci et al., 2020; Van Helleputte et al., 2018). Whether or not acetylated α-tubulin levels are altered in diabetic neuropathy has not been investigated. To determine if there was a loss of α-tubulin acetylation associated with diabetic neuropathy, sciatic nerve tissues were taken from diabetic and citrate buffer-treated, non-diabetic control mice. The sciatic nerve was bisected into distal and proximal portions and the total tubulin and acetylated α-tubulin levels in each nerve portion were measured.

While streptozotocin-induced diabetic mice did not show a loss of total α-tubulin (**Figure 4-12** &**Figure 4-17**), a marked loss of α-tubulin acetylation was evident in both the proximal and distal sciatic nerves. The loss is more marked in the distal nerve, with three-quarters of the acetylated tubulin lost when compared to the non-diabetic citrate controls (**Figure 4-14** & **Figure 4-19**). It is unclear if this loss progresses more quickly in the distal sciatic nerve, or loss begins at an earlier time point, but with no statistically significant difference in total levels of α-tubulin, it is unlikely that the loss of nerve tissue is what is driving the acetylated α-tubulin difference – at least up until the 13 week time point. There is certainly evidence in the literature that a loss of nerve tissue occurs in diabetes, both in the peripheral nerves (Baptista

et al., 2019; Dyck et al., 1986), and corneal nerves (Ferdousi et al., 2020), and this may also be the case in this model of the disease was left to progress longer than the 13 weeks.

Future work to understand the progression of acetylated α-tubulin loss in the sciatic nerves of STZ-induced diabetic mice could prove valuable. It would also be of interest to determine if the loss of acetylated α-tubulin in the sciatic nerves corresponds with the onset of neuropathic pain symptoms in diabetic mice, and if the glycation of the lysine in the α-tubulin is driving the lowered levels of acetylated α-tubulin that have been shown here.

4.4.3.1 HDAC6 inhibition

If α-tubulin acetylation loss plays a role in the development and progression of peripheral neuropathy and neuropathic pain, one way to promote re-acetylation of α-tubulin is by selective histone deacetylase 6 (HDAC6) inhibition. Acetylation levels of α-tubulin is largely determined by the competing activities of two enzymes; α-tubulin acetyltransferase (α-TAT), which is responsible for lysine 40 (K40) acetylation, and HDAC6, which deacetylates K40 by, by removing the acetyl group (Reed et al., 2006). It has been demonstrated in mice, that the loss of HDAC6 (*hdac6*-knockout) leads to increased acetylated α-tubulin levels (Hubbert et al., 2002). Furthermore, treatment with an HDAC6 inhibitor drug has been shown to increase the amount of acetylated α-tubulin and ameliorate the neuropathic pain symptoms and motor dysfunction seen in CMT2A mice (Picci et al., 2020; Shen et al., 2021). Similar to the diabetic mice, CMT2A mice show a progressive and length-dependent degeneration of the nerve tissue, with distal sciatic nerve portions showing a marked decrease in acetylated α-tubulin levels with age (Picci et al., 2020). When these mice were treated daily with an HDAC6 inhibitor drug, either pre-symptomatically or post-symptomatically, there was an improvement in mechanical allodynia, thermal hyperalgesia and rotarod scores (Picci et al., 2020). Concomitant with the improvement in pain, there was also a rescue of acetylated α-tubulin to that of wildtype mice (Picci et al., 2020).

Other studies have similarly shown that HDAC6 inhibition can promote increased acetylated α-tubulin levels in the nerves, improve motor defects and decrease neuropathic pain; for example, chemotherapy-induced neuropathies in rodents (Castelli et al., 2018; Krukowski et al., 2015; Krukowski et al., 2017; Van Helleputte et al., 2018; Zhang et al., 2022). Similar to

other peripheral degenerative neuropathies, chemotherapy-induced neuropathy causes a dieback of nerve tissues from the distal end of the nerves (Malacrida et al., 2019). This means that often the chemotherapy drugs are dose limited. Different chemotherapy drugs seem to have slightly different mechanisms for causing nerve damage, but many that target microtubules to interrupt cell division in cancer cells, result in adversely disrupting the integrity and functioning of microtubules in axons leading to peripheral nerve damage (Castelli et al., 2018). Promoting α-tubulin acetylation by HDAC inhibition in this context appears to provide some protection to the axon (Castelli et al., 2018; Krukowski et al., 2015; Krukowski et al., 2017; Van Helleputte et al., 2018; Zhang et al., 2022).

Considering the loss of acetylated α-tubulin seen in the diabetic mice (Figure **4-14** & Figure **4-19**), it is reasonable to consider that treatment with an HDAC6 inhibitor could lead to an improvement in the nerve structure and function, and to neuropathic pain. Future work to determine if this is a valid treatment for diabetic neuropathy would prove invaluable.

4.4.4 Efficacy of cannabinoids to treat streptozotocin-induced neuropathic pain.

While the levels of α-tubulin acetylation may provide some insights to the pathogenesis of diabetic-induced peripheral neuropathy, the main purpose for developing and characterizing this model in the laboratory was that it might be used as a clinically relevant model of neuropathic pain in which cannabis isolates could be tested. The previous chapter (Efficacy of Cannabinoids to Treat Neuropathic Pain in a Mouse Model of Charcot-Marie-Tooth Disease, type 2A), of this work has shown that cannabis isolates, (12.5 mg/kg CBD, CBD:THC and a high CBD whole extract) show efficacy in treating established neuropathic pain symptoms in a genetic model of CMT2A (**Figure 3-16**). These cannabinoids could also show efficacy in diabetic-induced neuropathy. Although time constraints meant that this was not tested in this study, evidence in the literature suggests that certain cannabinoids are a viable option to improve painful diabetic neuropathy. One study, using STZ-induced diabetic rats, that were given high CDB whole extract daily for seven days at 30 mg/kg showed a rescue of both mechanical allodynia and thermal hypoalgesia (Comelli et al., 2009). It is interesting to note that these rats showed thermal hypoalgesia starting two weeks post-STZ administration, when the opposite, thermal hyperalgesia, was seen in this work. A second study has shown that CBD (10 mg/kg and 20 mg/kg) given to mice intraperitoneally at the onset of diabetes

slows the onset and development of neuropathic pain symptoms (Toth et al., 2010). However, the same result was not seen with the administration of the CBD once the mice had established a chronic neuropathic pain state (Toth et al., 2010).

As set out previously in section 4.4.3.1, there are also similarities between the nerve damage occurring with diabetes and that occurring with chemotherapy-induced neuropathy. Of the latter, CBD has also been shown to have efficacy in preventing and ameliorating the neuropathic pain. Mice injected with either 2.5 mg/kg or 5 mg/kg of CBD 15 min before administration of a chemotherapy drug, paclitaxel, prevented the development of mechanical allodynia (Ward et al., 2014). CBD at 5 mg/kg and 10 mg/kg was also able to prevent the development of both cold and mechanical allodynia associated with paclitaxel-induced neuropathic pain in female mice (Ward et al., 2011). The overall theme seems to be that CBD could have some efficacy at preventing neuropathic pain when it is started early and given frequently. Future work using this mouse diabetic-induced peripheral neuropathy model to determine the efficacy of early and/or long-term treatment with the cannabis isolates, would provide further insight into the whether this phenomenon is generalisable to other painful peripheral neuropathies.

4.5 Conclusion

The administration of a single high dose of STZ to induce diabetes and consequently establish a model of diabetic-induced neuropathic pain was relatively robust and successful. The mice reliably showed high blood glucose within two weeks post-STZ administration, good survival rates, and limited adverse symptoms that are normally associated with diabetes. All mice that became diabetic went on to display thermal hyperalgesia symptoms, and nearly 40% showed mechanical allodynia symptoms. The time taken to develop neuropathic pain symptoms varied from four to eleven weeks post-STZ administration and there was no loss of motor function within the 13 weeks of the study. Although no treatment with cannabinoids was given to these mice, future work can be carried out with confidence now that the model has been established and characterised.

A marked loss of acetylated α-tubulin was found in both the proximal and distal sciatic nerves of the diabetic mice. This loss was greater in the distal sciatic nerve and was unlikely to reflect nerve degeneration as total α-tubulin levels were unchanged. Acetylated α-tubulin in microtubules is important for efficient transport of mitochondria and other cargos along the long axons of peripheral nerve cells. This large reduction in the acetylated α-tubulin levels would undoubtably impact axonal transport and could exacerbate (or even precede) the nerve dysfunction and damage that occurs with diabetes. There has been some success with the use of HDAC6 inhibitor drugs to ameliorate the loss of acetylated α-tubulin in other neuropathies, namely CMT2A and chemotherapy-induced neuropathic pain. An HDAC6 inhibitor could prove to be a valid treatment for improving transport and the associated neuropathic pain in an STZ-induced diabetic model.

5 Conclusions and Future Work

This work aimed to determine the analgesic efficacy of specific cannabis extracts in a pre-clinical model of neuropathic pain; this was completed in three parts. Firstly, a dose-response trial was carried out to using gene expression biomarkers to determine what doses of orally administered CBD in an olive oil vehicle had a biological effect in dorsal root ganglia in peripheral nerves of mice. The next step determined the efficacy of pure CBD, (dosed from 6.25 mg/kg to 100 mg/kg), a high CBD whole extract, and a CBD:THC mix in providing analgesia in a neuropathic pain model of CMT2A mice. Changes in thermal hyperalgesia and mechanical allodynia responses were measured before and after treatment with cannabinoids. Repeated responses were measured across four hours for a single oral dose of all the cannabinoids and across eight hours for pure CBD dosed at 12.5 mg/kg every two hours. The third objective was to characterise a wildtype B6:D2 male mouse model of a single high-dose of STZ-induced diabetic neuropathy. This was to determine the number of mice that develop neuropathic pain and the time of symptom onset.

The dose-response trial (using 25, 50, 100 & 150 mg/kg CBD) showed a U-shaped dose response with greatest biomarker change occurring for 25 and 100 mg/kg, while the middle dose of 50 mg/kg showed a lower response. Similarly, the 150 mg/kg dose showed very little change in gene expression; and as repeated doses at this concentration have been implicated in liver damage, this dose was not used moving forward. Because of this profile, the doses of 25, 50 and 100 mg/kg were all used in the behaviour trials.

The U-shaped dose-response seen with the biomarker dose-response trial was mirrored in terms of efficacy in treating thermal hyperalgesia in the CMT2A mice. Additionally, lower doses of 6.25 and 12.5 mg/kg CBD were tested to find the lowest therapeutic dose. As set out previously, this U-shaped dose-response is not unusual with CBD, many studies have shown this response in both pre-clinical and clinical trials.

Although all CBD doses showed some improvement of thermal hyperalgesia symptoms in the CMT2A mice, the lower dose of 12.5 mg/kg showed the most efficacy and was comparable to a clinically relevant dose of gabapentin, given orally at 40 mg/kg. This was noted for both the single oral dose and repeated doses across eight hours. In contrast to thermal hyperalgesia, none of the doses of CBD given to the mice were efficacious against mechanical allodynia.

Once the most effective dose of CBD was determined, trials using a high CBD whole extract (containing 12.5 mg/kg CBD, 0.867 mg/kg THC and smaller factions of other cannabinoids, terpenes, and flavonoids) and a CBD:THC mix (containing 12.5 mg/kg CBD and 0.867 mg/kg THC) were performed. A greater amelioration of thermal hyperalgesia symptoms in CMT2A mice was seen with high CBD whole extract when compared to the pure isolate of 12.5 mg/kg CBD, as well as some efficacy for mechanical allodynia. The improvement in treating thermal hyperalgesia and mechanical allodynia was not due to the addition of THC alone, as the pure isolate of CBD:THC with the same concentrations of CBD and THC as the high CBD whole extract, did not show the same improvement.

Although this work has shown that cannabinoids have therapeutic efficacy in ameliorating neuropathic pain symptoms in CMT2A mice, CMT is not the leading cause of neuropathic pain in the human population. Diabetic-induced neuropathy represents both the largest and fastest-growing group of patients who suffer from neuropathic pain. Therefore, to establish a more clinically relevant preclinical model that might be used to test cannabinoid isolates, a mouse model of STZ-induced diabetic neuropathy was established and characterised. Sixty-five percent of mice administered a single high dose of STZ (180 mg/kg) became diabetic within two weeks. The mice developed measurable neuropathic symptoms, in the form of thermal hyperalgesia and mechanical allodynia, but did not display motor dysfunction within 13-week period of diabetes. Interestingly, these diabetic mice also showed a marked loss of acetylated α-tubulin in sciatic nerve tissue when compared to citrate buffer-treated, non-diabetic control mice. This loss was seen in both the proximal and distal portions of the sciatic nerve, with a more marked loss seen in the distal portion. Other neuropathies that show a loss of acetylated α-tubulin have shown pre-clinical improvements with the use of HDAC6 inhibitor drugs, this includes CMT2A and chemotherapy-induced neuropathy. This model could be used in the future to test the efficacy of cannabinoids to ameliorate painful diabetic-induced neuropathy.

Future work could also include biomarker analysis of lower CBD doses (e.g. 6.25 mg/kg and 12.5 mg/kg) to determine what changes to biomarker gene transcription occur at these concentrations. This work could lead to greater insight into what pathways and mechanisms are involved in the analgesic properties of CBD, but also reinforce the utility of the biomarkers identified in this study for predicting what might be efficacious does of new or

uncharacterised cannabinoids prior to performing time consuming and laborious pain-related behavioural studies. In addition to new or uncharacterised cannabinoids, the ability to predict efficacious doses would also streamline the testing of different formulations of cannabinoids in both the mouse CMT2A model and diabetic neuropathy model of neuropathic pain.

References

Adalbert, R., Kaieda, A., Antoniou, C., Loreto, A., Yang, X., Gilley, J., Hoshino, T., Uga, K., Makhija, M. T., & Coleman, M. P. (2020, 2020/02/05). Novel HDAC6 Inhibitors Increase Tubulin Acetylation and Rescue Axonal Transport of Mitochondria in a Model of Charcot–Marie–Tooth Type 2F. *ACS Chemical Neuroscience, 11*(3), 258-267. https://doi.org/10.1021/acschemneuro.9b00338

Adelizzi, R. A. (1999). COX-1 and COX-2 in health and disease. *The Journal of the American Osteopathic Association, 99*(11_suppl), S7-S12. https://doi.org/10.7556/jaoa.1999.99.11.S7

Ahimsadasan, N., Reddy, V., Suheb, M. Z. K., & Kumar, A. (2022). *Neuroanatomy, Dorsal Root Ganglion* https://www.ncbi.nlm.nih.gov/books/NBK532291/

Akio, N., & Ritsuko, K. (2021). Advanced Glycation End Products and Oxidative Stress in a Hyperglycaemic Environment. In R. Alok & A. Jamal (Eds.), *Fundamentals of Glycosylation* (pp. Ch. 2). IntechOpen. https://doi.org/10.5772/intechopen.97234

Aksu, I., Ates, M., Baykara, B., Kiray, M., Sisman, A. R., Buyuk, E., Baykara, B., Cetinkaya, C., Gumus, H., & Uysal, N. (2012). Anxiety correlates to decreased blood and prefrontal cortex IGF-1 levels in streptozotocin induced diabetes. *Neuroscience Letters, 531*(2), 176-181. https://doi.org//10.1016/j.neulet.2012.10.045

Al-Chalabi, A., & Miller, C. C. J. (2003). Neurofilaments and neurological disease. *BioEssays, 25*(4), 346-355. https://doi.org/10.1002/bies.10251

Alger, B. E. (2013). Getting high on the endocannabinoid system. *Cerebrum : the Dana forum on brain science, 2013*, 14-14. https://www.ncbi.nlm.nih.gov/pubmed/24765232

Ameri, A. (1999). The effects of cannabinoids on the brain. *Progress in Neurobiology, 58*(4), 315-348. https://doi.org/10.1016/s0301-0082(98)00087-2

American-Diabetes-Association. (2013, Jan). Diagnosis and classification of diabetes mellitus. *Diabetes Care, 36 Suppl 1*, S67-74. https://doi.org/10.2337/dc13-S067

Anand, U., Jones, B., Korchev, Y., Bloom, S. R., Pacchetti, B., Anand, P., & Sodergren, M. H. (2020). CBD Effects on TRPV1 Signaling Pathways in Cultured DRG Neurons. *J Pain Res, 13*, 2269-2278. https://doi.org/10.2147/jpr.S258433

Andersohn, F., Schade, R., Willich, S. N., & Garbe, E. (2010, Jul 27). Use of antiepileptic drugs in epilepsy and the risk of self-harm or suicidal behavior. *Neurology, 75*(4), 335-340. https://doi.org/10.1212/WNL.0b013e3181ea157e

Anderson, L. L., Low, I. K., Banister, S. D., McGregor, I. S., & Arnold, J. C. (2019, Nov 22). Pharmacokinetics of Phytocannabinoid Acids and Anticonvulsant Effect of Cannabidiolic Acid in a Mouse Model of Dravet Syndrome. *J Nat Prod, 82*(11), 3047-3055. https://doi.org/10.1021/acs.jnatprod.9b00600

Appendino, G., Gibbons, S., Giana, A., Pagani, A., Grassi, G., Stavri, M., Smith, E., & Rahman, M. M. (2008, 2008/08/01). Antibacterial Cannabinoids from Cannabis sativa: A Structure−Activity Study. *Journal of Natural Products, 71*(8), 1427-1430. https://doi.org/10.1021/np8002673

Argoff, C. E., Cole, B. E., Fishbain, D. A., & Irving, G. A. (2006). Diabetic Peripheral Neuropathic Pain: Clinical and Quality-of-Life Issues. *Mayo Clinic Proceedings, 81*(4, Supplement), S3-S11. https://doi.org//10.1016/S0025-6196(11)61474-2

Ashton, C. H. (2001). Pharmacology and effects of cannabis: A brief review. *British Journal of Psychiatry, 178*(2), 101-106. https://doi.org/10.1192/bjp.178.2.101

Atalay, S., Jarocka-Karpowicz, I., & Skrzydlewska, E. (2020). Antioxidative and anti-inflammatory properties of cannabidiol. *Antioxidants, 9*(1), 21. https://doi.org//10.3390/antiox9010021

Atwal, N., Casey, S. L., Mitchell, V. A., & Vaughan, C. W. (2019). THC and gabapentin interactions in a mouse neuropathic pain model. *Neuropharmacology, 144*, 115-121. https://doi.org/10.1016/j.neuropharm.2018.10.006

Backonja, M., & Glanzman, R. L. (2003). Gabapentin dosing for neuropathic pain: Evidence from randomized, placebo-controlled clinical trials. *Clinical Therapeutics, 25*(1), 81-104. https://doi.org//10.1016/S0149-2918(03)90011-7

Banerjee, S., & McCormack, S. (2019). *Medical Cannabis for the Treatment of Chronic Pain: A Review of Clinical Effectiveness and Guidelines*. Canadian Agency for Drugs and Technologies in Health. https://www.ncbi.nlm.nih.gov/pubmed/31532599

Baptista, F. I., Pinheiro, H., Gomes, C. A., & Ambrósio, A. F. (2019, Mar). Impairment of Axonal Transport in Diabetes: Focus on the Putative Mechanisms Underlying Peripheral and Central Neuropathies. *Mol Neurobiol, 56*(3), 2202-2210. https://doi.org/10.1007/s12035-018-1227-1

Baron, E. P. (2018). Medicinal Properties of Cannabinoids, Terpenes, and Flavonoids in Cannabis, and Benefits in Migraine, Headache, and Pain: An Update on Current Evidence and Cannabis Science. *Headache: The Journal of Head and Face Pain, 58*(7), 1139-1186. https://doi.org//10.1111/head.13345

Baron, R. G., J. . (2016). Neuropathic Pain. *Seminars in Neurology, 36*(05), 462-468. https://doi.org//10.1055%2Fs-0036-1584950

Barrett, M. L., Scutt, A. M., & Evans, F. J. (1986, 1986/04/01). Cannflavin A and B, prenylated flavones fromCannabis sativa L. *Experientia, 42*(4), 452-453. https://doi.org/10.1007/BF02118655

Barrie, N., & Manolios, N. (2017). The endocannabinoid system in pain and inflammation: Its relevance to rheumatic disease. *European journal of rheumatology, 4*(3), 210-218. https://doi.org/10.5152/eurjrheum.2017.17025

Basbaum, A. I., Bautista, D. M., Scherrer, G., & Julius, D. (2009). Cellular and Molecular Mechanisms of Pain. *Cell, 139*(2), 267-284. https://doi.org//10.1016/j.cell.2009.09.028

Basu, S., Ray, A., & Dittel, B. N. (2011). Cannabinoid receptor 2 is critical for the homing and retention of marginal zone B lineage cells and for efficient T-independent immune responses. *Journal of immunology (Baltimore, Md. : 1950), 187*(11), 5720-5732. https://doi.org/10.4049/jimmunol.1102195

Beaulieu, P. (2005). Toxic effects of cannabis and cannabinoids: Animal data. *Pain Research and Management, 10*(Suppl A), 23A-26A. https://doi.org//10.1155/2005/763623

Ben-Shabat, S., Fride, E., Sheskin, T., Tamiri, T., Rhee, M.-H., Vogel, Z., Bisogno, T., De Petrocellis, L., Di Marzo, V., & Mechoulam, R. (1998). An entourage effect: inactive endogenous fatty acid glycerol esters enhance 2-arachidonoyl-glycerol cannabinoid activity. *European journal of pharmacology, 353*(1), 23-31. https://doi.org//10.1016/S0014-2999(98)00392-6

Bennett, M. I., & Simpson, K. H. (2004, Jan). Gabapentin in the treatment of neuropathic pain. *Palliat Med, 18*(1), 5-11. https://doi.org/10.1191/0269216304pm845ra

Binns, D., Dimmer, E., Huntley, R., Barrell, D., O'Donovan, C., & Apweiler, R. (2009, Nov 15). QuickGO: a web-based tool for Gene Ontology searching. *Bioinformatics, 25*(22), 3045-3046. https://doi.org/10.1093/bioinformatics/btp536

Bonnet, U., Richter, E. L., Isbruch, K., & Scherbaum, N. (2018, Jun). On the addictive power of gabapentinoids: a mini-review. *Psychiatr Danub, 30*(2), 142-149. https://doi.org/10.24869/psyd.2018.142

Bouhassira, D., Lanteri-Minet, M., Attal, N., Laurent, B., & Touboul, C. (2008, Jun). Prevalence of chronic pain with neuropathic characteristics in the general population. *Pain, 136*(3), 380-387. https://doi.org/10.1016/j.pain.2007.08.013

Bowery, N. G., & Smart, T. G. (2006). GABA and glycine as neurotransmitters: a brief history. *British journal of pharmacology, 147 Suppl 1*(Suppl 1), S109-S119. https://doi.org/10.1038/sj.bjp.0706443

Brand, E. J., & Zhao, Z. (2017). Cannabis in Chinese Medicine: Are Some Traditional Indications Referenced in Ancient Literature Related to Cannabinoids? *Frontiers in pharmacology, 8*, 108-108. https://doi.org/10.3389/fphar.2017.00108

Bridgeman, M. B., & Abazia, D. T. (2017). Medicinal Cannabis: History, Pharmacology, And Implications for the Acute Care Setting. *P & T : a peer-reviewed journal for formulary management, 42*(3), 180-188. https://www.ncbi.nlm.nih.gov/pubmed/28250701

Bridgestock, C., & Rae, C. P. (2013). Anatomy, physiology and pharmacology of pain. *Anaesthesia & Intensive Care Medicine, 14*(11), 480-483. https://doi.org//10.1016/j.mpaic.2013.08.004

Brito-Casillas, Y., Melian, C., & Wagner, A. M. (2016, Aug-Sep). Study of the pathogenesis and treatment of diabetes mellitus through animal models. *Endocrinol Nutr, 63*(7), 345-353. https://doi.org/10.1016/j.endonu.2016.03.011

Brown, M. J., & Asbury, A. K. (1984). Diabetic neuropathy. *Annals of Neurology: Official Journal of the American Neurological Association and the Child Neurology Society, 15*(1), 2-12. https://doi.org//10.1002/ana.410150103

Bult, C. J., Blake, J. A., Smith, C. L., Kadin, J. A., & Richardson, J. E. (2019, Jan 8). Mouse Genome Database (MGD) 2019. *Nucleic Acids Res, 47*(D1), D801-d806. https://doi.org/10.1093/nar/gky1056

Buntin-Mushock, C., Phillip, L., Moriyama, K., & Palmer, P. P. (2005, Jun). Age-dependent opioid escalation in chronic pain patients. *Anesth Analg, 100*(6), 1740-1745. https://doi.org/10.1213/01.Ane.0000152191.29311.9b

Burks, S. S., Levi, D. J., Hayes, S., & Levi, A. D. (2014). Challenges in sciatic nerve repair: anatomical considerations. *Journal of neurosurgery, 121*(1), 210-218. https://doi.org//10.3171/2014.2.jns131667

Burstein, S. (2015). Cannabidiol (CBD) and its analogs: a review of their effects on inflammation. *Bioorganic & Medicinal Chemistry, 23*(7), 1377-1385. https://doi.org//10.1016/j.bmc.2015.01.059

Burston, J. J., & Woodhams, S. G. (2014). Endocannabinoid system and pain: an introduction. *Proceedings of the Nutrition Society, 73*(1), 106-117. https://doi.org/10.1017/S0029665113003650

Bustin, S. A., Benes, V., Garson, J. A., Hellemans, J., Huggett, J., Kubista, M., Mueller, R., Nolan, T., Pfaffl, M. W., Shipley, G. L., Vandesompele, J., & Wittwer, C. T. (2009, Apr). The MIQE guidelines: minimum information for publication of quantitative real-time PCR experiments. *Clin Chem, 55*(4), 611-622. https://doi.org/10.1373/clinchem.2008.112797

Cabrera, C. L. R., Keir-Rudman, S., Horniman, N., Clarkson, N., & Page, C. (2021). The anti-inflammatory effects of cannabidiol and cannabigerol alone, and in combination. *Pulmonary Pharmacology & Therapeutics, 69*, 102047. https://doi.org//10.1016/j.pupt.2021.102047

Campos, A. C., & Guimarães, F. S. (2008, 2008/08/01). Involvement of 5HT1A receptors in the anxiolytic-like effects of cannabidiol injected into the dorsolateral periaqueductal gray of rats. *Psychopharmacology, 199*(2), 223-230. https://doi.org/10.1007/s00213-008-1168-x

Carter, G. T., Jensen, M. P., Galer, B. S., Kraft, G. H., Crabtree, L. D., Beardsley, R. M., Abresch, R. T., & Bird, T. D. (1998). Neuropathic pain in Charcot-Marie-tooth disease. *Archives of physical medicine and rehabilitation, 79*(12), 1560-1564. https://doi.org//10.1016/S0003-9993(98)90421-X

Casey, S. L., Atwal, N., & Vaughan, C. W. (2017). Cannabis constituent synergy in a mouse neuropathic pain model. *Pain, 158*(12), 2452-2460. https://doi.org/10.1097/j.pain.0000000000001051

Castelli, V., Palumbo, P., d'Angelo, M., Moorthy, N. K., Antonosante, A., Catanesi, M., Lombardi, F., Iannotta, D., Cinque, B., Benedetti, E., Ippoliti, R., Cifone, M. G., & Cimini, A. (2018, Jun 15). Probiotic DSF counteracts chemotherapy induced neuropathic pain. *Oncotarget, 9*(46), 27998-28008. https://doi.org/10.18632/oncotarget.25524

Caterina, M. J., & Julius, D. (2001). The vanilloid receptor: a molecular gateway to the pain pathway. *Annu Rev Neurosci, 24*, 487-517. https://doi.org/10.1146/annurev.neuro.24.1.487

Chaplan, S. R., Bach, F. W., Pogrel, J. W., Chung, J. M., & Yaksh, T. L. (1994). Quantitative assessment of tactile allodynia in the rat paw. *Journal of Neuroscience Methods, 53*(1), 55-63. https://doi.org//10.1016/0165-0270(94)90144-9

Cheah, M., Fawcett, J. W., & Andrews, M. R. (2017). Assessment of Thermal Pain Sensation in Rats and Mice Using the Hargreaves Test. *Bio-protocol, 7*(16), e2506. https://doi.org/10.21769/BioProtoc.2506

Chen, L., Deng, H., Cui, H., Fang, J., Zuo, Z., Deng, J., Li, Y., Wang, X., & Zhao, L. (2017). Inflammatory responses and inflammation-associated diseases in organs. *Oncotarget, 9*(6), 7204-7218. https://doi.org/10.18632/oncotarget.23208

Chopra, K., & Tiwari, V. (2012). Alcoholic neuropathy: possible mechanisms and future treatment possibilities. *British Journal of Clinical Pharmacology, 73*(3), 348-362. https://doi.org//10.1111/j.1365-2125.2011.04111.x

Cogan, P. S. (2020, Aug). The 'entourage effect' or 'hodge-podge hashish': the questionable rebranding, marketing, and expectations of cannabis polypharmacy. *Expert Rev Clin Pharmacol, 13*(8), 835-845. https://doi.org/10.1080/17512433.2020.1721281

Colleoni, M., & Sacerdote, P. (2010). Murine models of human neuropathic pain. *Biochimica et Biophysica Acta (BBA) - Molecular Basis of Disease, 1802*(10), 924-933. https://doi.org//10.1016/j.bbadis.2009.10.012

Comelli, F., Bettoni, I., Colleoni, M., Giagnoni, G., & Costa, B. (2009). Beneficial effects of a Cannabis sativa extract treatment on diabetes-induced neuropathy and oxidative stress. *Phytotherapy Research, 23*(12), 1678-1684. https://doi.org/10.1002/ptr.2806

Costa, B., Giagnoni, G., Franke, C., Trovato, A. E., & Colleoni, M. (2004, Sep). Vanilloid TRPV1 receptor mediates the antihyperalgesic effect of the nonpsychoactive cannabinoid, cannabidiol, in a rat model of acute inflammation. *British journal of pharmacology, 143*(2), 247-250. https://doi.org/10.1038/sj.bjp.0705920

Costa, B., Trovato, A. E., Comelli, F., Giagnoni, G., & Colleoni, M. (2007). The non-psychoactive cannabis constituent cannabidiol is an orally effective therapeutic agent in rat chronic inflammatory and neuropathic pain. *European journal of pharmacology, 556*(1-3), 75-83. https://doi.org/10.1016/j.ejphar.2006.11.006

Cruccu, G., & Truini, A. (2009). Tools for assessing neuropathic pain. *PLoS medicine, 6*(4), e1000045-e1000045. https://doi.org/10.1371/journal.pmed.1000045

Davis, W. M., & Hatoum, N. S. (1983). Neurobehavioral actions of cannabichromene and interactions with delta 9-tetrahydrocannabinol. *Gen Pharmacol, 14*(2), 247-252. https://doi.org/10.1016/0306-3623(83)90004-6

Dayanandan, P., & Kaufman, P. B. (1976). Trichomes of Cannabis Sativa L. (Cannabaceae). *American Journal of Botany, 63*(5), 578-591. https://doi.org/10.1002/j.1537-2197.1976.tb11846.x

de Almeida, D. L., & Devi, L. A. (2020, Dec). Diversity of molecular targets and signaling pathways for CBD. *Pharmacol Res Perspect, 8*(6), e00682. https://doi.org/10.1002/prp2.682

De Gregorio, D., McLaughlin, R. J., Posa, L., Ochoa-Sanchez, R., Enns, J., Lopez-Canul, M., Aboud, M., Maione, S., Comai, S., & Gobbi, G. (2019, Jan). Cannabidiol modulates serotonergic transmission and reverses both allodynia and anxiety-like behavior in a model of neuropathic pain. *Pain, 160*(1), 136-150. https://doi.org/10.1097/j.pain.0000000000001386

De Vriendt, E., Van Hul, M., Timmerman, V., Verhoeven, K., Jordanova, A., Robberecht, W., Roelens, F., Vance, J. M., Züchner, S., Saifi, G. M., Lupski, J. R., Szigeti, K., Butler, I. J., Mancias, P., Shy, M. E., Schröder, J. M., Weis, J., Christen, H.-J., Tournev, I., Guergueltcheva, V., Nelis, E., De Jonghe, P., Claeys, K. G., Seeman, P., Mazanec, R., Kochanski, A., Ryniewicz, B., Auer-Grumbach, M., Milic Rasic, V., Nevo, Y., Vieregge, P., Vinci, P., Moreno, M. T., Ceuterick, C., De Bleecker, J., Van Coster, R., Van den Bergh, P., Verellen, C., & Goemans, N. (2006). MFN2 mutation distribution and genotype/phenotype correlation in Charcot–Marie–Tooth type 2. *Brain, 129*(8), 2093-2102. https://doi.org/10.1093/brain/awl126

Deacon, R. M. J. (2013). Measuring motor coordination in mice. *Journal of visualized experiments : JoVE*(75), e2609-e2609. https://doi.org/10.3791/2609

Deeds, M. C., Anderson, J. M., Armstrong, A. S., Gastineau, D. A., Hiddinga, H. J., Jahangir, A., Eberhardt, N. L., & Kudva, Y. C. (2011). Single dose streptozotocin-induced diabetes: considerations for study design in islet transplantation models. *Laboratory animals, 45*(3), 131-140. https://doi.org/10.1258/la.2010.010090

Deiana, S., Watanabe, A., Yamasaki, Y., Amada, N., Arthur, M., Fleming, S., Woodcock, H., Dorward, P., Pigliacampo, B., Close, S., Platt, B., & Riedel, G. (2012, February 01). Plasma and brain pharmacokinetic profile of cannabidiol (CBD), cannabidivarine (CBDV), Δ9-tetrahydrocannabivarin (THCV) and cannabigerol (CBG) in rats and mice following oral and intraperitoneal administration and CBD action on obsessive–compulsive behaviour [journal article]. *Psychopharmacology, 219*(3), 859-873. https://doi.org/10.1007/s00213-011-2415-0

DeLong, G. T., Wolf, C. E., Poklis, A., & Lichtman, A. H. (2010). Pharmacological evaluation of the natural constituent of Cannabis sativa, cannabichromene and its modulation by Δ(9)-tetrahydrocannabinol. *Drug and alcohol dependence, 112*(1-2), 126-133. https://doi.org/10.1016/j.drugalcdep.2010.05.019

Demuth, D. G., & Molleman, A. (2006). Cannabinoid signalling. *Life sciences, 78*(6), 549-563. https://doi.org//10.1016/j.lfs.2005.05.055

Deshpande, A., Mailis-Gagnon, A., Zoheiry, N., & Lakha, S. F. (2015). Efficacy and adverse effects of medical marijuana for chronic noncancer pain: Systematic review of randomized controlled trials. *Canadian family physician Medecin de famille canadien, 61*(8), e372-e381. https://pubmed.ncbi.nlm.nih.gov/26505059

Detmer, S. A., & Chan, D. C. (2007, 11/01/online). Functions and dysfunctions of mitochondrial dynamics [Review Article]. *Nature Reviews Molecular Cell Biology, 8*, 870. https://doi.org/10.1038/nrm2275

Devane, W. A., Dysarz, F. r., Johnson, M. R., Melvin, L. S., & Howlett, A. C. (1988). Determination and characterization of a cannabinoid receptor in rat brain. *Molecular pharmacology, 34*(5), 605-613.

Donvito, G., Nass, S. R., Wilkerson, J. L., Curry, Z. A., Schurman, L. D., Kinsey, S. G., & Lichtman, A. H. (2018). The Endogenous Cannabinoid System: A Budding Source of Targets for Treating Inflammatory and Neuropathic Pain. *Neuropsychopharmacology : official publication of the American College of Neuropsychopharmacology, 43*(1), 52-79. https://doi.org/10.1038/npp.2017.204

Dubin, A. E., & Patapoutian, A. (2010). Nociceptors: the sensors of the pain pathway. *The Journal of clinical investigation, 120*(11), 3760-3772. https://doi.org/10.1172/JCI42843

Dyck, P. J., Karnes, J. L., O'Brien, P., Okazaki, H., Lais, A., & Engelstad, J. (1986). The spatial distribution of fiber loss in diabetic polyneuropathy suggests ischemia. *Annals of Neurology, 19*(5), 440-449. https://doi.org//10.1002/ana.410190504

Evans, F. J. (1991). Cannabinoids: The Separation of Central from Peripheral Effects on a Structural Basis. *Planta Medical, 57*(S 1), 60-67. https://doi.org/10.1055/s-2006-960231

Ewing, L. E., Skinner, C. M., Quick, C. M., Kennon-McGill, S., McGill, M. R., Walker, L. A., ElSohly, M. A., Gurley, B. J., & Koturbash, I. (2019). Hepatotoxicity of a Cannabidiol-Rich Cannabis Extract in the Mouse Model. *Molecules (Basel, Switzerland), 24*(9), 1694. https://doi.org/10.3390/molecules24091694

Feely, S. M. E., Laura, M., Siskind, C. E., Sottile, S., Davis, M., Gibbons, V. S., Reilly, M. M., & Shy, M. E. (2011). MFN2 mutations cause severe phenotypes in most patients with CMT2A. *Neurology, 76*(20), 1690. https://doi.org/10.1212/WNL.0b013e31821a441e

Feldman, E. L., Callaghan, B. C., Pop-Busui, R., Zochodne, D. W., Wright, D. E., Bennett, D. L., Bril, V., Russell, J. W., & Viswanathan, V. (2019, 2019/06/13). Diabetic neuropathy. *Nature Reviews Disease Primers, 5*(1), 41. https://doi.org/10.1038/s41572-019-0092-1

Ferdousi, M., Kalteniece, A., Azmi, S., Petropoulos, I. N., Ponirakis, G., Alam, U., Asghar, O., Marshall, A., Fullwood, C., Jeziorska, M., Abbott, C., Lauria, G., Faber, C. G., Soran, H., Efron, N., Boulton, A. J. M., & Malik, R. A. (2020). Diagnosis of Neuropathy and Risk Factors for Corneal Nerve Loss in Type 1 and Type 2 Diabetes: A Corneal Confocal

Microscopy Study. *Diabetes Care, 44*(1), 150-156. https://doi.org/10.2337/dc20-1482

Ferguson, J. M. (2001). SSRI Antidepressant Medications: Adverse Effects and Tolerability. *Primary care companion to the Journal of clinical psychiatry, 3*(1), 22-27. https://doi.org/10.4088/pcc.v03n0105

Filev, R., Engelke, D. S., Da Silveira, D. X., Mello, L. E., & Santos-Junior, J. G. (2017). THC inhibits the expression of ethanol-induced locomotor sensitization in mice. *Alcohol (Fayetteville, N.Y.), 65*, 31-35. https://doi.org/10.1016/j.alcohol.2017.06.004

Fine, P. G., & Rosenfeld, M. J. (2014). Cannabinoids for neuropathic pain. *Current Pain and Headache Reports, 18*(10), 451-451. https://doi.org/10.1007/s11916-014-0451-2

Finnerup, N. B., Haroutounian, S., Kamerman, P., Baron, R., Bennett, D. L., Bouhassira, D., Cruccu, G., Freeman, R., Hansson, P., Nurmikko, T., Raja, S. N., Rice, A. S., Serra, J., Smith, B. H., Treede, R. D., & Jensen, T. S. (2016, Aug). Neuropathic pain: an updated grading system for research and clinical practice. *Pain, 157*(8), 1599-1606. https://doi.org/10.1097/j.pain.0000000000000492

Formato, M., Crescente, G., Scognamiglio, M., Fiorentino, A., Pecoraro, M. T., Piccolella, S., Catauro, M., & Pacifico, S. (2020). (–)-Cannabidiolic Acid, a Still Overlooked Bioactive Compound: An Introductory Review and Preliminary Research. *Molecules (Basel, Switzerland), 25*(11), 2638. https://doi.org/10.3390/molecules25112638

Fornasari, D. (2014, Sep). Pain pharmacology: focus on opioids. *Clin Cases Miner Bone Metab, 11*(3), 165-168.

Fornasari, D. (2017). Pharmacotherapy for Neuropathic Pain: A Review. *Pain and therapy, 6*(Suppl 1), 25-33. https://doi.org/10.1007/s40122-017-0091-4

Foss, J. D., Farkas, D. J., Huynh, L. M., Kinney, W. A., Brenneman, D. E., & Ward, S. J. (2021). Behavioural and pharmacological effects of cannabidiol (CBD) and the cannabidiol analogue KLS-13019 in mouse models of pain and reinforcement. *British journal of pharmacology, 178*(15), 3067-3078. https://doi.org//10.1111/bph.15486

Fox, A., Eastwood, C., Gentry, C., Manning, D., & Urban, L. (1999, Jun). Critical evaluation of the streptozotocin model of painful diabetic neuropathy in the rat. *Pain, 81*(3), 307-316. https://doi.org/10.1016/s0304-3959(99)00024-x

Fride, E., Perchuk, A., Hall, F. S., Uhl, G. R., & Onaivi, E. S. (2006). Behavioral Methods in Cannabinoid Research. In E. S. Onaivi (Ed.), *Marijuana and Cannabinoid Research: Methods and Protocols* (pp. 269-290). Humana Press. https://doi.org/10.1385/1-59259-999-0:269

Friedman, D., & Sirven, J. I. (2017). Historical perspective on the medical use of cannabis for epilepsy: Ancient times to the 1980s. *Epilepsy & Behavior, 70*, 298-301. https://doi.org//10.1016/j.yebeh.2016.11.033

Furman, B. L. (2015, Sep 1). Streptozotocin-Induced Diabetic Models in Mice and Rats. *Curr Protoc Pharmacol, 70*, 5.47.41-20. https://doi.org/10.1002/0471141755.ph0547s70

Garland, E. L. (2012). Pain processing in the human nervous system: a selective review of nociceptive and biobehavioral pathways. *Primary care, 39*(3), 561-571. https://doi.org/10.1016/j.pop.2012.06.013

Genaro, K., Fabris, D., Arantes, A. L. F., Zuardi, A. W., Crippa, J. A. S., & Prado, W. A. (2017). Cannabidiol Is a Potential Therapeutic for the Affective-Motivational Dimension of Incision Pain in Rats. *Front Pharmacol, 8*, 391. https://doi.org/10.3389/fphar.2017.00391

Giuliano, F., & Warner, T. D. (2002). Origins of Prostaglandin E2: Involvements of Cyclooxygenase (COX)-1 and COX-2 in Human and Rat Systems. *Journal of Pharmacology and Experimental Therapeutics, 303*(3), 1001-1006. https://doi.org/10.1124/jpet.102.041244

Glozak, M. A., Sengupta, N., Zhang, X., & Seto, E. (2005). Acetylation and deacetylation of non-histone proteins. *Gene, 363*, 15-23. https://doi.org//10.1016/j.gene.2005.09.010

Grotenhermen, F. (2003, 2003/04/01). Pharmacokinetics and Pharmacodynamics of Cannabinoids. *Clinical Pharmacokinetics, 42*(4), 327-360. https://doi.org/10.2165/00003088-200342040-00003

Guimarães, F. S., Chiaretti, T. M., Graeff, F. G., & Zuardi, A. W. (1990, 1990/04/01). Antianxiety effect of cannabidiol in the elevated plus-maze. *Psychopharmacology, 100*(4), 558-559. https://doi.org/10.1007/BF02244012

Gupta, D., Radhakrishnan, M., & Kurhe, Y. (2014, 2014/09/01). Insulin reverses anxiety-like behavior evoked by streptozotocin-induced diabetes in mice. *Metabolic Brain Disease, 29*(3), 737-746. https://doi.org/10.1007/s11011-014-9540-5

Gustafsson, H., Flood, K., Berge, O.-G., Brodin, E., Olgart, L., & Stiller, C.-O. (2003). Gabapentin reverses mechanical allodynia induced by sciatic nerve ischemia and formalin-induced nociception in mice. *Experimental Neurology, 182*(2), 427-434. https://doi.org//10.1016/S0014-4886(03)00097-9

Harding, A. E., & Thomas, P. K. (1980). The Clinical Features of Hereditary Motor and Sensory Neuropathy Types I and II. *Brain, 103*(2), 259-280. https://doi.org/10.1093/brain/103.2.259

Hargreaves, K., Dubner, R., Brown, F., Flores, C., & Joris, J. (1988). A new and sensitive method for measuring thermal nociception in cutaneous hyperalgesia. *Pain, 32*(1), 77-88. https://doi.org//10.1016/0304-3959(88)90026-7

Harris, H. M., Sufka, K. J., Gul, W., & ElSohly, M. A. (2016). Effects of Delta-9-Tetrahydrocannabinol and Cannabidiol on Cisplatin-Induced Neuropathy in Mice. *Planta medica, 82*(13), 1169-1172. https://doi.org/10.1055/s-0042-106303

Hartsel, J. A., Eades, J., Hickory, B., & Makriyannis, A. (2016). Chapter 53 - Cannabis sativa and Hemp. In R. C. Gupta (Ed.), *Nutraceuticals* (pp. 735-754). Academic Press. https://doi.org//10.1016/B978-0-12-802147-7.00053-X

Haschek, W. M., Rousseaux, C. G., & Wallig, M. A. (2013). Toxicologic Pathology: An Introduction. In W. M. Haschek, C. G. Rousseaux, & M. A. Wallig (Eds.), *Haschek and Rousseaux's Handbook of Toxicologic Pathology (Third Edition)* (pp. 1-9). Academic Press. https://doi.org//10.1016/B978-0-12-415759-0.00094-7

Henshaw, F. R., Dewsbury, L. S., Lim, C. K., & Steiner, G. Z. (2021). The effects of cannabinoids on pro-and anti-inflammatory cytokines: a systematic review of in vivo studies. *Cannabis and cannabinoid research, 6*(3), 177-195. https://doi.org//10.1089/can.2020.0105

Hložek, T., Uttl, L., Kadeřábek, L., Balíková, M., Lhotková, E., Horsley, R. R., Nováková, P., Šíchová, K., Štefková, K., Tylš, F., Kuchař, M., & Páleníček, T. (2017, 2017/12/01/). Pharmacokinetic and behavioural profile of THC, CBD, and THC+CBD combination after pulmonary, oral, and subcutaneous administration in rats and confirmation of conversion in vivo of CBD to THC. *European Neuropsychopharmacology, 27*(12), 1223-1237. https://doi.org//10.1016/j.euroneuro.2017.10.037

Hoggart, B., Ratcliffe, S., Ehler, E., Simpson, K. H., Hovorka, J., Lejčko, J., Taylor, L., Lauder, H., & Serpell, M. (2015, 2015/01/01). A multicentre, open-label, follow-on study to assess the long-term maintenance of effect, tolerance and safety of THC/CBD oromucosal spray in the management of neuropathic pain. *Journal of Neurology, 262*(1), 27-40. https://doi.org/10.1007/s00415-014-7502-9

Hosking, R. D., & Zajicek, J. P. (2008, Jul). Therapeutic potential of cannabis in pain medicine. *Br J Anaesth, 101*(1), 59-68. https://doi.org/10.1093/bja/aen119

Howlett, A., Barth, F., Bonner, T., Cabral, G., Casellas, P., Devane, W., Felder, C., Herkenham, M., Mackie, K., & Martin, B. (2002). International Union of Pharmacology. XXVII. Classification of cannabinoid receptors. *Pharmacological reviews, 54*(2), 161-202. https://doi.org//10.1124/pr.54.2.161

Hubbert, C., Guardiola, A., Shao, R., Kawaguchi, Y., Ito, A., Nixon, A., Yoshida, M., Wang, X.-F., & Yao, T.-P. (2002, 05/23/online). HDAC6 is a microtubule-associated deacetylase. *Nature, 417*, 455. https://doi.org/10.1038/417455a

Hudson, L. J., Bevan, S., Wotherspoon, G., Gentry, C., Fox, A., & Winter, J. (2001, Jun). VR1 protein expression increases in undamaged DRG neurons after partial nerve injury. *Eur J Neurosci, 13*(11), 2105-2114. https://doi.org/10.1046/j.0953-816x.2001.01591.x

Huestis, M. A. (2005). Pharmacokinetics and metabolism of the plant cannabinoids, delta9-tetrahydrocannabinol, cannabidiol and cannabinol. *Handb Exp Pharmacol*(168), 657-690. https://doi.org/10.1007/3-540-26573-2_23

Huestis, M. A. (2007). Human cannabinoid pharmacokinetics. *Chemistry & biodiversity, 4*(8), 1770. https://doi.org//10.1002%2Fcbdv.200790152

Iannotti, F. A., Hill, C. L., Leo, A., Alhusaini, A., Soubrane, C., Mazzarella, E., Russo, E., Whalley, B. J., Di Marzo, V., & Stephens, G. J. (2014, 2014/11/19). Nonpsychotropic Plant Cannabinoids, Cannabidivarin (CBDV) and Cannabidiol (CBD), Activate and Desensitize Transient Receptor Potential Vanilloid 1 (TRPV1) Channels in Vitro: Potential for the Treatment of Neuronal Hyperexcitability. *ACS Chemical Neuroscience, 5*(11), 1131-1141. https://doi.org/10.1021/cn5000524

Izzo, A. A., Borrelli, F., Capasso, R., Di Marzo, V., & Mechoulam, R. (2009, 2009/10/01/). Non-psychotropic plant cannabinoids: new therapeutic opportunities from an ancient herb. *Trends in pharmacological sciences, 30*(10), 515-527. https://doi.org//10.1016/j.tips.2009.07.006

Izzo, A. A., Capasso, R., Aviello, G., Borrelli, F., Romano, B., Piscitelli, F., Gallo, L., Capasso, F., Orlando, P., & Di Marzo, V. (2012). Inhibitory effect of cannabichromene, a major non-psychotropic cannabinoid extracted from Cannabis sativa, on inflammation-induced hypermotility in mice. *British journal of pharmacology, 166*(4), 1444-1460. https://doi.org/10.1111/j.1476-5381.2012.01879.x

Jaggi, A. S., Jain, V., & Singh, N. (2011, Feb). Animal models of neuropathic pain. *Fundam Clin Pharmacol, 25*(1), 1-28. https://doi.org/10.1111/j.1472-8206.2009.00801.x

Janke, C., & Montagnac, G. (2017). Causes and Consequences of Microtubule Acetylation. *Current Biology, 27*(23), R1287-R1292. https://doi.org/10.1016/j.cub.2017.10.044

Jensen, T. S. (2002). Anticonvulsants in neuropathic pain: rationale and clinical evidence. *European Journal of Pain, 6*(SA), 61-68. https://doi.org/10.1053/eujp.2001.0324

Jensen, T. S., & Finnerup, N. B. (2014). Allodynia and hyperalgesia in neuropathic pain: clinical manifestations and mechanisms. *The Lancet Neurology, 13*(9), 924-935. https://doi.org//10.1016/S1474-4422(14)70102-4

Jesus, C. H. A., Redivo, D. D. B., Gasparin, A. T., Sotomaior, B. B., de Carvalho, M. C., Genaro, K., Zuardi, A. W., Hallak, J. E. C., Crippa, J. A., Zanoveli, J. M., & da Cunha, J. M. (2019). Cannabidiol attenuates mechanical allodynia in streptozotocin-induced diabetic rats via serotonergic system activation through 5-HT1A receptors. *Brain Research, 1715*, 156-164. https://doi.org//10.1016/j.brainres.2019.03.014

Jett, J., Stone, E., Warren, G., & Cummings, K. M. (2018). Cannabis Use, Lung Cancer, and Related Issues. *Journal of Thoracic Oncology, 13*(4), 480-487. https://doi.org//10.1016/j.jtho.2017.12.013

Jolivalt, C. G., Frizzi, K. E., Guernsey, L., Marquez, A., Ochoa, J., Rodriguez, M., & Calcutt, N. A. (2016). Peripheral Neuropathy in Mouse Models of Diabetes. *Current protocols in mouse biology, 6*(3), 223-255. https://doi.org/10.1002/cpmo.11

Jung, J., Meyer, M. R., Maurer, H. H., Neusüß, C., Weinmann, W., & Auwärter, V. (2009). Studies on the metabolism of the Δ9-tetrahydrocannabinol precursor Δ9-tetrahydrocannabinolic acid A (Δ9-THCA-A) in rat using LC-MS/MS, LC-QTOF MS and GC-MS techniques. *Journal of Mass Spectrometry, 44*(10), 1423-1433. https://doi.org/10.1002/jms.1624

Kaminski, N. E. (1996, Oct 25). Immune regulation by cannabinoid compounds through the inhibition of the cyclic AMP signaling cascade and altered gene expression. *Biochem Pharmacol, 52*(8), 1133-1140. https://doi.org/10.1016/0006-2952(96)00480-7

Karniol, I., & Carlini, E. (1973). Pharmacological interaction between cannabidiol and δ9-tetrahydrocannabinol. *Psychopharmacologia, 33*(1), 53-70.

Karniol, I. G., Shirakawa, I., Kasinski, N., Pfeferman, A., & Carlini, E. A. (1974). Cannabidiol interferes with the effects of Δ9-tetrahydrocannabinol in man. *European journal of pharmacology, 28*(1), 172-177.

Katalin, S., & Attila, K. (2017). Cannabis: A Treasure Trove or Pandora's Box? *Mini-Reviews in Medicinal Chemistry, 17*(13), 1223-1291. https://doi.org//10.2174/1389557516666161004162133

King, K. M., Myers, A. M., Soroka-Monzo, A. J., Tuma, R. F., Tallarida, R. J., Walker, E. A., & Ward, S. J. (2017). Single and combined effects of Δ(9) -tetrahydrocannabinol and cannabidiol in a mouse model of chemotherapy-induced neuropathic pain. *British journal of pharmacology, 174*(17), 2832-2841. https://doi.org/10.1111/bph.13887

Kingery, W. S. (1997). A critical review of controlled clinical trials for peripheral neuropathic pain and complex regional pain syndromes. *Pain, 73*(2), 123-139. https://doi.org/10.1016/s0304-3959(97)00049-3

Kirkpatrick, L. L. B., S. T; . (1999). Basic Neurochemistry: Molecular, Cellular and Medical Aspects. In G. J. A. Siegel, B. W; Albers R. W. (Ed.), *Components of the Neuronal Cytoskeleton*. Lippincott-Raven. https://www.ncbi.nlm.nih.gov/books/NBK28122/

Klauke, A. L., Racz, I., Pradier, B., Markert, A., Zimmer, A. M., Gertsch, J., & Zimmer, A. (2014). The cannabinoid CB2 receptor-selective phytocannabinoid beta-caryophyllene exerts analgesic effects in mouse models of inflammatory and neuropathic pain. *European Neuropsychopharmacology, 24*(4), 608-620. https://doi.org//10.1016/j.euroneuro.2013.10.008

Kogan, N. M., Melamed, E., Wasserman, E., Raphael, B., Breuer, A., Stok, K. S., Sondergaard, R., Escudero, A. V., Baraghithy, S., Attar-Namdar, M., Friedlander-Barenboim, S., Mathavan, N., Isaksson, H., Mechoulam, R., Müller, R., Bajayo, A., Gabet, Y., & Bab, I.

(2015). Cannabidiol, a Major Non-Psychotropic Cannabis Constituent Enhances Fracture Healing and Stimulates Lysyl Hydroxylase Activity in Osteoblasts. *Journal of Bone and Mineral Research, 30*(10), 1905-1913. https://doi.org//10.1002/jbmr.2513

Krukowski, K., Heijnen, C. J., Golonzhka, O., Gutti, T., Jarpe, M., & Kavelaars, A. (2015). An HDAC6 inhibitor for treatment of chemotherapy-induced peripheral numbness and pain in a mouse model. *Brain, Behavior, and Immunity, 49*, e28. https://doi.org//10.1016/j.bbi.2015.06.114

Krukowski, K., Ma, J., Golonzhka, O., Laumet, G. O., Gutti, T., van Duzer, J. H., Mazitschek, R., Jarpe, M. B., Heijnen, C. J., & Kavelaars, A. (2017, Jun). HDAC6 inhibition effectively reverses chemotherapy-induced peripheral neuropathy. *Pain, 158*(6), 1126-1137. https://doi.org/10.1097/j.pain.0000000000000893

Kukkar, A., Bali, A., Singh, N., & Jaggi, A. S. (2013, 2013/03/01). Implications and mechanism of action of gabapentin in neuropathic pain. *Archives of Pharmacal Research, 36*(3), 237-251. https://doi.org/10.1007/s12272-013-0057-y

Kusunose, N., Koyanagi, S., Hamamura, K., Matsunaga, N., Yoshida, M., Uchida, T., Tsuda, M., Inoue, K., & Ohdo, S. (2010, 2010/01/01). Molecular Basis for the Dosing Time-Dependency of Anti-Allodynic Effects of Gabapentin in a Mouse Model of Neuropathic Pain. *Molecular pain, 6*, 1744-8069-1746-1783. https://doi.org/10.1186/1744-8069-6-83

Labianca, R., Sarzi-Puttini, P., Zuccaro, S. M., Cherubino, P., Vellucci, R., & Fornasari, D. (2012, Feb 22). Adverse effects associated with non-opioid and opioid treatment in patients with chronic pain. *Clin Drug Investig, 32 Suppl 1*, 53-63. https://doi.org/10.2165/11630080-000000000-00000

Latremoliere, A., & Woolf, C. J. (2009, Sep). Central sensitization: a generator of pain hypersensitivity by central neural plasticity. *J Pain, 10*(9), 895-926. https://doi.org/10.1016/j.jpain.2009.06.012

Laursen, L. (2015, 2015/09/01). Botany: The cultivation of weed. *Nature, 525*(7570), S4-S5. https://doi.org/10.1038/525S4a

Lawrence, D. K., & Gill, E. W. (1975, Sep). The effects of delta1-tetrahydrocannabinol and other cannabinoids on spin-labeled liposomes and their relationship to mechanisms of general anesthesia. *Mol Pharmacol, 11*(5), 595-602.

Le May, C., Chu, K., Hu, M., Ortega, C. S., Simpson, E. R., Korach, K. S., Tsai, M. J., & Mauvais-Jarvis, F. (2006, Jun 13). Estrogens protect pancreatic beta-cells from apoptosis and prevent insulin-deficient diabetes mellitus in mice. *Proc Natl Acad Sci U S A, 103*(24), 9232-9237. https://doi.org/10.1073/pnas.0602956103

Lee, G., Grovey, B., Furnish, T., & Wallace, M. (2018, February 01). Medical Cannabis for Neuropathic Pain [journal article]. *Current Pain and Headache Reports, 22*(1), 8. https://doi.org/10.1007/s11916-018-0658-8

Lee, M. A. (2012). *Smoke signals: A social history of Marijuana-Medical, Recreational and Scientific*. Simon and Schuster. https://books.google.co.nz/books?hl=en&lr=&id=eVU_4QMn2kAC&oi=fnd&pg=PA1&dq=Lee,+M.+A.+(2012).+Smoke+signals:+A+social+history+of+Marijuana-Medical,+Recreational+and+Scientific.+Simon+and+Schuster.&ots=f6xB4Q1z9c&sig=47_Hi8_1naTftNdVXKI87cOnWGQ&redir_esc=y#v=onepage&q=Lee%2C%20M.%20A.%20(2012).%20Smoke%20signals%3A%20A%20social%20history%20of%20Marijuana-Medical%2C%20Recreational%20and%20Scientific.%20Simon%20and%20Schuster.&f=false

Lefaucheur, J.-P. (2019). Chapter 8 - Clinical neurophysiology of pain. In K. H. Levin & P. Chauvel (Eds.), *Handbook of Clinical Neurology* (Vol. 161, pp. 121-148). Elsevier. https://doi.org//10.1016/B978-0-444-64142-7.00045-X

Lehmann, C., Fisher, N. B., Tugwell, B., Szczesniak, A., Kelly, M., & Zhou, J. (2016). Experimental cannabidiol treatment reduces early pancreatic inflammation in type 1 diabetes. *Clinical hemorheology and microcirculation, 64*(4), 655-662. https://doi.org/10.3233/CH-168021

Lekan, H. A., Carlton, S. M., & Coggeshall, R. E. (1996, Apr 26). Sprouting of A beta fibers into lamina II of the rat dorsal horn in peripheral neuropathy. *Neurosci Lett, 208*(3), 147-150. https://doi.org/10.1016/0304-3940(96)12566-0

Leone, S., Pascale, R., Vitale, M., & Esposito, S. (2012). [Epidemiology of diabetic foot]. *Infez Med, 20 Suppl 1*, 8-13. (Epidemiologia del piede diabetico.)

Levin, S., Pearsall, G., & Ruderman, R. J. (1978). Von Frey's method of measuring pressure sensibility in the hand: An engineering analysis of the Weinstein-Semmes pressure aesthesiometer. *Journal of Hand Surgery, 3*(3), 211-216. https://doi.org/10.1016/S0363-5023(78)80084-7

Li, X., Kaminski, N. E., & Fischer, L. J. (2001). Examination of the immunosuppressive effect of delta9-tetrahydrocannabinol in streptozotocin-induced autoimmune diabetes. *International immunopharmacology, 1*(4), 699-712. https://doi.org/10.1016/s1567-5769(01)00003-0

Liao, L., Hua, H., Zhao, J. N., Luo, H., & Yang, A. D. (2014, Mar). Pharmacokinetics and relative bioavailability of THC and THC-solid dispersion orally to mice at single dose. *Zhongguo Zhong Yao Za Zhi, 39*(6), 1101-1106.

Lieberman, J. A., 3rd. (2004). Managing anticholinergic side effects. *Primary care companion to the Journal of clinical psychiatry, 6*(Suppl 2), 20-23. https://www.ncbi.nlm.nih.gov/pubmed/16001097

Linares, I. M., Zuardi, A. W., Pereira, L. C., Queiroz, R. H., Mechoulam, R., Guimarães, F. S., & Crippa, J. A. (2018). Cannabidiol presents an inverted U-shaped dose-response curve in a simulated public speaking test. *Brazilian Journal of Psychiatry, 41*, 9-14. https://doi.org//10.1590/1516-4446-2017-0015

Livak, K. J., & Schmittgen, T. D. (2001, Dec). Analysis of relative gene expression data using real-time quantitative PCR and the 2(-Delta Delta C(T)) Method. *Methods, 25*(4), 402-408. https://doi.org/10.1006/meth.2001.1262

Lodish H, B. A., Zipursky SL, et al. (2000). *Molecular Cell Biology* (4th ed.). W. H. Freeman. https://www.ncbi.nlm.nih.gov/books/NBK21475/

Lorenzetti, B. B., Souza, G. E. P., Sarti, S. J., Santos Filho, D., & Ferreira, S. H. (1991). Myrcene mimics the peripheral analgesic activity of lemongrass tea. *Journal of Ethnopharmacology, 34*(1), 43-48. https://doi.org//10.1016/0378-8741(91)90187-I

Lotsch, J., Weyer-Menkhoff, I., & Tegeder, I. (2018, Mar). Current evidence of cannabinoid-based analgesia obtained in preclinical and human experimental settings. *Eur J Pain, 22*(3), 471-484. https://doi.org/10.1002/ejp.1148

Lu, H.-C., & Mackie, K. (2016). An Introduction to the Endogenous Cannabinoid System. *Biological psychiatry, 79*(7), 516-525. https://doi.org/10.1016/j.biopsych.2015.07.028

Ma, W., Zhang, Y., Bantel, C., & Eisenach, J. C. (2005, Feb). Medium and large injured dorsal root ganglion cells increase TRPV-1, accompanied by increased alpha2C-adrenoceptor co-expression and functional inhibition by clonidine. *Pain, 113*(3), 386-394. https://doi.org/10.1016/j.pain.2004.11.018

MacCallum, C. A., & Russo, E. B. (2018, Mar). Practical considerations in medical cannabis administration and dosing. *Eur J Intern Med, 49*, 12-19. https://doi.org/10.1016/j.ejim.2018.01.004

Machholz, E., Mulder, G., Ruiz, C., Corning, B. F., & Pritchett-Corning, K. R. (2012). Manual restraint and common compound administration routes in mice and rats. *Journal of visualized experiments : JoVE*(67), 2771. https://doi.org/10.3791/2771

Mackie, K. (2006, 2006/04/01). Mechanisms of CB1 receptor signaling: endocannabinoid modulation of synaptic strength. *International Journal of Obesity, 30*(1), S19-S23. https://doi.org/10.1038/sj.ijo.0803273

Malacrida, A., Meregalli, C., Rodriguez-Menendez, V., & Nicolini, G. (2019, May 9). Chemotherapy-Induced Peripheral Neuropathy and Changes in Cytoskeleton. *International journal of molecular sciences, 20*(9). https://doi.org/10.3390/ijms20092287

Malfait, A. M., Gallily, R., Sumariwalla, P. F., Malik, A. S., Andreakos, E., Mechoulam, R., & Feldmann, M. (2000). The nonpsychoactive cannabis constituent cannabidiol is an oral anti-arthritic therapeutic in murine collagen-induced arthritis. *Proceedings of the National Academy of Sciences of the United States of America, 97*(17), 9561-9566. https://doi.org/10.1073/pnas.160105897

Malik, R. (1997). The Pathology of Human Diabetic Neuropathy. *Diabetes, 46*(Supplement_2), S50-S53. https://doi.org/10.2337/diab.46.2.S50

Maneuf, Y. P., Luo, Z. D., & Lee, K. (2006). α2δ and the mechanism of action of gabapentin in the treatment of pain. *Seminars in Cell & Developmental Biology, 17*(5), 565-570. https://doi.org//10.1016/j.semcdb.2006.09.003

Mannion, R. J., Doubell, T. P., Coggeshall, R. E., & Woolf, C. J. (1996). Collateral sprouting of uninjured primary afferent A-fibers into the superficial dorsal horn of the adult rat spinal cord after topical capsaicin treatment to the sciatic nerve. *J Neurosci, 16*(16), 5189-5195. https://doi.org//10.1523/jneurosci.16-16-05189.1996

Marcu, J. P. (2016). Chapter 62 - An Overview of Major and Minor Phytocannabinoids. In V. R. Preedy (Ed.), *Neuropathology of Drug Addictions and Substance Misuse* (pp. 672-678). Academic Press. https://doi.org//10.1016/B978-0-12-800213-1.00062-6

Martin, S. L., Reid, A. J., Verkhratsky, A., Magnaghi, V., & Faroni, A. (2019, Jun). Gene expression changes in dorsal root ganglia following peripheral nerve injury: roles in inflammation, cell death and nociception. *Neural Regen Res, 14*(6), 939-947. https://doi.org/10.4103/1673-5374.250566

Martinou, J.-C., Cartoni, R., Arnaud, E., Médard, J.-J., Poirot, O., Chrast, R., & Courvoisier, D. S. (2010). Expression of mitofusin 2R94Q in a transgenic mouse leads to Charcot–Marie–Tooth neuropathy type 2A. *Brain, 133*(5), 1460-1469. https://doi.org/10.1093/brain/awq082 %J Brain

Matsuda, L. A., Lolait, S. J., Brownstein, M. J., Young, A. C., & Bonner, T. I. (1990, Aug 9). Structure of a cannabinoid receptor and functional expression of the cloned cDNA. *Nature, 346*(6284), 561-564. https://doi.org/10.1038/346561a0

Matsumoto, M., Inoue, M., Hald, A., Xie, W., & Ueda, H. (2006, Aug). Inhibition of paclitaxel-induced A-fiber hypersensitization by gabapentin. *J Pharmacol Exp Ther, 318*(2), 735-740. https://doi.org/10.1124/jpet.106.103614

McClements, D. J. (2020). Enhancing Efficacy, Performance, and Reliability of Cannabis Edibles: Insights from Lipid Bioavailability Studies. *Annual Review of Food Science and Technology, 11*(1), 45-70. https://doi.org/10.1146/annurev-food-032519-051834

McCorquodale, D., Pucillo, E. M., & Johnson, N. E. (2016). Management of Charcot-Marie-Tooth disease: improving long-term care with a multidisciplinary approach. *Journal of multidisciplinary healthcare, 9*, 7-19. https://doi.org/10.2147/JMDH.S69979

McPartland, J. M., & Russo, E. B. (2001, 2001/06/01). Cannabis and Cannabis Extracts. *Journal of Cannabis Therapeutics, 1*(3-4), 103-132. https://doi.org/10.1300/J175v01n03_08

Mechoulam, R., & Hanuš, L. r. (2002). Cannabidiol: an overview of some chemical and pharmacological aspects. Part I: chemical aspects. *Chemistry and Physics of Lipids, 121*(1), 35-43. https://doi.org//10.1016/S0009-3084(02)00144-5

Mechoulam, R., Peters, M., Murillo-Rodriguez, E., & Hanuš, L. O. (2007). Cannabidiol–recent advances. *Chemistry & biodiversity, 4*(8), 1678-1692. https://doi.org//10.1002/cbdv.200790147

Menorca, R. M. G., Fussell, T. S., & Elfar, J. C. (2013). Nerve Physiology: Mechanisms of Injury and Recovery. *Hand Clinics, 29*(3), 317-330. https://doi.org//10.1016/j.hcl.2013.04.002

Meyer, R. A. (2006). Peripheral mechanisms of cutaneous nociception. *Wall and Melzack's textbook of pain*. https://doi.org//10.1016/B0-443-07287-6/50006-0

Millar, S. A., Stone, N. L., Yates, A. S., & O'Sullivan, S. E. (2018). A Systematic Review on the Pharmacokinetics of Cannabidiol in Humans. *Frontiers in pharmacology, 9*, 1365-1365. https://doi.org/10.3389/fphar.2018.01365

Misuse of Drugs Act, § 2A (1975). https://www.legislation.govt.nz/act/public/1975/0116/latest/LMS148483.html?search=ts_act%40bill%40regulation%40deemedreg_misuse+of+drugs+act_resel_25_a&p=1

Mitchell, V. A., Harley, J., Casey, S. L., Vaughan, A. C., Winters, B. L., & Vaughan, C. W. (2021). Oral efficacy of Δ(9)-tetrahydrocannabinol and cannabidiol in a mouse neuropathic pain model. *Neuropharmacology, 189*, 108529. https://doi.org//10.1016/j.neuropharm.2021.108529

Morales, P., Reggio, P. H., & Jagerovic, N. (2017). An Overview on Medicinal Chemistry of Synthetic and Natural Derivatives of Cannabidiol. *Frontiers in pharmacology, 8*, 422-422. https://doi.org/10.3389/fphar.2017.00422

Moreno-Sanz, G. (2016). Can You Pass the Acid Test? Critical Review and Novel Therapeutic Perspectives of Δ(9)-Tetrahydrocannabinolic Acid A. *Cannabis and cannabinoid research, 1*(1), 124-130. https://doi.org/10.1089/can.2016.0008

Morgan, M. M., & Christie, M. J. (2011, Oct). Analysis of opioid efficacy, tolerance, addiction and dependence from cell culture to human. *British journal of pharmacology, 164*(4), 1322-1334. https://doi.org/10.1111/j.1476-5381.2011.01335.x

Mucke, M., Phillips, T., Radbruch, L., Petzke, F., & Hauser, W. (2018, Mar 7). Cannabis-based medicines for chronic neuropathic pain in adults. *Cochrane Database Syst Rev, 3*, Cd012182. https://doi.org/10.1002/14651858.CD012182.pub2

Muller, C., Morales, P., & Reggio, P. H. (2019). Cannabinoid Ligands Targeting TRP Channels. *Frontiers in molecular neuroscience, 11*, 487-487. https://doi.org/10.3389/fnmol.2018.00487

Munro, S., Thomas, K. L., & Abu-Shaar, M. (1993, Sep 2). Molecular characterization of a peripheral receptor for cannabinoids. *Nature, 365*(6441), 61-65. https://doi.org/10.1038/365061a0

Murnion, B. P. (2018). Neuropathic pain: current definition and review of drug treatment. *Australian prescriber, 41*(3), 60-63. https://doi.org/10.18773/austprescr.2018.022

Nascimento, A. I., Mar, F. M., & Sousa, M. M. (2018, 2018/09/01/). The intriguing nature of dorsal root ganglion neurons: Linking structure with polarity and function. *Progress in Neurobiology, 168*, 86-103. https://doi.org//10.1016/j.pneurobio.2018.05.002

Nazario, L. R., Antonioli, R., Capiotti, K. M., Hallak, J. E. C., Zuardi, A. W., Crippa, J. A. S., Bonan, C. D., & da Silva, R. S. (2015). Reprint of "Caffeine protects against memory loss induced by high and non-anxiolytic dose of cannabidiol in adult zebrafish (Danio rerio)". *Pharmacology Biochemistry and Behavior, 139*, 134-140. https://doi.org//10.1016/j.pbb.2015.11.002

NCBI. (2022). *NCBI Primer Blast*. https://www.ncbi.nlm.nih.gov/tools/primer-blast/

Nedelescu, H., Wagner, G. E., De Ness, G. L., Carroll, A., Kerr, T. M., Wang, J., Zhang, S., Chang, S., Than, A. H., & Emerson, N. E. (2022). Cannabidiol Produces Distinct U-Shaped Dose-Response Effects on Cocaine-Induced Conditioned Place Preference

and Associated Recruitment of Prelimbic Neurons in Male Rats. *Biological psychiatry global open science, 2*(1), 70-78. https://doi.org//10.1016/j.bpsgos.2021.06.014

NetPrimer. (2022). Biosoft. http://www.premierbiosoft.com/NetPrimer/AnalyzePrimer.jsp

Nishiyori, M., & Ueda, H. (2008). Prolonged gabapentin analgesia in an experimental mouse model of fibromyalgia. *Molecular pain, 4*, 52-52. https://doi.org/10.1186/1744-8069-4-52

Nordstrom, B. R., & Hart, C. L. (2006). Assessing cognitive functioning in cannabis users: cannabis use history an important consideration. *Neuropsychopharmacology : official publication of the American College of Neuropsychopharmacology, 31*(12), 2798-2799. https://doi.org//10.1038/sj.npp.1301210

O'Brien, P. D., Sakowski, S. A., & Feldman, E. L. (2014). Mouse models of diabetic neuropathy. *ILAR journal, 54*(3), 259-272. https://doi.org//10.1093/ilar/ilt052

O'Connor, C. M., Anoushiravani, A. A., Adams, C., Young, J. R., Richardson, K., & Rosenbaum, A. J. (2020, Aug). Cannabinoid Use in Musculoskeletal Illness: a Review of the Current Evidence. *Curr Rev Musculoskelet Med, 13*(4), 379-384. https://doi.org/10.1007/s12178-020-09635-x

Obata, H. (2017). Analgesic Mechanisms of Antidepressants for Neuropathic Pain. *International journal of molecular sciences, 18*(11), 2483. https://doi.org/10.3390/ijms18112483

Obrosova, I. G. (2009). Diabetic Painful and Insensate Neuropathy: Pathogenesis and Potential Treatments. *Neurotherapeutics, 6*(4), 638-647. https://doi.org//10.1016/j.nurt.2009.07.004

Ogborne, A. C., Smart, R. G., Weber, T., & Birchmore-Timney, C. (2000, Oct-Dec). Who is using cannabis as a medicine and why: an exploratory study. *J Psychoactive Drugs, 32*(4), 435-443. https://doi.org/10.1080/02791072.2000.10400245

Padua, L., Aprile, I., Cavallaro, T., Commodari, I., La Torre, G., Pareyson, D., Quattrone, A., Rizzuto, N., Vita, G., Tonali, P., Schenone, A., & Group, f. t. I. C. Q. S. (2006, December 01). Variables influencing quality of life and disability in Charcot Marie Tooth (CMT) patients: Italian multicentre study [journal article]. *Neurological Sciences, 27*(6), 417-423. https://doi.org/10.1007/s10072-006-0722-8

Park, J. Y., Pillinger, M. H., & Abramson, S. B. (2006). Prostaglandin E2 synthesis and secretion: The role of PGE2 synthases. *Clinical Immunology, 119*(3), 229-240. https://doi.org//10.1016/j.clim.2006.01.016

Paton, W. D. M. (1973). Cannabis and its Problems. *Proceedings of the Royal Society of Medicine, 66*(7), 718-722. https://doi.org/10.1177/003591577306600753

Patorno, E., Bohn, R. L., Wahl, P. M., Avorn, J., Patrick, A. R., Liu, J., & Schneeweiss, S. (2010, Apr 14). Anticonvulsant medications and the risk of suicide, attempted suicide, or violent death. *JAMA, 303*(14), 1401-1409. https://doi.org/10.1001/jama.2010.410

Peckham, A. M., Evoy, K. E., Ochs, L., & Covvey, J. R. (2018). Gabapentin for Off-Label Use: Evidence-Based or Cause for Concern? *Subst Abuse, 12*, 1178221818801311. https://doi.org/10.1177/1178221818801311

Perrotin-Brunel, H., Buijs, W., Spronsen, J. v., Roosmalen, M. J. E. v., Peters, C. J., Verpoorte, R., & Witkamp, G.-J. (2011). Decarboxylation of Δ9-tetrahydrocannabinol: Kinetics and molecular modeling. *Journal of Molecular Structure, 987*(1), 67-73. https://doi.org//10.1016/j.molstruc.2010.11.061

Pertwee, R. G. (2005). Pharmacological actions of cannabinoids. In *Cannabinoids* (pp. 1-51). Springer. https://doi.org//10.1007/3-540-26573-2_1

Pertwee, R. G. (2006). Cannabinoid pharmacology: the first 66 years. *British journal of pharmacology, 147 Suppl 1*(Suppl 1), S163-S171. https://doi.org/10.1038/sj.bjp.0706406

Pertwee, R. G. (2008). The diverse CB1 and CB2 receptor pharmacology of three plant cannabinoids: delta9-tetrahydrocannabinol, cannabidiol and delta9-tetrahydrocannabivarin. *British journal of pharmacology, 153*(2), 199-215. https://doi.org/10.1038/sj.bjp.0707442

Peterson, C. L., & Laniel, M.-A. (2004). Histones and histone modifications. *Current Biology, 14*(14), R546-R551. https://doi.org//10.1016/j.cub.2004.07.007

Pfaffl, M. W. (2001, May 1). A new mathematical model for relative quantification in real-time RT-PCR. *Nucleic Acids Res, 29*(9), e45. https://doi.org/10.1093/nar/29.9.e45

Pfizer. (2020). *Neurotn New Zealand Data Sheet* Pfizer New Zealand Ltd. Retrieved 6/7/22 from https://www.medsafe.govt.nz/profs/Datasheet/n/Neurontincaptab.pdf

Picci, C., Wong, V. S. C., Costa, C. J., McKinnon, M. C., Goldberg, D. C., Swift, M., Alam, N. M., Prusky, G. T., Shen, S., Kozikowski, A. P., Willis, D. E., & Langley, B. (2020). HDAC6 inhibition promotes α-tubulin acetylation and ameliorates CMT2A peripheral neuropathy in mice. *Experimental Neurology*, 113281-113281. https://doi.org/10.1016/j.expneurol.2020.113281

Pittenger, G. L., Ray, M., Burcus, N. I., McNulty, P., Basta, B., & Vinik, A. I. (2004). Intraepidermal Nerve Fibers Are Indicators of Small-Fiber Neuropathy in Both

Diabetic and Nondiabetic Patients. *Diabetes Care, 27*(8), 1974-1979. https://doi.org/10.2337/diacare.27.8.1974

Planells-Cases, R., Garcìa-Sanz, N., Morenilla-Palao, C., & Ferrer-Montiel, A. (2005, 2005/10/01). Functional aspects and mechanisms of TRPV1 involvement in neurogenic inflammation that leads to thermal hyperalgesia. *Pflügers Archiv, 451*(1), 151-159. https://doi.org/10.1007/s00424-005-1423-5

Quasthoff, S., & Hartung, H. P. (2002, 2002/01/01). Chemotherapy-induced peripheral neuropathy. *Journal of Neurology, 249*(1), 9-17. https://doi.org/10.1007/PL00007853

Quintero, G. C. (2017). Review about gabapentin misuse, interactions, contraindications and side effects. *J Exp Pharmacol, 9*, 13-21. https://doi.org/10.2147/jep.S124391

Rabgay, K., Waranuch, N., Chaiyakunapruk, N., Sawangjit, R., Ingkaninan, K., & Dilokthornsakul, P. (2019). The effects of cannabis, cannabinoids, and their administration routes on pain control efficacy and safety: A systematic review and network meta-analysis. *Journal of the American Pharmacists Association*. https://doi.org//10.1016/j.japh.2019.07.015

Radulovic, L. L., Türck, D., von Hodenberg, A., Vollmer, K. O., McNally, W. P., DeHart, P. D., Hanson, B. J., Bockbrader, H. N., & Chang, T. (1995). Disposition of gabapentin (neurontin) in mice, rats, dogs, and monkeys. *Drug Metabolism and Disposition, 23*(4), 441. http://dmd.aspetjournals.org/content/23/4/441.abstract

Rahn, E., Makriyannis, A., & Hohmann, A. (2007). Activation of cannabinoid CB1 and CB2 receptors suppresses neuropathic nociception evoked by the chemotherapeutic agent vincristine in rats. *British journal of pharmacology, 152*(5), 765-777. https://doi.org//10.1038%2Fsj.bjp.0707333

Ramaekers, J. G., Mason, N. L., & Theunissen, E. L. (2020). Blunted highs: Pharmacodynamic and behavioral models of cannabis tolerance. *European Neuropsychopharmacology, 36*, 191-205. https://doi.org//10.1016/j.euroneuro.2020.01.006

Ramaekers, J. G., Theunissen, E. L., de Brouwer, M., Toennes, S. W., Moeller, M. R., & Kauert, G. (2011, 2011/03/01). Tolerance and cross-tolerance to neurocognitive effects of THC and alcohol in heavy cannabis users. *Psychopharmacology, 214*(2), 391-401. https://doi.org/10.1007/s00213-010-2042-1

Ramakers, C., Ruijter, J. M., Deprez, R. H., & Moorman, A. F. (2003, Mar 13). Assumption-free analysis of quantitative real-time polymerase chain reaction (PCR) data. *Neurosci Lett, 339*(1), 62-66. https://doi.org/10.1016/s0304-3940(02)01423-4

Raphael-Mizrahi, B., & Gabet, Y. (2020, Oct). The Cannabinoids Effect on Bone Formation and Bone Healing. *Curr Osteoporos Rep, 18*(5), 433-438. https://doi.org/10.1007/s11914-020-00607-1

Reda, H. M., Zaitone, S. A., & Moustafa, Y. M. (2016). Effect of levetiracetam versus gabapentin on peripheral neuropathy and sciatic degeneration in streptozotocin-diabetic mice: Influence on spinal microglia and astrocytes. *European journal of pharmacology, 771*, 162-172. https://doi.org//10.1016/j.ejphar.2015.12.035

Reed, N. A., Cai, D., Blasius, T. L., Jih, G. T., Meyhofer, E., Gaertig, J., & Verhey, K. J. (2006). Microtubule Acetylation Promotes Kinesin-1 Binding and Transport. *Current Biology, 16*(21), 2166-2172. https://doi.org//10.1016/j.cub.2006.09.014

Richner, M., Jager, S. B., Siupka, P., & Vaegter, C. B. (2017, 2017/01/22/). Hydraulic Extrusion of the Spinal Cord and Isolation of Dorsal Root Ganglia in Rodents. *JoVE*(119), e55226. https://doi.org/doi:10.3791/55226

Ringkamp, M., Dougherty, P. M., & Raja, S. N. (2018). Chapter 1 - Anatomy and Physiology of the Pain Signaling Process. In H. T. Benzon, S. N. Raja, S. S. Liu, S. M. Fishman, & S. P. Cohen (Eds.), *Essentials of Pain Medicine (Fourth Edition)* (pp. 3-10.e11). Elsevier. https://doi.org//10.1016/B978-0-323-40196-8.00001-2

Rock, E. M., Kopstick, R. L., Limebeer, C. L., & Parker, L. A. (2013). Tetrahydrocannabinolic acid reduces nausea-induced conditioned gaping in rats and vomiting in Suncus murinus. *British journal of pharmacology, 170*(3), 641-648. https://doi.org/10.1111/bph.12316

Rock, E. M., Limebeer, C. L., & Parker, L. A. (2018, 2018/11/01). Effect of cannabidiolic acid and Δ9-tetrahydrocannabinol on carrageenan-induced hyperalgesia and edema in a rodent model of inflammatory pain. *Psychopharmacology, 235*(11), 3259-3271. https://doi.org/10.1007/s00213-018-5034-1

Rog, D. J., Nurmikko, T. J., & Young, C. A. (2007). Oromucosal Δ9-tetrahydrocannabinol/cannabidiol for neuropathic pain associated with multiple sclerosis: An uncontrolled, open-label, 2-year extension trial. *Clinical Therapeutics, 29*(9), 2068-2079. https://doi.org//10.1016/j.clinthera.2007.09.013

Rose, M. A., & Kam, P. C. A. (2002). Gabapentin: pharmacology and its use in pain management. *Anaesthesia, 57*(5), 451-462. https://doi.org//10.1046/j.0003-2409.2001.02399.x

Rosenbaum, T., & Simon, S. A. (2006). TRPV1 receptors and signal transduction. In W. H. Liedtke, S (Ed.), *TRP ion channel function in sensory transduction and cellular signaling cascades* (pp. 83-98). CRC Press. https://www.ncbi.nlm.nih.gov/books/NBK5260/

Rosenberger, D. C., Blechschmidt, V., Timmerman, H., Wolff, A., & Treede, R. D. (2020, Apr). Challenges of neuropathic pain: focus on diabetic neuropathy. *J Neural Transm (Vienna), 127*(4), 589-624. https://doi.org/10.1007/s00702-020-02145-7

Ruhaak, L. R., Felth, J., Karlsson, P. C., Rafter, J. J., Verpoorte, R., & Bohlin, L. (2011). Evaluation of the Cyclooxygenase Inhibiting Effects of Six Major Cannabinoids Isolated from Cannabis sativa. *Biological and Pharmaceutical Bulletin, 34*(5), 774-778. https://doi.org/10.1248/bpb.34.774

Russell, C., Rueda, S., Room, R., Tyndall, M., & Fischer, B. (2018). Routes of administration for cannabis use - basic prevalence and related health outcomes: A scoping review and synthesis. *The International journal on drug policy, 52*, 87-96. https://doi.org/10.1016/j.drugpo.2017.11.008

Russell, J. W., & Zilliox, L. A. (2014). Diabetic neuropathies. *Continuum (Minneapolis, Minn.), 20*(5 Peripheral Nervous System Disorders), 1226-1240. https://doi.org/10.1212/01.CON.0000455884.29545.d2

Russo, E., & Guy, G. W. (2006). A tale of two cannabinoids: The therapeutic rationale for combining tetrahydrocannabinol and cannabidiol. *Medical Hypotheses, 66*(2), 234-246. https://doi.org//10.1016/j.mehy.2005.08.026

Russo, E. B. (2007). History of Cannabis and Its Preparations in Saga, Science, and Sobriquet. *Chemistry & biodiversity, 4*(8), 1614-1648. https://doi.org/10.1002/cbdv.200790144

Russo, E. B. (2011). Taming THC: potential cannabis synergy and phytocannabinoid-terpenoid entourage effects. *British journal of pharmacology, 163*(7), 1344-1364. https://doi.org/10.1111/j.1476-5381.2011.01238.x

Russo, E. B. (2019). The Case for the Entourage Effect and Conventional Breeding of Clinical Cannabis: No "Strain," No Gain. *Frontiers in plant science, 9*, 1969-1969. https://doi.org/10.3389/fpls.2018.01969

Russo, E. B., & Marcu, J. (2017). Cannabis Pharmacology: The Usual Suspects and a Few Promising Leads. *Adv Pharmacol, 80*, 67-134. https://doi.org/10.1016/bs.apha.2017.03.004

Saarto, T., & Wiffen, P. J. (2007). Antidepressants for neuropathic pain. *Cochrane Database of Systematic Reviews*(4). https://doi.org/10.1002/14651858.CD005454.pub2

Saito, M., Hayashi, Y., Suzuki, T., Tanaka, H., Hozumi, I., & Tsuji, S. (1997). Linkage mapping of the gene for Charcot-Marie-Tooth disease type 2 to chromosome 1p (CMT2A) and the clinical features of CMT2A. *Neurology, 49*(6), 1630. https://doi.org/10.1212/WNL.49.6.1630

Sandkühler, J. (2009). Models and Mechanisms of Hyperalgesia and Allodynia. *Physiological Reviews, 89*(2), 707-758. https://doi.org/10.1152/physrev.00025.2008

Sayers, E. W., Bolton, E. E., Brister, J. R., Canese, K., Chan, J., Comeau, D. C., Connor, R., Funk, K., Kelly, C., Kim, S., Madej, T., Marchler-Bauer, A., Lanczycki, C., Lathrop, S., Lu, Z., Thibaud-Nissen, F., Murphy, T., Phan, L., Skripchenko, Y., Tse, T., Wang, J., Williams, R., Trawick, B. W., Pruitt, K. D., & Sherry, S. T. (2022, Jan 7). Database resources of the national center for biotechnology information. *Nucleic Acids Res, 50*(D1), D20-d26. https://doi.org/10.1093/nar/gkab1112

Schembri, E. (2019, 2019/01/01). Are Opioids Effective in Relieving Neuropathic Pain? *SN Comprehensive Clinical Medicine, 1*(1), 30-46. https://doi.org/10.1007/s42399-018-0009-4

Scherer, S. S. (2011). CMT2A. *Neurology, 76*(20), 1686. https://doi.org/10.1212/WNL.0b013e31821bcc42

Schmalbruch, H. (1986, May). Fiber composition of the rat sciatic nerve. *Anat Rec, 215*(1), 71-81. https://doi.org/10.1002/ar.1092150111

Schneider, C. A., Rasband, W. S., & Eliceiri, K. W. (2012, Jul). NIH Image to ImageJ: 25 years of image analysis. *Nat Methods, 9*(7), 671-675. https://doi.org/10.1038/nmeth.2089

Scuteri, D., Berliocchi, L., Rombolà, L., Morrone, L. A., Tonin, P., Bagetta, G., & Corasaniti, M. T. (2020, 2020-May-08). Effects of Aging on Formalin-Induced Pain Behavior and Analgesic Activity of Gabapentin in C57BL/6 Mice [Brief Research Report]. *Frontiers in pharmacology, 11*. https://doi.org/10.3389/fphar.2020.00663

Shang, Y., & Tang, Y. (2017, 2017/09/02). The central cannabinoid receptor type-2 (CB2) and chronic pain. *International Journal of Neuroscience, 127*(9), 812-823. https://doi.org/10.1080/00207454.2016.1257992

Shen, S., Picci, C., Ustinova, K., Benoy, V., Kutil, Z., Zhang, G., Tavares, M. T., Pavlíček, J., Zimprich, C. A., Robers, M. B., Van Den Bosch, L., Bařinka, C., Langley, B., & Kozikowski, A. P. (2021, Apr 22). Tetrahydroquinoline-Capped Histone Deacetylase 6 Inhibitor SW-101 Ameliorates Pathological Phenotypes in a Charcot-Marie-Tooth Type 2A Mouse Model. *J Med Chem, 64*(8), 4810-4840. https://doi.org/10.1021/acs.jmedchem.0c02210

Shir, Y., & Seltzer, Z. e. (1990). A-fibers mediate mechanical hyperesthesia and allodynia and C-fibers mediate thermal hyperalgesia in a new model of causalgiform pain disorders in rats. *Neuroscience Letters, 115*(1), 62-67. https://doi.org//10.1016/0304-3940(90)90518-E

Shortland, P., Kinman, E., & Molander, C. (1997). Sprouting of A-fibre primary afferents into lamina II in two rat models of neuropathic pain. *Eur J Pain, 1*(3), 215-227. https://doi.org//10.1016/s1090-3801(97)90107-5

Shun, C. T., Chang, Y. C., Wu, H. P., Hsieh, S. C., Lin, W. M., Lin, Y. H., Tai, T. Y., & Hsieh, S. T. (2004, Jul). Skin denervation in type 2 diabetes: correlations with diabetic duration and functional impairments. *Brain, 127*(Pt 7), 1593-1605. https://doi.org/10.1093/brain/awh180

Shy, M. E., Garbern, J. Y., & Kamholz, J. (2002). Hereditary motor and sensory neuropathies: a biological perspective. *The Lancet Neurology, 1*(2), 110-118. https://doi.org/10.1016/S1474-4422(02)00042-X

Silva-Cardoso, G. K., Lazarini-Lopes, W., Hallak, J. E., Crippa, J. A., Zuardi, A. W., Garcia-Cairasco, N., & Leite-Panissi, C. R. A. (2021). Cannabidiol effectively reverses mechanical and thermal allodynia, hyperalgesia, and anxious behaviors in a neuropathic pain model: Possible role of CB1 and TRPV1 receptors. *Neuropharmacology, 197*, 108712. https://doi.org//10.1016/j.neuropharm.2021.108712

Singh, K. P., Miaskowski, C., Dhruva, A. A., Flowers, E., & Kober, K. M. (2018, Jul). Mechanisms and Measurement of Changes in Gene Expression. *Biol Res Nurs, 20*(4), 369-382. https://doi.org/10.1177/1099800418772161

Skre, H. (1974). Genetic and clinical aspects of Charcot-Marie-Tooth's disease. *Clinical Genetics, 6*(2), 98-118. https://doi.org/10.1111/j.1399-0004.1974.tb00638.x

Sleigh, J. N., Weir, G. A., & Schiavo, G. (2016). A simple, step-by-step dissection protocol for the rapid isolation of mouse dorsal root ganglia. *BMC research notes, 9*, 82-82. https://doi.org/10.1186/s13104-016-1915-8

Sleigh, J. N., West, S. J., & Schiavo, G. (2020, 2020/06/24). A video protocol for rapid dissection of mouse dorsal root ganglia from defined spinal levels. *BMC research notes, 13*(1), 302. https://doi.org/10.1186/s13104-020-05147-6

Smirnov, M. S., & Kiyatkin, E. A. (2008). Behavioral and temperature effects of delta 9-tetrahydrocannabinol in human-relevant doses in rats. *Brain Research, 1228*, 145-160. https://doi.org/10.1016/j.brainres.2008.06.069

Souayah, N., Potian, J. G., Garcia, C. C., Krivitskaya, N., Boone, C., Routh, V. H., & McArdle, J. J. (2009). Motor unit number estimate as a predictor of motor dysfunction in an animal model of type 1 diabetes. *American Journal of Physiology-Endocrinology and Metabolism, 297*(3), E602-E608. https://doi.org/10.1152/ajpendo.00245.2009

Stout, S. M., & Cimino, N. M. (2014, 2014/02/01). Exogenous cannabinoids as substrates, inhibitors, and inducers of human drug metabolizing enzymes: a systematic review. *Drug Metabolism Reviews, 46*(1), 86-95. https://doi.org/10.3109/03602532.2013.849268

Sugimoto, K., Yasujima, M., & Yagihashi, S. (2008). Role of advanced glycation end products in diabetic neuropathy. *Current Pharmaceutical Design, 14*(10), 953-961. https://doi.org//10.2174/138161208784139774

Sumner, C. J., Sheth, S., Griffin, J. W., Cornblath, D. R., & Polydefkis, M. (2003). The spectrum of neuropathy in diabetes and impaired glucose tolerance. *Neurology, 60*(1), 108-111. https://doi.org/10.1212/wnl.60.1.108

Takeda, S., Misawa, K., Yamamoto, I., & Watanabe, K. (2008). Cannabidiolic Acid as a Selective Cyclooxygenase-2 Inhibitory Component in Cannabis. *Drug Metabolism and Disposition, 36*(9), 1917. https://doi.org/10.1124/dmd.108.020909

Taura, F., Sirikantaramas, S., Shoyama, Y., Shoyama, Y., & Morimoto, S. (2007). Phytocannabinoids in Cannabis sativa: Recent Studies on Biosynthetic Enzymes. *Chemistry & biodiversity, 4*(8), 1649-1663. https://doi.org/10.1002/cbdv.200790145

Tesch, G. H., & Allen, T. J. (2007, Jun). Rodent models of streptozotocin-induced diabetic nephropathy. *Nephrology (Carlton), 12*(3), 261-266. https://doi.org/10.1111/j.1440-1797.2007.00796.x

Tikhonova, I. G., & Costanzi, S. (2009). Unraveling the structure and function of G protein-coupled receptors through NMR spectroscopy. *Current Pharmaceutical Design, 15*(35), 4003-4016. https://doi.org/10.2174/138161209789824803

Todd, A. J. (2010, Dec). Neuronal circuitry for pain processing in the dorsal horn. *Nat Rev Neurosci, 11*(12), 823-836. https://doi.org/10.1038/nrn2947

Toth, C. C., Jedrzejewski, N. M., Ellis, C. L., & Frey, W. H. (2010). Cannabinoid-Mediated Modulation of Neuropathic Pain and Microglial Accumulation in a Model of Murine Type I Diabetic Peripheral Neuropathic Pain. *Molecular pain, 6*, 1744-8069-1746-1716. https://doi.org/10.1186/1744-8069-6-16

Treede, R. D., Jensen, T. S., Campbell, J. N., Cruccu, G., Dostrovsky, J. O., Griffin, J. W., Hansson, P., Hughes, R., Nurmikko, T., & Serra, J. (2008). Neuropathic pain. *Neurology, 70*(18), 1630. https://doi.org/10.1212/01.wnl.0000282763.29778.59

Turkanis, S. A., Karler, R., & Partlow, L. M. (1991). Differential effects of delta-9-tetrahydrocannabinol and its 11-hydroxy metabolite on sodium current in neuroblastoma cells. *Brain Research, 560*(1), 245-250. https://doi.org//10.1016/0006-8993(91)91239-W

Udoh, M., Santiago, M., Devenish, S., McGregor, I. S., & Connor, M. (2019). Cannabichromene is a cannabinoid CB2 receptor agonist. *British journal of pharmacology, 176*(23), 4537-4547. https://doi.org/10.1111/bph.14815

Van Helleputte, L., Kater, M., Cook, D. P., Eykens, C., Rossaert, E., Haeck, W., Jaspers, T., Geens, N., Vanden Berghe, P., Gysemans, C., Mathieu, C., Robberecht, W., Van Damme, P., Cavaletti, G., Jarpe, M., & Van Den Bosch, L. (2018). Inhibition of histone deacetylase 6 (HDAC6) protects against vincristine-induced peripheral neuropathies and inhibits tumor growth. *Neurobiology of Disease, 111*, 59-69. https://doi.org//10.1016/j.nbd.2017.11.011

Vane, J. R., Bakhle, Y. S., & Botting, R. M. (1998). Cyclooxygenases 1 and 2. *Annual Review of Pharmacology and Toxicology, 38*, 97-120. https://doi.org/10.1146/annurev.pharmtox.38.1.97

Vane, J. R., & Botting, R. M. (2003). The mechanism of action of aspirin. *Thrombosis Research, 110*(5), 255-258. https://doi.org/10.1016/S0049-3848(03)00379-7

Verhoeckx, K. C. M., Korthout, H. A. A. J., van Meeteren-Kreikamp, A. P., Ehlert, K. A., Wang, M., van der Greef, J., Rodenburg, R. J. T., & Witkamp, R. F. (2006). Unheated Cannabis sativa extracts and its major compound THC-acid have potential immuno-modulating properties not mediated by CB1 and CB2 receptor coupled pathways. *International immunopharmacology, 6*(4), 656-665. https://doi.org//10.1016/j.intimp.2005.10.002

Vincenzetti, S., Pucciarelli, S., Huang, Y., Ricciutelli, M., Lambertucci, C., Volpini, R., Scuppa, G., Soverchia, L., Ubaldi, M., & Polzonetti, V. (2019). Biomarkers mapping of neuropathic pain in a nerve chronic constriction injury mice model. *Biochimie, 158*, 172-179. https://doi.org//10.1016/j.biochi.2019.01.005

Viudez-Martínez, A., García-Gutiérrez, M. S., Medrano-Relinque, J., Navarrón, C. M., Navarrete, F., & Manzanares, J. (2019, 2019/03/01). Cannabidiol does not display drug abuse potential in mice behavior. *Acta Pharmacologica Sinica, 40*(3), 358-364. https://doi.org/10.1038/s41401-018-0032-8

Vlassara, H., Brownlee, M., & Cerami, A. (1981, Aug). Nonenzymatic glycosylation of peripheral nerve protein in diabetes mellitus. *Proc Natl Acad Sci U S A, 78*(8), 5190-5192. https://doi.org/10.1073/pnas.78.8.5190

Vučković, S., Srebro, D., Vujović, K. S., Vučetić, Č., & Prostran, M. (2018). Cannabinoids and Pain: New Insights From Old Molecules. *Frontiers in pharmacology, 9*, 1259-1259. https://doi.org/10.3389/fphar.2018.01259

Walker, K., Fox, A. J., & Urban, L. A. (1999). Animal models for pain research. *Molecular Medicine Today, 5*(7), 319-321. https://doi.org/10.1016/S1357-4310(99)01493-8

Ward, S. J., McAllister, S. D., Kawamura, R., Murase, R., Neelakantan, H., & Walker, E. A. (2014, Feb). Cannabidiol inhibits paclitaxel-induced neuropathic pain through 5-HT(1A) receptors without diminishing nervous system function or chemotherapy efficacy. *British journal of pharmacology, 171*(3), 636-645. https://doi.org//10.1111/bph.12439

Ward, S. J., Ramirez, M. D., Neelakantan, H., & Walker, E. A. (2011, Oct). Cannabidiol prevents the development of cold and mechanical allodynia in paclitaxel-treated female C57Bl6 mice. *Anesth Analg, 113*(4), 947-950. https://doi.org/10.1213/ANE.0b013e3182283486

Ware, M. A., Wang, T., Shapiro, S., Collet, J.-P., Boulanger, A., Esdaile, J. M., Gordon, A., Lynch, M., Moulin, D. E., & O'Connell, C. (2015). Cannabis for the Management of

Pain: Assessment of Safety Study (COMPASS). *The Journal of Pain, 16*(12), 1233-1242. https://doi.org//10.1016/j.jpain.2015.07.014

Ware, M. A., Wang, T., Shapiro, S., Robinson, A., Ducruet, T., Huynh, T., Gamsa, A., Bennett, G. J., & Collet, J.-P. (2010). Smoked cannabis for chronic neuropathic pain: a randomized controlled trial. *Canadian Medical Association Journal, 182*(14), E694-E701. https://doi.org/10.1503/cmaj.091414

Waymire, J. C. (2018). *Cellular and Molecular Neurobiology* https://nba.uth.tmc.edu/neuroscience/m/s1/chapter08.html

Welburn, P. J., Starmer, G. A., Chesher, G. B., & Jackson, D. M. (1976). Effect of cannabinoids on the abdominal constriction response in mice: within cannabinoid interactions. *Psychopharmacologia, 46*(1), 83-85. https://doi.org/10.1007/bf00421553

Whitlow, C. T., Freedland, C. S., & Porrino, L. J. (2002). Metabolic mapping of the time-dependent effects of delta 9-tetrahydrocannabinol administration in the rat. *Psychopharmacology, 161*(2), 129-136. https://doi.org/10.1007/s00213-002-1001-x

WHO. (2016). *Management of substance abuse: Cannabis* https://www.who.int/substance_abuse/facts/cannabis/en/

Wiffen, P. J., Derry, S., Bell, R. F., Rice, A. S., Tölle, T. R., Phillips, T., & Moore, R. A. (2017). Gabapentin for chronic neuropathic pain in adults. *The Cochrane database of systematic reviews, 6*(6), CD007938-CD007938. https://doi.org/10.1002/14651858.CD007938.pub4

Wild, S., Roglic, G., Green, A., Sicree, R., & King, H. (2004). Global Prevalence of Diabetes. *Diabetes Care, 27*(5), 1047. https://doi.org/10.2337/diacare.27.5.1047

Wilsey, B., Marcotte, T., Deutsch, R., Gouaux, B., Sakai, S., & Donaghe, H. (2013). Low-dose vaporized cannabis significantly improves neuropathic pain. *The journal of pain : official journal of the American Pain Society, 14*(2), 136-148. https://doi.org/10.1016/j.jpain.2012.10.009

Wirth, P. W., Sue Watson, E., ElSohly, M., Turner, C. E., & Murphy, J. C. (1980). Anti-inflammatory properties of cannabichromene. *Life sciences, 26*(23), 1991-1995. https://doi.org/10.1016/0024-3205(80)90631-1

Woodhams, S. G., Sagar, D. R., Burston, J. J., & Chapman, V. (2015). The role of the endocannabinoid system in pain. *Handb Exp Pharmacol, 227*, 119-143. https://doi.org/10.1007/978-3-662-46450-2_7

Woolf, C. J. (2011). Central sensitization: implications for the diagnosis and treatment of pain. *Pain, 152*(3 Suppl), S2-S15. https://doi.org/10.1016/j.pain.2010.09.030

Woolf, C. J., & Mannion, R. J. (1999). Neuropathic pain: aetiology, symptoms, mechanisms, and management. *The Lancet, 353*(9168), 1959-1964. https://doi.org//10.1016/S0140-6736(99)01307-0

Woolf, C. J., & Thompson, S. W. (1991, Mar). The induction and maintenance of central sensitization is dependent on N-methyl-D-aspartic acid receptor activation; implications for the treatment of post-injury pain hypersensitivity states. *Pain, 44*(3), 293-299. https://doi.org/10.1016/0304-3959(91)90100-c

World-Health-Organization. (2018, 30 October 2018). *Diabetes*. Retrieved 29 August 2019 from https://www.who.int/news-room/fact-sheets/detail/diabetes

Wu, K. K., & Huan, Y. (2008). Streptozotocin-Induced Diabetic Models in Mice and Rats. *Current Protocols in Pharmacology, 40*(1), 5.47.41-45.47.14. https://doi.org/10.1002/0471141755.ph0547s40

Xu, C., Chang, T., Du, Y., Yu, C., Tan, X., & Li, X. (2019). Pharmacokinetics of oral and intravenous cannabidiol and its antidepressant-like effects in chronic mild stress mouse model. *Environmental Toxicology and Pharmacology, 70*, 103202. https://doi.org//10.1016/j.etap.2019.103202

Yagihashi, S., Mizukami, H., & Sugimoto, K. (2011). Mechanism of diabetic neuropathy: Where are we now and where to go? *Journal of diabetes investigation, 2*(1), 18-32. https://doi.org/10.1111/j.2040-1124.2010.00070.x

Yam, M. F., Loh, Y. C., Tan, C. S., Khadijah Adam, S., Abdul Manan, N., & Basir, R. (2018). General Pathways of Pain Sensation and the Major Neurotransmitters Involved in Pain Regulation. *International journal of molecular sciences, 19*(8), 2164. https://doi.org/10.3390/ijms19082164

Yamamoto, H., Uchigata, Y., & Okamoto, H. (1981, 1981/11/01). Streptozotocin and alloxan induce DNA strand breaks and poly(ADP–ribose) synthetase in pancreatic islets. *Nature, 294*(5838), 284-286. https://doi.org/10.1038/294284a0

Zgair, A., Lee, J. B., Wong, J. C. M., Taha, D. A., Aram, J., Di Virgilio, D., McArthur, J. W., Cheng, Y.-K., Hennig, I. M., Barrett, D. A., Fischer, P. M., Constantinescu, C. S., & Gershkovich, P. (2017, 2017/11/06). Oral administration of cannabis with lipids leads to high levels of cannabinoids in the intestinal lymphatic system and prominent immunomodulation. *Scientific Reports, 7*(1), 14542. https://doi.org/10.1038/s41598-017-15026-z

Zgair, A., Wong, J. C., Lee, J. B., Mistry, J., Sivak, O., Wasan, K. M., Hennig, I. M., Barrett, D. A., Constantinescu, C. S., Fischer, P. M., & Gershkovich, P. (2016). Dietary fats and pharmaceutical lipid excipients increase systemic exposure to orally administered cannabis and cannabis-based medicines. *American journal of translational research, 8*(8), 3448-3459. https://pubmed.ncbi.nlm.nih.gov/27648135

Zhang, J., Ma, J., Trinh, R. T., Heijnen, C. J., & Kavelaars, A. (2022). An HDAC6 inhibitor reverses chemotherapy-induced mechanical hypersensitivity via an IL-10 and macrophage dependent pathway. *Brain, Behavior, and Immunity, 100*, 287-296. https://doi.org//10.1016/j.bbi.2021.12.005

Zilliox, L., & Russell, J. W. (2011, Apr). Treatment of diabetic sensory polyneuropathy. *Curr Treat Options Neurol, 13*(2), 143-159. https://doi.org/10.1007/s11940-011-0113-1

Zou, S., & Kumar, U. (2018). Cannabinoid Receptors and the Endocannabinoid System: Signaling and Function in the Central Nervous System. *International journal of molecular sciences, 19*(3), 833. https://doi.org/10.3390/ijms19030833

Zuardi, A. W. (2006, Jun). History of cannabis as a medicine: a review. *Braz J Psychiatry, 28*(2), 153-157. https://doi.org/10.1590/s1516-44462006000200015

Zuardi, A. W., Rodrigues, N. P., Silva, A. L., Bernardo, S. A., Hallak, J. E., Guimarães, F. S., & Crippa, J. A. (2017). Inverted U-shaped dose-response curve of the anxiolytic effect of cannabidiol during public speaking in real life. *Frontiers in pharmacology*, 259. https://doi.org//10.3389/fphar.2017.00259

Züchner, S., Mersiyanova, I. V., Muglia, M., Bissar-Tadmouri, N., Rochelle, J., Dadali, E. L., Zappia, M., Nelis, E., Patitucci, A., Senderek, J., Parman, Y., Evgrafov, O., Jonghe, P. D., Takahashi, Y., Tsuji, S., Pericak-Vance, M. A., Quattrone, A., Battologlu, E., Polyakov, A. V., Timmerman, V., Schröder, J. M., & Vance, J. M. (2004, 04/04/online).

Mutations in the mitochondrial GTPase mitofusin 2 cause Charcot-Marie-Tooth neuropathy type 2A. *Nature Genetics, 36*, 449. https://doi.org/10.1038/ng1341

Appendices

Dose Response Appendix

A.1 Ethics approval coversheet

UNIVERSITY OF WAIKATO ANIMAL ETHICS COMMITTEE

THE UNIVERSITY OF WAIKATO

Protocol Number: 1093

APPLICATION COVER SHEET

Project Details (Do not use acronyms)
Full Protocol Title: Medical Cannabis for Neuropathic Pain **Name of Primary Applicant:** Brett Langley **Faculty/School/Department:** School of Health, HECS **Expected start date:** August 1, 2020 **Expected completion date:** April 30, 2023 **Animals species:** Mice **Number to be used over entire project:** (common name) **Impact Level:** Grade B; Little Impact (E.g. No Impact, Little Impact, Moderate Impact. See Q 6 Animal Use Statistics Form – Appendix 1):

Type of Application (Can tick more than one box):	X Research ☐ Part of research thesis ☐ Teaching ☐ Other (Specify)
Standard Operating Procedures:	☐ No X Yes: SOP Number/ Title SOP#5 / The Housing and Care of Lab/Domestic and Wild Rodents SOP#9 / Euthanasia of Rodents by CO2 Asphyxiation SOP#10 / Administration of a substance by Intraperitoneal Injection in rats and mice SOP#15 / Euthanasia of rodents by CO2 anesthesia and decapitation SOP#22 / Administration of substance by oral gavage in mice SOP#TBD / Rodent Genotyping (Ear Punch and Tail Biopsy) – to be considered by the Committee If yes, have you been trained in this/these SOP(s)? Yes
Other AEC approval:	Has this application been submitted any other AEC for approval X No ☐ Yes (Specify Committee) Was the application approved ☐ No ☐ Yes Details:
Funding support:	Is this research part of a funding grant either received or pending ☐ No X Yes (Specify funding source) Details: Callaghan Innovation and Cannasouth Medical Therapeutics

OFFICE USE ONLY This proposal is approved for the period: **From: 1 August 2020**	***Protocol Number:*** **To: 30 April 2023**
Signature AEC Chair:	**Date: 30 July 2020**

A.2 Certificate of analysis for cannabis extracts - CBD

cannasouth

Cannasouth Biosciences Limited, Hamilton, New Zealand

CERTIFICATE OF ANALYSIS

DATE:	**18-Jan-22**	**Batch ID:**	**NA**
			Controlled drug Entry
Report date:	18-Jan-22	Method:	SOP012

High Performance Liquid Chromatography Cannabinoid Analysis

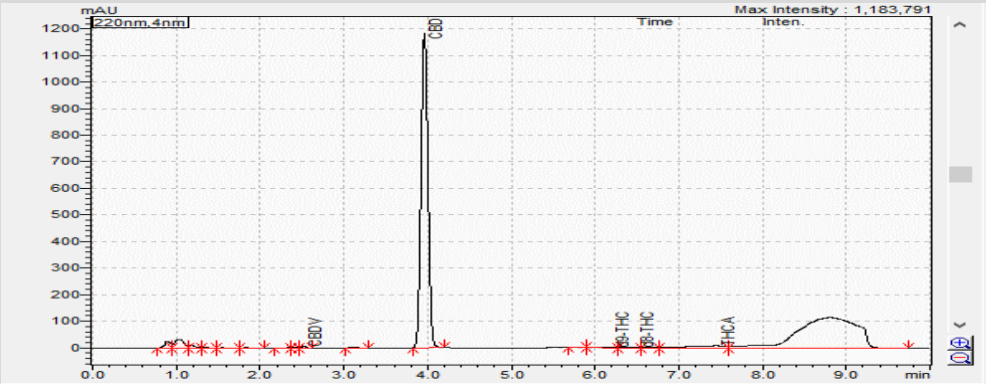

CANNABINOID PROFILE

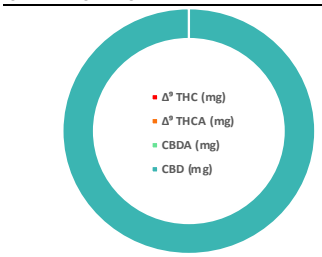

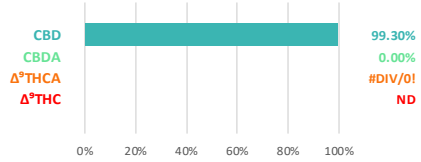

Compound	Result (mg)	Result (mg/g)	%
Delta 9-Tetrahydrocannabinol (Δ⁹ THC)	0.00	#DIV/0!	ND
Delta 9-Tetrahydrocannabinolic acid (Δ⁹ THCA)	0.00	#DIV/0!	ND
Cannabidiolic acid (CBDA)	0.00	#DIV/0!	ND
Cannabidiol (CBD)	0.00	993.00	99.30%
Delta 8-Tetrahydrocannabinolic acid (Δ⁸ THCA)	0.00	#DIV/0!	ND
Cannabinol (CBN)	0.00	#DIV/0!	ND
Cannabigerolic acid (CBGA)	0.00	#DIV/0!	ND
Cannabigerol (CBG)	0.00	#DIV/0!	ND
Tetrahydrocannabivarin (THCV)	0.00	#DIV/0!	ND
Cannabichromene (CBC)	0.00	#DIV/0!	ND

Total Cannabinoids*	**993.00**	**mg/g**
Total Potential THC**	0.00	mg/g
Total Potential CBD**	993.00	mg/g

ND = Non-detect

% = % (w/w) = Percent (Weight of Analyte / Weight of Product)

* Total Cannabinoids result reflects the absolute sum of all cannabinoids detected.
** Total Potential THC/CBD is calculated using the following formulas to take into account the loss of a carboxyl group during decarboxylation.
Total THC = THC + (THCa *(0.877)) and Total CBD = CBD + (CBDa *(0.877))

NOTES:

Number of replicates (n) = 3
Analyte sample weight extracted = g

Enter blurb here

FINAL APPROVAL

D.Reason 18-Jan-22	P.Squire 18-Jan-22
PREPARED BY / DATE	APPROVED BY / DATE

A.3 Dose-response in wildtype mice - dose schedule and mouse data

CBD DOSING EXPERIMENT in WT mice

Dose mg/kg	0	25	50	100	150	Total #n
# mice	6	6	6	6	6	**30**
Average weight g	25	25	25	25	25	
Volume ul	50	50	50	50	50	
Concentration ug/ul (for 50ul gavage)	**0**	**12.5**	**25**	**50**	**75**	
Total Volume per day ul	**300**	**300**	**300**	**300**	**300**	
Volume for four days ul	**1,200**	**1,200**	**1,200**	**1,200**	**1,200**	

mg/kg of CBD	Mouse I.D	Weight (g)	Dose vol (uL)	Total vol. (uL)	Fri 30th	Sat 31st	Sun 1st	Mon 2nd	Tue 3rd	Wed 4th	Thur 5th	Fri 6th	Time of final dose	Time of euthanisia	Time
0 mg/kg	1.1	38	50		Dose 1	Dose 2	Dose 3	Dose 4/Harvest					10:34:00	11:30:00	00:56:00
G1/1 male	1.2	44	50		Dose 1	Dose 2	Dose 3	Dose 4/Harvest					11:13:00	12:20:00	01:07:00
	1.3	51	50		Dose 1	Dose 2	Dose 3	Dose 4/Harvest					12:08:00	13:30:00	01:22:00
G1/2 Female	1.4	30	50		Dose 1	Dose 2	Dose 3	Dose 4/Harvest					13:00:00	14:30:00	01:30:00
	1.5	19	50		Dose 1	Dose 2	Dose 3	Dose 4/Harvest					13:30:00	15:00:00	01:30:00
	1.6	25	50		Dose 1	Dose 2	Dose 3	Dose 4/Harvest					14:30:00	15:45:00	01:15:00
25 mg/kg			**300**	**1200**											
G2/1 Male	2.1	49	98			Dose 1	Dose 2	Dose 3	Dose 4/Harvest				09:58:00	11:15:00	01:17:00
	2.2	44	88			Dose 1	Dose 2	Dose 3	Dose 4/Harvest				10:35:00	11:50:00	01:15:00
	2.3	49	98			Dose 1	Dose 2	Dose 3	Dose 4/Harvest				11:02:00	12:30:00	01:28:00
G2/2 Female	2.4	31	62			Dose 1	Dose 2	Dose 3	Dose 4/Harvest				11:46:00	13:05:00	01:19:00
	2.5	25	50			Dose 1	Dose 2	Dose 3	Dose 4/Harvest				13:00:00	14:15:00	01:15:00
	2.6	23	46			Dose 1	Dose 2	Dose 3	Dose 4/Harvest				13:40:00	14:45:00	01:05:00
50 mg/kg			**442**	**1768**											
G3/1 Male	3.1	46	92				Dose 1	Dose 2	Dose 3	Dose 4/Harvest			09:43:00	10:45:00	01:02:00
	3.2	28	56				Dose 1	Dose 2	Dose 3	Dose 4/Harvest			10:20:00	11:30:00	01:10:00
	3.3	38	76				Dose 1	Dose 2	Dose 3	Dose 4/Harvest			11:25:00	12:50:00	01:25:00
G3/2 Female	3.4	28	56				Dose 1	Dose 2	Dose 3	Dose 4/Harvest			12:05:00	13:28:00	01:23:00
	3.5	28	56				Dose 1	Dose 2	Dose 3	Dose 4/Harvest			12:40:00	14:00:00	01:20:00
	3.6	22	44				Dose 1	Dose 2	Dose 3	Dose 4/Harvest			13:25:00	14:45:00	01:20:00
100 mg/kg			**380**	**1520**											
G4/1 Male	4.1	47	94					Dose 1	Dose 2	Dose 3	Dose 4/Harvest		09:51:00	11:10:00	01:19:00
	4.2	35	70					Dose 1	Dose 2	Dose 3	Dose 4/Harvest		10:27:00	11:45:00	01:18:00
	4.3	32	64					Dose 1	Dose 2	Dose 3	Dose 4/Harvest		11:07:00	12:35:00	01:28:00
G4/2 Female	4.4	21	42					Dose 1	Dose 2	Dose 3	Dose 4/Harvest		11:43:00	13:05:00	01:22:00
	4.5	25	50					Dose 1	Dose 2	Dose 3	Dose 4/Harvest		12:32:00	13:45:00	01:13:00
	4.6	18	36					Dose 1	Dose 2	Dose 3	Dose 4/Harvest		13:02:00	14:20:00	01:18:00
150 mg/kg			**356**	**1424**											
G5/1 Male	5.1	43	86						Dose 1	Dose 2	Dose 3	Dose 4/Harvest	09:38:00	10:55:00	01:17:00
	5.2	35	70						Dose 1	Dose 2	Dose 3	Dose 4/Harvest	10:15:00	11:30:00	01:15:00
	5.3	36	72						Dose 1	Dose 2	Dose 3	Dose 4/Harvest	10:53:00	12:10:00	01:17:00
G5/2 Female	5.4	30	60						Dose 1	Dose 2	Dose 3	Dose 4/Harvest	11:25:00	12:53:00	01:28:00
	5.5	23	46						Dose 1	Dose 2	Dose 3	Dose 4/Harvest	12:00:00	13:20:00	01:20:00
	5.6	28	56						Dose 1	Dose 2	Dose 3	Dose 4/Harvest	12:34:00	13:50:00	01:16:00
			390	**1560**											
Total #n for the day					**6**	**12**	**18**	**24**	**24**	**18**	**12**	**6**			

A.4. RNA quality and quantity of DRGs for dose response work

	CBD dose response RNA from DRGs								120 ng RNA	
CBD conc. mg/kg	Sample ID	Nucleic Acid	Unit	A260 (Abs)	A280 (Abs)	260/280	260/230	Sample Type	Vol to load cDNA	H2O
Ctrl	1.1 CBD dose	25.8	ng/µl	0.646	0.397	1.63	0.87	RNA	4.65	0.35
Ctrl	1.2 CBD dose	31.5	ng/µl	0.788	0.486	1.62	0.33	RNA	3.81	1.19
Ctrl	1.3 CBD dose	56.5	ng/µl	1.412	0.8	1.76	0.83	RNA	2.12	2.88
Ctrl	1.4 CBD dose	65.2	ng/µl	1.629	0.924	1.76	0.69	RNA	1.84	3.16
Ctrl	1.5 CBD dose	43.5	ng/µl	1.088	0.655	1.66	0.4	RNA	2.76	2.24
Ctrl	1.6 CBD dose	69.1	ng/µl	1.727	0.932	1.85	0.64	RNA	1.74	3.26
25	2.1 CBD dose	499.3	ng/µl	12.482	6.681	1.87	1.73	RNA	0.24	4.76
25	2.2 CBD dose	71.4	ng/µl	1.785	0.972	1.84	1.2	RNA	1.68	3.32
25	2.3 CBD dose	23.2	ng/µl	0.581	0.333	1.74	0.37	RNA	5.17	-0.17
25	2.4 CBD dose	55.3	ng/µl	1.382	0.76	1.82	0.65	RNA	2.17	2.83
25	2.5 CBD dose	127.4	ng/µl	3.184	1.695	1.88	0.64	RNA	0.94	4.06
25	2.6 CBD dose	106.7	ng/µl	2.668	1.422	1.88	0.94	RNA	1.12	3.88
50	3.1 CBD dose	107.8	ng/µl	2.695	1.426	1.89	1.38	RNA	1.11	3.89
50	3.2 CBD dose	65.3	ng/µl	1.632	0.883	1.85	0.86	RNA	1.84	3.16
50	3.3 CBD dose	69.3	ng/µl	1.733	0.939	1.85	0.96	RNA	1.73	3.27
50	3.4 CBD dose	58.8	ng/µl	1.471	0.785	1.87	0.69	RNA	2.04	2.96
50	3.5 CBD dose	83.6	ng/µl	2.089	1.106	1.89	1.08	RNA	1.44	3.56
50	3.6 CBD dose	101.2	ng/µl	2.53	1.337	1.89	1	RNA	1.19	3.81
100	4.1 CBD dose	41	ng/µl	1.025	0.612	1.67	0.23	RNA	2.93	2.07
100	4.2 CBD dose	52.3	ng/µl	1.308	0.727	1.8	0.41	RNA	2.29	2.71
100	4.3 CBD dose	139.6	ng/µl	3.49	1.896	1.84	0.72	RNA	0.86	4.14
100	4.4 CBD dose	69.4	ng/µl	1.735	0.955	1.82	0.63	RNA	1.73	3.27
100	4.5 CBD dose	545.1	ng/µl	13.628	6.89	1.98	1.74	RNA	0.22	4.78
100	4.6 CBD dose	91.9	ng/µl	2.298	1.207	1.9	1.15	RNA	1.31	3.69
150	5.1 CBD dose	91.8	ng/µl	2.294	1.253	1.83	1.12	RNA	1.31	3.69
150	5.2 CBD dose	102.2	ng/µl	2.554	1.416	1.8	1.11	RNA	1.17	3.83
150	5.3 CBD dose	191.8	ng/µl	4.795	2.601	1.84	0.95	RNA	0.63	4.37
150	5.4 CBD dose	376.9	ng/µl	9.423	5.405	1.74	1.2	RNA	0.32	4.68
150	5.5 CBD dose	290.5	ng/µl	7.262	3.875	1.87	0.82	RNA	0.41	4.59
150	5.6 CBD dose	374.8	ng/µl	9.371	4.917	1.91	1.89	RNA	0.32	4.68

A.5. Dose-response for qPCR in mice - dose schedule and mouse data

CBD dose response in CMT2A mice

Dose mg/kg	0	25	50	100	Total #n
# mice	3	3	3	3	12
Average weight g	25	25	25	25	
Volume ul	50	50	50	50	
Concentration ug/ul (for 50ul gavage)	0	12.5	25	50	
Total Volume per day ul	150	150	150	150	
Volume for four days ul	600	600	600	600	

mg/kg of CBD	Mouse I.D	Weight (g)	Dose vol (uL)	Total vol for 4 days (ul	Sunday 21 March	Monday 22 March	Tuesday 23 March	Wednesday 24 March	Thursday 25 March	Friday 26 March	Time of final dose	Time of euthanisia	Time
0 mg/kg	28.2	20	50	200	Dose 1	Dose 2	Dose 3	Dose 4/ Harvest			09:10:00	10:25:00	01:15:00
	27.1	27	50	200		Dose 1	Dose 2	Dose 3	Dose 4/ Harvest		09:30:00	10:45:00	01:15:00
	26.1	17	50	200			Dose 1	Dose 2	Dose 3	Dose 4/ Harvest	10:55:00	12:10:00	01:15:00
25 mg/kg				600									
	1.2	15	30	120	Dose 1	Dose 2	Dose 3	Dose 4/ Harvest			10:22:00	11:35:00	01:13:00
	1.3	15	30	120		Dose 1	Dose 2	Dose 3	Dose 4/ Harvest		10:45:00	11:55:00	01:10:00
	25.1	22	44	176			Dose 1	Dose 2	Dose 3	Dose 4/ Harvest	10:00:00	11:10:00	01:10:00
50 mg/kg				416									
	22.2	28	56	224	Dose 1	Dose 2	Dose 3	Dose 4/ Harvest			11:30:00	12:48:00	01:18:00
	26.2	18	36	144		Dose 1	Dose 2	Dose 3	Dose 4/ Harvest		11:35:00	12:45:00	01:10:00
	12.2	23	46	184			Dose 1	Dose 2	Dose 3	Dose 4/ Harvest	11:30:00	12:40:00	01:10:00
100 mg/kg				552									
	24.1	23	46	184	Dose 1	Dose 2	Dose 3	Dose 4/ Harvest			12:45:00	14:00:00	01:15:00
	24.4	17	34	136		Dose 1	Dose 2	Dose 3	Dose 4/ Harvest		12:25:00	13:35:00	01:10:00
	25.2	23	46	184			Dose 1	Dose 2	Dose 3	Dose 4/ Harvest	09:15:00	10:27:00	01:12:00
				504									
Total #n for the day					4	8	12	12	8	4			

A.6 Flow chart of data generated from GENEWIZ

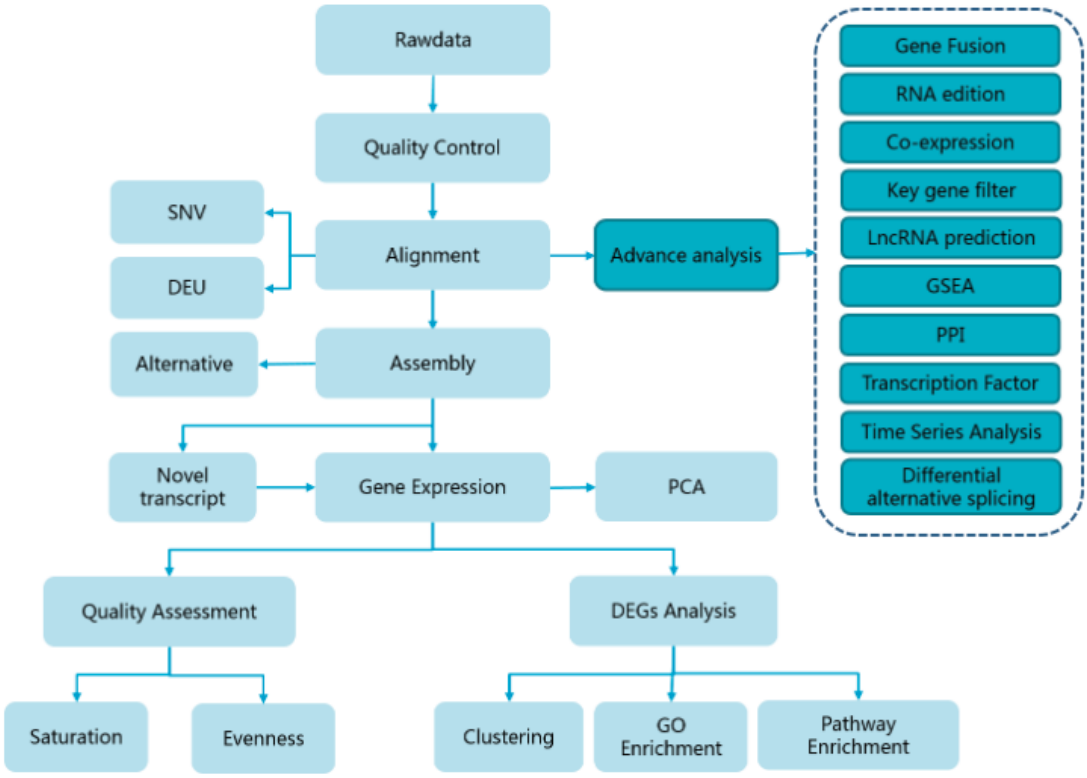

Figure A.6. Flowchart of data and workflow generated by GENEWIZ for transcriptomics data

A.7 Volcano plots of changes to differential gene expression

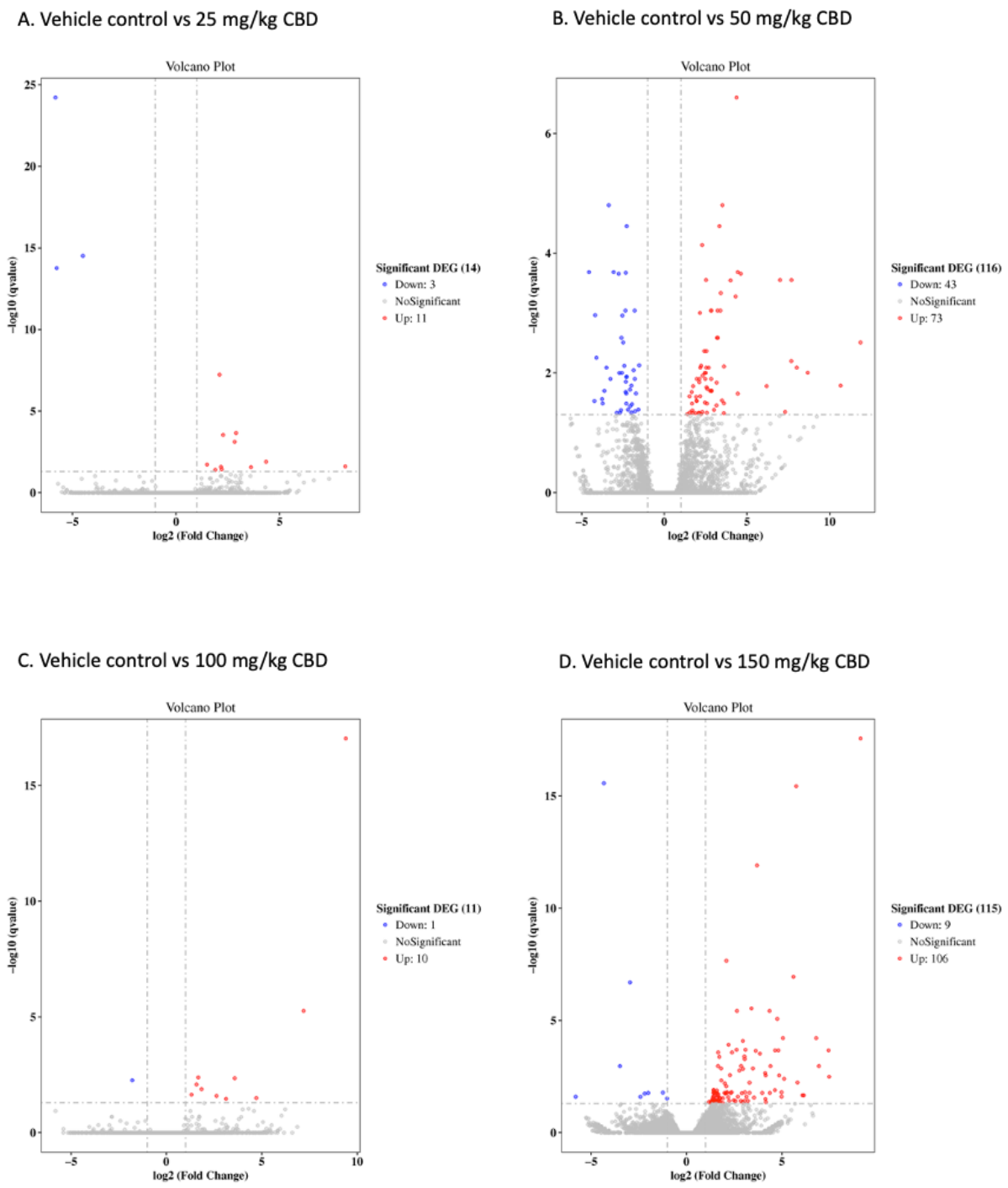

Figure A.7. Volcano plots showing changes to gene transcription in mice given orally administered CBD. A) Vehicle verses 25 mg/kg CBD. B) Vehicle verses 50 mg/kg CBD. C) Vehicle verses 100 mg/kg CBD. D) Vehicle verses 150 mg/kg CBD.

Efficacy in CMT2A Appendix

B.1 Certificate of analysis for high CBD whole extract (WEX)

cannasouth

Cannasouth Plant Research New Zealand Ltd, Hamilton, NZ

CERTIFICATE OF ANALYSIS

DATE:	**17-Mar-22**	**Batch ID:**	**Callaghan Extract**
			Controlled drug Entry
Report date:	17-Mar-22	Method:	High Sensitivity
		CD Type	**Extract**

High Performance Liquid Chromatography Cannabinoid Analysis

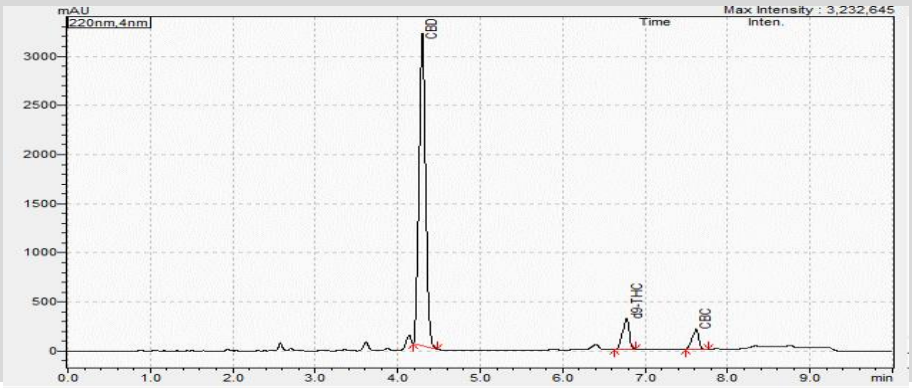

CANNABINOID PROFILE

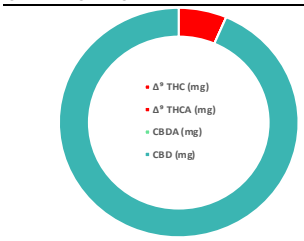

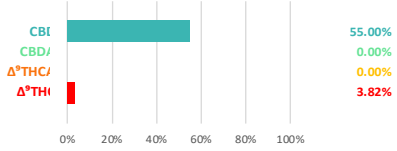

Compound	Result (mg/g)	%
Delta 9-Tetrahydrocannabinol (Δ⁹ THC)	38.2	3.82%
Delta 9-Tetrahydrocannabinolic acid (Δ⁹ THCA)	0	0.00%
Cannabidiolic acid (CBDA)	0	0.00%
Cannabidiol (CBD)	550	55.00%
Delta 8-Tetrahydrocannabinolic acid (Δ⁸ THCA)	ND	ND
Cannabinol (CBN)	ND	ND
Cannabigerolic acid (CBGA)	ND	ND
Cannabigerol (CBG)	ND	ND
Tetrahydrocannabivarin (THCV)	ND	ND
Cannabichromene (CBC)	ND	ND

Total Cannabinoids*	**588.20**	**mg/g**
Total Potential THC**	38.20	mg/g
Total Potential CBD**	0.00	mg/g

% = % (w/w) = Percent (Weight of Analyte / Weight of Product)

ND = Non-detect

* Total Cannabinoids result reflects the absolute sum of all cannabinoids detected.
** Total Potential THC/CBD is calculated using the following formulas to take into account the loss of a carboxyl group during decarboxylation.
Total THC = THC + (THCa *(0.877)) and Total CBD = CBD + (CBDa *(0.877))

NOTES:

Entered By	D. Reason

B.2 Certificate of analysis for CBD: THC

cannasouth

Cannasouth Plant Research New Zealand Ltd, Hamilton, NZ

CERTIFICATE OF ANALYSIS

DATE:	**17-Mar-22**	**Batch ID:**	**Marion Sample**
			Controlled drug Entry
Report date:	17-Mar-22	Method:	High Sensitivity
		CD Type	**Extract**

High Performance Liquid Chromatography Cannabinoid Analysis

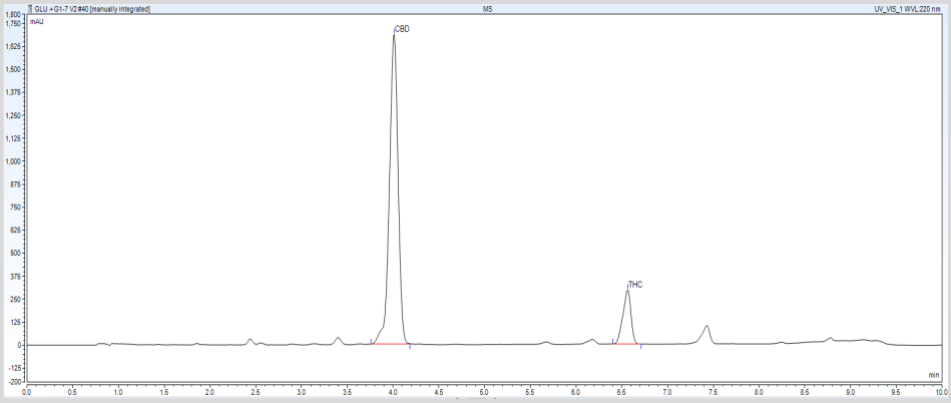

CANNABINOID PROFILE

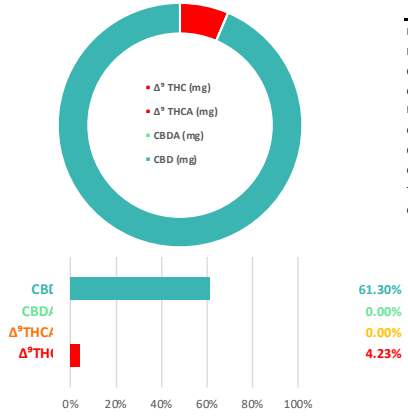

Compound	Result (mg/g)	%
Delta 9-Tetrahydrocannabinol (Δ⁹ THC)	42.3	4.23%
Delta 9-Tetrahydrocannabinolic acid (Δ⁹ THCA)	0	0.00%
Cannabidiolic acid (CBDA)	0	0.00%
Cannabidiol (CBD)	613	61.30%
Delta 8-Tetrahydrocannabinolic acid (Δ⁸ THCA)	ND	ND
Cannabinol (CBN)	ND	ND
Cannabigerolic acid (CBGA)	ND	ND
Cannabigerol (CBG)	ND	ND
Tetrahydrocannabivarin (THCV)	ND	ND
Cannabichromene (CBC)	ND	ND

Total Cannabinoids*	**655.30**	**mg/g**
Total Potential THC**	42.30	mg/g
Total Potential CBD**	0.00	mg/g

% = % (w/w) = Percent (Weight of Analyte / Weight of Product)

ND = Non-detect

* Total Cannabinoids result reflects the absolute sum of all cannabinoids detected.
** Total Potential THC/CBD is calculated using the following formulas to take into account the loss of a carboxyl group during decarboxylation.
Total THC = THC + (THCa *(0.877)) and Total CBD = CBD + (CBDa *(0.877))

NOTES:

Entered By	D. Reason

B.3. Paw withdrawal latency in wildtype mice given orally administered CBD

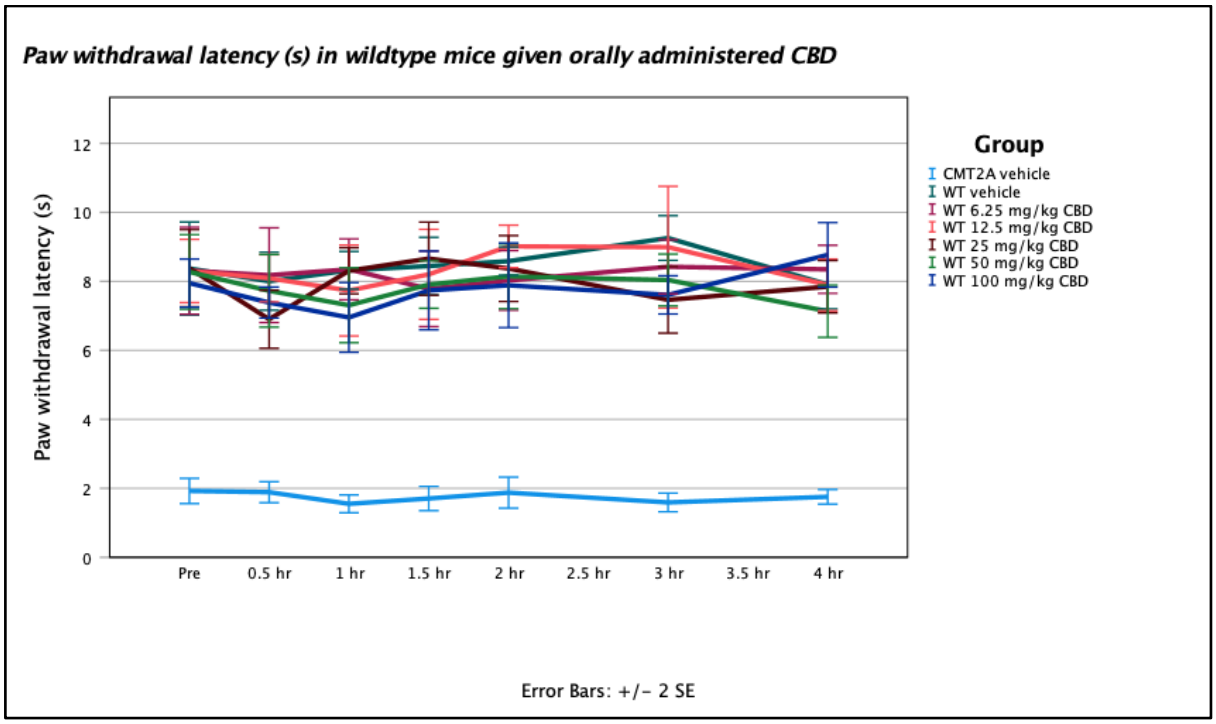

Figure B.3. Paw withdrawal latency (s) in wildtype mice (WT) given orally administered CBD. n = 8. No statistically significant change to paw withdrawal latency (s) was seen in the wildtype mice given orally administered CBD at any of the doses given.

B.4. Paw withdrawal threshold in wildtype mice given orally administered CBD

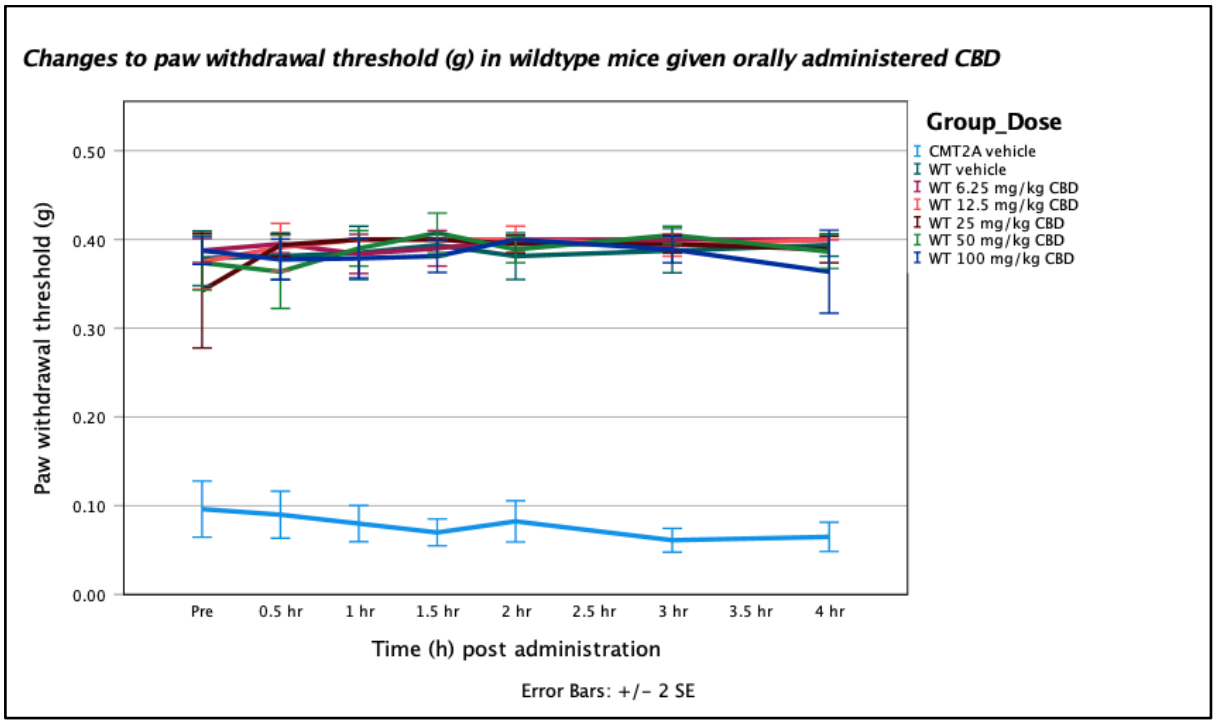

Figure B.4 Changes to paw withdrawal threshold (g) in wildtype mice (WT) given orally administered CBD. n = 8. There were no statistically significant changes to paw withdrawal threshold in wildtype mice that were given orally administered CBD at any of the doses given.

STZ-Induced Diabetes Appendix

C.1. Streptozotocin dosing charts

Table C.1.1. Streptozotocin dosing chart group one mice

STZ mice	STZ administered 4/05/21					
Dose mg/kg	**180**		180mg/kg, mouse weight = 0.025kg. 180 x 0.025 = 4.5gm per mouse			
Average weight g	25		**Vol = 0.15 ml. 1/0.15 x 4.5 = 30mg/ml**			
Volume ul	150		Conc. 30mg/ml (30 x 1)/4.5 = 0.15			
Concentration mg/ml (for 150 ul IP)	30					
Excess for needle (uL)	3					
Total Volume (uL)	**1920.6**					
Amount of STZ needed (g)	57.618					
Mouse I.D.	**Group**	**Weight pre STZ**	**vol. (uL) of STZ**	**Excess for needle (+3ul)**	**Cull weight (g)**	
12.3	STZ	22	132	135	17.6	
12.4	STZ	25	150	153	20.0	
20.2	STZ	22	132	135	17.6	
20.3	STZ	26	156	159	20.8	
25.3	STZ	20	120	123	16.0	
25.4	STZ	22	132	135	17.6	
27.2	STZ	23	138	141	18.4	
32.3	STZ	25	150	153	20.0	
31.2	STZ	24	144	147	19.2	
31.1	STZ	24	144	147	19.2	
32.1	STZ	29	174	177	23.2	
50.1	STZ	23	138	141	18.4	

Table C.1.2. Streptozotocin dosing chart group two mice

STZ mice	STZ administered 9/2/22					
Dose mg/kg	**180**	Tube A				
Average weight g	25	Citrate (uL)	STZ (mg)			
Volume ul	150	1079.1	32.373			
Concentration mg/ml (for 150ul IP)	30					
Excess for needle (uL)	3	Tube B				
Total Volume (uL)	**2006.4**	Citrate (uL)	STZ (mg)			
Amount of STZ needed (mg)	60.192	910.8	27.324			
Mouse I.D.	**Group**	**Weight pre STZ**	**vol. (uL) of STZ**	**Excess for needle (+3ul)**	**Cull weight (g)**	Tube
WT 14.1	STZ	35	210	213	28	Tube A
WT 15.1	STZ	28	168	171	22.4	Tube A
12.1	STZ	42	252	255	33.6	Tube A
13.1	STZ	27	162	165	21.6	Tube A
WT 60.1	STZ	29	174	177	23.2	Tube A
WT 60.2	STZ	29	174	177	23.2	Tube B
WT 60.3	STZ	31	186	189	24.8	Tube B
16.2	STZ	27	162	165	21.6	Tube B
16.4	STZ	26	156	159	20.8	Tube B
17.1	STZ	25	150	153	20	Tube B
13.2	Citrate	24	144	147	19.2	
16.6	Citrate	25	150	153	20	

Table C.1.3. Streptozotocin dosing chart group three mice

STZ mice	STZ administered 3/5/22					
Dose mg/kg	**180**	Tube A				
Average weight g	25	Citrate (uL)	STZ (mg)			
Volume ul	150	1240.8	37.224			
Concentration mg/ml (for 150ul IP)	30					
Excess for needle (uL)	3	Tube B				
Total Volume (uL)	**2376**	Citrate (uL)	STZ (mg)			
Amount of STZ needed (g)	71.28	1135.2	34.056			
Mouse I.D.	**Group**	**Weight pre STZ**	**vol. (uL) of STZ**	**Excess for needle (+3ul)**	**Cull weight (g)**	
A1	Citrate	33	198	201	26.4	
A2	STZ	33	198	201	26.4	Tube A
A3	STZ	34	204	207	27.2	Tube A
B1	Citrate	27	162	165	21.6	
B2	STZ	28	168	171	22.4	Tube A
B3	STZ	34	204	207	27.2	Tube A
C1	Citrate	34	204	207	27.2	
C2	STZ	27	162	165	21.6	Tube A
D1	STZ	29	174	177	23.2	Tube A
E1	Citrate	32	192	195	25.6	
E2	STZ	27	162	165	21.6	Tube B
E3	STZ	32	192	195	25.6	Tube B
F1	STZ	27	162	165	21.6	Tube B
F2	STZ	27	162	165	21.6	Tube B
G2	citrate	26	156	159	20.8	
G3	STZ	28	168	171	22.4	Tube B
28.2	Citrate	27	162	165	21.6	
28.3	STZ	28	168	171	22.4	Tube B

C.2. Animal welfare form for diabetic mice

UNIVERSITY OF WAIKATO ANIMAL ETHICS COMMITTEE

Appendix 3 - Daily Health Monitoring Sheet
(from the Animal Welfare Score Sheet in the Good Practice Guide for the use of animals in research, testing and teaching)

One sheet per animal to record parameters listed below

Animal/Species #				**Date of Treatment/Operation:**								
Pre-study Bodyweight:											**AEC #:**	
Date												
Day												
BODY WEIGHT & B.A.R. SCORE (score normal animal as 0; score 1, 2, 3 for ↑ in severity)												
Body weight yesterday												
Body weight today												
Body weight change												
BAR (bright, alert, responsive)												
Approach response												
(inquisitive behaviour investigates your presence)												
GENERAL CLINICAL SIGNS (score normal animal as 0; score 1, 2, 3 for ↑ in severity)												
Inactive												
Hunched posture												
Coat rough, fur on end												
Red eye/nose discharges												
Pink staining of neck												
Dehydration – Skin turgor test (see reverse)												
BEHAVIOURAL SIGNS OF PAIN	**(score as √ each time when sign is observed)**											
Back arch Hunched up with arched back												
Belly press Presses belly to cage floor												
Writhe Twisting of body or flank												
Stagger Sudden loss of balance/gait												
Twitch Sudden spasm of flank muscles												
Fall — falls over												
Signature												

C.3. Rotarod data

Table C.3. Rotarod data on diabetic mice across 13 weeks. Mouse 50.1 was excluded from the data analysis as he refused to run on the Rotarod. All mice were given 180 mg/kg streptozotocin, mice 25.3, 32.3, 31.1 and 50.1 did not become diabetic so were not included in the analysis. The latency to fall for each day is an average of three trials.

	Rotarod results Group 1 STZ mice								
		Latency to fall (secs)							
	Mouse I.D	Pre STZ	day 8 post	day 15 post	day 23 post	day 30 post	day 37 post	day 44 post	day 51 post	day 101 post
	12.3	300	300	224	204	237	222	198	273	248
	12.4	300	300	300	300	300	300	240	174	93
	20.2	186	182	50	52	116	107	192	248	210
	20.3	156	230	76	294	164	208	179	230	93
	25.4	219	148	290	164	300	276	286	300	255
	27.2	300	300	300	300	300	300	300	300	271
	31.2	300	300	300	213	244	296	228	300	300
	32.1	155	150	300	300	136	95	282	300	300
Not diabetic	25.3	230	210	300	300	280	227	300	300	238
	32.3	156	188	238	129	138	170	295	219	
	31.1	300	300	254	242	300	300	263	300	300
	50.1	31	30	20	30	15	13	17	6	

C.4. Protein quantification

Table C.4. Protein quantification data for sciatic nerve tissue harvested from diabetic mice after the 13 week trial.

			5.0	ug	
Mouse I.D	**Distal**	**Conc. Ug/ul**	**vol ripa buffer uL**	**Vol lysate uL**	**Samples run**
STZ	50.1	1.441727273	21.5	3.5	x
	31.1	1.055	20.3	4.7	
	32.1	1.740772727	22.1	2.9	x
	20.3	1.455772727	21.6	3.4	x
	27.2	1.479363636	21.6	3.4	x
	25.3	1.152409091	20.7	4.3	
	31.2	0.939681818	19.7	5.3	
	25.4	1.232045455	20.9	4.1	x
	20.2	1.388136364	21.4	3.6	x
	12.4	1.608863636	21.9	3.1	x
	12.3	1.623227273	21.9	3.1	x
Ctrl	Distal				
	38.3	1.784318182	22.2	2.8	x
	42.1	1.807818182	22.2	2.8	x
	42.2	1.374818182	21.4	3.6	
	38.1	1.643136364	22.0	3.0	x
	39.1	1.506090909	21.7	3.3	x
	34.1	1.645318182	22.0	3.0	x
	Proximal				
STZ	50.1	1.320772727	21.2	3.8	x
	31.1	1.423272727	21.5	3.5	x
	32.1	1.357772727	21.3	3.7	x
	20.3	1.451181818	21.6	3.4	x
	27.2	1.401681818	21.4	3.6	x
	25.3	1.051	20.2	4.8	
	31.2	1.9785	22.5	2.5	x
	25.4	1.211136364	20.9	4.1	
	20.2	1.446227273	21.5	3.5	x
	12.4	1.028909091	20.1	4.9	
	12.3	1.523	21.7	3.3	x
Ctrl	Proximal				
	38.3	0.889863636	19.4	5.6	
	42.1	1.202227273	20.8	4.2	x
	42.2	1.1855	20.8	4.2	x
	38.1	1.445545455	21.5	3.5	x
	39.1	1.571363636	21.8	3.2	x
	34.1	1.476227273	21.6	3.4	x

C.5. Immunoblot quantification data

Table C.5. Quantification of immunoblot data to determine the changes to levels of acetylated α - tubulin in STZ-induced diabetic mice.

Distal acetylated alpha tub			GAPDH	Normalised	Normalised			GAPDH	Normalised	Normalised		Ratio acetyl			
STZ	Mouse ID	acety tub	acetyl	to GAPDH	acetyl tub	Percentage	total tub	total tub	to GAPDH	total tub	Percentage	tub/tot tub		Percentage	
	50.1	7547.057	53021.759	0.65346546	11549.2823	30.2405824	12431.978	23124.999	0.59415596	20923.7623	139.478093	0.55196968		19.7089806	**22.0442696**
	32.1	3587.581	56535.446	0.69676981	5148.87549	13.4817896	6628.803	30287.877	0.77819344	8518.1944	56.7824035	0.60445621		21.5830981	
	20.3	5524.38	66428.274	0.81869374	6747.798	17.6684002	19679.434	31476.362	0.80872946	24333.7667	162.209231	0.27730183		9.90151561	
	27.2	3391.045	81139.345	1	3391.045	8.8790951	5265.388	35969.099	0.92416239	5697.47053	37.9794186	0.5951843		21.2520294	
	25.4	14827.362	65944.324	0.81272931	18243.912	47.7697669	22414.505	24935.534	0.64067445	34985.795	233.215801	0.52146627		18.6198065	
	12.4	12273.626	70240.626	0.86567899	14178.0339	37.1236923	21808.676	36319.279	0.93315965	23370.7877	155.789999	0.60665623		21.6616534	
	12.3	32825.082	71154.103	0.87693711	37431.5119	98.0104817	25388.534	30743.007	0.7898872	32141.9742	214.258851	1.16456792		41.5828033	
					13812.9226	**36.1676869**				**21424.5358**	**142.816257**	**0.61737177**			
Ctrl	Distal														
	38.3	30790.212	67572.082	0.83279058	36972.3347	96.8081745	14604.563	30716.484	0.78920574	18505.3938	123.357215	1.99792207		71.3390772	**100**
	42.1	30806.718	65382.851	0.80580945	38230.7728	100.103262	8863.066	38920.756	1	8863.066	59.0813225	4.31349296		154.020325	
	38.1	30271.555	61693.002	0.76033399	39813.4969	104.247459	13123.714	37324.747	0.95899337	13684.885	91.2236356	2.90930446		103.881477	
	39.1	27777.321	70396.931	0.86760536	32016.078	83.8307368	9640.673	33384.333	0.8577514	11239.4722	74.9224793	2.84853928		101.711757	
	34.1	39882.496	73673.617	0.90798881	43923.9952	115.010367	22637.484	38788.747	0.99660826	22714.5257	151.415347	1.93374036		69.0473643	
					38191.3355	**100**				**15001.4685**	100	**2.80059983**			
Proximal acetylated tub															
STZ	50.1	44883.123	42716.467	0.77923369	57599.0538	96.9001436	66610.404	31036.404	0.52137849	127758.251	149.975608	0.4508441		64.015902	**58.2396245**
	31.1	28717.304	64444.701	1.17560008	24427.7834	41.0953924	50848.011	55067.215	0.92507049	54966.6339	64.5254164	0.44441112		63.1024751	
	32.1	29972.475	54818.558	1	29972.475	50.4233479	54692.739	52584.751	0.88336774	61913.8966	72.6808187	0.48409932		68.7378504	
	20.3	14233.258	55975.659	1.02110783	13939.0352	23.4499427	44916.07	51249.266	0.86093302	52171.3874	61.2440722	0.26717777		37.9368969	
	27.2	15066.744	49095.517	0.8956003	16823.0672	28.3018125	31765.676	41920.153	0.70421387	45107.9955	52.9523456	0.37295089		52.9557505	
	31.2	13646.844	43055.040	0.78540993	17375.441	29.2310832	24551.141	39746.333	0.66769601	36769.9382	43.1642872	0.47254474		67.0972027	
	20.2	20510.2	30713.848	0.56028194	36606.9269	61.584631	56588.685	28381.655	0.47678154	118688.918	139.329104	0.30842751		43.7939963	
	12.3	30700.818	23639.250	0.43122714	71194.0765	119.771347	58777.605	23631.907	0.39699084	148057.838	173.805324	0.48085314	**0.41016357**	68.2769221	
					33492.2324	56.3447125				**80679.3573**	94.709622				
Ctrl	Proximal														
	42.1	46533.224	33306.726	0.60758121	76587.661	128.845091	64192.948	31355.362	0.52673665	121869.151	143.062385	0.62844173		89.2332058	**100**
	42.2	44891.789	29396.635	0.53625334	83713.7699	140.8335	58874.17	28913.220	0.48571126	121212.281	142.291283	0.69063769		98.0644856	
	38.1	46245.446	37251.362	0.67953925	68054.1201	114.48893	52450.848	37544.283	0.63070392	83162.3944	97.6244631	0.81832805		116.195395	
	39.1	24560.756	57754.780	1.05356255	23312.1004	39.2184545	38750.333	46021.002	0.77310376	50123.069	58.839548	0.46509723		66.0397205	
	34.1	39312.446	47321.496	0.86323861	45540.6482	76.614025	49563.203	59527.588	1	49563.203	58.1823205	0.91883989	**0.70426892**	130.467193	
					59441.6599	100				**85186.0197**	100				